



Reduced Proximal Tubular Expression of Megalin and Neonatal Fc Receptor in Proteinuria: The Role of Matrix Metalloproteinases

Thesis submitted for the degree of
Doctor of Philosophy
at the University of Leicester

By

Hiwa Ramadhan Fatah MSc

Department of Infection, Immunity and Inflammation
University of Leicester

November 2017

Statement of originality

This accompanying thesis submitted for the degree of PhD entitled “*Reduced Proximal Tubular Expression of Megalin and Neonatal Fc Receptor in Proteinuria: The Role of Matrix Metalloproteinases*” is based on work conducted by the author at the University of Leicester mainly during the period between November 2013 and October 2016.

All the work recorded in this thesis is original unless otherwise acknowledged in the text or by references.

None of the work has been submitted for another degree in this or any other University.

Signed: _____

Date: _____

Reduced Proximal Tubular Expression of Megalin and Neonatal Fc Receptor in Proteinuria: The Role of Matrix Metalloproteinases

Hiwa Ramadhan Fatah

Abstract

Proteinuria is clearly associated with the progression of chronic kidney disease (CKD) but the mechanisms underlying this relationship remain unclear. Recent evidence suggests that altered proximal tubular (PT) handling of filtered proteins may significantly modulate urine protein excretion and progressive renal disease. Megalin and neonatal Fc receptor (FcRn) are endocytic receptors responsible for the PT reabsorption of glomerular ultrafiltered proteins by receptor-mediated endocytosis (RME) and transcytosis, and are expressed on the luminal surface of the PT. This study aimed to investigate the expression and turnover of megalin and FcRn in proteinuria, and the possible mechanisms underlying down-regulation of expression of these receptors.

In protein overload proteinuria (POP), the PT expression of megalin and FcRn were both downregulated compared to control animals. In addition, significant amount of both receptor were detected in the urine of proteinuric animals. This reduction in megalin and FcRn protein expression was accompanied by a significant increase in the urinary excretion of plasma proteins including the most abundant albumin. Increased expression and activity of both matrix metalloproteinase (MMP) and gamma secretase (γ -secretase) was evident in proteinuric animals and was paralleled with the urinary excretion of both megalin and FcRn.

Megalin was previously identified to undergo regulated intramembrane proteolysis (RIP). RIP includes the MMP-mediated cleavage of the extracellular domain of megalin which in turn excreted into the urine, and the subsequent cleavage of the intracellular domain by γ -secretase. A synthetic inhibitor of MMPs, batimastat (BB-94) significantly reduced urinary excretion and also preserved the PT expression of megalin. In addition, inhibition of MMPs appeared to be antiproteinuric by markedly reducing urinary excretion of albumin and plasma proteins. The urinary excretion of FcRn was also reduced in BB-94 treated animals but the mechanism of this reduction was not clear. Further, BB-94 treatment preserved PT expression of FcRn in proteinuric animals.

The POP model was developed to investigate the degree of tubulointerstitial damage in experimental animals. Injury was detected in the interstitium of proteinuric animals with significant increases in inflammatory markers including tumour necrosis factor alpha (TNF- α), interleukin-6 (IL-6) and the transforming growth factor-beta (TGF- β) as well as interstitial collagen deposition and marked interstitial infiltration of macrophages (F4/80). Blockade of MMP in proteinuric animals significantly reduced the expression of these markers in the kidney and abrogated the progression of interstitial inflammation and fibrosis.

In summary this is the first study to correlate the reduced expression of megalin and FcRn, and the urinary excretion of these receptors with the increased cellular activity of MMP and the possible occurrence of RIP in vivo. Inhibition of MMP could be of great importance in treating proteinuria and the progression of tubulointerstitial inflammation and fibrosis, the most characteristic features of CKD.

Acknowledgments

“Thanks to Almighty ALLAH for giving me strength and ability to understand, learn and complete this work”

Firstly, I would like to express my sincere gratitude to my supervisor Professor Nigel Brunskill for the continuous support of my PhD study, for his patience, motivation, and immense knowledge. His guidance helped me in all the time of research and writing of this thesis. I could not have imagined having a better supervisor and mentor for my PhD study.

I would also like to thank my PRP members, Professor Jonathan Barret, and Dr Alan Bevington, for their insightful comments and encouragement, but also for the hard question, which incited me to widen my research from various perspectives.

My special thank goes to Dr Ravi who helped me to learn various techniques during my Lab work and I never forget his nice words. I would like to thank my dear friend Sami who helped me during animal work and in establishing the present animal models.

I want to thank all the people in 3i department and labmates for their continuous support. Very special thanks also to the University of Leicester for giving me an opportunity to complete this study.

I would like to thank Ministry of Higher Education in Kurdistan/HCDP for sponsoring and financially support me throughout my PhD study.

I would especially like to thank my family. My parents, brothers (especially Dr Azad) and sisters have been extremely supported me during this study and without them I could never be successful. My special thanks goes to my wife “Narmeen” for her patience and support in very hard times.

Dedication,

This thesis is dedicated to the soul of my father who taught me the meaning of life.

Publications and Posters

Reduced proximal tubular expression of protein endocytic receptors in proteinuria is associated with urinary receptor shedding.

Fatah, H., Benfaed, N., Chana, R.S., Chunara, M.H., Barratt, J., Baines, R.J. and Brunskill, N.J., 2017. *Nephrology Dialysis Transplantation*.

Urinary shedding of tubular protein receptors in proteinuric states. UK Kidney Week conference, British Renal Society, Birmingham, June 2016. Hiwa Fatah and Nigel J Brunskill.

Albumin overload, a successful model of proteinuria in BALB/c mice. 3Rs Conference, Leicester UK, March 2016. Hiwa Fatah and Nigel J Brunskill.

Table of Contents

1 Introduction	1
1.1 The kidney structure	1
1.2 Kidney anatomy	2
1.3 The nephron	2
1.3.1 Glomerular filtration barrier.....	3
1.3.1.1 Endothelial cells	4
1.3.1.2 Glomerular basement membrane.....	7
1.3.1.3 Podocytes	8
1.3.2 The proximal tubule.....	10
1.4 Mechanisms of proteinuria	12
1.4.1 Glomerular proteinuria.....	12
1.4.2 Tubular proteinuria	14
1.5 Renal handling of protein	15
1.5.1 Glomerular filtration of albumin	16
1.5.2 Tubular reabsorption of proteins	17
1.6 Tubular receptors for endocytosis of proteins	19
1.6.1 Megalin.....	19
1.6.1.1 The structure of megalin.....	19
1.6.1.2 Megalin cytoplasmic tail and its phosphorylation role.....	20
1.6.1.3 Regulated intramembrane proteolysis.....	21
1.6.1.4 The biological role of megalin.....	24
1.6.1.5 Megalin as a receptor for albumin	25
1.6.1.6 Regulation of megalin expression	25
1.6.1.6.1 Regulation of megalin mRNA and protein expression	26
1.6.1.6.2 Regulation of megalin cell surface distribution and protein levels	26
1.6.2 Cubilin	27
1.6.3 The neonatal Fc receptor (FcRn)	29
1.7 Tubular toxicity of proteinuria (Figure 1.11)	33
1.7.1 Cell culture studies	33

1.7.2 In vivo studies	35
1.8 Importance of proteinuria in CKD	38
1.8.1 Correlation between proteinuria and renal failure.....	38
1.8.1.1 Correlation in animal studies	38
1.8.1.1.1 Remnant kidney	38
1.8.1.1.2 Puromycin aminonucleoside nephrosis model	39
1.8.1.1.3 Protein overload proteinuria	40
1.8.1.2 Correlation in human studies.....	41
1.9 Matrix metalloproteinases	42
1.9.1 MMP structure.....	43
1.9.2 MMP activation and expression	44
1.9.3 The beneficial effect of MMP inhibition in animal models.....	45
1.9.4 Mechanisms of MMP in kidney diseases.....	47
1.10 Synthetic Inhibitor batimastat.....	47
1.11 Aims and objectives.....	49
1.12 Hypothesis.....	49
2 Materials and Methods	50
2.1 Materials.....	50
2.1.1 Experimental animals.....	50
2.1.2 Chemicals, reagents and solutions	50
2.1.3 Antibodies	54
2.1.4 TaqMan gene expression assays.....	54
2.1.5 Commercial kits.....	54
2.2 Methods	58
2.2.1 Unilateral nephrectomy	58
2.2.2 Experiment 1: Protein overload proteinuria model (Figure 2.1).....	58
2.2.3 Experiment 2: Protein overload proteinuria plus batimastat (BB-94) model (Figure 2.2).....	58
2.2.4 Collection of urine and blood.....	59
2.2.5 Animal killing and tissue collection	59
2.2.6 Preparation of urine for megalin and FcRn determination.....	62

2.2.7 Urine analysis.....	62
2.2.7.1 Determination of protein concentration.....	62
2.2.7.2. SDS-PAGE of urinary protein.....	63
2.2.7.3 SDS-PAGE of urinary megalin.....	63
2.2.7.4 Determination of urine albumin concentration.....	63
2.2.7.5 Determination of urine megalin concentration.....	64
2.2.7.6 Determination of urine FcRn concentration.....	65
2.2.7.6.1 Preparation of wash buffer (1X).....	65
2.2.7.6.2 Preparation of biotin-antibody (1X).....	65
2.2.7.6.3 Preparation of HRP-avidin (1X).....	65
2.2.8 Analysis of serum.....	66
2.2.8.1 Determination of serum creatinine.....	66
2.2.8.2 Determination of total serum protein.....	66
2.2.9 Preparation of homogenate from mouse renal cortex.....	66
2.2.10 Determination of protein concentration in kidney homogenates.....	67
2.2.11 Western blot analysis.....	67
2.2.12 Coomassie blue staining.....	68
2.2.13 Analysis of western blot images.....	68
2.2.14 Immunohistochemistry.....	70
2.2.15 Analysis of immunohistochemical images.....	72
2.2.16 TGF- β scoring.....	72
2.2.17 Histological analysis.....	72
2.2.17.1 Haematoxylin and eosin (H&E) staining.....	72
2.2.17.1.1 Analysis of H&E images.....	73
2.2.17.2 Sirius red staining.....	73
2.2.17.2.1 Analysis of sirius red staining images.....	73
2.2.18 Determination of transforming growth factor beta-1 (TGF β -1) concentration in kidney homogenates.....	74
2.2.19 Determination of tumour necrosis factor- α (TNF- α) concentration in kidney homogenates.....	75
2.2.20 Total RNA isolation and purification.....	75
2.2.21 RNA integrity and quantification.....	76
2.2.22 Reverse transcription reaction.....	76
2.2.23 Quantitative real-time PCR (qPCR).....	76

2.2.24 MMP assays.....	77
2.2.25 Data analysis.....	77
3 Expression of Tubular Protein Receptors in Normal and Proteinuric Mice.....	78
3.1 Introduction	78
3.2 Results	79
3.2.1 Effects of POP on kidney function.....	79
3.2.2 Effects of POP on serum total protein concentration.....	79
3.2.3 Proteinuria in mice following unilateral nephrectomy with POP.....	82
3.2.4 Protein expression of megalin in the kidneys of POP mice	84
3.2.5 mRNA expression of megalin in the kidney of POP mice.....	88
3.2.6 Urinary excretion of megalin in saline-treated control and POP mice	91
3.2.7 Protein expression of FcRn in the kidneys of saline-treated control and POP mice	94
3.2.8 mRNA expression of FcRn in the kidney of POP mice.....	98
3.2.9 Urinary excretion of FcRn by proteinuric mice.....	100
3.3 Discussion	102
3.4 Summary.....	106
3.5 Conclusions.....	106
4 Expression and Shedding of Proximal Tubular Receptors and the Effect of Matrix Metalloproteinase Inhibition in Proteinuria.....	107
4.1 Introduction	107
4.2 Results	108
4.2.1 Effect of POP on MMP activity in uni-nephrectomised mice.....	108
4.2.2 Effect of POP on γ -secretase activity in uni-nephrectomised mice .	110
4.2.3 The effect of the MMP inhibitor BB-94 on serum creatinine levels in POP mice	114
4.2.4 Total serum protein concentration in BB-94 treated and non-BB-94 treated mice	116

4.2.5 BB-94 treatment reduced urinary albumin and total protein excretion in POP mice	118
4.2.6 BB-94 treatment reduced the enzymatic activity of MMP in POP mice	120
4.2.7 Assessment of MMP-9 expression in POP mice after BB-94 treatment	122
4.2.8 BB-94 treatment reduced MMP-9 mRNA expression in POP mice .	123
4.2.9 BB-94 preserves the expression of megalin in proximal tubules in mice with POP	128
4.2.10 The effect of BB-94 treatment on megalin mRNA expression in POP mice	129
4.2.11 Assessment of FcRn protein expression after BB-94 treatment in POP mice	134
4.2.12 mRNA expression of FcRn receptor in proteinuric mice after BB-94 treatment	135
4.2.13 BB-94 treatment leads to reduced urinary excretion of megalin in POP mice	140
4.2.14 BB-94 treatment leads to reduced urinary excretion of FcRn in POP mice	142
4.3 Discussion	144
4.4 Conclusions.....	150
5 Matrix Metalloproteinase Inhibitor (BB-94) Reduces Renal Tubulointerstitial Fibrosis in Proteinuric Mice	151
5.1 Introduction	151
5.2 Results	152
5.2.1 Effects of BB-94 treatment on morphological changes in the kidney of POP mice	152
5.2.2 BB-94 treatment reduced collagen deposition in POP mice	155
5.2.3 Effect of BB-94 treatment on the interstitial accumulation of inflammatory cells in mice with POP	158
5.2.4 BB-94 treatment reduced mRNA expression of F4/80 in the kidney of POP mice	159

5.2.5 Effect of BB-94 treatment on transforming growth factor-beta (TGF- β) expression in the kidney of POP mice.....	164
5.2.6 Effect of BB-94 treatment on tumour necrosis factor-alpha (TNF- α) expression in POP mice.....	169
5.2.7 Effects of BB-94 treatment on interleukin-6 (IL-6) expression in POP mice	175
5.3 Discussion.....	179
5.4 Conclusions.....	185
6 Thesis discussion.....	186
6.1 Thesis Summary	186
6.2 Conclusions.....	190
6.3 Future Work.....	190
7 Appendices.....	192
7.1 Appendix A - Buffers and solutions used in this study	192
7.2 Appendix B - Standard curves	195
7.3 Appendix C - Automated image analysis macro code.....	199
8 References.....	200

List of Tables

Table 2.1: Chemicals, reagents and solutions used throughout for immunohistochemistry and western blot analysis.	51
Table 2.2: Primary antibodies used in immunohistochemistry and western blot analysis.	55
Table 2.3: Secondary antibodies used in immunohistochemistry and western blot analysis.	56
Table 2.4: TaqMan gene expression assays used in qPCR analysis.....	56
Table 2.5: Supplier information for assay kits.....	57
Table 2.6: Primary and secondary antibody dilutions for western blot analysis.	69
Table 2.7: Primary and secondary antibody dilutions for immunohistochemistry.	71
Table 3.1: RNA integrity number in 10 samples from mouse kidney analysed by 2100 bioanalyzer (Agilent Technologies).	88

List of Figures

Figure 1.1: Structure of mammalian kidney depicting the important parts.....	1
Figure 1.2: Schematic diagram of the nephron system.	3
Figure 1.3: Schematic diagram of the renal glomerulus.	4
Figure 1.4: Structure of the glomerular filtration barrier (GFB).	5
Figure 1.5: Fenestration area of the glomerular endothelium.....	6
Figure 1.6: The structure of the slit diaphragm and podocyte foot process showing important proteins.	9
Figure 1.7: (A) Schematic diagram of the three segments of the proximal tubule. (B)Transmission electron microscopy showing the ultrastructure of the three segments of the proximal tubule cells in the rat kidney.	12
Figure 1.8: Schematic diagram showing both endocytosis mediated by megalin, cubilin and amnionless, and transcytosis mediated by FcRn.	18
Figure 1.9: Mechanism of megalin ectodomain shedding (RIP).	23
Figure 1.10: The structure of megalin (C), cubilin (B) and FcRn (A) showing known motifs and domains.....	32
Figure 1.11: Mechanisms of protein overload proteinuria leading to tubular toxicity and kidney damage.	37
Figure 1.12: Proposed mechanism of MMP inhibition and protection of megalin ectodomain shedding.	46
Figure 1.13: Schematic diagram showing signalling pathways of MMP synthesis by various stimuli and inhibition of MMP production by different MMP inhibitors, including batimastat.	48
Figure 2.1: Schematic diagram showing the model of protein overload proteinuria in wild type BALB/c mice.....	60
Figure 2.2: Schematic diagram showing the model of protein overload proteinuria+BB-94 in wild type BALB/c mice.	61

Figure 3.1: Effect of POP on serum creatinine level in uni-nephrectomised mice.	80
Figure 3.2: Effect of POP on serum total protein level in uni-nephrectomised mice.	81
Figure 3.3: Urinary protein excretion in saline-treated control and POP mice.	83
Figure 3.4: Effect of POP on renal megalin protein expression in uni-nephrectomised mice.	85
Figure 3.5: Expression of megalin in the cortex of kidneys from saline-injected control and POP mice.	86
Figure 3.6: Quantification of renal megalin staining in saline-treated control and POP mice.	87
Figure 3.7: Effect of POP on renal megalin mRNA expression in uni-nephrectomised mice.	89
Figure 3.8: Gel electrophoresis of total RNA isolated from mouse kidney.	90
Figure 3.9: Urinary excretion of megalin in saline-treated control and POP mice.	92
Figure 3.10: PAGE and WB of urine from saline-treated control and POP mice.	93
Figure 3.11: Effects of POP on renal FcRn protein expression in uni-nephrectomised mice.	95
Figure 3.12: Expression of FcRn in the cortex of kidneys from saline-treated control and POP groups.	96
Figure 3.13: Quantification of renal FcRn staining in saline-treated control and POP groups.	97
Figure 3.14: Effect of POP on renal FcRn mRNA expression in uni-nephrectomised mice.	99
Figure 3.15: Urinary FcRn excretion in saline-treated control and POP mice.	101

Figure 4.1: Effect of POP on MMP activity in uni-nephrectomised mice.	109
Figure 4.2: Effect POP on renal PS-1 expression in uni-nephrectomised mice.	111
Figure 4.3: Expression of PS-1 in the cortex of kidneys from saline-treated control and POP groups.....	112
Figure 4.4: Quantification of renal PS-1 staining in saline-treated control and POP groups.....	113
Figure 4.5: Effect of MMP inhibitor (BB-94) treatment on serum creatinine level in proteinuria-induced mice.	115
Figure 4.6: Effect of BB-94 treatment on serum total protein level in POP mice.	117
Figure 4.7: BB-94 treatment of proteinuria-induced mice decreases urinary albumin and protein excretion.	119
Figure 4.8: Effect of synthetic inhibitor BB-94 treatment on MMPs activity in proteinuria-induced mice.....	121
Figure 4.9: BB-94 treatment reduced MMP-9 expression in POP mice.	124
Figure 4.10: Expression of MMP-9 in the cortex of kidneys from saline-treated control, POP and POP+BB-94 groups.	125
Figure 4.11: Quantification of renal MMP-9 staining in saline-treated control, POP and POP+BB-94 groups.....	126
Figure 4.12: Effect of BB-94 treatment on MMP-9 mRNA expression in POP mice.	127
Figure 4.13: Downregulation of megalin in POP mice is prevented with BB-94 treatment.....	130
Figure 4.14: Expression of megalin in the cortex of kidneys from saline-treated control, POP and POP+BB-94 mice.....	131
Figure 4.15: Quantification of renal megalin staining in saline-treated control, POP and POP+BB-94 groups.....	132

Figure 4.16: Effect of BB-94 treatment on renal megalin mRNA levels in POP group.....	133
Figure 4.17: Downregulation of FcRn in POP mice is prevented with BB-94 treatment.....	136
Figure 4.18: Expression of FcRn in the cortex of kidneys from saline-treated control, POP and POP+BB-94 groups.	137
Figure 4.19: Quantification of renal FcRn staining in saline-treated control, POP and POP+BB-94 groups.....	138
Figure 4.20: Effect of BB-94 treatment on renal FcRn mRNA levels in POP mice.	139
Figure 4.21: Increased urinary excretion of megalin in POP mice is reduced by BB-94 treatment.....	141
Figure 4.22: Increased urinary excretion of FcRn in POP mice is reduced by BB-94 treatment.....	143
Figure 5.1: Representative photomicrographs of H&E staining of the kidney of saline-treated control (A), POP (B) and POP+BB-94 groups.	153
Figure 5.2: BB-94 treatment attenuated renal tubular injury scores in POP mice.	154
Figure 5.3: Representative photomicrographs of sirius red staining showing collagen deposition in the kidney of saline-treated control (A), POP (B) and POP+BB-94 (C) groups.....	156
Figure 5.4: BB-94 treatment reduced collagen deposition in the kidney of POP mice	157
Figure 5.5: BB-94 treatment reduced macrophage infiltration into the kidney of POP mice.....	160
Figure 5.6: Representative photomicrographs showing macrophage infiltration into renal interstitium assessed by immunohistochemistry of F4/80 in the saline-treated control (B), POP (C), and POP+BB-94 (D) groups at day 14.....	161

Figure 5.7: Quantification of macrophage infiltration in the kidney of saline-treated control, POP and POP+BB-94 groups.	162
Figure 5.8: BB-94 treatment reduced mRNA expression of F4/80 in POP mice.	163
Figure 5.9: Effects of BB-94 treatment on renal TGF- β expression in POP mice.	165
Figure 5.10: Expression of TGF- β in the cortex of kidneys from saline-treated control, POP and POP+BB-94 groups.	166
Figure 5.11: Immunostaining score for TGF- β staining in the kidney of saline-treated control, POP and POP+BB-94 groups.	167
Figure 5.12: Effects of BB-94 treatment on renal TGF- β levels in POP mice.	168
Figure 5.13: BB-94 treatment reduced TNF- α expression in the kidney of POP mice.	171
Figure 5.14: Expression of TNF- α in the cortex of kidneys from saline-treated control, POP and POP+BB-94 groups.	172
Figure 5.15: Quantification of TNF- α staining in the kidneys of saline-treated control, POP and POP+BB-94 groups.	173
Figure 5.16: Effects of BB-94 treatment on renal TNF- α levels in POP mice.	174
Figure 5.17: Effects of BB-94 treatment on renal IL-6 expression in POP mice.	176
Figure 5.18: Expression of IL-6 in the cortex of kidneys from saline-treated control, POP and POP+BB-94 groups.	177
Figure 5.19: Quantification of IL-6 staining in the kidneys of saline-treated control, POP and POP+BB-94 groups.	178
Figure 5.20: Mechanisms of MMP inhibition preventing renal tubulointerstitial inflammation and fibrosis.	184

Figure 6.1: Schematic view of endocytic receptor down-regulation in proteinuria	187
Figure 6.2: Schematic view showing how MMPs inhibition preserves cell surface expression of endocytic receptors in the proximal tubule cells in the kidney..	187
Figure 6.3: Schematic diagram showing how inhibition of MMPs activity reduces interstitial fibrosis and inflammation.	189

List of Abbreviations

ACE	Angiotensin converting enzyme
AKI	Acute kidney injury
AMN	Amnionless
BB-94	Batimastat
BSA	Bovine serum albumin
CKD	Chronic kidney disease
CT	Cytoplasmic tail
D.W	Distilled Water
DAB	Diaminobenzidine
DN	Diabetic nephropathy
ECM	Extracellular matrix
EGF	Epidermal growth factor
ELISA	Enzyme-linked immunosorbent assay
EMT	Epithelial mesenchymal transition
ERK	Extracellular signal-regulated kinase
ESL	Endothelial cell surface layer
FcRn	Neonatal Fc receptor
FP	Foot processes
FPE	Foot processes effacement
GBM	Glomerular basement membrane
GFB	Glomerular filtration barrier
GFR	Glomerular filtration rate
GSK3	Glycogen synthase kinase 3
H&E	Haematoxylin and eosin
HDL	High density lipoprotein
HMW	High molecular weight
HRP	Horseradish peroxidase
HSPGs	Heparan sulfate proteoglycans
i.p.	Intraperitoneal
IF-B12	Intrinsic factor-cobalamin complex
IHC	Immunohistochemistry
IP-10	Interferon-inducible protein-10
KO	Knockout
LDLR	Low-density lipoprotein receptor
LMW	Low molecular weight

MAPK	Mitogen-activated protein kinase
MCNS	Minimal change nephrotic syndrome
MCP-1	Monocyte chemoattractant protein-1
MCTF	Megalin C-terminus fragment
MCTF	Megalin carboxyl terminal fragment
MHC	Major histocompatibility-complex
MICD	Megalin intracellular domain
MMP	Matrix metalloproteinase
MN	Membranous nephropathy
NS	Nephrotic syndrome
OPN	Osteopontin
PAN	Puromycin aminonucleoside
PBS	Phosphate buffered saline
PKB	Protein kinase B
PKC	Protein kinase C
PMSF	Phenylmethanesulfonyl fluoride
POP	Protein overload proteinuria
PPARs	Peroxisome proliferator-activated receptors
PS-1	Presenilin-1
PT	Proximal tubule
PTEC	Proximal tubular epithelial cells
qPCR	Quantitative real-time PCR
RANTES	Regulated upon activation, normal T cell expressed and secreted
RAP	Receptor associated protein
RBP	Retinol-binding protein
RME	Receptor-mediated endocytosis
RFU	Relative fluorescence unit
RIP	Regulated intramembrane proteolysis
RIPA	Radioimmunoprecipitation assay
ROS	Reactive oxygen species
SD	Slit diaphragm
SDS	Sodium dodecyl sulphate
SDS-PAGE	Sodium dodecyl sulphate polyacrylamide gel electrophoresis
STAT	Signal transducer activator of transcription
TBS	Tris-buffered saline
TBST	Tris-buffered saline with tween 20
TGF- β	Transforming growth factor-beta

TMB	3,3',5,5'-tetramethylbenzidine
TNF- α	Tumour necrosis factor alpha
UUO	Unilateral ureteral obstruction
VDBP	Vitamin D binding protein
WB	Western blot
β ME	Beta mercaptoethanol

1 Introduction

1.1 The kidney structure

The kidneys are paired bean-shaped organs that are located below the ribs external to the peritoneal cavity on the posterior abdominal wall on each side of the vertebral column. Each human kidney is approximately 10 cm in length, 5 cm in width and 2.5 cm in thickness. The approximate weight of human kidney is 125 to 170 g in adult male and from 115 to 155 g in the adult female. The structure of the kidney is the three distinct area, the outer renal cortex where the urine production occur contains renal corpuscles, segments of the proximal and distal convoluted tubules, as well as portions of the collecting ducts, the inner renal medulla where the urine collection occur consists of specialised segment of the nephron, the Loops of Henle, associated vasculature (vasa recta and venulae recta) and the collecting ducts, and the third part is the renal capsule that surrounds the internal structures of the kidney. Located to the middle of each kidney in the concave notch away from the cortex there is the renal hilum where the renal artery and vein, lymphatics and nerve plexus, and renal pelvis and ureter enter and exit the kidney (Figure 1.1) (van Leeuwen and Bladh, 2016).

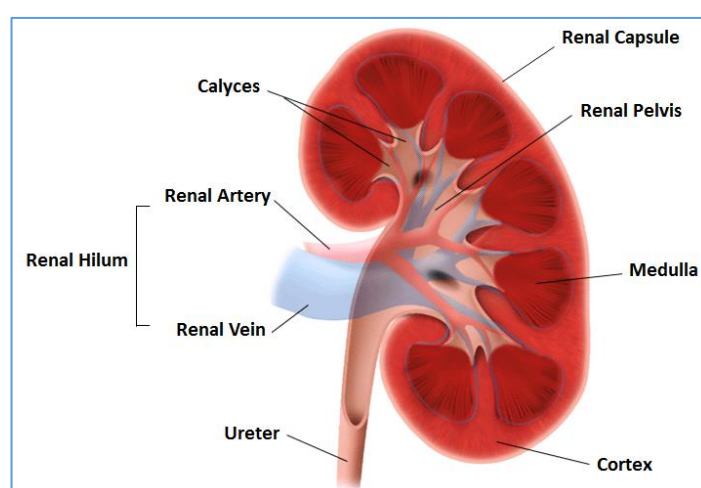


Figure 1.1: Structure of mammalian kidney depicting the important parts. (Modified from Guyton, A. C. and Hall, J. E., 2000. Textbook of Medical Physiology. Philadelphia WB Saunders Company).

1.2 Kidney anatomy

The kidneys perform a number of important functions and play a crucial role in maintaining acid-base homeostasis through the excretion of waste products, regulation of body fluid volume and composition, and production and secretion of hormones and enzymes such as erythropoietin and renin that regulate blood pressure, calcium balance and production of red blood cells. Blood carrying waste products is filtered in the kidney to produce a primary filtrate which is then modified in the nephron to produce the final urine. This section will focus on the most important components of nephron system.

1.3 The nephron

The nephrons are tiny tubules numbering more than one million in each human kidney (van Leeuwen and Bladh, 2016). Nephrons constitute the major part of the kidney cortex, and represent the functional and structural unit of the kidney (Taal et al., 2011). The nephrons consist of the renal corpuscle filtering unit, consisting of the glomerulus and the glomerular (Bowman's) capsule, and the renal tubule including the proximal tubule, loop of Henle, distal tubule and collecting duct system (Figure 1.2).

The glomerulus is composed of capillaries supplied by an afferent glomerular arteriole with a relatively higher diameter, and drained by an efferent glomerular arteriole (Figure 1.3) (Koeppen and Stanton, 2012). The blood plasma is filtered through the glomerular capillaries or capillary bed due to the higher hydraulic pressure in these capillaries and the intrinsic permeability of the glomerular wall, into the Bowman's- or urinary-space that is located between the glomerulus and the Bowman's capsule (Mirpuri and Patel, 2000). The Bowman's capsule is a cup-shaped, double-layered epithelial wall that surrounds the entire glomerulus and extend to the beginning of the PTs (Dudek, 2006).

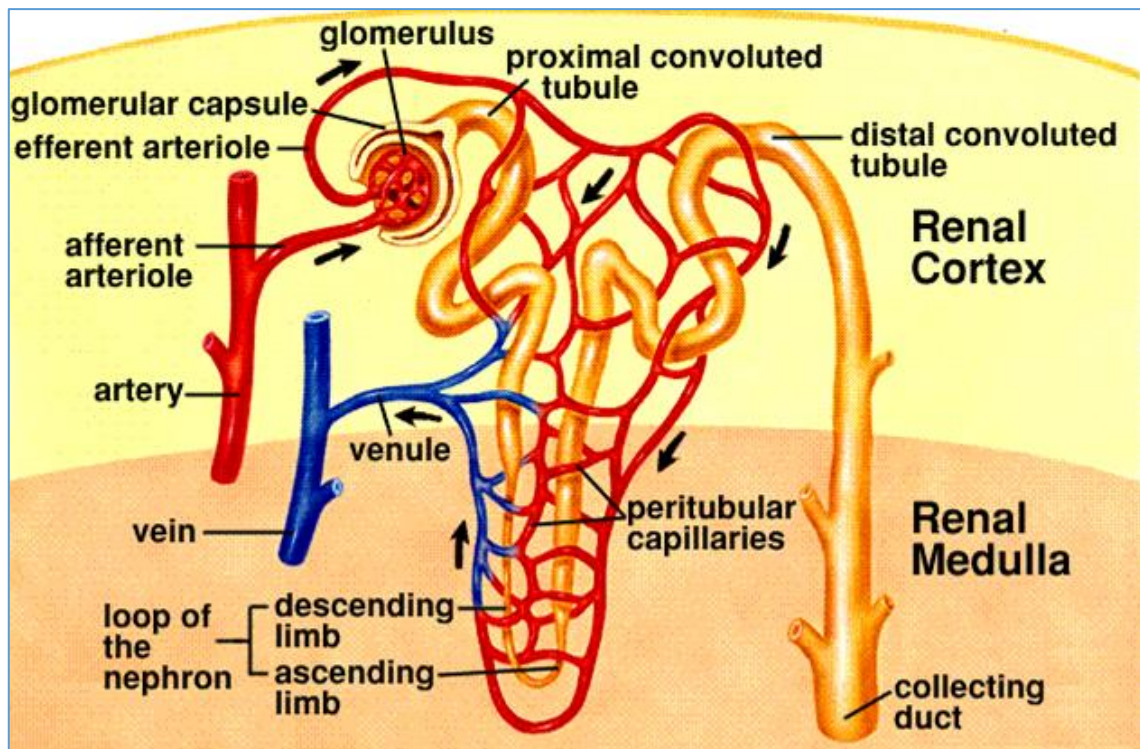


Figure 1.2: Schematic diagram of the nephron system.

Adapted from <http://www.mhhe.com/biosci/ap/dynamichuman2/content/gifs/0176.gif>

1.3.1 Glomerular filtration barrier

The kidney glomerular filtration barrier (GFB) is composed of, from the capillary lumen to the urinary space: endothelial cells and associated glycocalyx, the glomerular basement membrane (GBM), and the podocytes with their “slit diaphragms” (Figure 1.4) (Menon et al., 2012). The GFB has reported to have a surface area of around 0.203 mm² in human kidney (Guasch and Myers, 1994) and 0.184 mm² in the rat kidney (Shea and Morrison, 1975).

Glomerular endothelial cells are attached to the GBM that is covered by podocytes on its opposite surface. The presence of different cells and components in GFB together maintain the integrity and patency of the barrier, to permitting, under normal conditions, passage only of small and midsize molecules such as water, and restricting the passage of macromolecules such as proteins. In addition to size-selective permeability, GFB has a charge-selective property that also limits the free passage of macromolecules into the urinary space (Chang et al., 1975, Ohlson et al., 2001). According to previous

research, distortion of the components of any layer of the GFB has been linked to proteinuria (Kalluri, 2006, Jarad and Miner, 2009).

Loss of GFB integrity often results in increased filtration of macromolecules such as albumin and the appearance of glomerular proteinuria (Menon et al., 2012). The herein described model of protein overload proteinuria (POP) is associated with the increased glomerular permeability to proteins such as albumin. Once filtered however the presence of receptors for ultrafiltered macromolecules on the proximal tubular epithelial cells (PTEC) may further modify the composition of the glomerular filtrate and determine the quality and quantity of the final proteinuria.

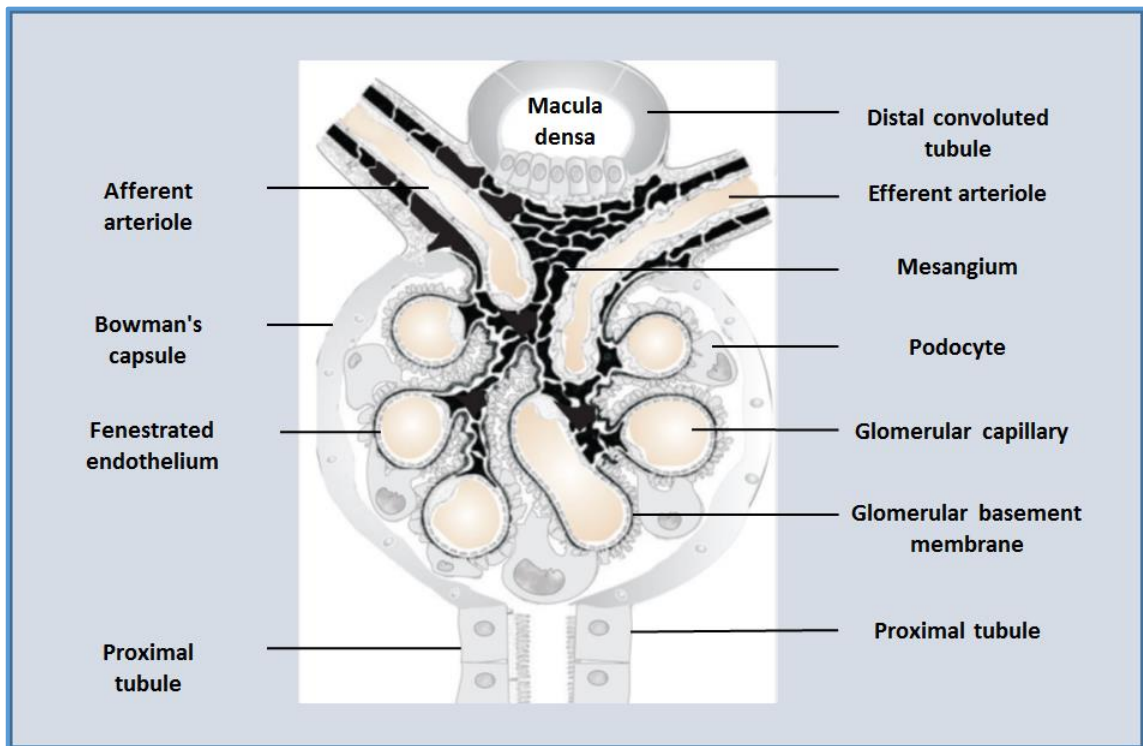


Figure 1.3: Schematic diagram of the renal glomerulus. Taken from Toblli et al. (2012).

1.3.1.1 Endothelial cells

The endothelium of glomerular capillaries is characteristic and differs from other capillary endothelia by having large fenestrations constituting 20–50% of the entire endothelial surface (Figure 1.5) (Bulger et al., 1983, Haraldsson et al., 2008).

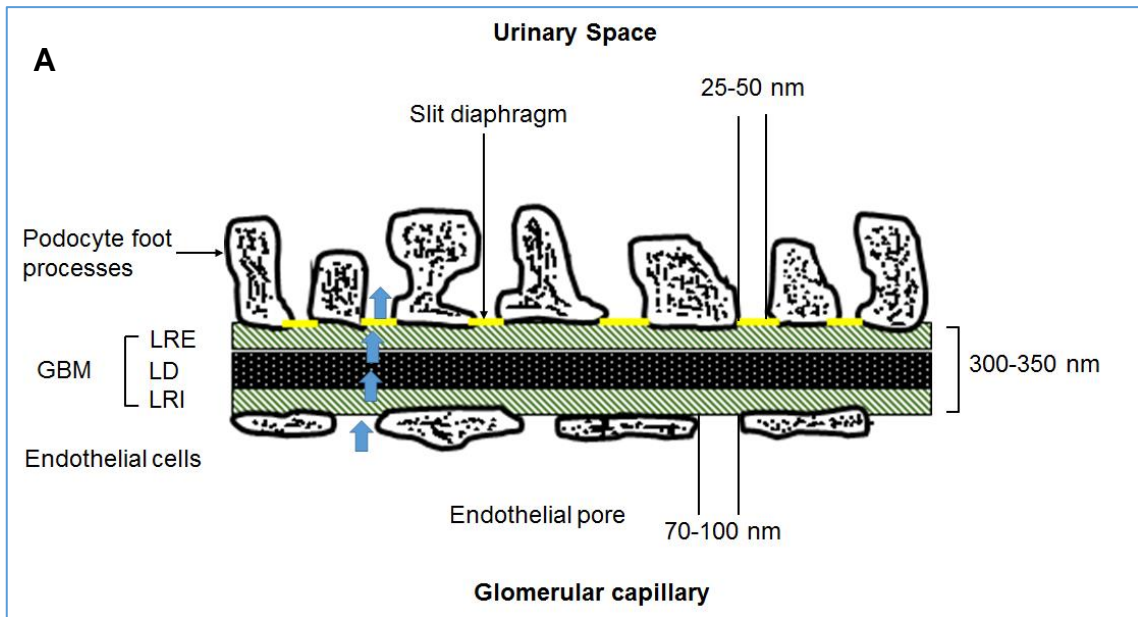


Figure 1.4: Structure of the glomerular filtration barrier (GFB). GFB forms the sieve between the blood and urinary space through which initial filtrate (urine) is formed (arrows). (A) Schematic diagram showing the components of GFB; the fenestrated endothelial cells, the three layers of the GBM, and the podocytes. The slit diaphragm is the highly specialised structure between the podocytes that forms the final barrier in the system to loss protein. LRE = Lamina rara externa, LD = Lamina densa, LRI = Lamina rara interna. (B) Transmission electron micrograph of the rat glomerular capillary loop showing the three layers of GFB. Taken from Pavenstädt et al. (2003). US = Urinary Space, P = Podocytes, GBM = Glomerular basement membrane, EC = Endothelial cells, GC=Glomerular capillary.

The fenestrated area contains pores, or fenestrae, that in human kidney range from 70 to 100 nm in diameter (Pollak et al., 2014). These pores are freely permeable to water, small solutes and small proteins but do not allow large proteins, red blood cells, white blood cells and platelets to pass (Taal et al., 2011).

Originally the endothelium was not regarded as a major component of the GFB (Menon et al., 2012) because of the large diameter of its pores which exceed that of albumin which has a diameter 3.6 nm (Haraldsson et al., 2008). However recent studies have revealed that the entire endothelium of glomerular capillaries is coated with a gel-like layer called endothelial cell surface layer (ESL) (Jeansson and Haraldsson, 2003, Jeansson and Haraldsson, 2006). The ESL is composed of glycocalyx and glycoproteins which are both synthesised and expressed by the endothelium itself. This is highly negatively charged and minimises the filtration into Bowman's space of positively charged molecules such as albumin (Sörensson et al., 2003, Koeppen and Stanton, 2012). The ESL projects around 200 nm into the capillary lumen thus further preventing albumin and other small proteins from moving towards the capillary pores and reaching the urinary space (Jeansson and Haraldsson, 2003). Recent studies have shown that disruption of ESL by hyaluronidase and adriamycin treatment leads to proteinuria in experimental animals, indicating the importance of this layer in the GFB (Hjalmarsson et al., 2004, Jeansson et al., 2009).

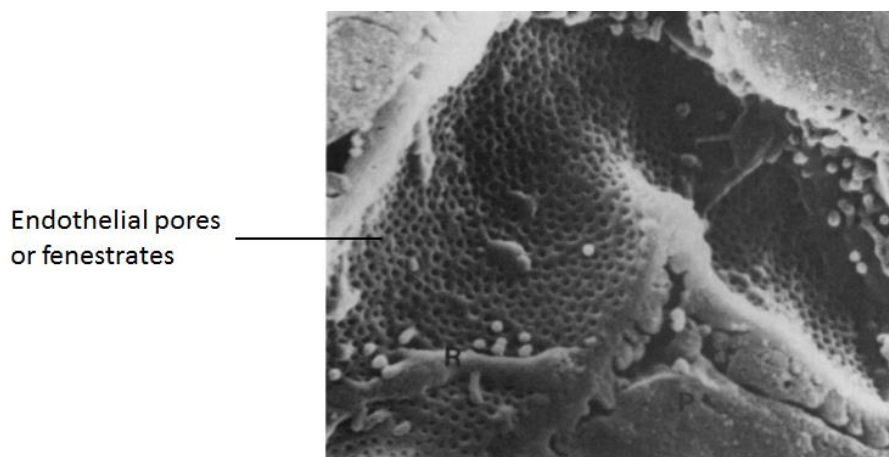


Figure 1.5: Fenestration area of the glomerular endothelium. Taken from Bulger et al. (1883).

1.3.1.2 Glomerular basement membrane

The visceral epithelial, or podocyte, layer of Bowman's capsule (urinary space) and the endothelial layer of glomerular capillaries (vasculature) are separated by a thick network (300-350 nm) layer called glomerular basement membrane (GBM), the extracellular matrix component of the GFB (Comper et al., 1993, Miner, 2012). The GBM is composed of three layers, the middle thick lamina densa consists of type IV collagen, entactin (nidogen) and laminin, and the two thinner lamina rara interna from the endothelial side and the lamina rara externa from the podocyte layer (Taal et al., 2011, Pollak et al., 2014). The last two thin layers contain heparan sulfate proteoglycans (perlecan, collagen XVIII, and agrin) and measure approximately 20-40 nm in thickness (Jørgensen, 1966). The presence of these negatively charged proteins in the structure of GBM is an important filtration barrier to plasma proteins. In the absence of heparan sulfate side chains removed by enzymatic digestion in vitro, for example, the permeability of GMB to ferritin (Kanwar et al., 1980) and bovine serum albumin (Rosenzweig and Kanwar, 1982) has shown to be increased, suggesting the role of these glycosaminoglycans in determining the charge-selectivity of GBM to plasma proteins. This property of GBM is also detected in studies that show the distribution and pattern of ferritin and dextran are restricted to the subendothelial side of GBM in normal rats and dramatically changed after treatment with puromycin to induce proteinuria (Farquhar and Palade 1960, Caulfield and Farquhar, 1975). Further, it has been demonstrated that perlecan deficient mice are more susceptible to develop proteinuria when overloaded with protein (Morita et al., 2005).

Laminin especially laminin β 2 is another basic component of the GBM that plays an important function in the GFB. This is clear from Lamb2^{-/-} mice as these animals showed mild proteinuria at birth without any changes in the endothelium and podocyte initially (Jarad et al., 2006), but thereafter urinary albumin excretion increases significantly, the podocyte foot processes become effaced, and the mice died about 1 month after birth (Miner et al., 2006). In conditions such as membranous nephropathy (MN) and diabetic nephropathy (DN), the thickness of GBM is altered (Wasserstein, 1997, Adler, 2004).

1.3.1.3 Podocytes

The visceral epithelial layer of Bowman's capsule consists of terminally differentiated glomerular podocytes. Podocytes are attached to the collagen, fibronectin and laminin components of the GBM via $\alpha_3\beta_1$ integrins and support the glomerular capillary loop of the Bowman's space (Adler, 1992).

The glomerular podocytes pose long finger-like processes, called foot processes (FP) or pedicles that extend toward the capillary loop and interdigitate with each other to enwrap the glomerular capillaries (Mundel and Kriz, 1995, Pavenstädt et al., 2003). The FP of podocytes are separated by apparent filtration slits of approximately 25-60 nm wide and bridged with a thin diaphragm called the filtration slit diaphragm (SD) (Taal et al., 2011, Koeppen and Stanton, 2012) (Figure 1.6). This filtration slit and the luminal membrane of the podocyte are covered with a thick, negatively charged coat containing podocalyxin and other proteins essential for the GFB (Huang and Langlois, 1985, Sawada et al., 1986).

Many other proteins in FP and SD, such as nephrin, NEPH-1 and P-cadherin, function as a barrier restricting the passage of macromolecules such as albumin into the urinary space (Koeppen and Stanton, 2012). In addition to these proteins, ZO-1, CD2AP, podocin are important proteins that maintain the integrity and correct function of the SD (D'Amico and Bazzi, 2003). For example, congenital nephrotic syndrome (NS) of the Finnish type is caused by mutation in NPHS1, the gene encoding nephrin, suggesting that this protein is crucial for normal function or structure of the GFB (Kestilä et al., 1998). Furthermore, inactivation of nephrin in mice results in dramatic changes in podocyte structure including effaced FP and loss of SD as well as enlargement of Bowman's space and tubular dilation (Putaala et al., 2001). Moreover, mutation in NPHS2 gene which is responsible for encoding the protein podocin, are the principal cause of autosomal recessive (Machuca et al., 2009) and both familial and sporadic NS (McKenzie et al., 2007), and podocin absence in mice leads to focal segmental glomerulosclerosis and albuminuria due to foot processes effacement (FPE) (Mollet et al., 2009).

A further component of the GFB is the SD. The relationship of the FPE, a condition where the architecture of the podocyte foot projections are distorted or retracted (Menon et al., 2012), with proteinuria is under the debate. In patients with IgA nephropathy, it has been demonstrated that increased proteinuria is found with the increased ratio of effacement of the podocyte FP (Tewari et al., 2015) suggesting that normal structure of these projections play an important role in retaining plasma proteins. Similarly, in DN the FP of glomerular podocytes are greatly effaced and correlated with albuminuria (Adler 2004). Conversely, van den Berg et al. (2004) have reported that podocyte FPE is not correlated with proteinuria. In this study, treated patients with prednisolone that are with minimal change nephrotic syndrome (MCNS) significantly ameliorated podocyte FPE compared to non-treated patients, but there was no significant difference in proteinuria in both conditions as well as IgA nephropathy that exhibited more effacement than treated MCNS patients.

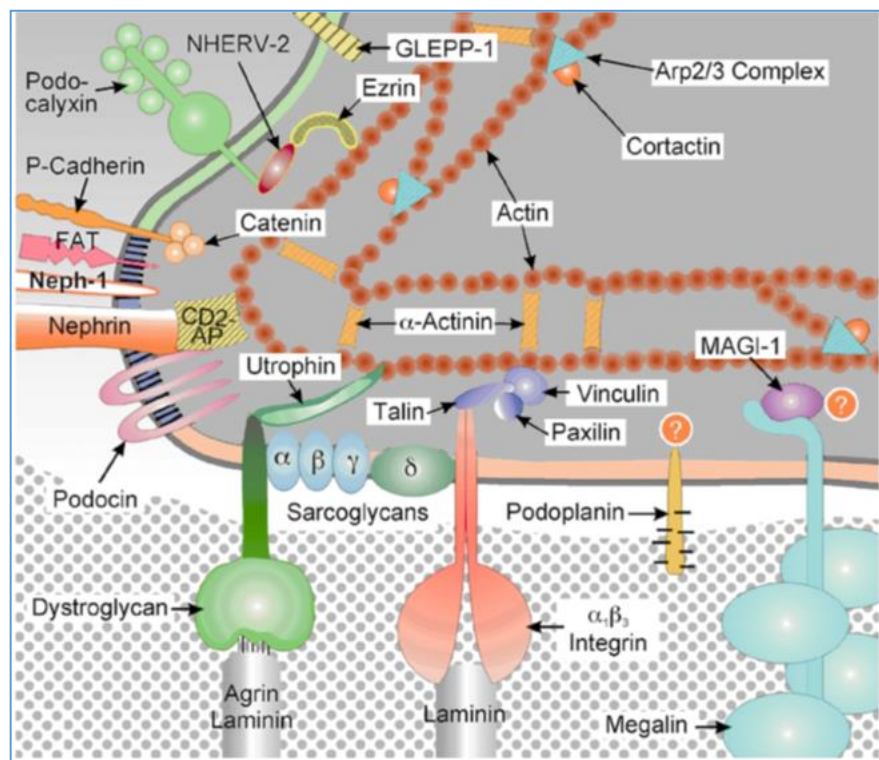


Figure 1.6: The structure of the slit diaphragm and podocyte foot process showing important proteins. Taken from Kerjaschki (2001).

1.3.2 The proximal tubule

The initial glomerular filtrate enters the urinary space and then enters the proximal tubule (PT), a 14mm length, narrow tubule lined with a single layer of cuboidal epithelial cells (Taal et al., 2011). The PT is composed of two distinct segments, the convoluted and the straight tubules (Maunsbach, 1966). The convoluted PT located in the cortical labyrinth, begins at the urinary pole of the glomerulus where the parietal layer of Bowman's capsule ends, and extends to the straight portion of the PT in the medullary rays of the cortex and outer medulla (Verlander, 1998). The PT is, morphologically, further subdivided into three distinguishable segments which are the S1, S2 and S3 (Figure 1.7A&B) (Maunsbach, 1966).

The epithelial cells in S1, the initial part of the convoluted portion, have numerous microvilli located to the luminal surface that increase the surface area of the PT and form the brush border membrane in the PT. The cells are tightly connected and attached to each other at the basolateral membrane through invaginations extending from the apical to the basal surface. These invaginations contain many elongated mitochondria that are different from thus found in the other segments, and prominent apical endocytic vesicles and lysosomal compartments can also be seen in the S1 of the PT (Welling and Welling, 1975, Taal et al., 2011).

The S2 occupies the last part of the convoluted portion and comes directly before the straight portion of the PT. Ultrastructurally, there is no difference between S2 and S1, however the cells in this segment are less tall and have shorter apical microvilli and brush border compared to those in S1. The basolateral plasma membrane invaginations are less prominent, and the cells have fewer small mitochondria and reduced number of lysosomal compartments and apical endocytic vesicles compared to the cells in S1. In addition, near to the cell basal membrane numerous cytoplasmic projections called micropedici can be observed which result from the shallow of membrane invaginations (Verlander, 1998, Taal et al., 2011).

S3 constitutes the last part of the straight portion of the PT. The cells in S3 are easily recognised and differentiated from the cells in S1 and S2 by lacking or less complicated basolateral membrane infoldings. They have fewer small mitochondria, apical endocytic vesicles and lysosomal elements (Verlander, 1998). Compared to the other segments, the length of brush border in this segment appears to be varied in various species. For example, the rat S3 has tall brush border, in the rabbit is fairly short and human kidney S3 contains intermediate brush border (Taal et al., 2011).

A particularly notable feature is the higher number and large size of mitochondria in the first segment of the PT compared to the other segments. Thus, it appears that the S1 is the place that reabsorption and transport are more active than the later segments of the PT (Ross et al., 1995).

In the nephron, the most vulnerable portion is the PT because it performs the majority of kidney function and occupies the greatest area of the cortical tissue (Bakoush et al., 2001). It therefore requires more oxygen to yield adequate metabolic energy for use solute transport.

In the PT, proteins and peptides bind to the PT brush border and are reabsorbed from glomerular filtrate by receptor-mediated endocytosis (RME) (Christensen et al., 1998). Reabsorbed proteins are then cleaved at the amino side of hydrophobic amino acids by enzymes present in the brush border including membrane metallo-endopeptidase (NEP; neutral endopeptidase, kidney-brush-border neutral proteinase, enkephalinase, EC 3.4.24.11) (Connelly et al., 1985, Inoue et al., 2003).

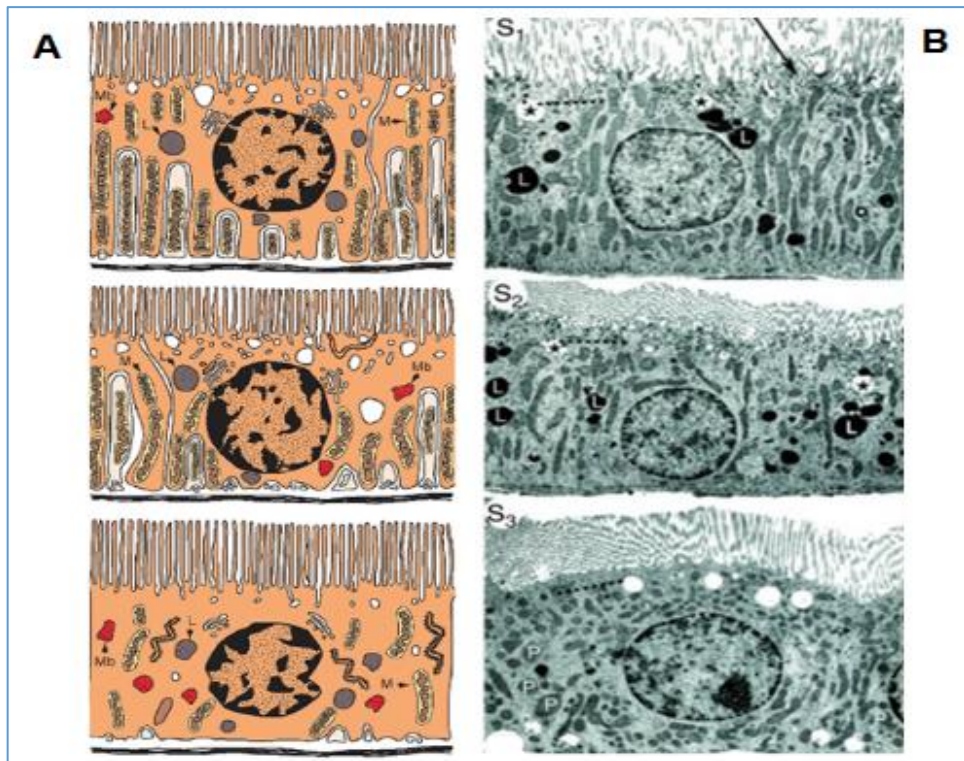


Figure 1.7: (A) Schematic diagram of the three segments of the proximal tubule. (B)Transmission electron microscopy showing the ultrastructure of the three segments of the proximal tubule cells in the rat kidney.Taken from (Mills, S.E., 2007. *Histology for pathologists*, 3rd Edition. Philadelphia), Zhuo and Li (2013).

1.4 Mechanisms of proteinuria

Proteinuria can be caused either by excess glomerular filtration of plasma proteins due to altered permselectivity of the GFB (glomerular proteinuria), or by reduced re-absorption of normally filtered low molecular weight (LMW) proteins by PT cells (tubular proteinuria).

1.4.1 Glomerular proteinuria

Glomerular proteinuria can be associated with alterations in one or all the three different levels of GFB, the endothelial cells, the GBM or the podocyte. Proteinuria due to change in the endothelium structure is clearly seen in the most common disease in women during pregnancy called pre-eclampsia, which is characterised by glomerular endotheliosis and loss of endothelial fenestrated (Lafayette et al., 1998). Numerous studies have confirmed that pre-eclamptic patients have different levels of proteinuria which in some reach nephrotic-range proteinuria (3.7 g/dl) and continues to increase (peak urine

protein/creatinine ratio 9), indicating the significance of endothelium in proteinuria in these patients (Stillman and Karumanchi, 2007). This relationship between proteinuria and endothelial damage has also been noticed in pregnant rats with pre-eclampsia (Maynard et al., 2003).

In terms of GBM, there are conditions that show the importance of the components of this structure in proteinuria. For example, mutation in one of the genes that encodes collagen IV may alter the structure of the GBM and this is clearly observed in Alport's syndrome that shows extensive GBM lamellations, fragmentations, and progressive glomerulosclerosis (Hudson et al., 2003, Sugimoto et al., 2006). Patients with this genetic disorder also have proteinuria and haematuria mainly due to these abnormalities in the GBM (Sugimoto et al., 2006). In mice, deficiency in the genes encoding collagen chains results in GBM thinning and proteinuria with podocyte FPE (Kalluri and Cosgrove, 2000, Miner and Sanes, 1996). Nail-patella syndrome is another genetic disorder caused by impaired function of the transcription factor LMX1B which leads to deterioration in the collagen IV structure and subsequent NS (Morello et al., 2001). Proteinuria is one of the characteristic feature of the ILK knockout (KO) mice because these animals have incorrect assembly in the GBM matrix components (El-Aouni et al., 2006).

Proteinuria exists in all the conditions related to the glomerular podocyte damage. Disruption of SD and FPE are most common in podocyte injury and perhaps the main causes of protein particularly albumin leakage in glomerular damage. Nephrin, among others, is considered as the most important protein in the composition of the glomerular podocyte that plays important role in the correct makeup of the SD. In diseases associated with nephrin abnormalities such as in Finnish-type congenital NS where the gene responsible for nephrin is mutated, the slit pores are disrupted and as a result proteinuria is massively developed (Ruotsalainen et al., 1999, Tryggvason, 1999). In MCNS, reduction of nephrin protein leads to enlargement of SD followed by massive non-selective proteinuria (Tojo and Kinugasa, 2012). Podocyte actin cytoskeleton is also crucial for the correct assembly of SD. Different models of podocyte injury with proteinuria have shown the abnormality of actin and reduction of SD molecules (Lee et al., 2004, Otaki et al., 2008, Greka and Mundel, 2012). Mice

with Cdc42 deficiency in their podocyte, one of the GTPases in Rho family that regulate actin cytoskeleton, develop heavy proteinuria associated with SD abnormality (Scott et al., 2012). All these studies indicate that abnormalities in the components of the GFB lead to abnormal passage of plasma proteins and in the absence of tubular function significant amount of these proteins may leave and found in the urine. In later section the importance of tubular dysfunction in determining final proteinuria will be described.

1.4.2 Tubular proteinuria

Tubular proteinuria is defined by the urinary excretion of significant amount of LMW proteins due to impaired tubular reabsorption of these proteins in the PT. LMW proteins such as α_1 - and β_2 -microglobulin, retinol-binding protein (RBP), urine protein 1 and β_2 -glycoprotein I (Norden et al., 2000) are normally filtered by the glomeruli because of their smaller size, charge and glomerular permeability to LMW proteins. On the other hand, intermediate and high molecular weight (HMW) proteins are largely retained by the glomeruli and only small amounts are found in the glomerular filtrate.

It has been demonstrated that using metabolic inhibitors to inhibit proximal reabsorption of filtered proteins (Maack et al., 1979, Sumpio and Maack, 1982), the glomerular sieving coefficient for lysozyme, a 14 600 molecular weight endogenous protein found in circulating plasma, is about 0.75 in both rat (Maack, 1975) and dog (Maack and Sigulem, 1974) comparing to the 0.01 for albumin estimated in the initial portion of the PTs by direct puncture method (Oken and Flamenbaum, 1971, Lewy and Pesce, 1973). These findings indicate that proteins of low molecular size can easily pass through GFB compared to the intermediate protein size such as albumin.

There is an agreement that normal glomeruli filter albumin but in a nephrotic range (Russo et al., 2007, Comper, 2008) and this amount is largely reabsorbed by the PTs (Marshansky et al., 1997, Tojo and Kinugasa, 2012). Numerous studies have demonstrated that tubular dysfunction may cause urinary excretion of significant amount of albumin. Russo et al. (2007) found that impairment of tubular function leads to albuminuria in nephrotic rats. Similarly, in patients with

acute tubular necrosis albuminuria is resulted from defective reabsorption of this protein by the endocytic receptors (West et al., 2006).

Furthermore, in proteinuric animals despite increasing glomerular permeability of circulating protein, it appears that the damage to tubulointerstitium determines the final proteinuria (Eddy, 1989, Eddy et al., 2000, Landgraf et al., 2014). Similarly, rats with (cy/+), a model for autosomal-dominant polycystic kidney disease develop proteinuria and that was due to the loss of endocytic machinery and tubular dysfunction (Obermüller et al., 2001). According to Gibb et al. (1989), urinary excretion of albumin, RBP, and N-acetyl-beta-D-glucosaminidase are all increased significantly in patients with early DN and that was present with tubular abnormalities indicating the loss of endocytic reabsorption of these proteins.

In addition, the fundamental role of tubular dysfunction in developing proteinuria can also be shown in genetic disorders. For instance, the reduced tubular function in Fanconi syndrome is clearly demonstrated by several studies, and the most important is that this genetic disorder is always accompanied by proteinuria indicating the positive link between proteinuria and tubular dysfunction (Leheste et al., 1999, Norden et al., 2001, Lang, 2009). Decreased resorption of proteins from glomerular filtrate can also be acquired and caused by tubulointerstitial damage. In this case tubular or interstitial injury prevents the PTs to reabsorb LMW proteins leading to tubular proteinuria (Viswanathan and Rani, 2016).

1.5 Renal handling of protein

Several techniques and studies have demonstrated that, in normal humans, urine contains a small amount of proteins. This is most likely because filtered proteins are reabsorbed effectively by PTEC. Deterioration in glomerulo-tubular balance may lead to loss large volume of essential proteins and excrete into the urine. For example, proteinuria results from glomerular damage and severe tubulointerstitial injury which may lead to adverse clinical outcomes.

1.5.1 Glomerular filtration of albumin

Under normal conditions, in addition to small molecular weight proteins, macromolecules such as albumin (66 kDa) and transferrin (81 kDa) are filtered, but in small amounts by glomeruli (Christensen et al., 2012). Various techniques have been identified to measure the amount of albumin which is normally found in the glomerular filtrate. According to these techniques, including micropuncture of rats and dogs, the concentration of albumin in the ultrafiltrate is between 1 and 50µg/ml which equates to 170 mg and 9 g/24h in normal humans (Birn and Christensen, 2006). The fractional filtration of albumin estimated by micropuncture in rats, is the concentration ratio between proximal tubular filtrate and blood and ranges between 0.0005 and 0.0007 (Tojo and Endou, 1992, Lund et al., 2003). The fractional filtration of albumin in humans is about 0.0001 (Norden et al., 2001).

Mogensen and Solling (1977) calculated the minimum albumin concentration in glomerular filtrate to be 281 µg /min, corresponding to about 400 mg/24h whilst blocking tubular albumin uptake with lysine in humans. Similarly, inhibition of tubular albumin reabsorption by lysine in rats led to the excretion of approximately 2.5–25 mg/24h, which equates to 0.7–7 g/24h in humans (Tencer et al., 1998, Thelle et al., 2006).

Micropuncture and inhibition of tubular albumin uptake are considered to be conventional techniques and largely depend on immunoassay for detecting albumin in the urine. A significant amount of albumin fragments are detected in the urine rats and humans using radiolabelled albumin and high-performance liquid chromatography. These fragments are thought to result from degradation of filtered albumin by proximal tubular cells. Standard urinalysis by radioimmunoassay does not detect these fragments in the urine (Comper et al., 2004, Osicka et al., 1997, Gudehithlu et al., 2004). Thus, according to the findings of these studies; a significant amount of albumin is filtered and subsequently reabsorbed by PTECs.

1.5.2 Tubular reabsorption of proteins

Although the GFB is highly permselective, some proteins do enter the glomerular filtrate. However the urine is almost free from protein, as a consequence of these proteins being effectively reabsorbed by PTEC (Christensen et al., 2012). Under normal conditions, only small amount of albumin, the most abundant protein in the circulation, can pass through GFB due to size and charge selectivity of the barrier towards proteins of intermediate and HMW. Whereas, the passage of LMW proteins (40,000 D and radius lower than 30 Å) is not restricted by the glomerular barrier and reach the proximal lumen freely. The majority of these proteins that enter the proximal lumen are reabsorbed by RME in the PT and back to circulation and only traces are found in the urine (D'Amico and Bazzi, 2003).

This protein reabsorption including albumin and other macromolecules by the PTEC occurs via endocytosis. During endocytosis, small plasma membrane invaginations are formed at the microvillar base and these invaginations contain some tubular fluid in which molecules are dissolved. The endocytic invaginations break away from the membrane and form early endocytic vesicles which subsequently transport their contents to the sorting endosomal compartment. From early endosomes, the cargo is transported to the lysosomal compartment where receptor-ligand dissociation occurs due to falling pH. Reabsorbed proteins may either be transcytosed to the opposite pole of the cell, or subject to proteolysis with reabsorption of constituent amino acids. Receptors are trafficked back to the apical membrane via recycling endosomes (Gekle, 2005) (Figure 1.8).

There are two main types of endocytosis, fluid-phase endocytosis and RME (Conner and Schmid, 2003). In the PT, fluid-phase endocytosis seems to be less important (Park and Maack, 1984). For example, inulin infused into animals is freely filtered by the glomerulus and is reabsorbed by fluid-phase endocytosis in the PT. High levels of urinary inulin excretion indicates that fluid-phase endocytosis is an inefficient process (Gekle, 2005).

RME, on the other hand, is an important and efficient mechanism of protein uptake in the PT and is essentially involved in the reabsorption of tubular albumin (Gekle, 2005). Identification of two different binding sites for albumin in

OK cells is an important evidence supporting the idea that this protein is mostly reabsorbed by RME (Brunskill et al., 1997). The endocytic process of albumin is very well documented by electron microscopy. The presence of numerous gold particles which are bound to plasma membrane and mostly restricted to the plasma membrane invaginations indicates the uptake of gold-albumin in OK cells (Brunskill et al., 1996).

It has been identified that RME is subdivided into three types according to the vesicle formation which are clathrin-coated endocytosis, caveolae-mediated endocytosis, and clathrin- and caveolae-independent endocytosis (Conner and Schmid, 2003, Mukherjee et al., 1997, Schmid, 1997).

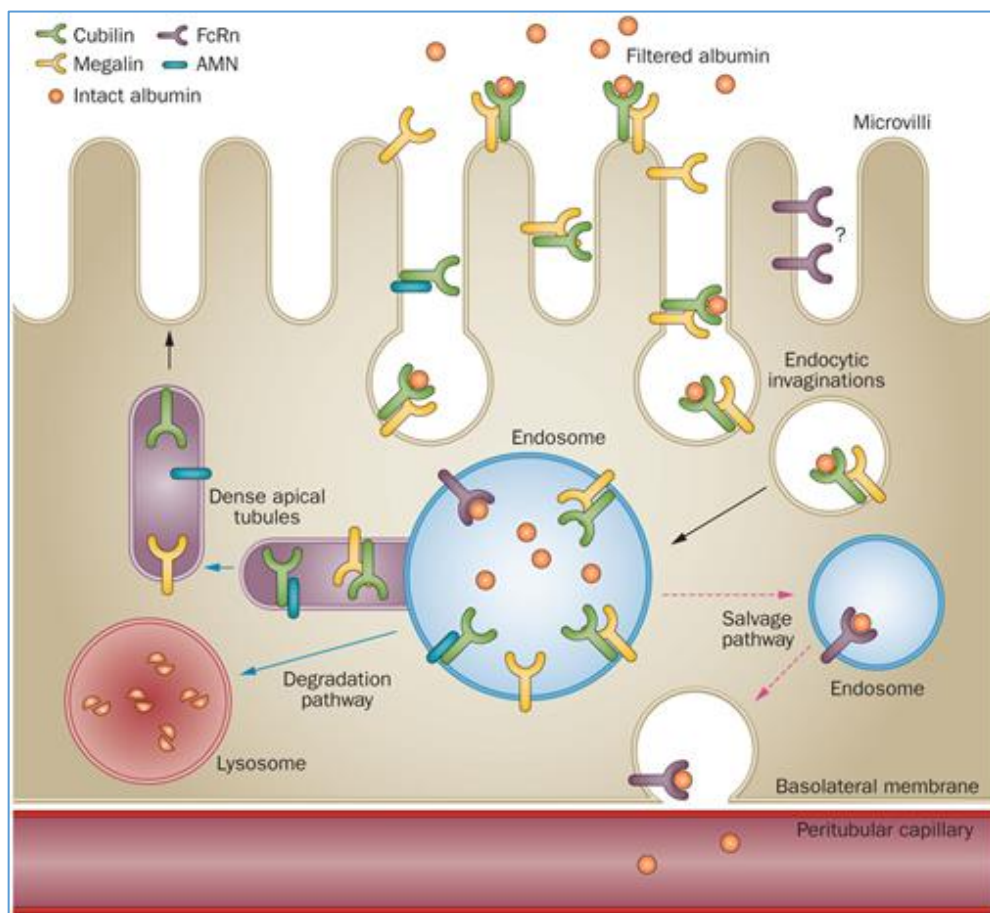


Figure 1.8: Schematic diagram showing both endocytosis mediated by megalin, cubilin and amnionless, and transcytosis mediated by FcRn. Taken from Christensen and Birn (2013).

1.6 Tubular receptors for endocytosis of proteins

The brush border of the PT possesses receptors that function to reclaim glomerular filtered proteins by both RME and transcytosis. This section will briefly describe the expression, structure and importance of these receptors in the kidney.

1.6.1 Megalin

1.6.1.1 The structure of megalin

Megalyn is a giant glycoprotein member that belongs to the low-density lipoprotein receptor (LDLR) protein family (Motoyoshi et al., 2008). It is highly expressed at the apical surface of many absorptive epithelia, including PTEC in the kidney, the small intestine, the parathyroid gland and the visceral yolk sac. Megalin is composed of a very large extracellular domain consisting of four clusters of cysteine-rich ligand-binding repeats, perhaps constituting the ligand binding region. These clusters are separated by 17 epidermal growth factor (EGF) type repeats and 8 spacer regions containing YWTD repeats, which are responsible for the dissociation of ligands in an acidic endosomal compartment and receptor recycling to the surface membrane. In addition, megalin contains a single transmembrane domain (23 amino acids), which links the extracellular part to a short cytoplasmic domain of 209 amino acids (Marzolo and Farfan, 2011) (Figure 1.10).

The cytoplasmic tail (CT) of megalin contains several regions, including more than one Src-homology-3 (SH3) and one Src-homology-2 (SH2) recognition sites as well as two NPXY motifs and one NPXY-like motif (Christensen and Birn, 2002). NPXY motifs can mediate the binding of CT to adaptor proteins which in turn, regulate receptor trafficking and signaling functions. In addition to the NPXY motif, the CT of megalin contains NQNY motif, with unknown function (Marzolo and Farfan, 2011).

1.6.1.2 Megalin cytoplasmic tail and its phosphorylation role

Several binding sites for adaptor proteins have been identified within the CT of megalin that not only regulate receptor trafficking but also may function as signalling molecules (Marzolo and Farfán, 2011).

NPXY motifs are engaged by adaptor proteins, the first and third NPXY motifs are necessary for endocytosis whereas the second NPXY motif is very important for apical sorting and targeting (Takeda et al., 2003). Disabled 2 (Dab 2) (Oleinikov et al., 2000) and autosomal recessive hypercholesterolemia (ARH) (Shah et al. 2013) are adaptor proteins in the cytoplasm they interact with the NPXY motifs of the CT of megalin. In addition to protein interaction motifs, several potential phosphorylation sites within the CT of megalin have been identified for protein kinase C (PKC), protein kinase A (PKA), casein kinase-2 (CK-II) and glycogen synthase kinase-3 (GSK3) (Yuseff et al., 2007). Megalin is highly and constitutively phosphorylated at a PPPSP motif by GSK3 (Yuseff et al., 2007).

Phosphorylation of megalin tail depends on a PPPSP motif and GSK3 activity (Yuseff et al., 2007). This motif is well conserved in megalin sequences of different species (Marzolo and Farfán, 2011). A significant reduction in megalin phosphorylation has been observed in a PPPSP motif mutant receptor (Yuseff et al., 2007). The regulation of megalin recycling and trafficking is strongly related to the phosphorylation of PPPSP motif and GSK3 activity. Yuseff et al. (2007) emphasise that the PPPSP motif and GSK3 activity are very important for megalin phosphorylation to occur, and also found that both PPPSP motif phosphorylation and GSK3 activity negatively regulate receptor recycling. On the other hand, the internalization rate and endocytosis of megalin receptor is not affected by the PPPSP motif phosphorylation and GSK3 activity (Yuseff et al., 2007). Although some of the physiological events of megalin tail phosphorylation are defined, it still not fully understood.

1.6.1.3 Regulated intramembrane proteolysis

Regulated intramembrane proteolysis (RIP) plays an important role in the regulation of a large number of transmembrane proteins (Lal and Caplan, 2011, Medina and Dotti 2003). In the presence of various functional sheddases including MMPs and the intramembrane multiprotein gamma secretase as presenilin-1, the substrates of RIP are sequentially cleaved to release an extracellular domain and a small intracellular fragment called intracellular domain (ICD). RIP was first described in the receptor involved in cholesterol metabolism called sterol regulatory element binding protein by Brown and Goldstein in 1997. Brown and Goldstein (1997) found that this transmembrane protein undergoes a series of regulated proteolytic cleavages leading to the formation of ICD which translocates to the nucleus and involves in the transcriptional regulation of the specific genes of both fatty acids and cholesterol metabolism. Further, RIP is also best described and studied in Notch, a single 300 kD membrane receptor important for the development of brain, and amyloid precursor protein (APP) previously (Andersson et al., 2011, Lichtenthaler et al., 2011) . Lichtenthaler et al. (2011) have shown that RIP of APP produces an extracellular domain and ICD, and further processing of the extracellular domain owing to the production of a short peptide corresponding to the remainder of the extracellular domain after cleavage and parts of the intracellular domain. Evidence are available showing that the amyloid β peptides from APP cleavage are involved in the onset and progression of Alzheimer's disease (Murphy and LeVine III, 2010, Xu et al., 2016). It seems that Notch receptor is subjected to similar proteolytic cleavage as in APP and the products of this cleavage have now identified in cell fate in various tissues in both vertebrates and invertebrates similarly (Andersson et al., 2011, Biemesderfer, 2006).

RIP may be involved in the regulation of specific gene expression in the PTEC. Receptor function may be linked to gene transcription via the evolutionarily conserved process, RIP.

RIP of megalin occurs both constitutively and as a result of receptor-ligand interactions. The RIP process involves receptor ectodomain cleavage by PKC-dependent MMPs and subsequent cleavage of cytoplasmic tail fragment from

the remaining transmembrane region of the receptor by the γ -secretase family of proteases. In most instances the released C-terminus is considered to regulate the expression of specific genes after translocation to the nucleus and interaction with other regulatory molecules (Zou et al., 2004, Li et al., 2008, Yuseff et al., 2007, Biemesderfer, 2006).

Recent studies have shown that megalin is indeed subject to RIP as described above. Biemesderfer (2006) showed that the megalin ectodomain is cleaved by PKC-regulated, metalloprotease-mediated, ectodomain shedding to release a cytosolic receptor fragment termed membrane-associated C-terminal fragment (MCTF). MCTF then becomes a substrate for γ -secretase. Gamma-secretase then cleaves MCTF and forms a new fragment termed the megalin intracellular domain (MICD) (Figure 1.9) (Li et al., 2008).

To determine whether RIP of megalin may be involved in the regulation of PT gene expression, Li et al. (2008) designed a study of transfected MCTF (tMCTF) or transfected MICD (tMICD) overexpression in opossum kidney proximal tubule (OKP) cells. In this study the data showed that megalin protein expression significantly decreased, indicating the crucial role of MICD in the regulation of specific gene expression in the OKP cells (Li et al., 2008).

There is some evidence that RIP of megalin might occur in proteinuric patients. The presence of significant amounts of megalin extracellular domain in the urine of patients with DN and albuminuria is a good indicator of RIP of megalin and this is not seen in patients with non-albuminuric diabetes (Thraill et al., 2009b).

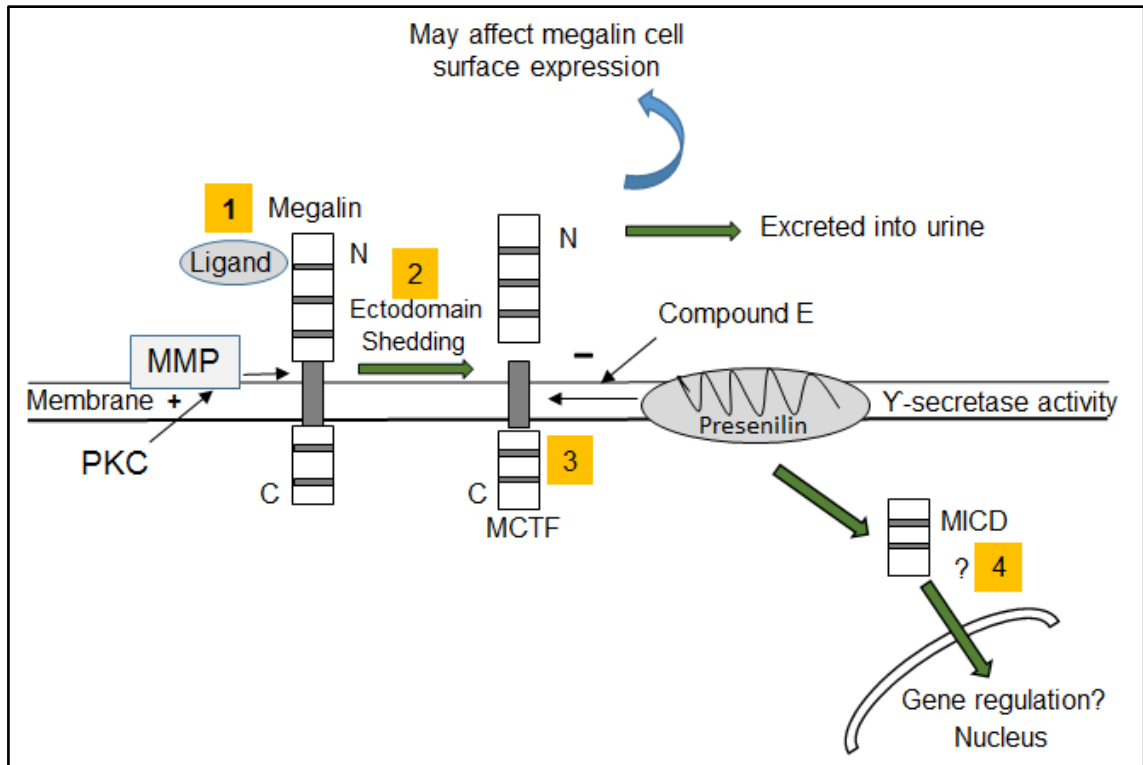


Figure 1.9: Mechanism of megalin ectodomain shedding (RIP). The first step (1) is the ligand binding to megalin and it is believed to be critical in the process. After ligand binding, the PKC-dependent MMP activation cleaves the ectodomain (N-terminus) of megalin and excreted into the urine (2). The remaining intracellular domain of megalin (MCTF) become a substrate to γ -secretase activity (3). Gamma secretase activity cleaves the MCTF and produces soluble megalin intracellular domain (MICD) (4) that translocates to the nucleus and activates transcription factors of specific gene having role in megalin gene expression regulation. Compound E can inhibit the activity of γ -secretase and prevent the cleavage of MCTF. MCTF = megalin C-terminus fragment, Compound E = an inhibitor of γ -secretase activity, MMP = matrix metalloproteinase. Modified from Biemesderfer (2006).

1.6.1.4 The biological role of megalin

The importance role of megalin during development and throughout adult life has been studied in megalin KO mice. Megalin deficient mice mostly die immediately after birth due to severe forebrain abnormalities and lung defects (Willnow et al., 1996) and megalin clearly has a critical role in the formation of brain structure (Willnow et al., 1996, Wicher et al., 2005).

In the kidney, megalin plays essential role in vitamin D metabolism and calcium homeostasis (Nykjaer et al., 2001). Megalin is involved in the reabsorption of vitamin D binding protein (VDBP), which mediates the endocytosis of this protein. Following endocytosis, reabsorbed VDBP is directed to the lysosomal compartment for degradation and subsequent intracellular conversion of 25-(OH) vitamin D3 to 1,25-(OH)₂ vitamin D3 and returning to circulation. This important function of megalin is clearly observed in megalin KO and/or deficient mice where significant amounts of VDBP are excreted in the urine, resulting in the reduction of plasma 1,25-(OH)₂ vitamin D3 levels (Kaseda et al., 2011). It is well-known that calcium homeostasis is regulated by 1,25-(OH)₂ vitamin D3. Therefore, decreased serum levels of 1,25-(OH)₂ vitamin D3 in the circulation as in megalin deficient mice may lead to bone diseases indicating the essential role of megalin in the calcium homeostasis (Nykjaer et al., 2001).

Megalin can also regulate apoptosis through interaction with protein kinase B (PKB) in the luminal membrane. In vitro studies of albumin overload have shown that a significant decrease in the megalin expression at the plasma membrane is associated with PKB activity and apoptosis (Caruso-Neves et al., 2006).

In addition, although the role of megalin in proteinuria has been confirmed by a number of elegant studies, mechanisms of megalin involved in proteinuria still remain unknown.

1.6.1.5 Megalin as a receptor for albumin

Disorders in megalin structure and function lead to proteinuria, suggesting a crucial role for megalin in PT reabsorption of albumin (Christensen and Birn, 2001). Megalin is an endocytic receptor and was initially identified as the primary antigen in Heymann nephritis, a rat model of human membranous glomerulonephritis (Kerjaschki and Farquhar, 1982). Its role as a receptor involved in the reabsorption of tubular albumin by endocytosis has been proposed by a number of functional studies in rat kidney (Cui et al., 1996). Studies of megalin deficient and megalin KO mice also supported this hypothesis. In megalin deficient mice, the presence of albumin in the urine is a good indicator supporting the critical role of megalin in the retrieval of filtered albumin. Furthermore, in megalin KO mice, a considerable increase in the urinary excretion of albumin is observed alongside absent tubular endocytosis of albumin (Birn et al., 2000). In addition, other studies have used the ability of receptor associated protein (RAP) to assess megalin-mediated uptake of albumin. RAP is an intracellular partner of megalin that inhibits the binding of extracellular ligands to megalin (Birn and Christensen, 2006). Thus it has been shown that RAP reduces albumin endocytosis due to its inhibition of albumin binding to megalin (Brunskill et al., 1997).

In PTEC megalin forms a complex with cubilin and they together act as a scavenger complex for albumin retrieval. In this complex megalin plays an important role in the internalisation of cubilin-albumin complexes (Gekle, 2005).

1.6.1.6 Regulation of megalin expression

Although the physiological role of megalin has been identified, the mechanisms of its cell surface expression are still not fully clarified. However, there are several potential mechanisms that might explain megalin availability at the cell surface, including the regulation of its protein synthesis, mRNA levels and trafficking of megalin to the cell membrane.

1.6.1.6.1 Regulation of megalin mRNA and protein expression

Megalín expression can be regulated by peroxisome proliferator-activated receptors (PPARs). PPARs are a group of nuclear proteins that function as transcription factors. Three PPAR isomers have been identified, PPAR- α , - β and - γ . PPARs heterodimerise with the 9-cis-retinoid X receptor (RXR) and together form an active heterodimer that binds to a specific DNA regions of target genes termed peroxisome proliferator response elements which are located in the promoters of PPAR responsive genes (Cabezas et al., 2011). In humans, three consensus regions for PPAR binding have been identified in the megalín promoter (Marzolo and Farfán, 2011).

In vitro and in vivo studies have confirmed that PPAR- α , and - γ can regulate megalín mRNA and protein synthesis expression. Cultured PTEC treated with PPAR- α and - γ agonists show a significant increase in megalín mRNA and protein levels. In mouse and rat kidney, megalín mRNA and protein levels can also be regulated by PPARs (Cabezas et al., 2011).

In addition, vitamin A and vitamin D which are megalín ligands can also regulate megalín mRNA expression. A considerable increase in megalín mRNA level has observed in various cells treated with vitamin A and vitamin D (Liu et al., 1998).

1.6.1.6.2 Regulation of megalín cell surface distribution and protein levels

Megalín distribution at the cell surface may be regulated by a number of factors. Potentially phosphorylation of megalín-CT by GSK3 may regulate expression, yet definite evidence is lacking. However recent study revealed that megalín phosphorylation negatively regulates megalín trafficking and recycling to the cell membrane (Yuseff et al., 2007). In this study, Yuseff et al. (2007) found that mutation in PPPSP motif and inhibition of GSK3 activity significantly decreases megalín phosphorylation and positively enhances receptor trafficking and recycling to the cell surface. Thus, it is likely that megalín cell surface expression depends at least in part on the phosphorylation of its CT.

A number of other candidates may be involved in the regulation of megalín protein levels. RAP, a megalín chaperone, appears to be crucial for normal megalín expression and function (Birn et al., 2000). RAP binds to megalín and inhibits the binding of other ligands to megalín. Recent studies have

demonstrated the crucial role of RAP in the regulation of megalin expression by its chaperone specificity that protects the newly synthesized receptor from binding other ligands inside the cell (Bu and Marzolo, 2000). In addition, a study of RAP KO mice has confirmed the importance role of RAP in megalin protein expression. These animals had less megalin expression (about 23% of normal megalin expression), and they also exhibited other phenotypes similar to that of megalin deficiency, including low molecular weight proteinuria (Birn et al., 2000).

1.6.2 Cubilin

Cubilin, a 460-kDa glycoprotein endocytic receptor, forms a complex with megalin. Together the megalin-cubilin complex functions to scavenge various glomerular ultrafiltered proteins, particularly albumin, in the PT (Christensen et al., 1998, Birn et al., 2000, Christensen and Birn, 2002). Unlike megalin, cubilin is not a member of the LDLR family and shares a very little homology to this family (Figure 1.10) (Birn, 2006, Christensen and Birn, 2002).

Cubilin lacks both transmembrane and cytoplasmic domains (Kristiansen et al., 1999), and therefore its internalisation is entirely dependent on cell surface availability of megalin (Amsellem et al., 2010). Cubilin is anchored to the plasma membrane by its N-terminal domain (Kristiansen et al., 1999). The N-terminal domain 110-amino acid consists of eight EGF-like repeats that contain an amphipathic α -helix resembling to that of the lipid-binding regions of apolipoproteins (Moestrup et al., 1998, Kristiansen et al., 1999). This α -helix structure, on one side, is proposed to contain conserved clustering of hydrophobic residues that embedded into the lipid bilayer of the plasma membrane (Kristiansen et al., 1999, Mishra and Palgunachari, 1996, Bernstein et al., 2000). In addition to hydrophobic residues, the N-terminal region has potential cysteine palmitoylation site which could also anchor cubilin in the membrane (Moestrup and Verroust 2001). The N-terminal domain of cubilin is followed by CUB domains (27 CUB domains), each contains 110-amino acid modules found in the components of the complement system, such as C1r/C1s, in the EGF related sea urchin protein (UEGF) and in the bone morphogenic peptide-1 (BMP-1) (Moestrup et al., 1998, Christensen and Birn, 2002).

Because of the presence of many potential CUB domains in the cubilin, the receptor has been shown to bind multiple ligands including intrinsic factor–cobalamin complex (IF–B12), RAP, albumin, immunoglobulin light chains, transferrin, haemoglobin, VDBP, clara cell secretory protein, apolipoprotein A-I/high density lipoprotein (HDL), Ca²⁺ and megalin (Christensen and Birn, 2002). Cubilin can also interact with amnionless (AMN), the other transmembrane protein receptor and generate cubilin-amnionless complex. This complex translocates from the ER to the cell membrane by the small transmembrane domain in the AMN (Fyfe et al., 2004). Cubilin mis-localisation has been observed in AMN-deficient cells, suggesting that AMN is responsible for cubilin direction in the PT (Nielsen et al., 2016). The strong correlation between cubilin and AMN expression has been detected in megalin-deficient mice as these animals show very little expression of cubilin (Coudroy et al., 2005).

Like megalin, cubilin is highly expressed on the apical membrane of several absorptive tissues, such as the renal PTEC (Sahali et al., 1992, Christensen et al., 1998, Barth and Argraves, 2001), the small intestine (Seetharam et al., 1981, Yammani et al., 2001), the visceral yolk sac (Sahali et al., 1993, Drake et al., 2004) and the male reproductive system (Van Praet et al., 2003). The importance of cubilin is clearly demonstrated in cubilin-deficient mice. In these mice, cubilin deficiency leads to LMW proteinuria, indicating the critical role of this receptor in tubular reabsorption of ultrafiltered proteins (Nielsen et al., 2016). It is very-well known that the correct expression of cubilin is important for normal functioning of PT and reabsorption of albumin, and it has been reported that cubilin function loss results in significant albuminuria associated with decreased albumin endocytosis in experimental animals (Fyfe et al., 1991a, Fyfe et al., 1991b, Xu et al., 1999).

Like cubilin-deficient mice and dogs, mutations in the cubilin gene in humans leads to Imlerslund-Grasbeck disease (IGS), a rare autosomal recessive disorder characterised by vitamin B₁₂ deficiency and LMW proteinuria (Broch et al., 1984, Aminoff et al., 1999). According to Nykjaer et al. (2001), both in dogs and human diseases characterised by inherited disorders and mutations in the CUB gene lead to abnormalities in the biosynthesis and dysfunction of cubilin, and eventually urinary excretion of 25(OH) vitamin D₃ and abnormal vitamin D

metabolism. Similarly, it is believed that vitamin D deficiency in patients with early-stage DN is highly associated with dysfunction of either megalin or cubilin receptor, indicating impaired endocytosis of vitamin D in the kidney of these patients (Kaseda et al., 2011).

Finally, cell surface expression of cubilin requires the correct expression of megalin. It has been demonstrated that cubilin expression is significantly reduced in megalin KO mice, suggesting the role of megalin in the regulation of cubilin in the PT (Birn et al., 2000).

1.6.3 The neonatal Fc receptor (FcRn)

FcRn is primarily responsible and function in transporting IgG from the blood of the mother to that of fetus across the placenta and the proximal small intestine during pregnancy, and from the milk of the mother to the neonate during the lactation period (Story et al., 1994, Jakoi et al., 1985, Roopenian and Akilesh 2007). Recent studies indicate that the FcRn can also bind albumin and maintain on the half-life of albumin in the serum (Sarav et al., 2009, Chen et al., 2010, Sand et al., 2015). Quantitatively, IgG and albumin are the two most abundant proteins in the bloodstream and constitute 80-90% of the total portion pool (Sand et al., 2015), and thus the importance of FcRn as a receptor for both protein is apparent.

Structurally, FcRn is a 42-44 kDa transmembrane heterodimeric protein consisting of a heavy chain containing three extracellular domains (α 1, α 2 and α 3) homologous to the α -chains of the classical and non-classical Class I major histocompatibility-complex (MHC) molecules. The extracellular domains are linked to the short cytoplasmic tail via a single transmembrane domain. The FcRn also contains β 2-microglobulin as a light chain, which non-covalently binds to the heavy α -chains (Figure 1.10) (Jones, 1972, Simister and Mostov, 1989, Haymann et al., 2000).

Albumin and IgG binding sites have been identified within both heavy and light chains. According to rat FcRn and IgG binding studies the binding sites for IgG lie in the heavy chain particularly α 2 domain including aspartic acid 137, an N-glycan moiety and N terminus of the light chain. (Vaughn et al., 1997). There is also binding site for IgG located within a pair of histidines in the α 3 domain of

the heavy chain (Raghavan et al., 1994). Studies have shown that mutation in histidine residues at positions 310 and 435 and replacement with alanine greatly reduces IgG binding to FcRn (Raghavan et al., 1995, Medesan et al., 1997, Kim et al., 1999). In addition, the $\alpha 3$ chain contains a binding site for albumin within the conserved histidine residue (H166) located on the opposite structural face of the FcRn from that which participates in binding IgG (Andersen et al., 2006, Chaudhury et al., 2006). It has been demonstrated that mutation and replacement of E54 with glutamine, a structure that surrounds the H166 resulted in low detectable binding of albumin (Andersen et al., 2012).

It seems that pH also plays an important role in the process of IgG and albumin binding to the FcRn receptor. Numerous studies have reported that both IgG and albumin have the ability to bind FcRn at acidic pH (6.0-6.5) and lose their affinity to bind or release at physiological pH (7.4) (Simister and Rees, 1985, Simister et al., 1996, Chaudhury et al., 2003, Chaudhury et al., 2006, Andersen et al., 2006). This is most likely to occur at the pH of gut but in the kidney due to neutral pH at the proximal membrane, the albumin-FcRn binding may occur inside the acidic endosomes (Dickson et al., 2014).

FcRn is expressed in multiple organs including intestine, mammary gland, placenta, lung, hematopoietic cells, kidney, liver, brain, eye and skin (Kuo et al., 2010). In the kidney, FcRn is expressed abundantly on both the podocyte of the glomerulus and the brush border of the PTEC (Sarav et al., 2009). Glomerular expression of FcRn is involved in the transcytosis of IgG from the basolateral side of the podocyte to the urinary space of the glomerulus, thereby preventing IgG from deposition and also to limit clogging of the filtration barrier (Roopenian and Akilesh, 2007, Akilesh et al., 2008). The transcytosed IgG then, at the PT, could interact with FcRn and move back into the circulation (Kobayashi et al., 2002).

In the PT, FcRn may also participate in albumin reabsorption by transcytosis (Figure 1.10). As indicated above, albumin binding to FcRn is pH dependent, however the pH of the luminal may not facilitate this interaction. It is well-known that endocytosed albumin dissociates from megalin/cubilin in acidified endocytic compartments. Dissociated albumin within the endosomal-sorting compartment may then bind to FcRn with high affinity due to low endosomal pH. Bound

albumin to FcRn is transcytosed to the basolateral surface and re-enters into the circulation. This function of FcRn may protect albumin from lysosomal degradation and help maintain normal serum levels of this protein (Tenten et al., 2013, Dickson et al., 2014). Indeed, it has been demonstrated that FcRn-deficient mice are both hypoalbuminemic and hypogammaglobulinemic (Kim et al., 2006, Roopenian et al., 2003)

Although it is not definitively demonstrated that FcRn is directly involved in the PT reabsorption of albumin, studies of FcRn-deficient mice have clearly shown the role of this receptor in albumin retrieval. Sarav et al. (2009) found that urinary albumin excretion is increased in the FcRn-deficient mice compared to normal mice. This observation was also confirmed in normal mice transplanted with FcRn-deficient kidney, indicating the contribution of FcRn in part in albumin reabsorption (Sarav et al., 2009). In addition, the same study examined the serum levels of albumin and found that FcRn-deficient mice had lower serum levels of albumin compared to normal and increased serum levels of albumin was observed in FcRn-deficient mice received an FcRn expressing kidney.

The effect of ultrafiltered proteins, especially albumin, on the expression of FcRn in the PT is unknown. The receptor might be subject to loss and downregulation in diseases associated with kidney because of its continuously interaction with proteins in the proximal lumen.

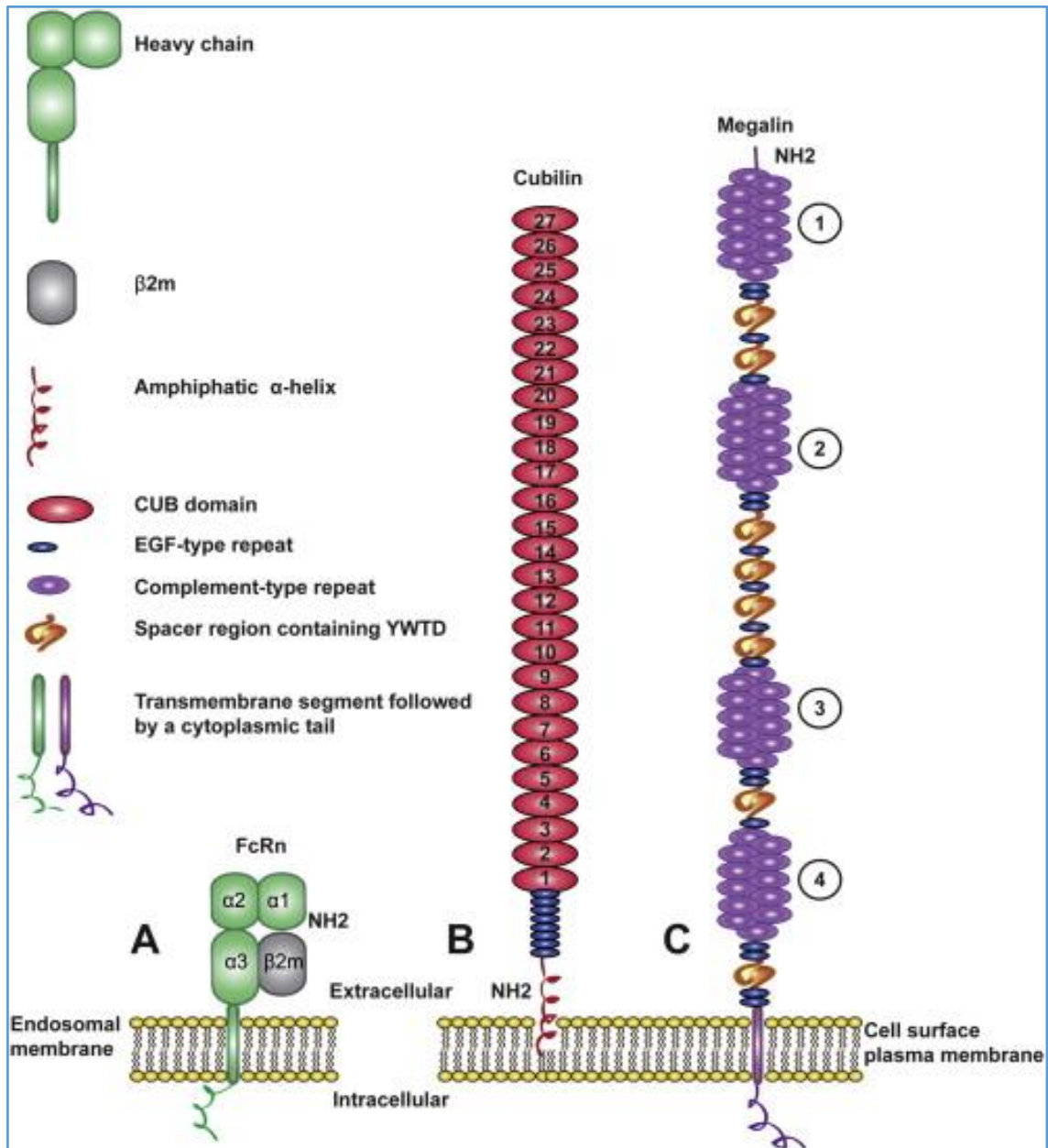


Figure 1.10: The structure of megalin (C), cubilin (B) and FcRn (A) showing known motifs and domains. Taken from Bern et al. (2015).

1.7 Tubular toxicity of proteinuria (Figure 1.11)

Proteinuria is characterised by the presence of abnormal amount of HMW and LMW proteins in the urine. As mentioned in the previous section glomerular diseases may increase filtration of macromolecules with the freely available LMW proteins in the proximal lumen. The toxic effects of the majority of these glomerular ultrafiltered macromolecules including the most abundant albumin, on the PTECs has been very well documented in cell culture and animal studies by having roles in activating of transcription and inflammatory cytokines, growth factors as well as effects on PTEC growth and causing apoptosis. In below the toxic effect of albumin on the PTEC in cell culture and animal studies are shown.

1.7.1 Cell culture studies

It is well known that abnormally filtered bioactive macromolecules have a direct toxicity to the PTEC (Baines and Brunskill, 2008). Albumin, the prevalent protein in the glomerular filtrate, exerts a toxic effect on the proximal epithelial cells through activation of signalling pathways and transcription factors. For example, NF- κ B is a transcription factor normally found in the cytoplasm of cell as inactive form and bound to inhibitory proteins (I κ B) (Takaya et al., 2003). Albumin has found to activate this nuclear factor in PTEC. Activation of NF- κ B leads to translation of NF κ B-dependent pro-inflammatory genes such as monocyte chemoattractant protein-1 (MCP-1) and regulated upon activation, normal T cell expressed and secreted (RANTES). These chemoattractant molecules increase the recruitment of inflammatory cells to the interstitium, resulting in release of potentially deleterious inflammatory cytokines and eventual tubular injury (Reich et al., 2005). In vitro studies have demonstrated that protein overload enhances the production of RANTES in the PTEC and a proposed role of this chemotactic and activating factor in the development of interstitial inflammation and kidney diseases (Zoja et al., 1998). Wheeler et al. (2011) have shown that activation of NF- κ B and TNF- α gene expression are both associated with albumin overload in the PTEC, and their contribution in renal inflammation and fibrosis has been very well-documented in obstructive and DN (Grande et al., 2010, Navarro-González and Mora-Fernández, 2008).

Albumin can also stimulate signal transducer and activator of transcription (STAT). It has been shown that albumin can activate STAT in murine PTEC (Nakajima et al., 2004). Similarly, stimulation of STAT leads to upregulation of MCP-1 and RANTES which in turn results in inflammatory cell infiltration and subsequent tubular damage (Rodríguez-Iturbe and García, 2010). Nakajima et al. (2004) found that STAT activation depends on the generation of reactive oxygen species (ROS) by albumin in the PTEC. ROS may itself contribute to the progression of renal disease. Evidence is available that increased albumin endocytosis by PTEC leads to activation of Rac1. Rac1 is a Rho-family small GTP-ase, which is responsible for activation of NADPH oxidase and ROS generation. Recent study has demonstrated that albumin overload increases the formation of ROS via activation of Rac1 and NADPH oxidase (Whaley-Connell et al., 2007).

Pearson et al. (2008) have reported that albumin overload in cultured PTEC activates signalling pathways such as p38 MAPK and ERK1 and 2, which in turn increases the production of proinflammatory markers of kidney damage including IL-6. According to Leonard et al. (1999), regulation of IL-6 synthesis is greatly dependent on both p38 and ERK/MAPK pathways in the PTEC and glomerular mesangial cells of the kidney nephron. It is believed that IL-6 may contribute to renal fibrosis via modulating TGF- β signalling (Pearson et al., 2008).

Another pathway activated by albumin in the PTEC is mitogen-activated protein kinase (MAPK). MAPK has shown to be involved in the regulation of MCP-1 and cell proliferation in PTEC (Takaya et al., 2003, Dixon and Brunskill, 2000).

It has been demonstrated that incubation of human PTEC with human serum albumin significantly increases the expression of proinflammatory markers (IL-6, IL-8, TNF- α , CCL-2, CCL-5) as well as α -SMA, and collagen IV, indicating the toxic effect of this plasma protein which may result in inflammation and fibrosis (Wu et al., 2014). Similarly, albumin is able to induce the production of IL-8, a potent chemokine that play a major role in attracting inflammatory cells particularly neutrophil to the site of inflammation and also promote angiogenesis in the PTEC, in human PTEC dose dependently, which occurs via NF- κ B–

dependent pathways through PKC activation and ROS generation (Tang et al., 2001). These proinflammatory markers, according to Kayama et al. (1997), are believed to be involved in the pathophysiology of CKD. TNF- α has long been identified as proinflammatory cytokine to play an important role in tissue damage and the progression of CKD (Vielhauer and Mayadas, 2007).

In addition to inflammation, interstitial fibrosis is the prognostic indicator of CKD and it is likely due to the chronic response of PTEC to the increased production of growth factors such as TGF- β (Zhao et al., 2013). There is evidence that albumin play a critical role in the activation and expression of this growth factor in the PTEC. For instance, Diwakar et al. (2007) have demonstrated that incubation of PTEC (opossum kidney cells and human kidney cell clone-8 cells) with albumin results in overproduction of TGF- β_1 . In this study, Diwakar et al. (2007) have also looked at the role of albumin endocytosis and its interaction with megalin in the secretion of TGF- β_1 and found that there is no correlation between the amount of TGF- β_1 produced by PTEC and the two processes, suggesting other mechanisms may be involved. Altogether, these studies have provided strong evidence that albumin overload, the most widely used protein in tissue culture studies and most abundant protein in glomerular filtrate, is toxic to the PTEC and may lead to inflammation and fibrosis, the main causes of CKD.

1.7.2 In vivo studies

Animal models of POP, a model of tubulointerstitial injury in experimental animals, have clearly demonstrated the toxic effects of glomerular ultrafiltered proteins on the PTEC which may lead to tubulointerstitial inflammation and fibrosis and ultimately chronic damage. In addition, there are other models of proteinuria that show the influence of filtered proteins due to glomerular permeability on the PTEC. In rats treated with increasing doses of bovine serum albumin (BSA) for two weeks, tubulointerstitial changes has been documented (Eddy, 1989). At one week, macrophage infiltration into the interstitium was clearly observed, subsequently followed by T helper and T cytotoxic cells. The PT showed increased expression of vimentin and increased deposition of complement component C3 and neoantigens. The severity of tubular damage was closely associated with proteinuria in these animals (Eddy, 1989). Likewise,

Landgraf et al. (2014) have found that POP produces significant changes in the kidney interstitium related with the increased levels of proinflammatory cytokines, TNF- α and IL-6. Tubulointerstitial fibrosis was detected as evaluated by marked collagen deposition.

Tubular injury has been reported by Takase et al. (2003) in POP rats. In these animals reduced tubulointerstitial damage induced by proteinuria was found to be associated with inactivation of NF- κ B, which in turn leads to suppression of MCP-1, TGF- β and fibronectin in tubulointerstitial injury lesions.

It is well-known that protein overload in mice results in proteinuria, interstitial inflammation and the development of interstitial fibrosis. Increased protein in the tubular lumen alters the mRNA levels of matrix genes procollagens α 1 (I), α 1 (III), and α 2 (IV) and TGF- β 1 and Timp-1 (Eddy et al., 2000). According to Eddy et al. (1995), POP in rats leads to activation of tubular NF- κ B with interstitial inflammation and upregulation of MCP-1 and osteopontin (OPN). Yang et al. (2011) have noticed that mice overloaded with protein shows tubular injury, increased macrophage infiltration in to the interstitium, assessed by F4/80 immunostaining, and that was associated with increased mRNA expression of MCP-1 and TNF- α .

In animal models of progressive proteinuric nephropathies (5/6 nephrectomy and passive Heymann nephritis), It has been shown that increased urinary excretion of protein over time is associated with remarkable increase in NF- κ B activity, which is being localised to the PTs (Donadelli et al., 2000). Activation of NF- κ B was paralleled by renal up-regulation of MCP-1 gene expression and subsequent accumulation of ED-1-positive monocytes/macrophages and CD8-positive T cells in the interstitium, suggesting that the initial recruitment of mononuclear cells may occur at least in part by MCP-1 dependent mechanism in these models.

The relationship between proteinuria and tubulointerstitial nephritis has long been recognised in puromycin aminonucleoside (PAN) nephrosis model (Tang et al., 1997). In this model, administration of PAN led to remarkable increase in MCP-1 and interferon-inducible protein-10 (IP-10) mRNA expression after 6-8 days and gradually declined by reaching day 21. The MCP-1 and IP-10 mRNA expression were mainly localised to the intrinsic tubulointerstitial cells and not to

infiltrating monocytes or macrophages. The most interesting is that using neutralising Ab to rat MCP-1 significantly reduced interstitial accumulation of macrophages and T lymphocytes, supporting the idea that inflammatory responses in the interstitium is greatly dependent on the MCP-1 mechanism.

The central role for TGF- β in the development of renal fibrosis has long been identified. TGF- β may contribute to renal scarring through activation of its downstream Smad signalling pathways (Lan, 2011). TGF- β can also leads to renal fibrosis through the induction of tubular cell epithelial–mesenchymal transition (EMT) (Zhao et al., 2013). In experimental animals, POP has been shown to upregulate the cortical mRNA and protein levels of TGF- β , which in turn leads to interstitial fibrosis and progressive renal injury (Eddy et al., 1995). Eddy (2001) believes that the initial inflammatory cells recruited in response to interstitial injury produced as a result of protein overload may participate in interstitial fibrosis. Infiltration of monocyte, the main source of TGF- β , into the interstitium in POP which might be explained by the recruitment mechanism of OPN, ICAM-I and VCAM-I expression, indicating the role of inflammatory cell infiltrate in the tubulointerstitial fibrosis (Eddy et al., 1995).

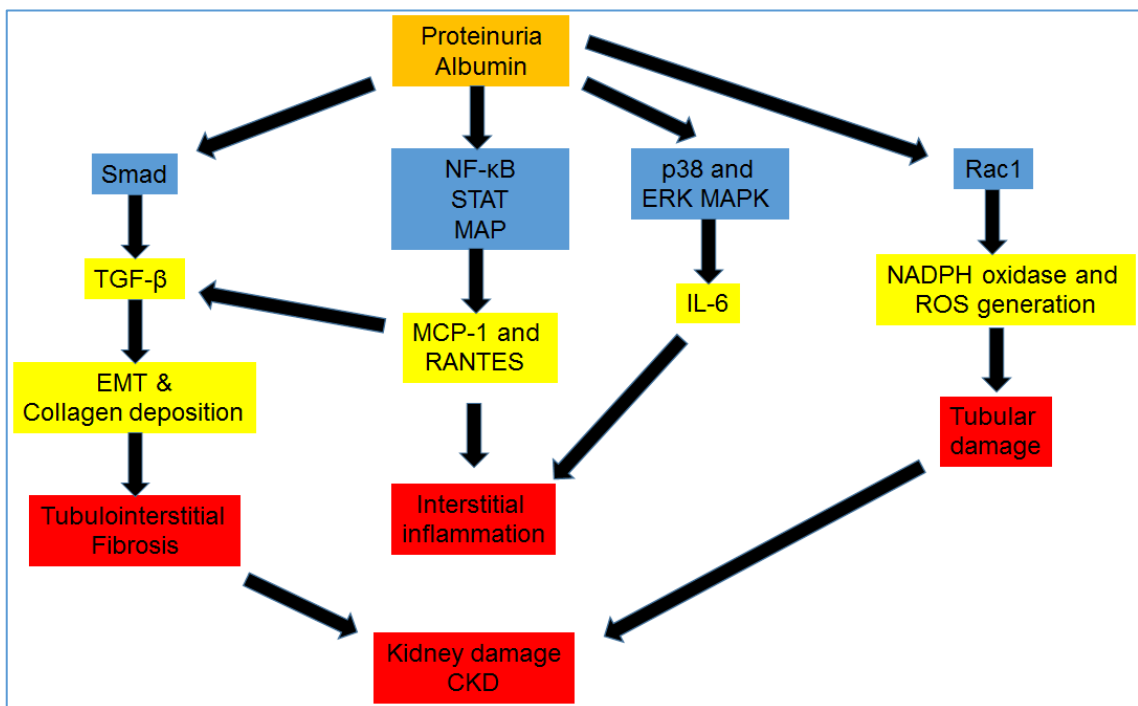


Figure 1.11: Mechanisms of protein overload proteinuria leading to tubular toxicity and kidney damage.

1.8 Importance of proteinuria in CKD

1.8.1 Correlation between proteinuria and renal failure

A strong correlation between the degree of proteinuria and the risk of progressive renal failure has been long recognized (Eddy, 2004). Proteinuria can be either glomerular and/or tubular in origin (Gorriz and Martinez-Castelao, 2012). Glomerular proteinuria appears when excess proteins pass through damaged or inflamed glomeruli and appear in the urine (Baines, 2010). Bioactive macromolecules which are present in the glomerular filtrate interact with PTEC, leading to progression of proteinuric nephropathy. The toxic effect of these molecules has clearly described such as activation of tubular-dependent pathways of interstitial fibrosis and inflammation, together with alterations in PTEC growth, apoptosis and gene transcription. Several animal and human studies have demonstrated that proteinuria is closely correlated with renal function loss.

1.8.1.1 Correlation in animal studies

1.8.1.1.1 Remnant kidney

In experimental animals, reduction in kidney mass leads to heavy proteinuria and progressive renal insufficiency. In these animals, reduction in proteinuria appears more beneficial because, according to Burton and Harris (1996), there is a strong correlation between proteinuria and the development of progressive renal failure. For example, in remnant kidney model, rats on low-protein diet exhibited less proteinuria and slowed the development of progressive renal impairment (Williams et al., 1987, El-Nahas et al., 1983). Similarly, rats with a remnant kidney and treated with angiotensin converting enzyme (ACE) inhibitors had a slightly different levels of proteinuria compared to controls and a minimum structural change in the glomeruli and tubulointerstitium (Anderson et al., 1986). Furthermore, ACE inhibitors can abrogate the development of renal injury in rats with reduced renal mass via reducing intraglomerular capillary pressure (Anderson et al., 1985). In another study, they used an alternative antihypertensive regimen in the treatment of rats with remnant kidney. These animals, surprisingly, had proteinuria at the same level as controls and

histological images of the glomerular structure and tubulointerstitium were similar to that as controls (Burton and Harris, 1996).

In addition, in the remnant kidney model, reduction in renal mass of rats may lead to glomerulosclerosis (Shimamura and Morrison, 1975). In these animals, the remaining glomeruli undergo several morphological and functional changes. These alterations may lead to increase in single nephron glomerular filtration rate (GFR) which may result in an increase in the intraglomerular pressure. Subsequently glomerular injury and eventual sclerosis may develop (Hostetter et al., 1981). In these animals a strong correlation between glomerulosclerosis and proteinuria has been detected (Williams and Coles 1994). Likely, Williams et al. (1987) proposed that protein restriction in diet is more beneficial as described before. There is direct evidence from animal and human studies that tubulointerstitial injury is more likely to be caused by poor control of systemic blood pressure which results from proteinuria in remnant kidney (Novick et al., 1991, Bidani et al., 1990). On the contrary, the better the control of systemic blood pressure the slower the rate of decline in GFR in the diseased kidney (Remuzzi et al., 1990). Deposition of complement components in the PTEC has been detected in remnant kidney, protein overload nephropathy and aminonucleoside nephrosis as a result of increased glomerular filtration of these molecules (Eddy, 1989, Abbate et al., 1998). Such observation has been recorded in patients with non-selective proteinuria and correlates with urinary complement excretion (Abbate et al., 1999). Over all, in this model, the amount of proteinuria, the degree of structural damage and the severity of renal insufficiency all are closely correlated.

1.8.1.1.2 Puromycin aminonucleoside nephrosis model

In puromycin aminonucleoside (PAN) nephrosis model, a single dose administration of PAN (15 mg/100g b.w.) to rats may lead to direct toxicity to the glomerular epithelial cells and the development of nephritic range proteinuria (Eddy et al., 1991). In these animals a remarkable change in the glomerular structure has observed. A detachment of podocyte FP from the GBM is the most prominent effect of PNA (Whiteside et al., 1993). According to Messina et al. (1987) and Whiteside et al. (1993), there is a positive correlation between

intensity of proteinuria and separation of podocyte from the GBM. It is clear that the extent of pro-inflammatory infiltrate and tubulointerstitial damage are closely correlated with the degree of proteinuria (Jones et al., 1992). Similarly, such relationship between an increased influx of pro-inflammatory cells such as macrophages and T lymphocytes into the interstitium and the degree of proteinuria has reported by Eddy et al. (1991) in PAN nephrosis. Another possible mechanism of podocyte detachment contributing to the renal impairment is that separation of these FP may alter the permeability of glomerular barrier as a result a huge amount of circulating macromolecules accumulate in the glomerulus and glomerulosclerosis develops, this correlation was clearly observed in the remnant kidney model in rats (El Nahas, 1989). Furthermore, according to Eddy and Michael (1988), a single intraperitoneal injection of PAN to rats produces considerable changes in the interstitium. Following these alterations, massive proteinuria develops and as a result the number of mononuclear cells penetrate the interstitium are significantly increased and hit the peak after 14 days. Therefore, the number of interstitial cells is greatly related to the degree of proteinuria. Additionally, in the PAN nephrosis model, rats exhibited a significant decline in GFR related to the extent of interstitial damage (Eddy and Michael, 1988).

1.8.1.1.3 Protein overload proteinuria

Similarly, in protein overload nephropathy model, intraperitoneal injection of large amount (1g/day) of BSA to rats may result in heavy proteinuria. There is no evidence that glomerular and/or interstitial damage is whether due to immune complex deposition or increased circulating of anti-BSA antibodies in the glomeruli or the interstitium. As proteinuria increases, there is an influx of chronic inflammatory cells into the interstitium and an accumulation of extracellular matrix (ECM) proteins (Eddy, 1989, Eddy et al., 1995). Furthermore, there is a significant increase in renal message for chemotactic MCP-1 and OPN (Eddy et al., 1995). In addition, Eddy et al. (1995) suggested that proteinuria is the only causative agent in this model, leading to recruitment of macrophages and T lymphocytes, with increased matrix protein synthesis and altered matrix degradation and remodeling participating in the interstitial fibrogenic process.

Further study of protein overload shows that injection of BSA to uninephrectomised rats leads to proteinuria and the development of acute tubulointerstitial nephritis. There is a significant increase in the number of macrophages and T lymphocytes in the interstitium in response to tubulointerstitial inflammation (Eddy et al., 1991). Tubular cell apoptosis also increases especially in the PTEC as a result of proteinuria (Thomas et al., 1999).

In experimental study, rats injected repeatedly with protein via i.v develop heavy proteinuria related to the increased permeability of glomerular properties. The subsequent toxic effects of filtered proteins are directly appeared on the PTs by increasing the process of reabsorption and recruitment of macrophages and T lymphocytes into the interstitium (Zoja et al., 1998).

Finally, incubation of PTEC with overload protein leads to upregulation of genes which are responsible for encoding of inflammatory cells. In this study, liberation of the inflammatory substances such as endothelin, chemokines and cytokines in high amount enhance other inflammatory cells migrate to inflamed area and fibrogenic reaction leading to renal failure (Zoja et al., 1999).

1.8.1.2 Correlation in human studies

In patients with diabetes the hallmark of DN is proteinuria. In these patients, proteinuria develops, especially when the GBM loss its selective-permeability, which is very common in diabetic kidney disease, for a diverse amount of proteins (Ruggenenti et al., 1998). Recent studies showed that, in diabetic patients, inhibition of ACE using different doses of ramipril reduces proteinuria through diminishing the size of large non-selective pores in the GFB (Morelli et al., 1990, Lewis et al., 1999). In addition, in experimental diabetes ACE inhibitors reduced intraglomerular capillary pressure and slowed the development of renal insufficiency (Zatz et al., 1986).

Likewise, patients with type 2 DN are of greater risk of proteinuria. Therefore, in these patients, reduction in proteinuria especially albuminuria to the lowest level is of major goal and particularly this is closely associated with the reducing of the higher risk of renal failure. For example, losartan, which is antiproteinuric therapy, can effectively reduce the higher risk of renal function loss in patients

with type 2 DN (De Zeeuw et al., 2004). Losartan has been recognized as an ACE inhibitor and/or angiotensin II receptor blocker which, in turn, can slow the progression of chronic renal failure (Hou et al., 2007).

Similarly, in type-1 diabetic patients the degree of diabetic glomerulosclerosis is associated with the intensity of proteinuria. It has been known that reducing proteinuria positively retard the progression of diabetic glomerulosclerosis. This is because lowering proteinuria might decrease the overflow of plasma lipoproteins through injured glomeruli (Hebert et al., 1994). For this reason, captopril has shown a renoprotective effect through decreasing proteinuria and lowering blood pressure. Recent studies have demonstrated that captopril can inhibit angiotensin II formation. It is well-known that angiotensin II stimulates formation of growth factors and TGF- β and these factors may lead to collagen formation and glomerular hypertrophy (Gibbons et al., 1992, Johnson et al., 1992). Captopril can also reduce proteinuria by its direct or indirect effects on GFB (Sorbi et al., 1993).

A study of the Modification of Diet in Renal Disease in 840 non-diabetic patients showed that proteinuria is the strongest predictor of the progressive renal failure among other baseline factors including serum creatinine, blood glucose, blood pressure and cholesterol levels (Peterson et al., 1995). In addition, De Zeeuw et al. (2004) found that baseline proteinuria can increase the riskiness of renal disease to end point by 5.2-fold, and an 8.1-fold increase risk for progressing to ESRD.

Overall, the degree of chronic renal insufficiency is closely correlated with the degree of proteinuria. Both restriction of protein in diet and using antiproteinuric agents might have a role in the slowing of progressive renal impairment.

1.9 Matrix metalloproteinases

Matrix metalloproteinases (MMPs) are a family of calcium containing zinc-dependent endopeptidases which are capable of degrading all components of ECM. These proteinases are also performing important roles, in addition to physiological and biological process such as embryonic development, tissue remodelling, cell migration, wound healing and angiogenesis, in diseases such as tissue ulceration, arthritis and cancer (Jones et al., 2003). Furthermore,

MMPs are greatly involved in the regulation of various molecules which are non-ECM including growth factors and their receptors, chemokines, cytokines, adhesion molecules, cell surface proteoglycans and various other enzymes (Peng et al., 2012).

Historically, collagenase MMP-1 was the first metalloproteinase discovered in the tail of tadpole undergoing metamorphosis by Gross and Lapiere in 1962 (Gross and Lapiere, 1962). To date, more than 20 MMPs have been identified in vertebrates and most of these proteinases are found in human tissues (Visse and Nagase, 2003). MMPs are also found in the other non-invertebrate organisms including sea urchins, *Caenorhabditis elegans*, soybean, and *Arabidopsis thaliana* (Nagase and Woessner, 1999), indicating the important role of these proteinases. In *Hydra* one MMP has been identified which regulates the foot process development and cell differentiation (Leontovich et al., 2000), and in the fruit fly *Drosophila melanogaster* two MMPs (Dm1-MMP and Dm2-MMP) have been cloned and sequenced (Llano et al., 2000). MMPs are classified, according to their structural homology and ability to degrade substrates, into six different groups which are, collagenases (MMP-1, -8, -13 and -18), the gelatinases (MMP-2 and -9), the stromelysins (MMP-3, -10 and -11), the matrilysins (MMP-7 and -26), membrane-types (MTs) (MMP-14, -15, -16, -17, -24 and -25), and others (MMP-12, -19, 20, -21, -22, -23, -27, -28 and -29) (Whittaker et al., 1999, Overall and López-Otín, 2002, Supuran and Scozzafaca, 2002, Visse and Nagase, 2003, Verma and Hansch, 2007, Gupta, 2012) .

1.9.1 MMP structure

The basic structure of the MMPs is similar and consists of four distinct domains, the propeptide domain, the catalytic domain, a linker peptide domain and a hemopexin (Hpx) domain (Nagase, 1997, Visse and Nagase, 2003). The propeptide domain contains about 80 amino acids and the PRCXXPD sequence in this domain is highly conserved. The cysteine “cysteine switch” residue within this motif maintains the pro-form (inactive form) or latency of these enzymes by binding to the zinc atoms in the active site and prevents from cleavage (Nagase and Woessner, 1999). The cysteine-zinc coordination can be cleaved by limited proteolysis of the pro-peptide, treatment with chaotropic agents or

organomercurials which in turn activates the enzyme (Van Wart and Birkedal-Hansen, 1990). There are also several potential furin recognition sites (RX(R/K)R) on the carboxy terminus of pro-peptide domain in several MMPs, which allow intracellular activation by furin-like pro-hormone convertases in the Golgi apparatus (Liu et al., 1997, Molloy et al., 1992, Nagase and Woessner, 1999).

The catalytic domain consists of 170 amino acids, with highly conserved zinc binding motif HEXXHXXGXXH (Bode et al., 1993). The catalytic zinc in this motif is supported by three histidine residues which forms a “Met-turn” (Sankari et al., 2016). The zinc binding motif and the conserved methionine in the catalytic domain are found in all members of the matrixin. In addition to catalytic zinc, MMPs have non-catalytic zinc and calcium ions to protect the tertiary structure of the enzyme, and the calcium ions play an important role in the expression of MMPs (Lovejoy et al., 1994, Zhang et al., 1997). The catalytic domain in all MMPs except MMP-7, -23 and -26, is linked to the Hpx domain by a proline-rich linker known as the hinge region (Peng et al., 2012).

1.9.2 MMP activation and expression

Initially, MMPs are produced and secreted in latent proenzyme form and then depending on the extracellular events they will be activated and changed to active-form (active MMPs) (Obermüller et al., 2001, Löffek et al., 2011). When released, MMPs can be activated by the already activated MMPs (Murphy et al., 1999) or other proteolytic enzymes (Ahmed, 2009). MMP-2 and MMP-9, among the other MMP species, are responsible for the cleavage of collagen types, especially collagen IV, and laminin, the basic components of tubular basement membrane (Catania et al., 2007). MMP-2 is mostly secreted by fibroblasts and endothelial cells, while MMP-9 is released by inflammatory cells (Corbel et al., 2001, Chadzinska et al., 2008).

Under normal conditions, MMPs are expressed at low levels and are tightly regulated via interactions between their activators and inhibitors (Ahmed, 2009, Tokito and Jougasaki, 2016). The expression of these peptidases has shown to be increased in response to high albumin doses in culture supernatants of podocytes (Fang et al., 2009). Similarly, in vitro albumin overload can induce

overexpression and activation of MMP-9 in the proximal epithelial cells (PECs) via the activation of P44/42 MAPK pathway (Zhang et al., 2015).

Eddy et al. (2000) found that the expression of MMP-9, the most expressed MMP with MMP-2 in the kidney, is increased modestly but not significantly in the kidney of proteinuric mice compared to control animals. It has also been shown that MMP-2, MMP-8 and MMP-9 levels are increased in the urine and serum of patients with DN, indicating that these endopeptidase enzymes may be involved in the progression of DN (Gharagozlian et al., 2009, Lauhio et al., 2008, Romanic et al., 2001, Tashiro et al., 2004, Thrailkill et al., 2009a, Van der Zijl et al., 2010). Further, upregulation of MMPs especially MMP-2 and MMP-9 has been reported in animal models of focal segmental glomerulosclerosis (FSGS), lupus nephritis and Thy-1.1 nephritis, a model for membranoproliferative glomerulonephritis (Liu et al., 2006, Tveita et al., 2008, Mitani et al., 2004).

Despite the great involvement of MMPs in degrading the ECM proteins in the kidney, these studies suggest that high levels of these endopeptidases may contribute to the development of various kidney diseases.

1.9.3 The beneficial effect of MMP inhibition in animal models

Overexpression or activation of MMPs have been shown to be associated with various kidney diseases. Using animal models of acute kidney injury (AKI), it has been demonstrated that the expression and activity of MMP-2, MMP-7 and MMP-9 are increased in kidney tissues exposed to ischemia reperfusion injury. Physiologically, inhibition the activity of MMPs in AKI models ameliorates the progression of acute tubular injury (ATI) and improves renal dysfunction at 24h (Kunugi et al., 2011).

Furthermore, inhibition of the MMPs activity has been widely used in animal models to treat various types of diseases. For example, in a rat model of autosomal-dominant polycystic kidney disease (cy/+) inhibition of MMP activity significantly reduced cyst numbers and kidney weight (Obermüller et al., 2001). In addition, in a mouse model of ischemic acute kidney injury (AKI) inhibition of MMPs activity significantly reduced reperfusion AKI (Kunugi et al., 2011).

The blockade of MMP-2 and MMP-9 in a murine model of bleomycin-induced pulmonary fibrosis was effective in reducing pulmonary fibrosis in mice (Corbel et al., 2001). Other studies have shown the importance of MMPs inhibitor in reducing the growth of tumours (Watson et al., 1996, Low et al., 1996, Prontera et al., 1999). Together, these findings suggest that MMPs inhibition might be important in the treatment of several of diseases.

As mentioned above, the extracellular domain of megalin can be cleaved by MMPs, therefore inhibition of these endocytic enzymes could be a useful strategy to prevent ectodomain shedding of megalin, and possibly FcRn (Figure 1.12). The importance of MMP inhibition in RIP has been reported in in vitro studies. MMP inhibitor III, a synthetic inhibitor of MMP, has shown to decrease the formation of megalin carboxylterminal fragment (MCTF) effectively. The MCTF is believed to be produced after the ectodomain shedding of megalin (Zou et al., 2004). Based on this, in order to investigate whether the inhibition of MMP activity may effectively reduce ectodomain shedding of both megalin and FcRn in mice, we used a synthetic inhibitor batimastat (BB-94).

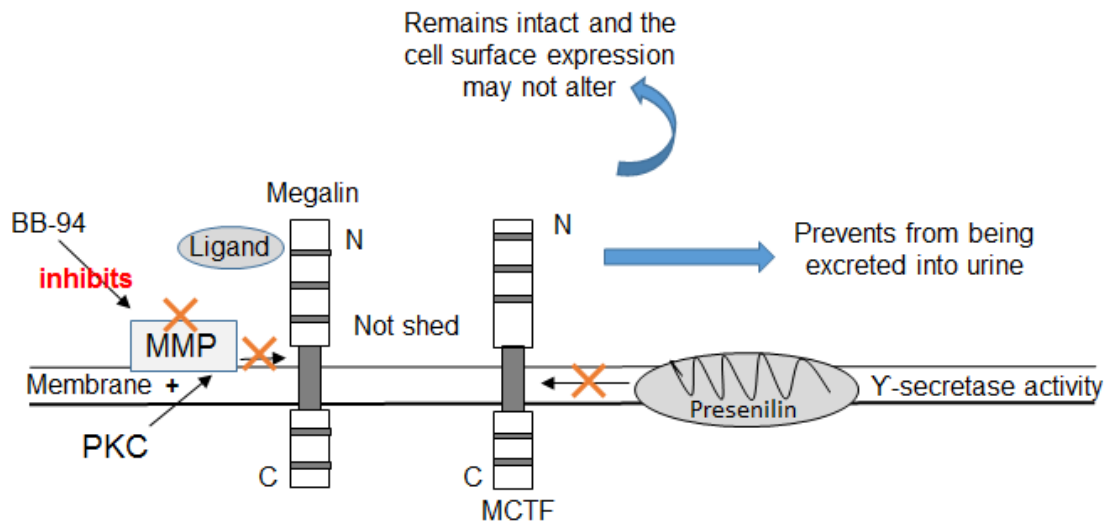


Figure 1.12: Proposed mechanism of MMP inhibition and protection of megalin ectodomain shedding. MMP blockade may prevent megalin ectodomain shedding and excretion into the urine which in turn may preserve cell surface expression of the receptor. The subsequent activation of γ -secretase and MCTF cleavage may not occur. BB-94= Broad spectrum MMP inhibitor, X = inhibition.

1.9.4 Mechanisms of MMP in kidney diseases

Several mechanisms may explain the contribution of MMPs to kidney diseases. Tan et al. (2010) and Cheng and Lovett (2003) have demonstrated that MMP-2 and MMP-9, the most expressed MMPs in the kidney, are involved in the progression of renal fibrosis through the induction of tubular cell epithelial-mesenchymal transition (EMT). The fact that MMP-2 and MMP-9 are responsible for the EMT is the collagen and laminin component of the tubular basement membrane (Lenz et al., 2000). Another possible mechanism of MMPs leading to kidney fibrosis is that products of collagen degradation have chemotactic properties for neutrophils and are also able to stimulate MMP-9 production (Xu et al., 2011). Furthermore, it has been long recognised that TGF- β and fibroblast growth factor (FGF)-2-binding proteins are components of ECM proteins and are released during ECM degradation (Benezra et al., 1993, Falcone et al., 1993, Taipale et al., 1992), which in turn, may regulate cell migration and induce EMT. Several other roles have been determined for MMPs in renal fibrosis such as destruction of the basement membrane, angiogenesis, cell migration, cell-cell adhesion and cell apoptosis (Gialeli et al., 2011, Morrison et al., 2009). Finally, recent studies have demonstrated that MMP-9 is able to cleave OPN, a potent macrophage chemoattractant; which in turn activates transforming growth factor-beta (TGF- β), a key inducer of renal fibrosis (Zheng et al., 2009, Tan et al., 2013).

1.10 Synthetic Inhibitor batimastat

Batimastat, also known as BB-94, is a potent broad spectrum and widely used MMP inhibitor. This synthetic low molecular weight inhibitor, blocks the activity of MMPs by directly binding to the Zn²⁺ ion in the active site of these enzymes (Brown, 1995, Beckett et al., 1996, Wojtowicz-Praga et al., 1997). Batimastat could also regulate MMPs at the transcriptional level by interfering with the signalling pathways of MMP production. It has been demonstrated that batimastat can reduce the activation of ERK1/2, p38 MAPK and AP-1 pathways in skeletal muscle of *mdx* mice, which in turn reduces the production of MMP (Kumar et al., 2010). Activation of other transcription factors such as NF- κ B and STAT by various stimuli may lead to an increase in MMP expression (Fanjul-

Fernández et al., 2010) , and reducing the activity of these transcription factors using different MMP inhibitors reduces the production of MMPs (Figure 1.13).

Batimastat was the first synthetic inhibitor used in clinical trials as an anti-cancer drug (Fingleton, 2007, Fingleton, 2008). BB-94 has been used in various animal models of kidney diseases and in clinical trials to treat cancer and prevent the growth of tumour in adult populations (Obermüller et al., 2001, Novak et al., 2010, Kunugi et al., 2011, Rasmussen and McCann, 1997, Wang et al., 1994). In addition, very low toxicity has been reported in animals treated with BB-94 (Wojtowicz-Praga et al., 1997).

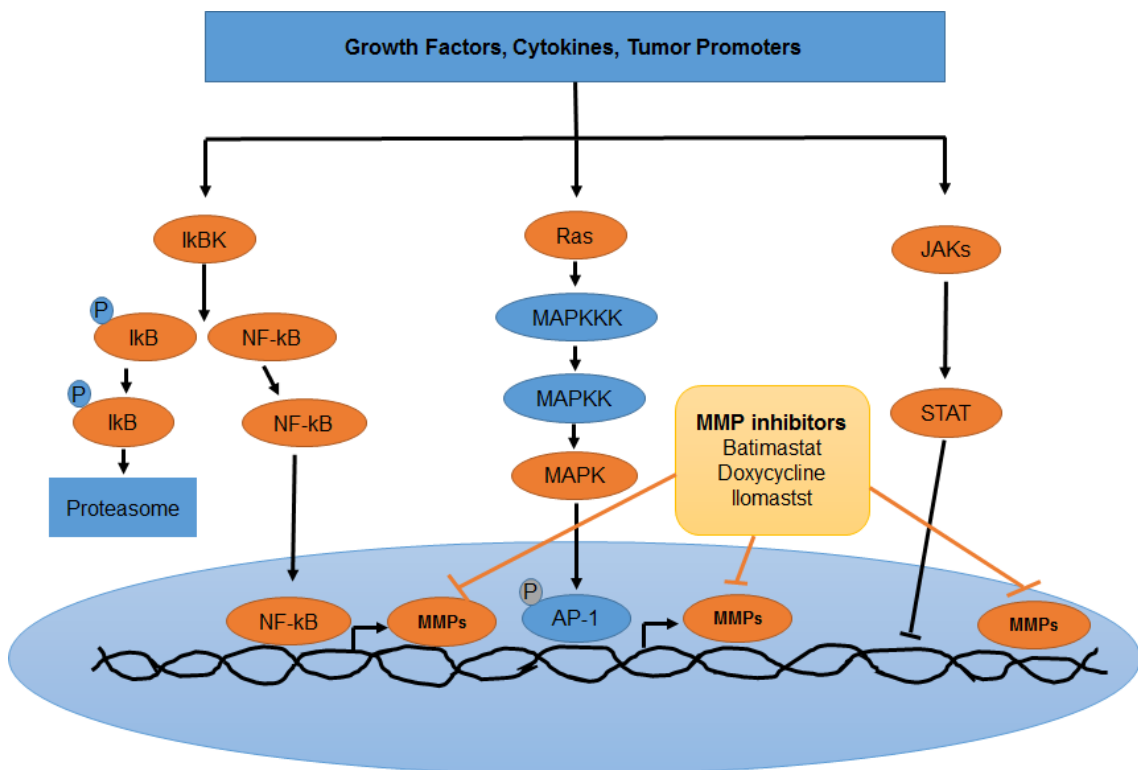


Figure 1.13: Schematic diagram showing signalling pathways of MMP synthesis by various stimuli and inhibition of MMP production by different MMP inhibitors, including batimastat. Modified from <http://www.selleckchem.com/products/bb-94.html>.

1.11 Aims and objectives

The strong correlation between proteinuria and the development of CKD showed by the previous investigators was the driving concept behind this thesis. Therefore, the current work was aimed to investigate the possible molecular mechanisms of proteinuria in proteinuric animals. To do this, a mouse model of POP was first established and the effect of protein overload on the expression of PT receptors including megalin and FcRn was studied. After this, a mouse model of POP and matrix metalloproteinase inhibitor (MMPI) was developed in order to determine whether this inhibitor can preserve the apical expression of these endocytic receptors and prevent proteinuria in proteinuric animals.

1.12 Hypothesis

In proteinuria altered expression of endocytic receptors is a central response in the PT. Altered expression of PT endocytic receptors is a maladaptive response to proteinuria and manipulating this process may potentially abrogate proteinuric nephropathy.

The specific objectives were:

- To study the effect of POP on the expression of endocytic receptors in the kidney of proteinuric mice.
- To determine the fate of endocytic receptors in proteinuric mice.
- To study the effect of MMP on the cell surface distribution of megalin and FcRn in the kidney of proteinuric mice.
- To investigate whether MMP inhibition could prevent proteinuria and influence megalin and FcRn expression in the PT of proteinuric mice.
- To study the importance of MMP blockade in the reducing tubulointerstitial inflammation and fibrosis in the kidney of proteinuric mice.

2 Materials and Methods

2.1 Materials

2.1.1 Experimental animals

Eight to ten week-old male BALB/c mice weighting 25-30 g were purchased from Charles River Laboratories. Upon arrival, mice were weighed, ear marked and caged in groups of four or five in standard housing. They were housed in a room with controlled temperature and a 12/12h light/dark cycle. Mice were fed standard diet and allowed to drink tap water *ad libitum*. Animals were cared for according to the guidelines of Home Office. All animal procedures were performed in accordance with the Animal (Scientific Procedures) Act 1986 research with approved laboratory practice protocols and assurance methods.

2.1.2 Chemicals, reagents and solutions

All chemicals used were of analytical grade and purchased from Thermo Fisher Scientific (Loughborough, UK), Sigma-Aldrich (Poole, UK), Acros Organics (Geel, Belgium), Invitrogen Life Technologies (Paisley, UK), Promega (Southampton, UK) and Santa Cruz Biotechnology (Heidelberg, Germany). Analytical-grade reagents were obtained from Sigma-Aldrich (Poole, UK) and Fisher Scientific (Loughborough, UK). Solutions for immunohistochemistry (IHC) and histological studies were purchased from Sigma-Aldrich (Poole, UK), Vector Laboratories (Peterborough, UK), Santa Cruz Biotechnology (Heidelberg, Germany), Abcam (Cambridge, UK), and Thermo Scientific Fisher (Loughborough, UK). Solutions for western blot (WB) analysis were bought from National Diagnostics (Atlanta, USA), Sigma-Aldrich (Poole, UK) and Bio-Rad Laboratories (Watford, UK). The full details of the chemicals, reagents and solution used in this study can be found in Table 2.1.

Table 2.1: Chemicals, reagents and solutions used throughout for immunohistochemistry and western blot analysis.

Chemicals, Reagents and Solutions	Product Code	Company
Bovine serum albumin (BSA)	BP9705-100	Fisher Scientific
Batimastat	SML0041-25MG	Sigma-Aldrich
Ammonium Persulfate (APS)	A/P470/46	Fisher Scientific
Sodium Chloride	PB358-212	Fisher Scientific
Albumin Standard	PJ208811	Thermo Scientific
OCT Embedding Medium 125ml	03804806	Thermo Scientific
PVDF Transfer Membrane	88518	Thermo Scientific
Sodium dodecyl sulfate (SDS)	L3771-100G	Sigma
Trizma Base	T1503-1KG	Sigma
Glycine	G8898-1KG	Sigma
Potassium Chloride	P-3911	Sigma
Potassium Phosphate	P-5379	Sigma
Protease Inhibitor Cocktail	P8340-1ML	Sigma
Albumin from Bovine Serum	A7511-5G	Sigma
Phenylmethanesulfonyl fluoride (PMSF)	P7626	Sigma
Sodium Citrate Tribasic	S4641-1KG	Sigma-Aldrich
Skim Milk Powder	70166-500G	Fluka
Sodium Phosphate Dibasic	448140010	ACROS ORGANICS
DTT	P/N Y00147	Invitrogen
TaqMan Universal Master Mix II, with UNG	4440038	Applied Biosystems

AMV Reverse Transcription System	A3500	Promega
RIPA Lysis Buffer System	Sc-24948A	Santa Cruz Biotechnology
ECL Western Blotting Detection reagents	RPN2106	GE Healthcare
2-Mercaptoethanol	M6250-100ML	Sigma-Aldrich
DPX mountant	44581	Sigma-Aldrich
Glycerol	G6279	Sigma
2-Propanol	19516-500ML	Sigma
Folin-Ciocalteu's phenol	F9252	Sigma
Tetramethylethylenediamine (TMED)	T9281-25ML	Sigma
Triton X-100	T-8532	Sigma
Dimethyl Sulfoxide (DMS)	D-8418-50ML	Sigma
Acetic Acid, minimum 99%	A6283	Sigma
Tween 20	P1379-250ML	Sigma-Aldrich
Xylene	X/0200/17	Fisher scientific
Isopentane	P/1030/08	Fisher Chemical
Methanol	–	Chemical Store, Leicester University
Absolute Ethanol	–	Chemical Store, Leicester University
Hydrogen peroxidase solution	H3410-500ML	Sigma-Aldrich
R.T.U Horse Radish Peroxidase Streptavidin	SA-5704	Vector Laboratories
Zymogen Developing Buffer	LC2671	Novex
Zymogen Renaturing Buffer	LC2670	Novex
Bio-Rad silver stain	161-0443, 161-0444, 161-0445, 161-0447	Bio-Rad Laboratories

LSAB Staining System	G3014	Santa Cruz Biotechnology
Acetic Acid Solution	ab150681	abcam
Picro Sirius Red Solution	ab150681	abcam
20% SDS Solution	EC-874	National Diagnostics
ProtoGel	EC-890	National Diagnostics
Brilliant Blue R Concentrate	B8647-1EA	Sigma
Eosin Y Solution Alcoholic	HT110132-1L	Sigma-Aldrich
Haematoxylin Solution	GHS132-1L	Sigma-Aldrich
Ponceau S Solution	P7170-1L	Sigma-Aldrich
Methyl Green	H-3402	Victor Laboratories
PageBlue Protein Staining Solution	24620	Thermo Scientific

2.1.3 Antibodies

The primary antibodies used throughout these studies for IHC and WB analysis (Table 2.2) are listed below. Primary antibodies were purchased from Proteintech (Manchester, UK), Bioss (Woburn, USA), OriGene (Rockville, USA), Abcam (Cambridge, UK), Aviva Systems Biology (San Diego, USA), Sigma-Aldrich (Darmstadt, Germany) and Santa Cruz Biotechnology (Heidelberg, Germany). Secondary antibodies (Table 2.3) were bought from Dako (Glostrup, Denmark), Sigma-Aldrich (Poole, UK) and Santa Cruz Biotechnology (Heidelberg, Germany).

2.1.4 TaqMan gene expression assays

The TaqMan gene expression assays used in these studies were purchased from Thermo Fisher Scientific (Loughborough, UK) and are listed in Table 2.4.

2.1.5 Commercial kits

ELISA kits for urinary megalin and FcRn were purchased from MyBioSource (San Diego, USA). ELISA kit for urinary albumin was bought from Bethyl Laboratories (Montgomery, USA). ELISA kits for TNF- α and TGF- β were obtained from R&D Systems (Abingdon, UK). Creatinine assay kit was provided by BioAssay Systems (Hayward, USA). Kits for IHC were purchased from Vector Laboratories (Peterborough, UK). MMP assay kit was obtained from Abcam (Cambridge, UK). Coomassie plus assay kit was purchased from Thermo Scientific (Loughborough, UK). Picrosirius red staining kit was provided by Abcam (Cambridge, UK). The full details for assay kits used in these studies can be found in Table 2.5.

Table 2.2: Primary antibodies used in immunohistochemistry and western blot analysis

Target Antibody	Host	Specificity	Product code	Company
LRP2	Rabbit	Human, Mouse	19700-1-AP	Proteintech
FCGRT/FcRn	Rabbit	Human, Mouse, Rat, Dog	bs-13151R	Bioss
MMP-3	Rabbit	Human, Mouse, Rat	TA300812	OriGene
MMP-7	Rabbit	Mouse, Human	ab5706	Abcam
MMP-9	Rabbit	Human, Mouse, Rat	OABB00316	Aviva Systems Biology
Presenilin-1	Rabbit	Mouse, Rat, Human	ab65293	Abcam
β -actin	Mouse	Mouse	A-5441	Sigma-Aldrich
F4/80	Rabbit	Mouse, Rat	Sc-25830	Santa Cruz Biotechnology
TNF- α	Goat	Mouse, Rat	Sc-1349	Santa Cruz Biotechnology
TGF- β	Rabbit	Mouse, Rat, Human	Sc-7892	Santa Cruz Biotechnology
IL-6	Rabbit	Mouse, Rat	Sc-1265-R	Santa Cruz Biotechnology

Table 2.3: Secondary antibodies used in immunohistochemistry and western blot analysis

Antibody	Product Code	Company
Polyclonal Swine Anti-Rabbit Immunoglobulins/Biotinylated Swine F(ab') ₂	E0431	Dako
Goat Anti-Rabbit Immunoglobulin (Peroxidase Conjugated)	A-6154	Sigma-Aldrich
Goat Anti-Mouse Immunoglobulin (Peroxidase Conjugated)	A-4416	Sigma-Aldrich
Donkey Anti-Goat IgG (HRP-Conjugated)	Sc-2020	Santa Cruz Biotechnology
Donkey Anti-Goat IgG/ Biotinylated	G30114	Santa Cruz Biotechnology

Table 2.4: TaqMan gene expression assays used in qPCR analysis

Target Gene	Species	TaqMan Assay ID	Reference ID	Company
LRP2	Mouse	Mm01328171_m1	NM_001081088.1	Thermo Fisher Scientific
Fcgrt	Mouse	Mm00438885_g1	NM_010189.3	Thermo Fisher Scientific
MMP3	Mouse	Mm01168406_g1	NM_010809.1	Thermo Fisher Scientific
MMP7	Mouse	Mm01168419_m1	NM_010810.4	Thermo Fisher Scientific
MMP9	Mouse	Mm01240563_g1	NM_013599.3	Thermo Fisher Scientific
GAPDH	Mouse	Mm99999915_g1	NM_001289726.1	Thermo Fisher Scientific
F4/80	Mouse	Mm00802529_m1	NM_010130.4	Thermo Fisher Scientific

Table 2.5: Supplier information for assay kits.

Commercial Kit	Target	Product Code	Company
Mouse Albumin ELISA Kit	Mouse Urine Albumin	E99-134	Bethyl Laboratories
QuantiChrom™ Creatinine Assay Kit	Mouse Serum and Urine Creatinine	DICT-500	BioAssay Systems
Coomassie Plus (Bradford) Assay Kit	Mouse Urine and Tissue Protein	23236	Thermo Scientific
RNeasy Plus Mini Kit	Total RNA Purification and Isolation	74134	Qiagen
LRP2 ELISA Kit	Mouse urine megalin	MBS068632	MyBioSource
FCGRT ELISA Kit	Mouse urine FcRn	MBS937874	MyBioSource
MMP Activity Assay Kit (Fluorometric-Green)	Mouse tissue MMPs Activity	ab112146	Abcam
Mouse TNF- α ELISA KIT	Mouse tissue TNF- α	DY410-05	R&D Systems
Mouse TGF- β 1 ELISA Kit	Mouse tissue TGF- β	DY1679-05	R&D Systems
Avidin/Biotin Blocking Kit	IHC	SP-2001	Vector Laboratories
Diaminobenzidine (DAB) Peroxidase Substrate kit	IHC	SK-4100	Vector Laboratories
Picro-Sirius Red Stain Kit	Collagen deposition	ab150681	Abcam

2.2 Methods

2.2.1 Unilateral nephrectomy

After an acclimatisation period of one week after arrival, eight-week old mice were subjected to unilateral nephrectomy. Unilateral nephrectomy was performed in a surgical theatre room in the animal house under anaesthesia (2.5% isoflurane in 1.5L/min oxygen).

Nephrectomy was carried out as described previously (Amann et al., 2000, Amann et al., 2001). The left kidney was exposed through a flank incision and then the renal vein, artery and ureter were all carefully ligated at the hilus using 6/0 polyglactin suture. The kidney was then excised. The muscle and skin were then closed separately using 6/0 polyglactin suture. Nephrectomised animals were monitored, pain scored according to the standard sheet, and injected daily intramuscularly with analgesics (meloxicam (5mg/kg) and buprenorphine (0.1mg/kg) for 5 days). The mice were allowed to recover completely (7 days) after surgery before starting BSA administration.

2.2.2 Experiment 1: Protein overload proteinuria model (Figure 2.1)

A mouse model of protein overload was used to induce proteinuria as described previously (Eddy, 1989, Ishola et al., 2005). Nephrectomised mice were injected with low endotoxin bovine serum albumin (BSA) for 14 days. BSA dissolved in 1ml of saline was administered by intraperitoneal (i.p) injection in increasing doses starting from 2mg/g body weight (bw) on day 1, to a maximum dose of 15mg/g bw on day 6 which was thereafter maintained. Control animals were received equal volumes of saline (1ml/animal). BSA solution (40%) was prepared using sodium chloride 0.9% (normal saline).

2.2.3 Experiment 2: Protein overload proteinuria plus batimastat (BB-94) model (Figure 2.2)

Proteinuria was induced in nephrectomised mice as described above. Proteinuric animals also received i.p injections of BB-94 30mg/kg, for two weeks starting on day 1 of BSA administration. A 30mg/kg dose of BB-94 was used in previous studies in mice and prepared as a suspension of 3 mg/ml in phosphate-buffered saline containing 0.01% Tween 80 (Corbel et al., 2001,

Kumar et al., 2010). Control animals received an equivalent volume of vehicle only.

2.2.4 Collection of urine and blood

Mice were placed individually in metabolic cages for 24h urine collection one day before sacrifice. To prevent the degradation of proteins in the urine, 25µl of protease inhibitor was placed in the urine collection tubes. Collected urines were then measured and transferred to microcentrifuge tubes and kept on ice. After that, they were centrifuged at 13,000 rpm for 5 min at 4°C to remove any excess debris. After centrifugation, the supernatants were transferred to a new 2 ml microcentrifuge tubes, labelled and stored at -20°C for later analysis.

Blood samples were collected from anaesthetised mice by cardiac puncture. An 18 gauge (40x1.2mm) hypodermic needle was inserted through the diaphragm into the heart and approximately 0.75 ml of blood was drawn into a 2.5 ml sterile syringe. Blood samples were then transferred to 2ml microcentrifuge tubes and incubated on ice/or at room temperature for 30-60 min and allowed to clot. The blood samples were then centrifuged at 13,000 rpm for 5 min at 4°C. Separated serum was then collected and transferred to fresh microcentrifuge tubes, labelled and stored at -20°C for serum total protein and serum creatinine measurement.

2.2.5 Animal killing and tissue collection

At the end of the experiment, animals were killed by cervical dislocation. Then kidneys were removed and transferred to a petri dish containing cold PBS. The kidneys were then carefully decapsulated and cut longitudinally with a sharp scalpel blade into two equal halves. Half of the kidney was preserved in 10% formalin for immunohistochemical and histological studies and the other half was processed further to remove cortical tissues. The cortices were snap-frozen in an isopentane bath on dry ice and then stored at -80°C for WB analysis and RNA isolation.

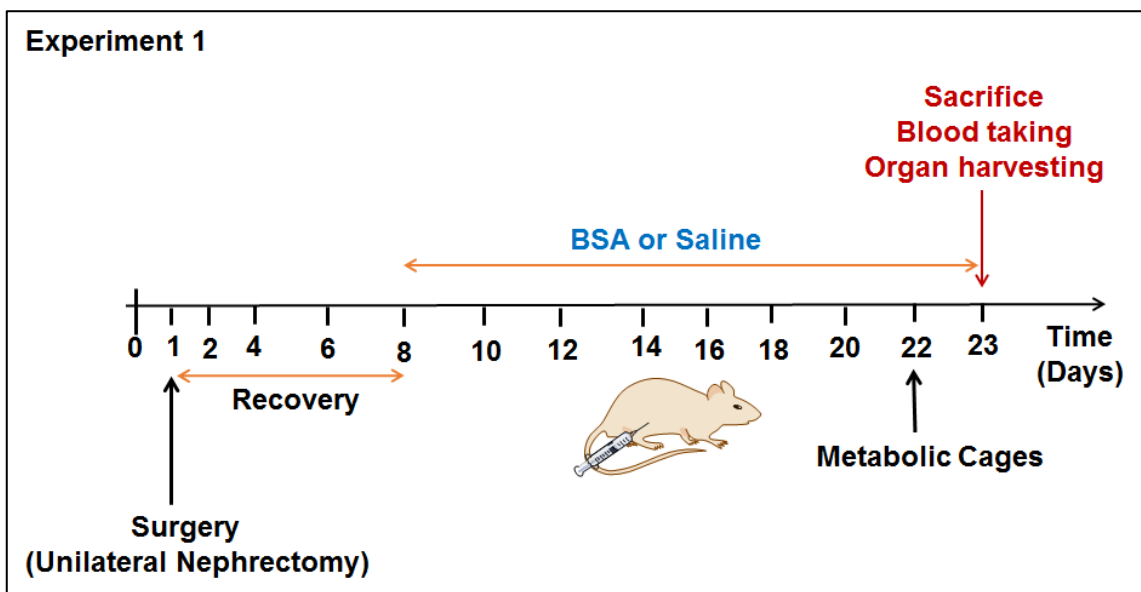


Figure 2.1: Schematic diagram showing the model of protein overload proteinuria in wild type BALB/c mice.

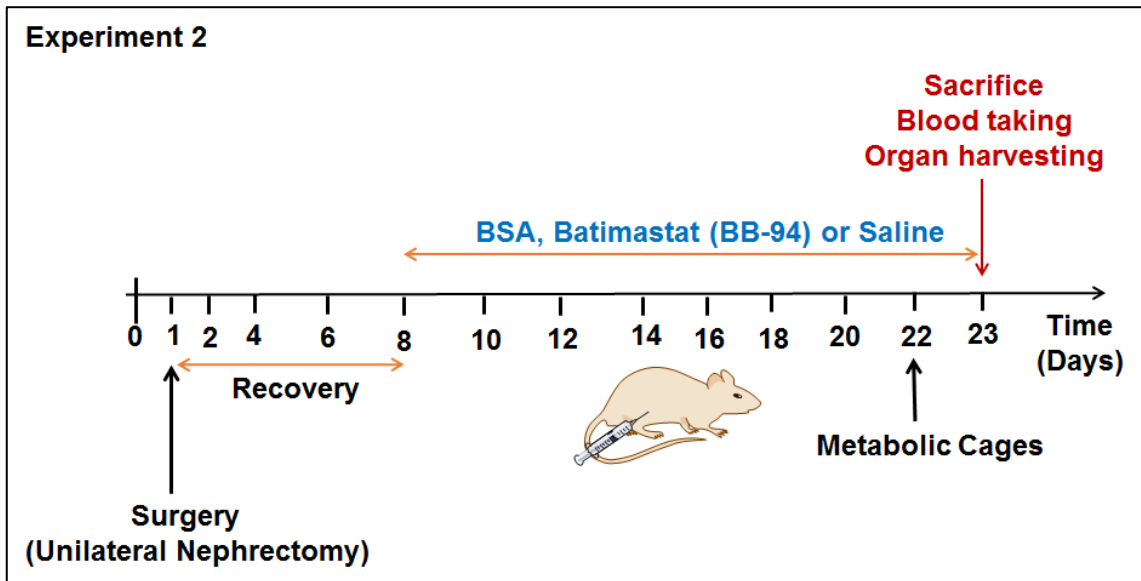


Figure 2.2: Schematic diagram showing the model of protein overload proteinuria+BB-94 in wild type BALB/c mice.

2.2.6 Preparation of urine for megalin and FcRn determination

Frozen urine samples were thawed and centrifuged at 17,000xg for 15 min at 4°C to remove whole cells, large membrane fragments and other debris from supernatants. The supernatants were further centrifuged at 200,000xg for 1h at 4°C to obtain low-density protein pellets (Pisitkun et al., 2004, Simpson et al., 2008). Both supernatants and pellets were collected. The supernatants were dialysed as described previously (Norden et al., 2002). A volume of urine equivalent to 2.5 µmol creatinine was dialysed (D9277-100FT dialysis tubing cellulose membrane; Sigma-Aldrich, Dorset, UK) for 3h in a cold room, with vigorous stirring, against 1L of 50 mM ammonium bicarbonate (A6141; Sigma-Aldrich), with one change after 1h. Dialysed urine samples were then collected from dialysis tubes and transferred to new microcentrifuge tubes. After that, dialysed urines were lyophilised to dryness in a freeze drier (ThermoSavant, -45°C, 70 microbars for overnight). Lyophilised urines were then resuspended in 0.25 ml of 50 mM ammonium bicarbonate buffer and stored at -20°C.

Pellets were resuspended in the same volume of 50 mM ammonium bicarbonate buffer as the original urine volume and dialysed as described above.

2.2.7 Urine analysis

2.2.7.1 Determination of protein concentration

The urine protein concentration was determined in 24h urine samples by Bradford protein assay, according to the manufacturer's instructions. Ten microliters of standards (50, 100, 200, 400 and 800 µg/ml) or diluted urine samples were added in duplicate to the wells of the 96-well microplate (FX9200; Alpha Laboratories Limited, Leicester, UK). 300µl of Coomassie plus reagent were added to the wells and the plate was shaken by hand for 30 sec. The plate was incubated at room temperature for 10 min. The optical density of the samples and standards was measured at 595 nm using a plate reader (TECAN, infinite F50) and plotted against standard (BSA) concentrations to create a standard curve. The standard curve was used to determine the protein concentration in urine samples.

2.2.7.2. SDS-PAGE of urinary protein

Urinary proteins were separated according to their molecular size using SDS-PAGE. In short, 1µl urine samples, normalised to urine creatinine, was applied to 10% SDS-PAGE and electrophoresed at 100 volts for approximately 1h. Two micrograms of BSA was also loaded as a positive control. Separated proteins were then visualised by staining the gel with Page blue protein staining solution (11852174; Thermo Fisher Scientific, Dublin, Ireland). To determine the molecular size of analysed proteins in the urine, a molecular weight protein marker was used as standard in the gel.

2.2.7.3 SDS-PAGE of urinary megalin

Lyophilised urines, which were resuspended in 0.25 ml of 50 mM ammonium bicarbonate buffer, were mixed with 0.25 ml loading buffer (62.5 mM Tris-HCl (pH 6.8) with 5% sodium dodecyl sulfate, 10% glycerol, and 0.003% bromphenol blue) and heated at 40°C for 30 min. Twenty five µl were loaded onto a 4% SDS-PAGE and electrophoresed at 100 V for approximately 2h and 30 min in 25 mM Tris, 0.192 M glycine. After that, the gel was stained with Page blue protein staining solution for overnight at room temperature and then destained with distilled water for 5 min with two changes.

2.2.7.4 Determination of urine albumin concentration

Mouse albumin ELISA kit (Cat. No. E99-134) was used to determine albumin concentration in 24h urine samples, according to the manufacturer's instructions. Standards (mouse albumin) or diluted urine samples (1:1000 in D.W) were pipetted in duplicate into the wells of the 96 well plate pre-coated with anti-mouse albumin antibody and incubated at room temperature for 1h. After incubation, the plate was washed 4 times with the provided wash solution. After washing, 100µl of mouse albumin detection antibody were added to the wells and the plate was incubated at room temperature for 1h. After removing any unbound substances, 100 µl of avidin conjugated horseradish peroxidase (HRP) solution A were added to the wells and the plate was incubated for 30 min at room temperature. Following the last wash and removing any unbound avidin-enzyme reagent, 100 µl of TMB substrate solution was added to the wells and the reaction was stopped immediately when the blue colour developed. The

intensity of blue colour was measured at 450nm using plate reader (TECAN, infinite F50). Obtained optical densities were used to create a standard curve and determine the concentration of albumin in the urine samples.

2.2.7.5 Determination of urine megalin concentration

The concentration of megalin was determined in 24h urine samples using a microplate solid phase quantitative sandwich ELISA (LRP2 ELISA kit, MBS068632, My-Biosource, USA), according to the manufacturer's instructions. Briefly, 50µl of sample diluent, standards (31.2, 62.5, 125, 250, 500 and 1000 ng/ml of recombinant full-length protein expressed in E. coli) or undiluted urine samples were pipetted into duplicate into the wells of a 96-well microplate pre-coated with rabbit polyclonal antibody specific for LRP2 (pre-coated microplate wells contained both capture and detection antibodies). After adding standards and urine samples, 100 µl of HRP-conjugated mouse anti-rabbit LRP2 antibody was added to the wells and the strip covered plate was incubated at 37°C for 1 h.

After incubation, the microplate was washed with 1X wash solution (one volume of wash solution (20X) diluted in 19 volumes of distilled water) four times and dried by inverting and blotting onto a paper towel. After removing any unbound avidin-enzyme reagent, 50µl of chromogen solution A and 50µl of chromogen solution B (substrates) were added to the wells successively. The microplate was then protected from light and incubated at 37°C for 15 min. The reaction was stopped by adding 50µl of stop solution to each well. The microplate was read at 450 nm with a microplate reader (TECAN, infinite F50) and optical density measurements were plotted against standard (BSA) concentrations to create standard curve. The standard curve was used to determine megalin concentration in urine samples.

2.2.7.6 Determination of urine FcRn concentration

The concentration of FcRn was determined in 24h urine samples using mouse IgG receptor FcRn large Subunit P51 ELISA Kit, according to the manufacturer's instructions. A 100 µl aliquot of sample diluent, standards (23.5, 47.94, 187.5, 375, 750 and 1500 pg/ml of recombinant full-length protein expressed in *E. coli*) or urine samples were pipetted in duplicate into the wells of a 96-well microplate pre-coated with antibody specific for FcRn. The plate was then covered with an adhesive strip and incubated at 37°C for 2h. After removing any unbound substances, the plate was incubated with biotinylated antibody (1X) at 37°C for 1h (100 µl/well). After washing with 1X wash buffer three times, 100 µl of avidin conjugated horseradish peroxidase (HRP) (1X) was added to the wells and the strip covered plate was incubated at 37°C for 1 hr. Following a wash to remove any unbound avidin-enzyme reagent, 90 µl of TMB substrate was added to the wells and the plate was incubated in dark for 30 min at 37°C. After the yellow colour developed, the reaction was stopped by adding 50 µl of stop solution to the wells.

The intensity of yellow colour was measured at 450nm with a plate reader and the optical densities were used to make standard curve. The standard curve was then used to determine the concentration of FcRn concentration in the urine samples.

2.2.7.6.1 Preparation of wash buffer (1X)

To prepare 1X wash buffer, 20 ml of concentrate wash solution (25X) were diluted in 480 Nanopure water to obtain 500 ml of 1X wash solution.

2.2.7.6.2 Preparation of biotin-antibody (1X)

1X biotin-antibody was prepared as follows: 10 µl of biotin-antibody were diluted in 990 µl of biotin-antibody diluent to make a 100-fold dilution.

2.2.7.6.3 Preparation of HRP-avidin (1X)

1X HRP-avidin was prepared as follows: 10 µl of HRP-avidin was diluted in 990 µl of HRP-avidin diluent to obtain a 100-fold dilution.

2.2.8 Analysis of serum

2.2.8.1 Determination of serum creatinine

Serum creatinine was determined using quantitative colorimetric creatinine assay (DICT-500; Universal Biologicals LTD, Cambridge, UK), according to the manufacturer's instructions. Thirty microliters of diluted standard (2mg/dL) or serum samples were added in duplicate to the wells of the 96-well standard plate. Then, 200µl of working reagent were added to the wells quickly and mixed gently. The plate was then incubated at room temperature and optical densities were taken at 1 min (OD1) and after 5 min (OD5) at 490 nm. The concentration of Serum creatinine was determined by using the following equation:

$$\text{Creatinine Con.} = \frac{\text{OD}_{\text{SAMPLE 5}} - \text{OD}_{\text{SAMPLE 1}}}{\text{OD}_{\text{STD 5}} - \text{OD}_{\text{STD 1}}} \times 2 \text{ (mg/dL)}$$

2.2.8.2 Determination of total serum protein

Total serum protein was determined by Bradford protein assay (Bradford, 10741945, Fischer Scientific Ireland Ltd.), according to the manufacturer's instructions. Ten microliters of standards or diluted serum samples were applied in duplicate to the wells of the 96-well plate. After that, 300 µl of Coomassie plus reagent were added to the wells and mixed with a microplate shaker for 30 sec. The plate was then incubated for 10 min at room temperature. The intensity of the blue colour was measured at 595 nm using plate reader. Optical densities were used to make a standard curve and to determine serum protein concentration.

2.2.9 Preparation of homogenate from mouse renal cortex

The renal capsule was removed and the cortex was dissected away from the medulla. The cortex was then homogenised in RIPA buffer containing PMSF (10µl/ml), sodium orthovanadate solution (10µl/ml) and protease inhibitor cocktail solution (20µl/ml) using four strokes of the homogenizer at maximum speed for 10 sec each. Homogenisation was performed on ice to reduce protein degradation. The homogenates were centrifuged at 10,000 g for 10 min at 4°C.

The supernatants were carefully collected and transferred to a fresh Eppendorf tube and stored at -20°C for protein expression studies.

2.2.10 Determination of protein concentration in kidney homogenates

The protein concentration in kidney homogenates was determined by Bradford protein assay. 10µl of standards or kidney homogenates were pipetted in duplicate into the wells of the 96-well standard plate. 300µl of Coomassie plus reagent were then added to the wells and the plate was shaken by hand for 30 sec. The plate was incubated at room temperature for 10 min. After incubation, produced blue colour was measured at 595 nm using plate reader and the measurements were plotted against standard concentrations to make a standard curve. The standard curve was used to determine protein concentration in kidney homogenates.

2.2.11 Western blot analysis

Forty µg of extracted protein from each lysate were mixed with an equal volume of 2X Laemmli loading buffer (100 mM tris (pH 6.8), 4% SDS, 0.2% bromphenol blue, 20% glycerol) containing 10% beta-mercaptoethanol and heated for 5 min at 95°C followed by a brief spin down. Samples were loaded onto 4% (for detection of megalin) or 10% (for lower molecular weight proteins) sodium dodecyl sulphate-polyacrylamide (SDS-PAGE) gels and electrophoresed at 100 V for 1h or 2.5h. Separated proteins were transferred onto Immobilon-P® PVDF transfer membrane (EMD Millipore Corporation, Billerica, MA, USA) using semi-dry transfer system (400 V, 62.5 mA for 2.30h).

The membrane was then blocked with blocking solution (5% skimmed milk powder in TBS) for 1h or 2h at room temperature. After blocking, the membrane was incubated with primary antibody (prepared in %5 milk solution) for overnight at 4°C or in the cold room, for antibody dilutions see Table 2.6. Following washing with TBST three times, the membrane was incubated with secondary antibody (prepared in 5% milk solution) for 1h or 2h at room temperature. After washing with TBST three times, the membrane was incubated with ECL reagent (RPN 2106, GE Healthcare) (1 volume reagent A mixed with 1 volume of reagent B) for 5 min at room temperature.

Blot images were taken on ChemiDoc™ Touch Gel Imaging System and analysed using Image Lab software or ImageJ software.

2.2.12 Coomassie blue staining

Once separated, proteins were visualised in SDS-PAGE gels with the use of Coomassie brilliant blue stain. The gel was incubated in Coomassie stain for 2h or overnight at room temperature and destained in destain solution (methanol:H₂O (1:1 v/v), glacial acetic acid) to remove excess Coomassie stain from the gel.

2.2.13 Analysis of western blot images

WB images were analysed using ImageJ software. All images were stored on 8 bit grayscale and the brightness and contrast of images were adjusted using adjustment tool. The intensity of protein bands was measured in samples from various experimental conditions. The intensity of the target protein was then divided by the intensity of the β -actin loading control for that sample. The target protein to loading control ratio was used to compare target protein abundance in various samples.

Protein content = Intensity of Target Protein / Intensity of Loading Control (β -actin)

Table 2.6: Primary and secondary antibody dilutions for western blot analysis.

Primary Antibody	Dilution	Secondary Antibody	Dilution
LRP2	1:1000	Goat anti-rabbit (HRP)	1:2000
FcRn	1:1000	Goat anti-rabbit (HRP)	1:2000
Presenilin-1	1:2000	Goat anti-rabbit (HRP)	1:4000
MMP-3	1:500	Goat anti-rabbit (HRP)	1:1000
MMP-7	1:2000	Goat anti-rabbit (HRP)	1:4000
MMP-9	1:1000	Goat anti-rabbit (HRP)	1:2000
F4/80	1:1000	Goat anti-rabbit (HRP)	1:2000
TGF- β	1:750	Goat anti-rabbit (HRP)	1:2000
TNF- α	1:750	Donkey anti-goat (HRP)	1:3000
IL-6	1:1000	Goat anti-rabbit (HRP)	1:2000
β -actin	1:2000	Goat anti-mouse (HRP)	1:4000

2.2.14 Immunohistochemistry

Paraffin embedded kidney sections were deparaffinised by immersing in xylene (2 x 5 min), and rehydrated in a series of graded alcohols (100% (2x), 90% and 70%) for 5 min each. Sections were then incubated in hydrogen peroxide solution (2.4ml of 30% hydrogen peroxide in 400ml PBS) for 10 min at room temperature to quench endogenous peroxidase activity. After that, slides were transferred to a container containing pre-heated sodium citrate (2.94g sodium citrate in 1000ml D.W, pH 6.0) and microwaved in an 800 W microwave oven for 12 min. This step was carried out to unmask the antigen epitopes in order to allow primary antibody to bind.

Following antigen retrieval, slides were allowed to cool at room temperature for 30 min and rinsed in D.W. To block non-specific binding, sections were incubated with blocking serum (0.5% BSA, 3% milk powder in 10 % goat serum) for 1h at room temperature, and then avidin/biotin blocking system was used to block endogenous biotin. Avidin was applied first for 15 min, followed by rinsing with PBS; biotin was then applied for 15 min and followed by rinsing with PBS. Sections were then incubated with primary antibody in a humidified chamber for overnight at 4°C, for antibody dilutions see Table 2.7. Primary antibody was replaced by 10% goat serum in negative controls. After washing with PBS three times, sections, including negative control were incubated with secondary antibody for 25 min at room temperature. Following washing with PBS three times, sections were incubated with horseradish peroxidase (HRP) streptavidin for 25 min at room temperature in humidified chamber.

To visualise bound antibodies, sections were incubated with diaminobenzidine (DAB) for 3 min at room temperature after three washes with PBS. When the brown colour developed, slides were quickly washed in tap water (3 x 5 min) to remove DAB solution from sections. After signal visualization, Slides were counterstained with haematoxylin for 10 sec, and then washed in running tap water for 10 min. Slides were dehydrated in increasing grades of ethanol (70% for 3 min, 90% for 3 min and 100% for 5 min) and cleared in xylene (2 x 5 min). After dehydration and clearing, slides were mounted with DPX mounting medium and examined with Olympus Cyto-system microscope (Adrian Building,

University of Leicester), Olympus microscope in Lab. 227 or Olympus CX41 in Lab 228.

Table 2.7: Primary and secondary antibody dilutions for immunohistochemistry.

Primary Antibody	Dilution	Secondary Antibody	Dilution
LRP2	1:200	Swine anti-rabbit (Biotinylated)	1:400
FcRn	1:100	Swine anti-rabbit (Biotinylated)	1:200
Presenilin-1	1:50	Swine anti-rabbit (Biotinylated)	1:200
MMP-3	1:100	Swine anti-rabbit (Biotinylated)	1:200
MMP-7	1:100	Swine anti-rabbit (Biotinylated)	1:200
MMP-9	1:100	Swine anti-rabbit (Biotinylated)	1:200
F4/80	1:100	Swine anti-rabbit (Biotinylated)	1:200
TGF- β	1:50	Swine anti-rabbit (Biotinylated)	1:100
TNF α	1:50	Donkey anti-goat (Biotinylated)	1:100
IL-6	1:100	Swine anti-rabbit (Biotinylated)	1:200

2.2.15 Analysis of immunohistochemical images

Analysis of digital images was performed using ImageJ software. To quantify IHC staining, images were opened with ImageJ software and converted to 8 bit grayscale using image tool. In order to measure the intensity of DAB staining accurately in various experimental conditions, the threshold of images was set to a similar pixel using threshold settings. After thresholding, the area of DAB staining in the images was measured automatically by entering the threshold values using plugin and macros tools. ImageJ software measured the intensity of IHC staining as the percentage of the stained area. For each experiment, the DAB staining of 30 images was measured. Comparison between the intensity of IHC staining in different conditions was made using GraphPad prism 6.0.

2.2.16 TGF- β scoring

The intensity of TGF- β staining was scored blinded and classified into 4 levels: 0: no staining, 1: weak staining, 2: mild staining, 3: moderate staining, 4: intense staining (Coppola et al., 1998, Culhaci et al., 2005).

2.2.17 Histological analysis

2.2.17.1 Haematoxylin and eosin (H&E) staining

Morphological changes in mouse kidneys were evaluated using H&E staining method. In brief, paraffin embedded kidney sections were dewaxed in xylene (2 x 5 min) and rehydrated in a series of graded alcohols (100%, 90% and 70%) for 2 min each. After rinsing with D.W, slides were stained with haematoxylin (Gill No. 1, GHS132-1L, Sigma-Aldrich) for 8 min then washed in running tap water for 5 min. Sections were then differentiated in 1% acetic alcohol for 30 sec and blued in 0.2% ammonia water for 30 sec to 1 min. After washing in running tap water for 5 min, slides were stained with acidified aqueous eosin solution (Eosin Y, HT110132-1L, Sigma-Aldrich) for 30 sec to 1 min. Slides were then dehydrated through 95% alcohol for 2 min and 100% alcohol (2 x 2 min) then cleared in xylene (2 X 5 min). After dehydration and clearing, slides were mounted with DPX mounting medium and examined under Olympus CX41 microscope in Lab 228.

2.2.17.1.1 Analysis of H&E images

Tubulointerstitial injury was evaluated and scored following H&E staining. Ten non-overlapping fields at x200 magnification from each section were captured using Olympus CX41 microscope and digital camera (Q Imaging MicroPublisher 5.0 RTV) with identical illumination and exposure. According to the previous studies, tubulointerstitial injury was scored as follows: 4 for severe tubular damage; 3 for moderate tubular damage; 2 for mild tubular damage; 1 for small focal areas and 0 for normal tubules (Takase et al., 2003, Guan et al., 2013). In addition, tubular damage was scored independently and blind by two researchers in the infection, immunity and inflammation department. The scores were then statistically analysed with GraphPad prism 6.0 using unpaired t-test.

2.2.17.2 Sirius red staining

To detect collagen deposition in kidney sections, sirius red staining was performed. Shortly, paraffin embedded kidney sections were dewaxed in xylene (2 x 5 min) and rehydrated in alcohol solutions (100% (2X), 95% (2X), 70% and 50%) each for 2 min. After rinsing with D.W, sections were stained with haematoxylin for 8 min and washed for 10 min in running tap water. Slides were then incubated in picrosirius red solution (Picro-Sirius Red Stain Kit, ab150681, Abcam) for 60 min at room temperature, then rinsed quickly in 0.5% acetic acid solution (2 x 10 sec). After removing most of the water from slides by physical shaking, slides were dehydrated in absolute alcohol (3 x 1 min) then cleared in xylene and cover-slipped using mounting (DPX) medium. Collagen deposition was examined using Olympus CX41 microscope in Lab 228.

2.2.17.2.1 Analysis of sirius red staining images

Ten non-overlapping fields at x200 magnification from each section were captured with Olympus CX41 microscope and digital camera (Q Imaging MicroPublisher 5.0 RTV) with identical illumination and exposure. Analysis of captured images was performed using ImageJ software. The images were stored on 8 bit grayscale and the threshold was set using colour adjustment tool. After threshold was adjusted, the intensity of stained particles was determined with plugins software. The results were expressed as a percentage of the stained area and statistically analysed by unpaired t-test.

2.2.18 Determination of transforming growth factor beta-1 (TGFb-1) concentration in kidney homogenates

The concentration of TGFb-1 was determined in kidney homogenates using a mouse TGF- β ELISA kit (R&D Systems, DY1679-05), according to the manufacturer's instructions. The wells of a 96-well plate were coated with 100 μ l of capture antibody (mouse anti-TGFb-1 diluted in PBS to a concentration of 2mg/ml) then sealed and incubated for overnight at room temperature.

After gently aspirating the liquid from the wells, the plate was washed with wash buffer (0.05% Tween 20 in PBS, pH 7.2-7.4) three times. To remove excess wash buffer from the wells, the plate was inverted and carefully blotted onto a paper towel several times. The plate was then blocked with the blocking buffer (5% Tween 20 in PBS, pH 7.2-7.4) (300 μ l/well) for 1h at room temperature. Following incubation, the wells were then gently aspirated and washed three times with wash buffer. After removing excess wash buffer from the wells, 100 μ l of samples (kidney homogenates with protein concentration adjusted to 25 μ g) or standards (31.3, 62.5, 125, 250, 500, 1000 and 2000 pg/ml of recombinant mouse TGFb-1 prepared in reagent diluent) were added to the wells in duplicate and the plate was sealed and incubated at room temperature for 2h. Following a second aspiration and wash step, 100 μ l of detection antibody (biotinylated chicken anti-TGFb-1 diluted in reagent diluent to a concentration of 0.25 μ g/ml) were added to the wells and the plate was incubated for 2h at room temperature.

The plate content was then aspirated and the wells were washed with wash buffer three times. After removal of excess wash buffer from the wells, 100 μ l of streptavidin-HRP working dilution (1:2000 in diluent reagent) were added to the wells. The plate was then incubated in dark for 20 min at room temperature. After the last aspiration and wash step, the remaining wash buffer was removed from the wells by inverting and blotting the plate onto a paper towel.

To visualise bound antibodies, 100 μ l of substrate solution tetramethylbenzidine (TMP) were added to the wells and the plate was incubated in dark for 20 min at room temperature. The enzymatic reaction was stopped by adding 50 μ l of stop

solution (2 N H₂SO₄) to each well. The plate was read at 450nm using plate reader (TECAN, infinite F50).

2.2.19 Determination of tumour necrosis factor- α (TNF- α) concentration in kidney homogenates

A mouse TNF- α ELISA kit (R&D Systems, DY410-05) was used to determine the concentration of TNF- α in kidney lysates. The plate was prepared as described in the previous section (2.2.19). Standards (recombinant mouse TNF- α), capture antibody (goat anti-mouse TNF- α), detection antibody (biotinylated goat anti-mouse TNF- α) and streptavidin-HRP were all prepared in the same way as TGF- β and according to the manufacturer's instructions.

2.2.20 Total RNA isolation and purification

RNA was isolated from mouse kidney tissues using RNeasy® plus Mini Kit (50) (74134, QIAGEN, GmbH, Hilden, Germany) according to the manufacturer's instructions. Kidney cortices (30mg) were homogenised in 600 μ l buffer RLT containing beta-mercaptoethanol (B-ME) (10 μ l/1ml) and reagent DX (prevent foam formation during homogenization) using four strokes of the homogeniser at maximum speed for 10 sec each. The homogenates were then incubated for 2h on ice on a shaker. After incubation, the homogenates were centrifuged for 3 min at maximum speed. The supernatants were carefully collected and transferred to gDNA eliminator spin columns placed in 2 ml collection tubes then centrifuged for 30 sec at 10,000 rpm. After discarding the spin columns, 350 μ l of 70% ethanol were added to the collection tubes containing flow-throughs and mixed well by pipetting. After that, 700 μ l of the flow-through/ethanol were transferred to RNeasy spin columns placed in 2 ml collection tubes and centrifuged for 15 sec at 10,000 rpm. After discarding the flow-throughs from collection tubes, 700 μ l of buffer RW1 were added to the RNeasy spin columns and centrifuged for 15 sec at 10,000 rpm. The flow-throughs were again discarded, and the spin columns were placed into collection tubes. To wash the spin columns membrane, 500 μ l of buffer RPE were added to the RNeasy spin columns and centrifuged for 15 sec at 10,000 rpm. The second wash of the spin columns membrane was performed at the same speed for 2 min. The RNeasy spin columns were transferred to new 1.5

ml collection tubes and 30-50 μ l of RNase-free water were added directly to the spin columns membrane. To elute RNA, the RNeasy spin columns were centrifuged for 1 min at 10,000 rpm.

2.2.21 RNA integrity and quantification

The quality and quantity of RNA were determined using the Agilent 2100 Bioanalyzer system (Agilent Technologies, Inc., 76337 Waldbronn, Germany). In brief, purified RNA samples (1 μ l) were applied to an RNA Nano Chip pre-loaded with RNA Gel-Dye mixture and run on an Agilent 2100 Bioanalyzer for 25 min or following the manufacturer's instructions. RNA with RNA integrity number (RIN) more than 6 were considered to be pure.

2.2.22 Reverse transcription reaction

First-strand cDNA synthesis from total RNA was carried out using the AMV reverse transcriptase system (Reverse Transcription System, A3500, and Promega, USA), according to the manufacturer's instructions. Briefly, 1 μ g of total RNA was transferred to a sterile RNase-free microfuge tube and incubated at 70°C for 10 min. After incubation, the tube was centrifuged briefly and placed on ice. To prepare a 20 μ l transcription reaction, the following components (4 μ l of 25mM MgCl₂, 2 μ l of reverse transcription 10X buffer, 2 μ l of 10 mM dNTP mixture, 0.5 μ l of recombinant RNasin ribonuclease inhibitor, 0.6 μ l of AMV reverse transcriptase, 1 μ l of Oligo (dT)₁₅ primer and 7.9 μ l of RNase free water) were mixed and added to the first tube containing RNA. The reaction was then incubated at 42°C for 15 min, then heated for 5 min at 95°C and incubated on ice for 5 min for direct use or stored in -20°C for later use.

2.2.23 Quantitative real-time PCR (qPCR)

qPCR was conducted using an Applied Biosystems 7500 fast qPCR according to the standard procedures. qPCR reactions contained 10 μ l TaqMan Universal PCR Master Mix, 1 μ l of specific TaqMan® Gene Expression Assay Mix, 4 μ l cDNA template and RNase free water to make a final volume of 20 μ l. After initial hold at 50°C for 2 min and initial denaturation at 95°C for 10 min, qPCR reactions were run for 40-55 cycles consisting of denaturation at 95°C for 15 sec and annealing/extension at 60°C for 60 sec. All samples were analyzed in

duplicates. The negative control contained water instead of cDNA. To compensate differences in the amount of RNA input and the efficiency of reverse transcriptase, transcript abundance of the housekeeping gene, GAPDH was also quantified.

Results were calculated using 7500 Software v2.0.6, Applied Biosystems and Microsoft Office Excel 2007. The Ct values of the housekeeping gene were used to normalize the Ct values of control and treatment samples. The Ct values of GAPDH were not changed by treatments. Relative changes in mRNA abundance was quantified using the $2^{-\Delta\Delta Ct}$ method.

2.2.24 MMP assays

Fold difference in MMP enzymatic activity was determined using the MMP activity assay kit (Fluorometric-Green, Abcam, ab112146), which measures the activity of a variety of MMPs, including MMP-1,2,3,7,8,9,10,11,12,13 and 14. Briefly, 50µl of kidney lysates with the protein concentration adjusted to 25µg, was pipetted in duplicates into the wells of 96 well plate and incubated for 15 min at room temperature. 50 µl of MMP green substrate solution was then added to each well and the plate was then covered and incubated at room temperature for 1h in the dark. The plate was read at an excitation 490 nm and an emission 525 nm using VarioskanFlash plate reader. The RFUs were then used to compare the MMPs activity between the groups.

2.2.25 Data analysis

The data were statistically analysed using GraphPad prism 6.0 and 7.0 (GraphPad Software, Inc., California, USA). All data are reported as mean \pm SEM. To determine between group differences, unpaired t-test or analysis of variance (ANOVA) with Tukey's multiple comparisons test was performed. Statistical significance was accepted at $p < 0.05$.

3 Expression of Tubular Protein Receptors in Normal and Proteinuric Mice

3.1 Introduction

Prolonged proteinuria may have an important contribution to the progression of CKD due to chronic loss of the kidney function. In the kidney ultrafiltered proteins from glomeruli are largely reabsorbed by RME and therefore they are protected from being excreted into the urine. The most involved receptors in this process are the large receptor megalin and its co-expressed FcRn (Christensen and Birn, 2001, Christensen et al., 2009, Tenten et al., 2013, Sand et al., 2015). There is no clear data showing that these receptors are affected in POP or even in normal state their expression has not been studied clearly previously. However in vitro studies and in other diseases like DN or animal models of CKD the expression of megalin has shown to be downregulated in the PT. It has been demonstrated that the expression of megalin is downregulated in the PTEC incubated with high albumin concentrations in vitro (Caruso-Neves et al., 2006, Cabezas et al., 2011).

In animal models of kidney disease the expression of megalin has been shown to be downregulated in the PTECs. For example, in diabetic rats, the expression of megalin is reduced and this was accompanied by decreased reabsorption of albumin in the PTECs (Akihiro et al., 2003). Megalin expression is also found to be down regulated in aged rats, as LMW proteinuria has been detected in these animals (Odera et al., 2007). Further, in a transgenic mouse (RenTg mic) model which exhibits characteristic features of CKD, the expression of megalin is down regulated alongside the expression of other proteins (Huby et al., 2009). In rats with early stages of DN, increased urinary excretion of LMW proteins are associated with decreased megalin expression and function (Tojo et al., 2001).

Therefore, the main objective of this chapter is to study the expression and shedding of megalin and FcRn in the kidney of normal and proteinuric mice in a mouse model of POP.

3.2 Results

3.2.1 Effects of POP on kidney function

The effect of POP on serum creatinine levels is shown in Figure 3.1. As demonstrated, the concentration of serum creatinine was increased significantly in POP mice ($40.22 \pm 1.57 \mu\text{mol/L}$) compared to saline-injected control mice ($25.34 \pm 1.76 \mu\text{mol/L}$). These data indicate that POP reduces kidney function in uni-nephrectomised mice.

3.2.2 Effects of POP on serum total protein concentration

The effect of POP on serum total protein concentration is shown in Figure 3.2. Administration of 15mg/g BSA for 14 days caused a significant increase in serum total protein concentration ($39.71 \pm 2.71 \text{ mg/ml}$) in comparison to saline-injected controls ($23.89 \pm 0.78 \text{ mg/ml}$).

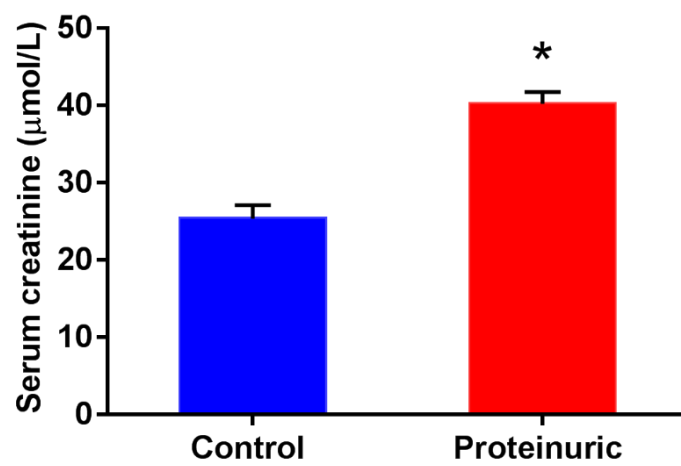


Figure 3.1: Effect of POP on serum creatinine level in uni-nephrectomised mice. Serum creatinine levels were measured in saline-injected control mice or POP mice. Results are expressed as mean \pm SEM of 5 mice per group. * $P < 0.05$ compared with saline-injected control group (t test).

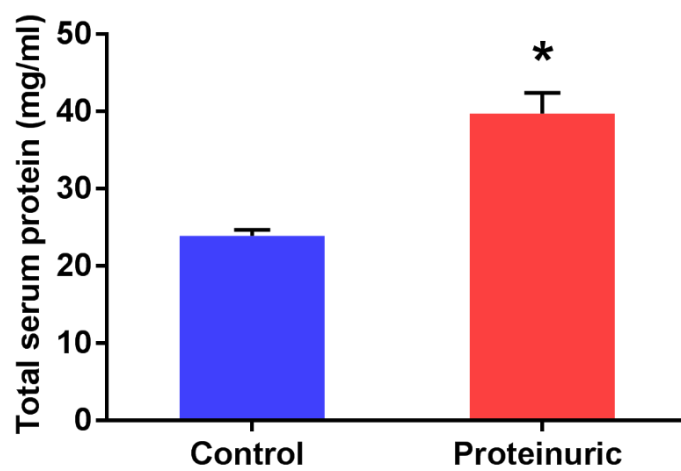


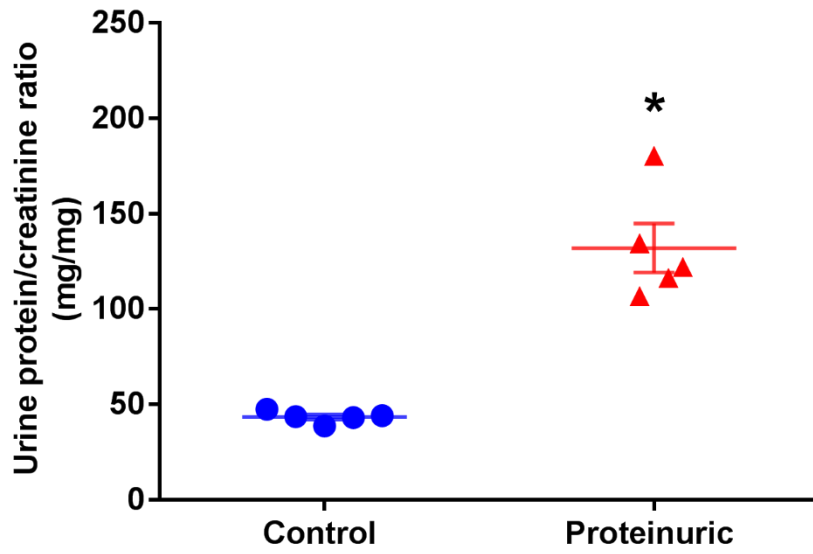
Figure 3.2: Effect of POP on serum total protein level in uni-nephrectomised mice. Serum total protein levels were measured in saline-injected control mice or POP mice. Results are expressed as mean \pm SEM of 5 mice per group. * $P < 0.05$ compared with saline-injected control group (t test).

3.2.3 Proteinuria in mice following unilateral nephrectomy with POP

To determine whether POP had an effect on kidney function and induced proteinuria in mice, the protein concentration was measured in the urine of saline-injected controls and POP mice using Bradford protein assay. The protein concentration in the urine was normalised to urine creatinine concentration. Following BSA overload at day 14, uni-nephrectomised mice exhibited significantly increased proteinuria (132 ± 12.87 mg/mg creatinine) to levels significantly greater than those seen in uni-nephrectomised, saline treated mice (43.43 ± 1.39 mg/mg creatinine) (Figure 3.3A).

To further investigate whether megalin and FcRn ligands were found in the urine of BSA treated mice, urine samples normalised to $2\mu\text{g}$ creatinine were electrophoresed on 10% SDS-PAGE and the gel was stained with Coomassie blue for the detection of separated proteins. Large quantities of both high and low molecular weight proteins were evident in the urine of BSA treated mice (Figure 3.3B). Saline-treated controls had very low levels of high and low molecular weight proteins in their urine (Figure 3.3B). More specifically, at approximately 66 kDa a very clear band was identified which was at the same molecular size of albumin loaded as a positive control (Figure 3.3B).

A



B

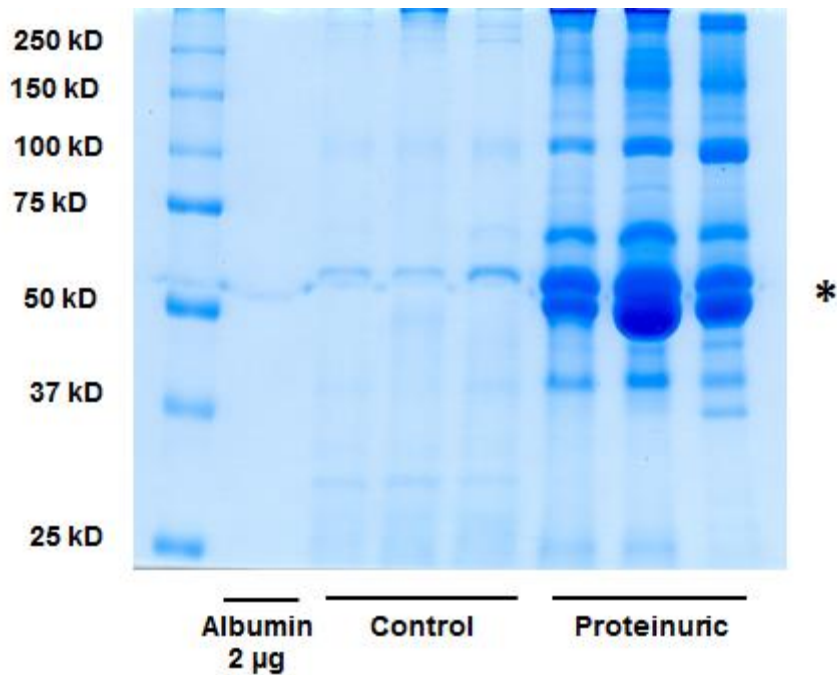


Figure 3.3: Urinary protein excretion in saline-treated control and POP mice. A) Quantitative measurement of proteinuria in saline-injected control mice and POP mice. Results are expressed as mean \pm SEM of 5 mice per group. * $P < 0.05$ compared with saline-treated control group (t test). B) Representative SDS-PAGE analysis of urine samples from saline-treated control mice and POP mice stained with Coomassie blue. Asterisk indicates albumin band.

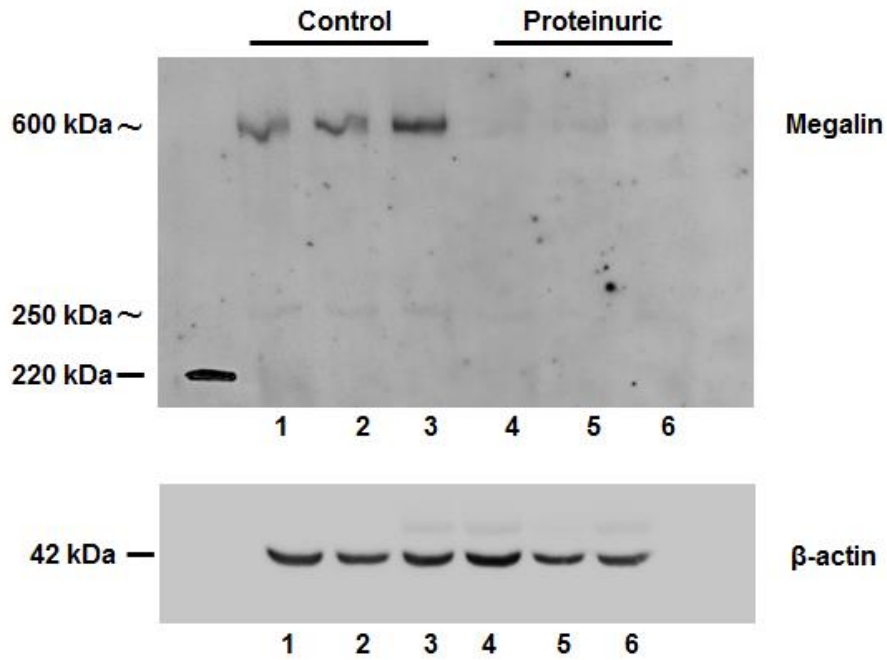
3.2.4 Protein expression of megalin in the kidneys of POP mice

To determine whether megalin protein expression is affected by POP, kidney tissues from saline-injected control and POP mice were analysed using WB and IHC. WB results revealed a significant decrease in megalin protein expression in POP mice (0.31 ± 0.12 relative intensity) compared to saline-injected control mice (2.38 ± 0.25 relative intensity) (Figure 3.4B). Figure 3.4A shows megalin bands in kidney tissue from saline-treated control and POP groups. The anti-LRP-2 antibody recognised protein bands at approximately 600 kDa. The megalin bands in the POP group were very faint in comparison to very prominent megalin bands in saline-treated control group. The intensity of megalin bands was determined using ImageJ software, and normalised to the intensity of β -actin bands (Figure 3.4B).

To confirm WB results, IHC analysis was performed. Figure 3.5 shows kidney localisation and expression of megalin in saline-treated control and POP mice. As demonstrated, megalin is mostly expressed at the apical membrane of the PTEC. The brown staining which represents megalin expression was very weak in POP group (Figure 3.5C) compared to very strong megalin staining in saline-injected control group (Figure 3.5B). No megalin staining was detected when the primary antibody was omitted as a negative control (Figure 3.5A). To quantify megalin expression, the intensity of brown staining was measured using ImageJ software (Figure 3.6). According to ImageJ analysis, megalin expression was decreased significantly in POP group (3.41 ± 0.52 % stained area) compared to saline-treated control group (8.33 ± 1.08 % stained area).

Both WB and IHC results showed that POP has a significant negative effect on the protein expression of megalin in the PT of the kidney.

A



B

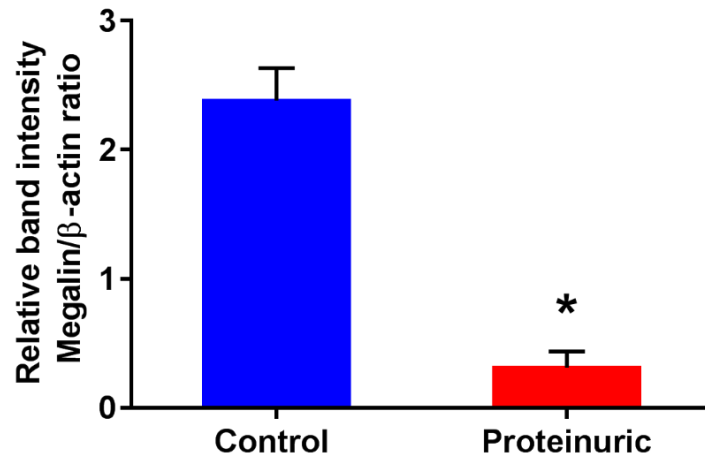


Figure 3.4: Effect of POP on renal megalin protein expression in uninephrectomised mice. A) Expression of megalin in kidney tissues from mice treated with BSA or saline was evaluated by western blot analysis. B) Densitometric analyses for megalin are presented as the relative ratio to β -actin. Results are expressed as mean \pm SEM of 3 mice per group. * $P < 0.05$ compared with saline-treated control mice (t test).

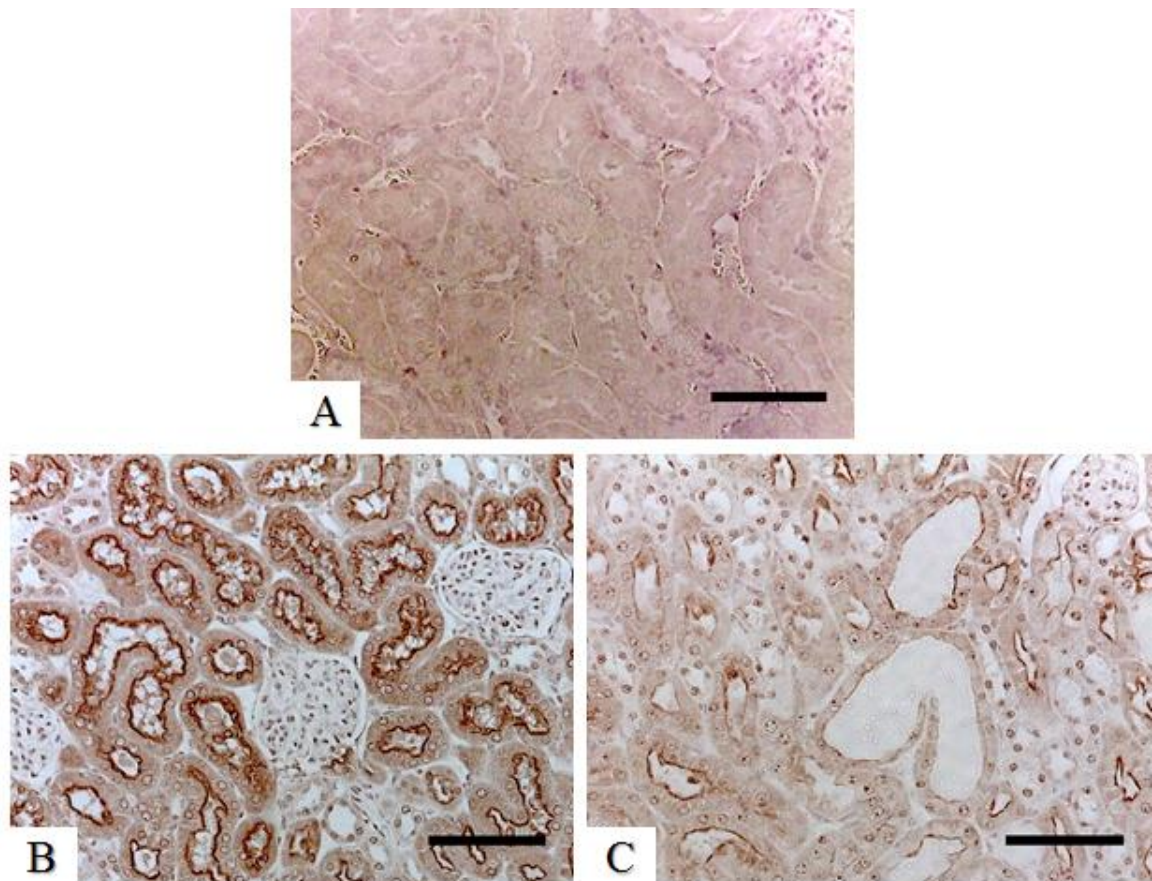


Figure 3.5: Expression of megalin in the cortex of kidneys from saline-injected control and POP mice. Representative photomicrographs showing megalin localisation and expression in the kidney of saline-injected control mice (B) or POP mice (C). (A) Negative control without primary antibody. Scale bar: 100 μ m.

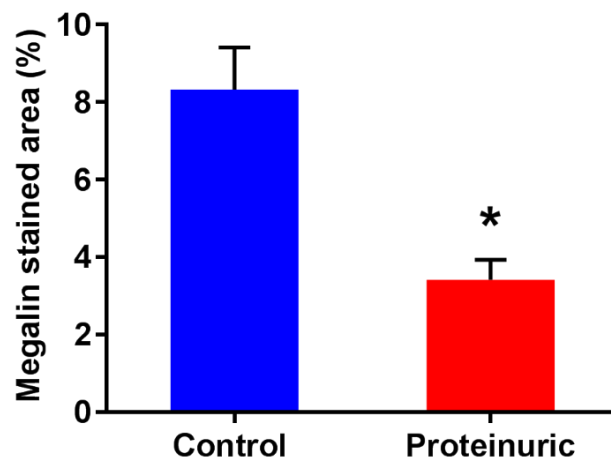


Figure 3.6: Quantification of renal megalin staining in saline-treated control and POP mice. Megalin staining was performed 14 days after BSA administration and quantified using ImageJ software and expressed as (%). Results are expressed as mean \pm SEM of 5 mice per group. * $P < 0.05$ compared with saline-treated control group (t test).

3.2.5 mRNA expression of megalin in the kidney of POP mice

To determine whether the levels of megalin mRNA are altered in the PTs of uninephrectomised mice treated with BSA, quantitative PCR (qPCR) analysis was used. Total RNA was isolated from kidney tissues of saline-treated control and POP mice (n=5 each group). The threshold cycle (Ct) values were determined using 7500 software system (Applied Biosystems) and normalised by subtracting the Ct values of the GAPDH. Figure 3.7 shows megalin mRNA expression expressed as fold change. Surprisingly, the mRNA expression of megalin was significantly increased (2.87 ± 0.29 fold increase) in POP mice compared to saline-treated control mice. These results indicate that down-regulation of megalin protein evaluated by WB and IHC analysis is not related to the mRNA levels in the kidney.

In order to exclude contamination by genomic DNA as an explanation for these results, the quality of RNA was checked by 2100 expert_Eukaryote Total RNA Nano system. The integrity of RNA in all samples is shown in Table 3.1. The all samples showed a high purity range of 6.2-9.3 and even in most of the samples the integrity of RNA was very close to the standard RNA integrity number (RIN) 10. In addition, gel electrophoresis revealed that RNA degradation was entirely absent in all of the samples and two clear bands at approximately of 18S and 28S ribosomal RNA were visualised (Figure 3.8).

Table 3.1: RNA integrity number in 10 samples from mouse kidney analysed by 2100 bioanalyzer (Agilent Technologies).

Samples	1	2	3	4	5	6	7	8	9	10
RIN	9	9.1	9	9.2	7.3	8.6	9.3	9	6.2	8.6

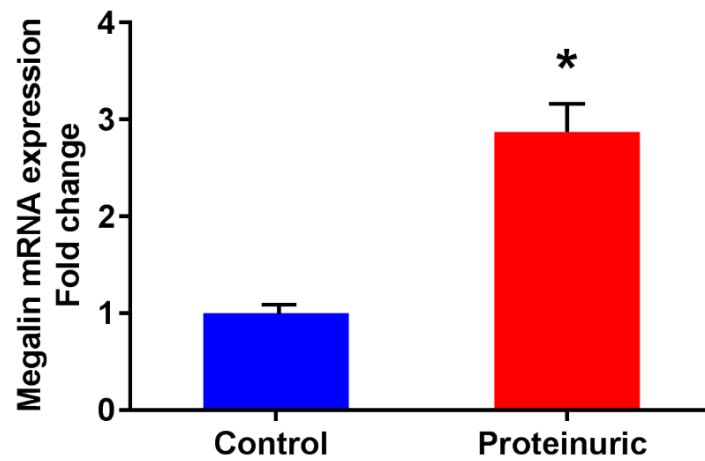


Figure 3.7: Effect of POP on renal megalin mRNA expression in uni-nephrectomised mice. Megalin mRNA levels were determined in saline-treated control mice or POP mice using qPCR analysis. Results are expressed as mean \pm SEM of 5 mice per group. * $P < 0.05$ compared with saline-injected control group (t test).

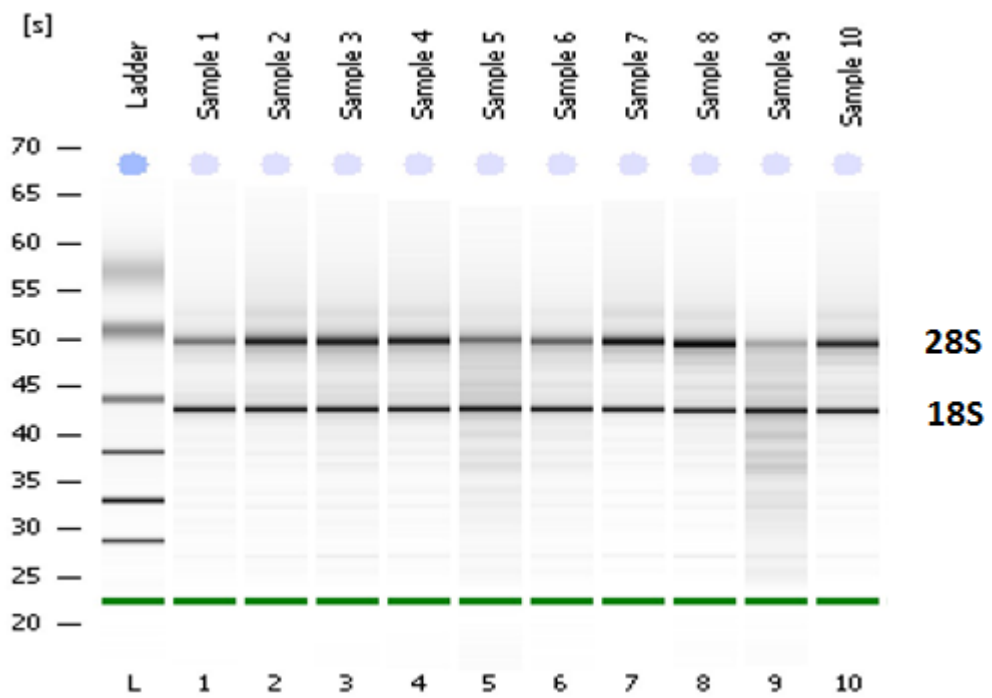


Figure 3.8: Gel electrophoresis of total RNA isolated from mouse kidney. Two clear bands in each sample were detected at 18S and 28S ribosomal RNA.

3.2.6 Urinary excretion of megalin in saline-treated control and POP mice

To investigate whether POP leads to urinary excretion of megalin, urine samples from saline-injected control and POP mice were analysed for the presence of megalin using ELISA. Figure 3.9 shows megalin excretion into the urine of saline-treated control and POP mice. The concentration of megalin in urine samples was normalised to urinary creatinine. As shown, BSA administration to uni-nephrectomised mice for two weeks caused a significant increase ($1.26 \pm 0.24 \mu\text{g}/\text{mg}$ creatinine) in urinary megalin excretion in comparison to the very low levels of megalin detected in the urine of saline-injected control animals ($0.04 \pm 0.01 \mu\text{g}/\text{mg}$ creatinine).

To support the ELISA results, silver staining and WB analysis were performed. Unfortunately, none of the above techniques was able to show clear results of megalin excretion in the urine of mice. Results of WB analysis and silver staining are shown in Figure 3.10. Rabbit polyclonal anti-LRP2 antibody recognised very faint bands at approximately 600 kDa, corresponding to the same molecular size of megalin (Figure 3.10A). These bands were only found in the urine of POP animals. In addition, silver staining revealed very faint bands at different molecular weights below 600 kDa (Figure 3.10B). Altogether, these data indicate that reduced megalin protein expression in POP animals might be caused by increased urinary excretion of megalin in these animals.

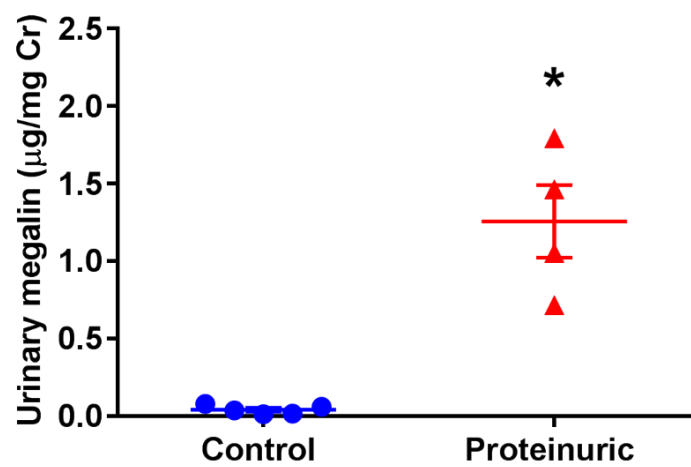


Figure 3.9: Urinary excretion of megalin in saline-treated control and POP mice. Urinary megalin excretion was determined in saline-injected control mice or POP mice using ELISA. Results are expressed as mean \pm SEM of 5 mice per group. * $P < 0.05$ compared with saline-treated control group (t test).

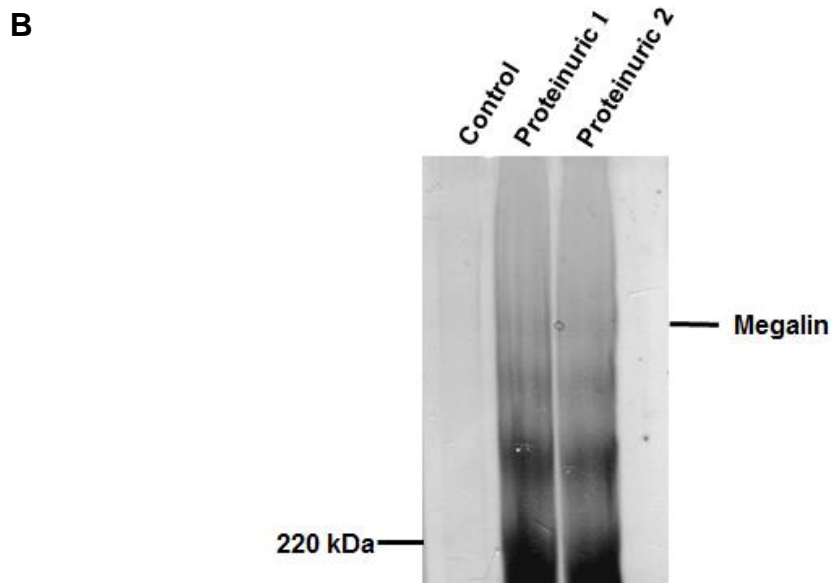
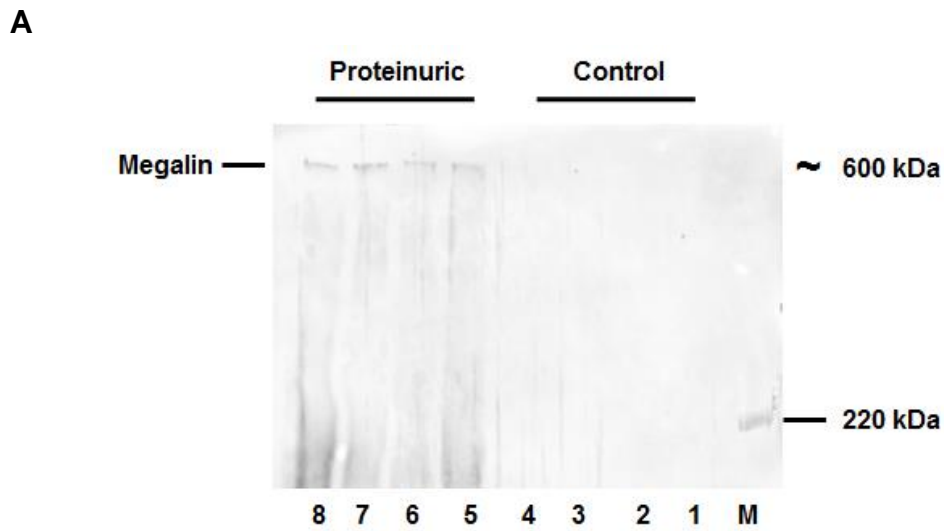


Figure 3.10: PAGE and WB of urine from saline-treated control and POP mice. Representative western blot (A) and silver staining (B) showing urinary megalin excretion in saline-treated control mice and POP mice. Very faint bands were detected in the urine of POP mice. No bands were detected in the urine of saline-injected control animals.

3.2.7 Protein expression of FcRn in the kidneys of saline-treated control and POP mice

In order to determine the effects of POP on FcRn protein expression in PTEC, kidney tissues from saline-treated control and POP mice were analysed using WB and IHC. WB results showed that FcRn expression was significantly decreased in POP mice (0.33 ± 0.11 relative intensity) compared to saline-treated control mice (1.04 ± 0.13 relative intensity). Figure 3.11A shows FcRn bands in saline-injected control and POP mice. FcRn antibody recognised protein bands at approximately 42 kDa. The intensity of FcRn bands in each sample was analysed using ImageJ and normalised to the intensity of β -actin bands (FcRn to β -actin ratio) (Figure 3.11B).

To confirm WB results, IHC analysis was performed. Figure 3.12 shows kidney localisation and expression of FcRn in saline-treated control and POP mice. As demonstrated, FcRn is expressed in both the glomeruli and the PTs of mouse kidney. The brown staining representing FcRn expression in PT was very weak in POP group (Figure 3.12C) compared to the much more prominent FcRn staining in saline-treated control group (Figure 3.12B). No FcRn staining was detected in the negative control sections where primary antibody was omitted (Figure 3.12A).

To quantify FcRn expression, staining was measured using ImageJ software (Figure. 3.13). Using ImageJ, the expression of FcRn was decreased significantly in POP group (1.08 ± 0.07 % stained area) compared to saline-treated control group (4.67 ± 0.47 % stained area). Both WB and IHC results confirmed that POP reduces FcRn protein expression in the PTs of the kidney.

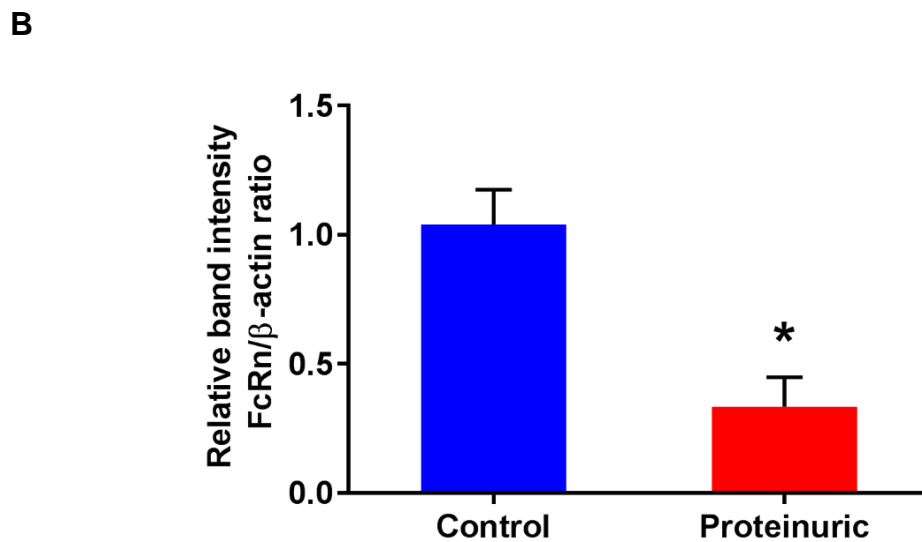
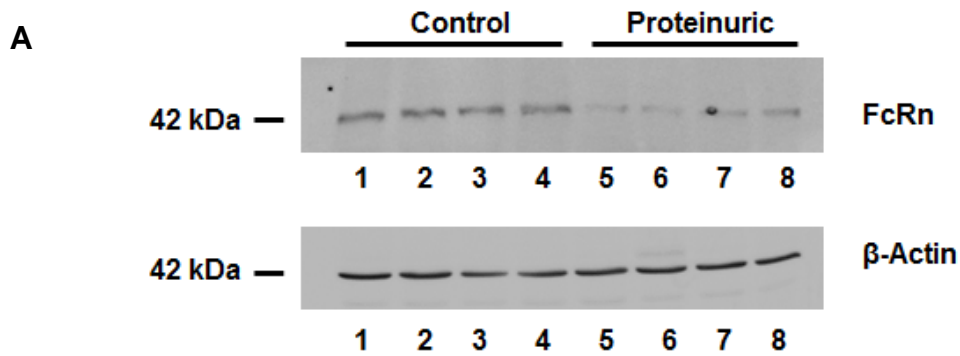


Figure 3.11: Effects of POP on renal FcRn protein expression in uninephrectomised mice. A) Expression of FcRn in kidney tissues from mice treated with BSA or saline was evaluated by western blot analysis. B) Densitometric analysis for FcRn are presented as the relative ratio to β -actin. Results are expressed as mean \pm SEM of 4 mice per group. * $P < 0.05$ compared with saline-injected control group (t test).

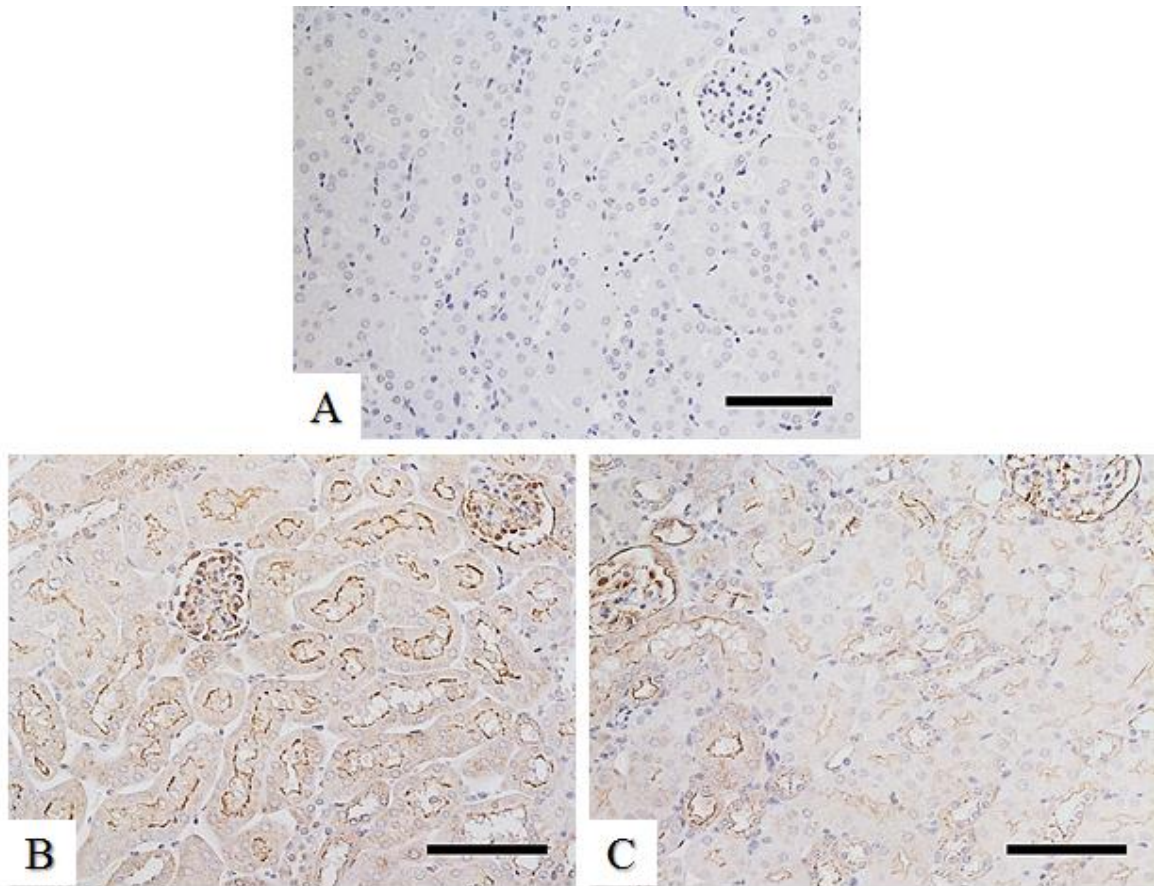


Figure 3.12: Expression of FcRn in the cortex of kidneys from saline-treated control and POP groups. Representative photomicrographs showing FcRn expression and localisation in the kidney of saline-injected control mice (B) or POP mice (C). (A) Negative control without primary antibody. Scale bar: 100 μ m.

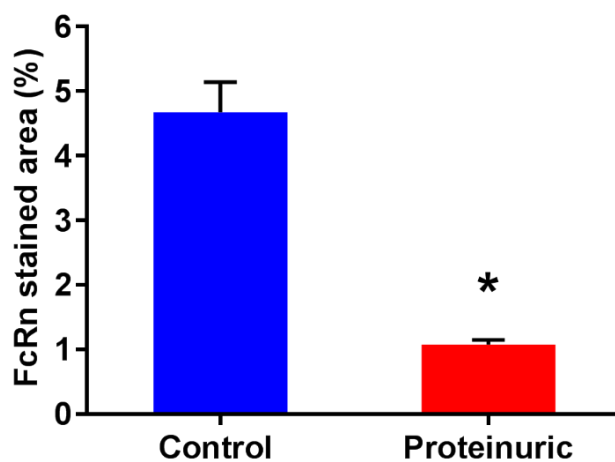


Figure 3.13: Quantification of renal FcRn staining in saline-treated control and POP groups. FcRn staining was performed 14 days after BSA administration and quantified using ImageJ software and expressed as (%). Results are expressed as mean \pm SEM of 5 mice per group. * $P < 0.05$ compared with saline-treated control mice (t test).

3.2.8 mRNA expression of FcRn in the kidney of POP mice

Quantitative PCR analysis was used to determine whether the mRNA levels of FcRn are altered in the PT cells of POP mice. Figure 3.14 shows the mRNA levels of FcRn expressed as fold change. As shown, the mRNA levels of FcRn were increased significantly in POP group (2.29 ± 0.19 fold increase) compared to saline-treated controls. Based on qPCR results there was no correlation between the protein and gene expression of FcRn in POP mice.

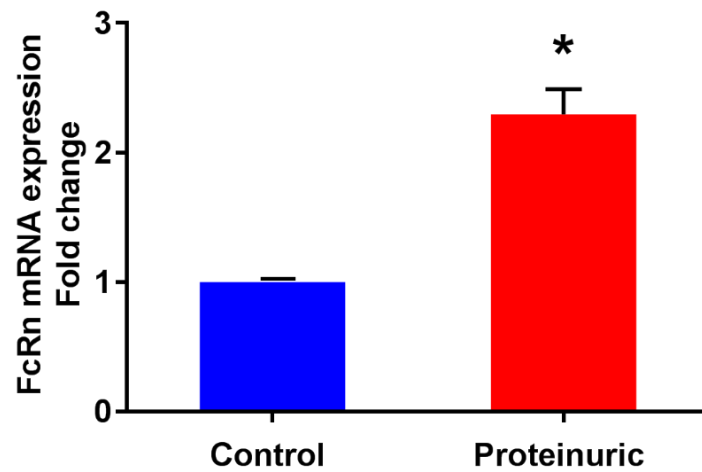


Figure 3.14: Effect of POP on renal FcRn mRNA expression in uni-nephrectomised mice. FcRn mRNA levels were determined in saline-treated control mice or POP mice using qPCR analysis. Results are expressed as mean \pm SEM of 5 mice per group. * $P < 0.05$ compared with saline-injected control group (t test).

3.2.9 Urinary excretion of FcRn by proteinuric mice

ELISA was used to determine whether the urine of POP mice contained the FcRn receptor. Urine samples from 5 saline-treated control animals were also analysed for the presence of FcRn. Figure 3.15 shows the amount of FcRn excreted into the urine of uni-nephrectomised mice. The concentration of FcRn in the urine was normalised to urinary creatinine. As shown, urinary excretion of FcRn was significantly increased in BSA-treated animals (1.62 ± 0.32 ng/mg creatinine) compared to saline-treated controls (0.3 ± 0.08 ng/mg creatinine). To confirm ELISA results, WB analysis was also performed. However, WB analysis was not able to show any immunoreactivity between anti-FcRn antibody and the FcRn protein if found in the urine of animals.

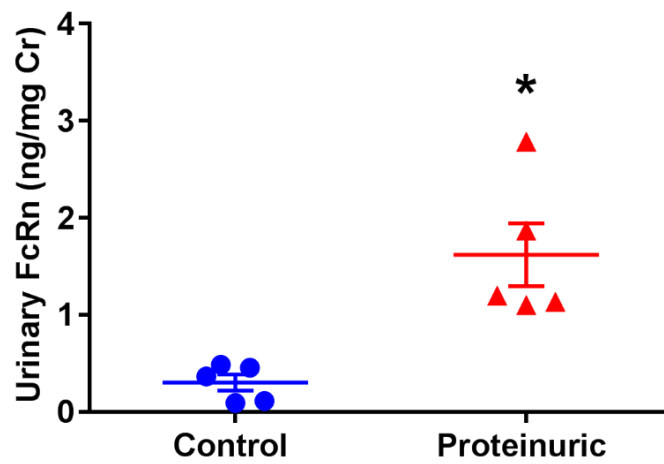


Figure 3.15: Urinary FcRn excretion in saline-treated control and POP mice. Urinary FcRn excretion was determined in saline-injected control or POP mice using ELISA. Results are expressed as mean \pm SEM of 5 mice per group. * $P < 0.05$ compared with saline-treated control group (t test).

3.3 Discussion

The results of the present study demonstrate that the expression of endocytic receptors are reduced at the apical membranes of the PTEC in proteinuric mice. In the current work, POP produced similar phenotypic results as described in the previous studies in mice (Eddy et al., 2000, Donadelli et al., 2003, Ishola et al., 2005), with a small rise in serum creatinine and an early significant rise in urinary protein excretion. Despite the presence of other mouse models such as adriamycin model that cause proteinuria by damaging the glycocalyx layer of glomerular endothelial cells (Jeansson et al., 2009), the POP model is closely associated with tubulointerstitial damage and is a non-immune and non-glomerular injury model (Eddy et al., 1995). In addition, the POP model allows to study the effect of ultrafiltered proteins such as albumin on the protein expression of endocytic receptors more effectively due to increased transcapillary movement of albumin into the urinary space.

In the present study, animals were injected with low endotoxin BSA to minimise tubular injury but it could be albumin bound to fatty acids that have more effect on the tubular damage and kidney injury (Kamijo et al., 2002, Thomas et al., 2002).

The effect of protein overload on megalin and FcRn expression appeared after 14 days of BSA administration. The protein downregulation of both megalin and FcRn was observed in PTEC of proteinuric animals. Whereas, the mRNA expression of megalin and FcRn are increased in the PTEC. Both receptors are detected in the urine of proteinuric mice in significant amount compared to saline-treated control animals.

In both proteinuric patients and animal models of kidney disease, increased urinary excretion of megalin has been documented by the previous researchers. In patients with early DN, the extracellular domain of megalin is detected in the urine and with the progression of this disease or in progressive DN the majority of megalin found in the urine is the full-length form of megalin (Thrailkill et al., 2009b, Ogasawara et al., 2012). In a mouse model of type1 diabetes, the expression of proximal tubular receptor megalin was reduced (Coffey et al., 2015). In diabetic Goto-Kakizaki rats, the PT expression of megalin is reduced

and was attenuated by the sulfonyleurea and gliquidone, which also reduces proteinuria in these animals (Ke et al., 2014).

Despite the tubular protein expression of megalin remained unchanged, strong correlation between urinary excretion of megalin and both proteinuria and severity of glomerular injury was recorded in IgA nephropathy (Seki et al., 2014). It appears that megalin expression, like in IgA nephropathy, did not alter in patients with MN ((Seki et al., 2014). Megalin was also observed in the urine of proteinuric dogs alongside other proteins in a model of Alport disease (Vinge et al., 2010).

Although these studies indicate that the increased urinary megalin excretion is associated with proteinuria-induced tubular injury (Remuzzi, 1999, Baines and Brunskill, 2011) in several proteinuric diseases, some proximal tubular disorders showed no correlation with the urinary loss of this receptor. In Fanconi syndrome produced as a result of nephropathic cystinosis, in addition to abnormal tubular functioning, the expression of megalin seemed not affected in the proximal tubular segments (Wilmer et al., 2008), and in both Dent's disease and Lowe syndrome urinary excretion of megalin showed no difference compared to normal individuals (Norden et al., 2002).

In contrast to the present study, Hathaway et al. (2015) have reported that megalin mRNA is downregulated in the kidney of Akita diabetic mice that are genetically modified to over-express TGF β 1. Our finding of increased megalin mRNA levels in proteinuric mice may be explained by the age difference and the duration of proteinuria in these animals compared to the Akita diabetic mice. In their study, Hathaway and colleagues used Akita mice that were 40 weeks, diabetic with a long duration of proteinuria, whereas the current work employed BALB/c mice that were 11 weeks, non-diabetic and proteinuric for two weeks. Therefore, the increased megalin mRNA expression in the early proteinuria could likely be downregulated in the later disease.

The expression of FcRn in the PTEC has been described previously (Haymann et al., 2000), and the role of this receptor in the transcytosis of albumin and immunoglobulin by podocytes and in the PT has only recently been identified (Tenten et al., 2013, Sand et al., 2015), therefore mice lack FcRn show

significant albuminuria. There are currently no data available on the modulation of this receptor in proteinuria, nor on urinary excretion of FcRn.

Although the mechanisms of megalin gene expression regulation in proteinuric kidneys are not clear yet, this receptor appears to be positively regulated at both gene and protein expression in the PTEC by peroxisome proliferator-activated receptor (PPAR) transcription factor α and γ (Cabezas et al., 2011). It was demonstrated, using agonists of PPAR α and γ the reduced expression of megalin gene and protein in the PTEC of proteinuric rats was upregulated indicating the role of PPAR α and γ in the regulation of megalin at the PT (Cabezas et al., 2011). However other studies showed activation of PPAR γ in the PTEC in proteinuric conditions (Arici et al., 2003) which give a good explanation for the upregulation of megalin mRNA expression in the kidney samples from POP mice. The expression of FcRn may be regulated through different inflammatory mediators in various tissues (Kuo et al., 2010), but currently there is no evidence showing the regulation of this receptor in the kidney under proteinuric conditions.

The reduced expression of megalin at the apical membrane of the PTEC could also be related to the significant urinary loss of this receptor. Megalin like other large transmembrane receptors has shown to undergo RIP (Lal and Caplan, 2011, Zou et al., 2004). In this process, the extracellular domain of megalin is cleaved by the PKC-regulated MMP activity and released into the urine, and leaves an intracellular domain which become a substrate for γ -secretase to form a soluble intracellular domain that may involve in the regulation of transcriptional genes (Zou et al., 2004, Li et al., 2008, Yuseff et al., 2007, Biemesderfer, 2006). Therefore, the presence of significant amount of megalin in the urine of POP mice, and the overall reduction of this receptor despite the increased mRNA expression in the PTEC observed in the current work could be explained by the RIP of megalin.

The existence of protein in the urine, particularly albumin is considered to be the result of both glomerular permselectivity and tubular reabsorption and this topic is under the debate (Comper et al., 2008, Peti-Peterdi, 2009, Dickson et al., 2014). There is currently evidence that inhibited tubular re-absorption of filtered

proteins contributes significantly to proteinuria in disease suggesting that losing glomerular permselectivity is not the only reason for increased urinary excretion of proteins (Comper et al., 2008, Dickson et al., 2014). Although the present study could not distinguish between the increased glomerular leakage and / or decreased PTEC re-absorption of proteins via megalin and FcRn, reduced tubular re-absorption of filtered proteins as a result of reduced expression of these endocytic receptors could likely be a part of the increased protein particularly albumin in the urine of proteinuric mice.

Finally, the results demonstrated that the expression of endocytic receptors are downregulated in the PTEC of proteinuric animals by the proposed mechanism RIP, but there might be other mechanisms such as phosphorylation of megalin cytoplasmic tail could regulate the protein and gene expression of these receptors particularly megalin in the PTEC of POP animals.

3.4 Summary

In this chapter, the expression and urinary shedding of endocytic receptors by PTEC are presented. As demonstrated the urinary shedding of the major endocytic receptors for glomerular filtered proteins is increased in proteinuric mice resulting in reduced expression of megalin and FcRn at the apical membrane of the PT. The results presented herein are very similar to the previously published data in human with the possible link between the urinary excretions of these receptors to the mechanisms of their downregulation in the PT. In addition, urinary excretion and reduced expression of endocytic receptors are best correlated with the urinary excretion of filtered proteins such as albumin in proteinuric mice.

3.5 Conclusions

- POP led to a significant reduction in renal function.
- Increased glomerular filtration of plasma proteins due to protein overload produced significant change in the protein and gene expressions of endocytic receptors, megalin and FcRn in the PTEC.
- Parallel with increased urinary protein excretion, significant amount of megalin and FcRn in the urine of proteinuric mice may contribute to the reduced apical membrane expression of these receptors in the kidney.

4 Expression and Shedding of Proximal Tubular Receptors and the Effect of Matrix Metalloproteinase Inhibition in Proteinuria

4.1 Introduction

In the previous chapter, the results have demonstrated that megalin and FcRn are markedly reduced in the kidney PT of proteinuric mice. Likely, the previous investigators have noticed the downregulation of these receptors especially megalin in the kidney of proteinuric and diabetic animals. Cabezas et al. (2011) have shown that megalin was downregulated in the Kidney of proteinuric mice. In diabetic rats, the expression of megalin is reduced and this was accompanied by decreased reabsorption of albumin in the PTEC (Akihiro et al., 2003). In rats with early stages of DN, increased urinary excretion of LMW proteins are associated with decreased megalin expression and function (Tojo et al., 2001).

Recent studies have also reported that megalin is shed in significant amount into the urine of patients with DN. In type 2 diabetes, both full length and ectodomain part of megalin were found in the urine in large quantities and increased urinary megalin excretion was parallel with increased albuminuria in these patients (Ogasawara et al., 2012). Similarly, megalin shedding is aberrantly increased in type 1 diabetes and was associated with increased albuminuria (Thrailkill et al., 2009b). In addition, the urine from patients with IgA nephropathy and MN contained high amounts of megalin (Seki et al., 2014).

The PT downregulation and presence of megalin in the urine of proteinuric animals and humans might be linked to RIP of this receptor in the kidney, which has been studied by previous researchers (Biemesderfer, 2006). There is no evidence that RIP occurs in proteinuric conditions, therefore the aim of the present work was to investigate whether RIP is activated in the POP model. Because RIP is dependent on MMP activity, the objectives were to: 1. study whether MMP activity is increased in POP and if so, 2. whether inhibition of these enzymes could protect ectodomain shedding and preserve cell surface expression of megalin in POP.

4.2 Results

4.2.1 Effect of POP on MMP activity in uni-nephrectomised mice

To determine whether POP activated renal MMPs, extracted proteins from kidney tissues were analysed for MMP activity using a fluorometric protein assay. The protein concentration in all the samples was adjusted to 25µg. Figure 4.1 shows the effect of POP on the MMP activity in mouse kidney. BSA administration resulted in a significant increase (1483 ± 69.51 RFUs) in MMPs activity compared to saline-treated controls (550.9 ± 26.39 RFUs).

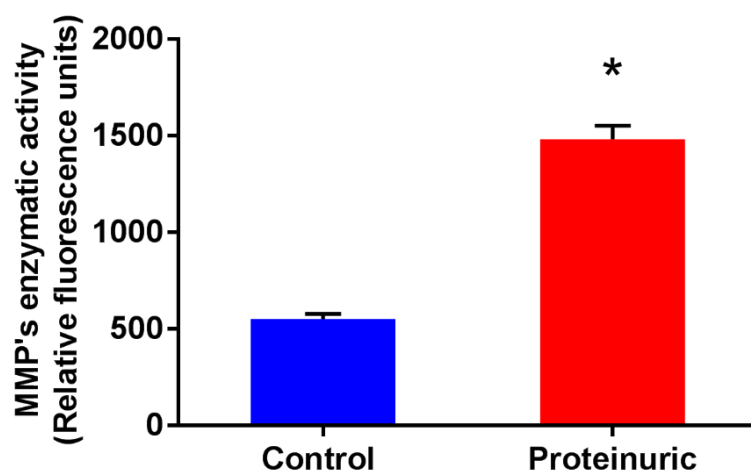


Figure 4.1: Effect of POP on MMP activity in uni-nephrectomised mice. MMP activity was measured in saline-treated control mice or POP mice using a fluorometric assay. Results are expressed as mean \pm SEM of 5 mice per group. * $P < 0.05$ compared with saline-treated control group (t test).

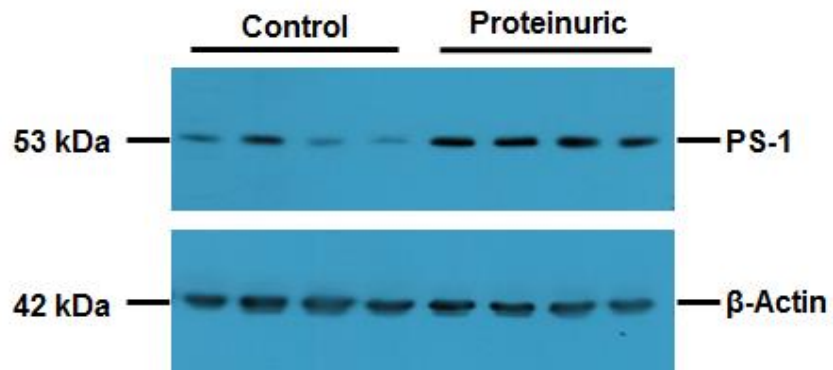
4.2.2 Effect of POP on γ -secretase activity in uni-nephrectomised mice

In order to investigate whether POP increased the level of γ -secretase, kidney tissues from saline-treated control and POP mice were analysed for the presence of presenilin-1 (PS-1) using WB and IHC.

WB results revealed a significant increase in PS-1 expression in POP mice (0.96 ± 0.09 relative intensity) compared to saline-injected control mice (0.25 ± 0.09 relative intensity). Figure 4.2A shows PS-1 bands in saline-treated control and POP mice. The PS-1 bands are fainter in saline-treated control samples compared to the PS-1 bands seen in POP samples. The intensity of protein bands were measured and normalised to the intensity of β -actin bands using ImageJ software (Figure 4.2B).

To confirm WB results, IHC analysis was performed. Figure 4.3 shows kidney localisation and expression of PS-1 in the kidney of saline-injected control and POP mice. In saline-treated control mice, PS-1 staining was very weak (Figure 4.3B), whereas the PS-1 staining in POP mice was more prominent (Figure 4.3C). No PS-1 staining was detected in negative control (primary antibody omitted) (Figure 4.3A). To quantify the expression of PS-1, the intensity of PS-1 staining was measured using ImageJ software. As shown in Figure 4.4, the expression of PS-1 was significantly increased (18.89 ± 1.02 % stained area) in POP group compared to saline-treated controls (6.61 ± 0.32 % stained area).

A



B

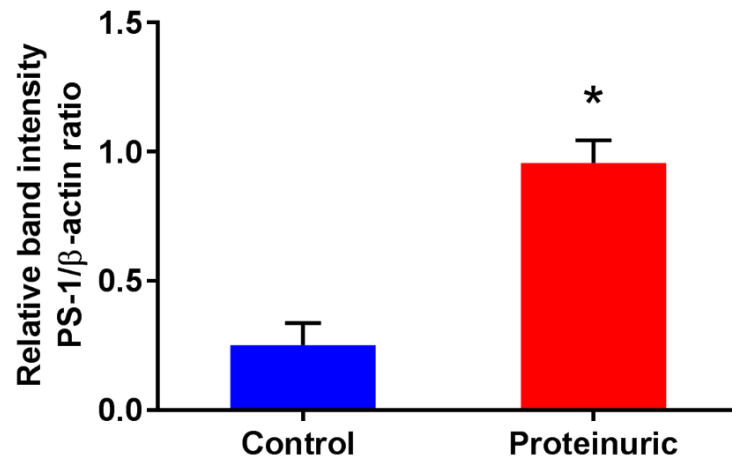


Figure 4.2: Effect POP on renal PS-1 expression in uni-nephrectomised mice. A) Expression of PS-1 in kidney tissues from mice treated with BSA or saline was evaluated by western blot analysis. B) Densitometric analysis for PS-1 are presented as the relative ratio to β -actin. Results are expressed as mean \pm SEM of 4 mice per group. * $P < 0.05$ compared with saline-injected control group (t test).

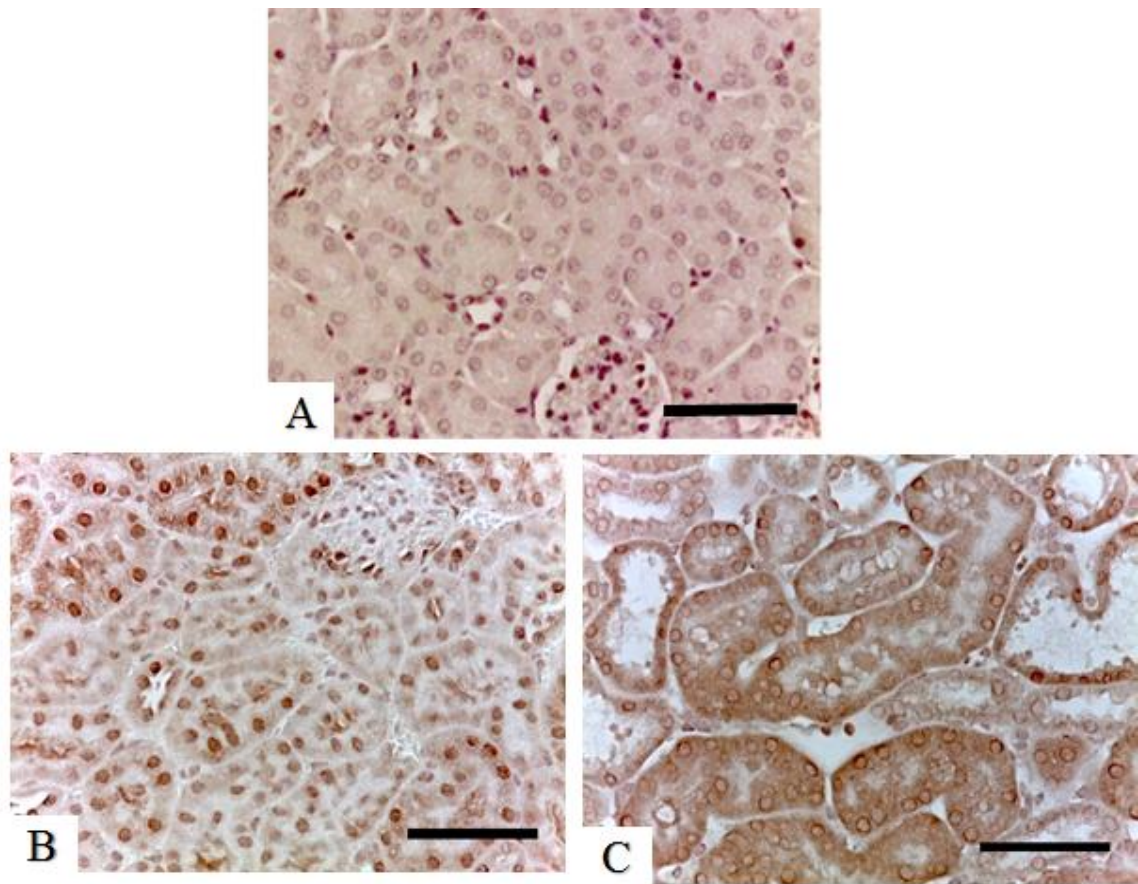


Figure 4.3: Expression of PS-1 in the cortex of kidneys from saline-treated control and POP groups. Representative photomicrographs showing immunohistochemical staining of PS-1 in the kidney of saline-injected control (B) and POP (C) mice. (A) Negative control without primary antibody. Scale bar: 100 μ m.

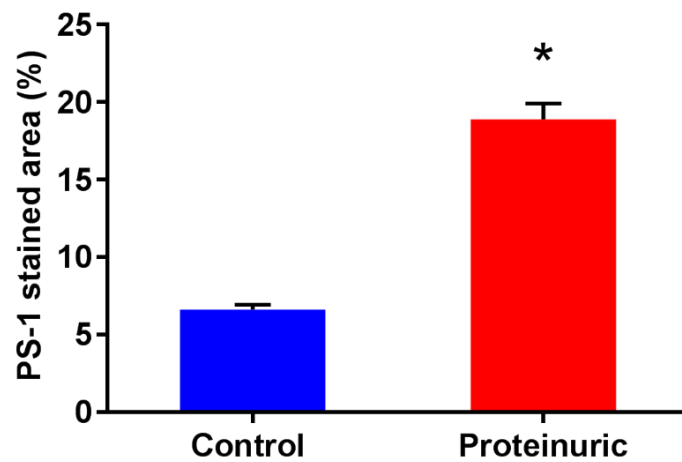


Figure 4.4: Quantification of renal PS-1 staining in saline-treated control and POP groups. PS-1 staining was performed 14 days after BSA administration and quantified using ImageJ software and expressed as (%). Results are expressed as mean \pm SEM of 5 mice per group. * $P < 0.05$ compared with saline-injected control mice (t test).

4.2.3 The effect of the MMP inhibitor BB-94 on serum creatinine levels in POP mice

The effect of BB-94 treatment on serum creatinine in mice is shown in Figure 4.5. Saline-injected control mice showed a normal serum creatinine level, whereas POP mice had a higher level of serum creatinine ($90.87 \pm 5.5 \mu\text{mol/L}$) compared to saline-treated controls ($31.71 \pm 3.42 \mu\text{mol/L}$). Treatment of POP mice with BB-94 significantly attenuated ($44.92 \pm 3.39 \mu\text{mol/L}$) the rise in serum creatinine in comparison to non-treated POP animals ($90.87 \pm 5.5 \mu\text{mol/L}$). There was no significant difference in serum creatinine level between saline-injected control and POP+BB-94 treated animals. These data confirm that renal function may be protected by BB-94 treatment.

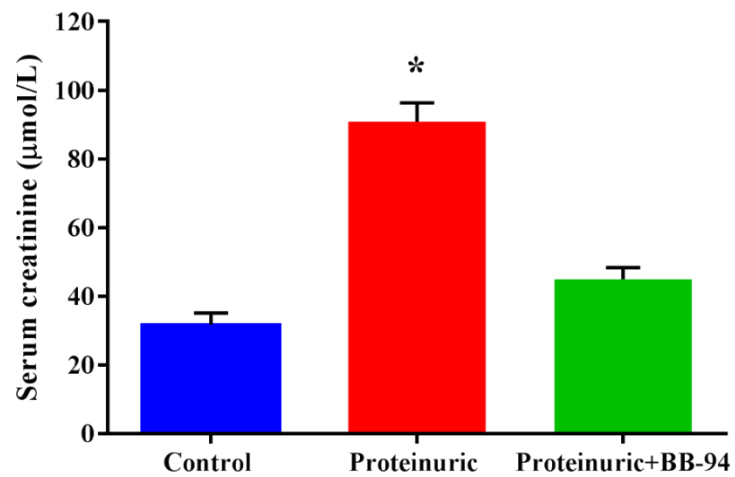


Figure 4.5: Effect of MMP inhibitor (BB-94) treatment on serum creatinine level in proteinuria-induced mice. Serum creatinine levels were measured in saline-injected control, POP and POP+BB-94 groups. Results are expressed as mean \pm SEM of 4 mice per group. * $P < 0.05$ compared with saline-injected control and POP+BB-94 groups (ANOVA).

4.2.4 Total serum protein concentration in BB-94 treated and non-BB-94 treated mice

As shown in Figure 4.6, mice treated with increasing doses of BSA had higher but not significant serum total protein concentration compared to saline-injected controls. In BB-94 treated mice, the total serum protein concentration was higher than non-BB-94 treated animals.

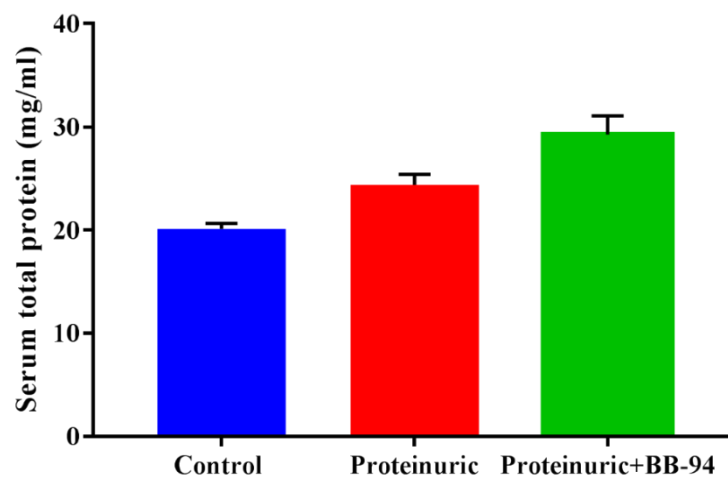
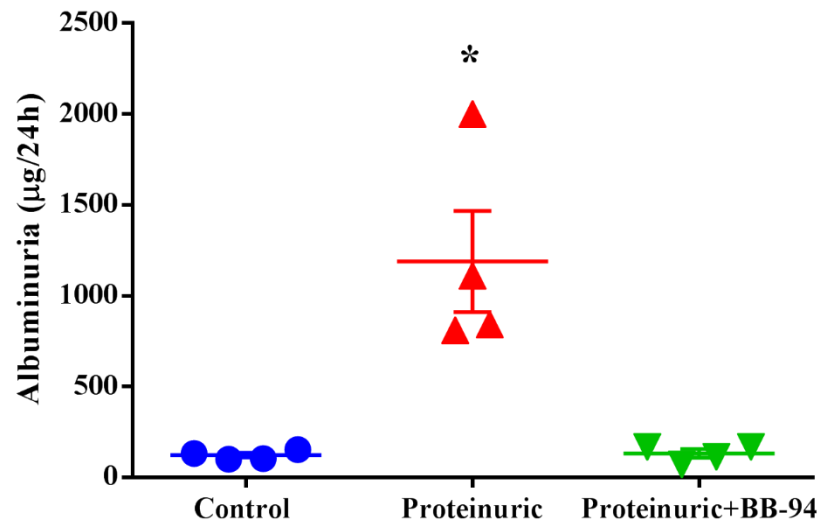


Figure 4.6: Effect of BB-94 treatment on serum total protein level in POP mice. Serum total protein levels were measured in saline-injected, POP or POP+BB-94 groups. Results are expressed as mean \pm SEM of 4 mice per group.

4.2.5 BB-94 treatment reduced urinary albumin and total protein excretion in POP mice

BSA-injected mice developed significant albuminuria and proteinuria, as measured by elevated urinary albumin and protein excretion (Figure 4.7A&B). Both albumin and protein excretion were increased more than nine-fold in the BSA-treated group compared with saline-treated control group. BB-94 treatment of BSA-injected mice resulted in a significant reduction in urinary albumin and protein excretion to control levels.

A



B

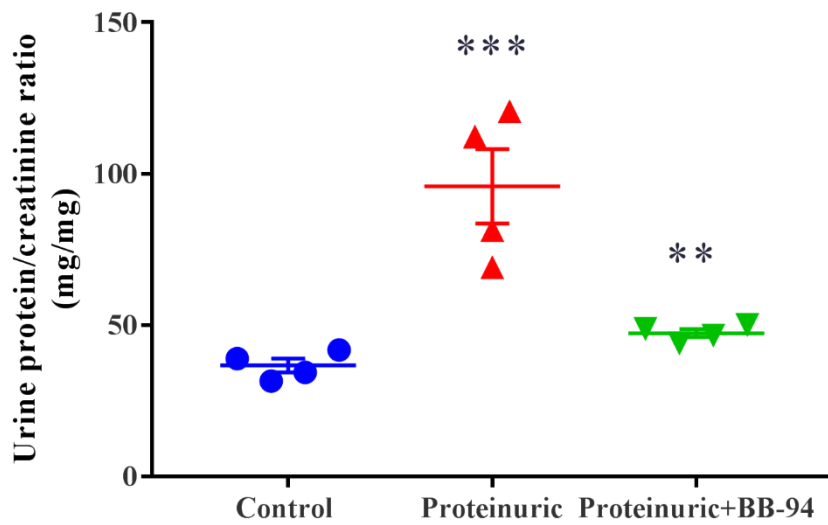


Figure 4.7: BB-94 treatment of proteinuria-induced mice decreases urinary albumin and protein excretion. Albumin (A) and protein (B) concentrations were measured in the urine of saline-treated control, POP and POP+BB-94 groups. Results are expressed as mean \pm SEM of 4 mice per group. *** $P < 0.05$ compared with saline-treated control group (ANOVA), ** $P < 0.05$ compared with POP group (ANOVA).

4.2.6 BB-94 treatment reduced the enzymatic activity of MMP in POP mice

To evaluate whether BB-94 treatment inhibit the enzymatic activity of MMPs in POP mice, a fluorimetric assay was employed. As shown in Figure 4.8, BSA administration (15mg/g) to mice significantly increased (1274 ± 152.2 RFUs) kidney MMP enzymatic activity compared to saline-treated control mice (777.8 ± 41.94 RFUs). Treatment of POP animals with BB-94 significantly reduced (491.3 ± 123.9 RFUs) kidney MMP activity compared to POP animals (1274 ± 152.2 RFUs). No significant difference in kidney MMP activity was found between POP+BB-94 group and saline-injected controls. These data confirmed that synthetic MMP inhibitor BB-94 indeed has an inhibitory effect on MMP activity in mouse kidney.

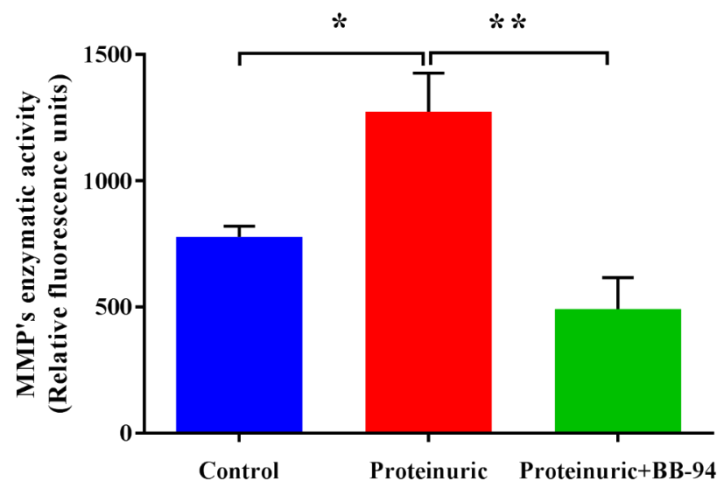


Figure 4.8: Effect of synthetic inhibitor BB-94 treatment on MMPs activity in proteinuria-induced mice. MMPs activity were measured in saline-injected control, POP and POP+BB-94 groups. Results are presented as mean \pm SEM of 4 mice per group. * $P < 0.05$ compared with saline-treated control group (ANOVA), ** $P < 0.05$ compared with the POP+BB-94 group (ANOVA).

4.2.7 Assessment of MMP-9 expression in POP mice after BB-94 treatment

It was of great importance to study the expression of MMPs in the kidney especially as some of these intracellular enzymes have shown to be involved in RIP of cellular receptors. Because there is no clear evidence which MMP is responsible for the cleavage of extracellular part of endocytic receptors, we examined the expression of three different MMPs in kidney homogenates; MMP-3, MMP-7 and MMP-9. Among these MMPs, MMP-9 showed the greatest expression in response to BSA overload in mice.

The expression of MMP-9 in mouse kidney was evaluated by WB and IHC. WB results showed a well-defined band at approximately 92kDa immunoreacting with polyclonal rabbit MMP-9 antibody. Figure 4.9A shows the bands of MMP-9 in the saline-treated controls, POP and POP+BB-94 animals. Increased MMP-9 expression was evident in kidney homogenates from POP animals but similar increased expression of MMP-9 was not found in kidney lysates from POP animals treated with BB-94. Saline-treated control lysates contained a very low levels of MMP-9.

Quantitative results obtained by means of densitometric analyses are shown in Figure 4.9B. MMP-9 expression was significantly increased (0.89 ± 0.01 relative intensity) in POP animals when compared with saline-treated control animals (0.47 ± 0.05 relative intensity). BB-94 treatment of POP animals resulted in a significant reduction (0.4 ± 0.11 relative intensity) in MMP-9 expression. MMP-9 expression was not significantly different in saline-injected controls and POP+BB-94 treated animals.

To confirm WB results, IHC was performed on kidney sections from saline-treated control, POP and POP+BB-94 treated animals. As shown in Figure 4.10, immunoreactivity for MMP-9 was prominent in POP sections and highly restricted to the PTs of the kidney. On the other hand, very weak signals of MMP-9 were observed in the kidney sections derived from saline-treated control and POP+BB-94 treated animals. In order to quantify the amount of MMP-9 stained immunohistochemically in kidney sections, ImageJ was employed. MMP-9 staining in kidney sections from POP mice was higher (6.7 ± 0.21 % stained area) than in kidney sections from saline-treated control (1.29 ± 0.1 %

stained area) and POP+BB-94 treated animals (1.04 ± 0.09 % stained area) (Figure 4.11). These data confirm that the effect of BSA overload on MMP-9 expression can be reduced with BB-94 treatment in mice.

4.2.8 BB-94 treatment reduced MMP-9 mRNA expression in POP mice

Results demonstrated that BB-94 treatment leads to a marked decrease in MMP-9 protein expression in the kidney of POP mice. In order to determine whether MMP-9 expression can also be regulated at the transcriptional level by BB-94 treatment, the mRNA expression of MMP-9 in the renal cortices from saline-treated control, POP and POP+BB-94 treated mice was determined using qPCR.

qPCR results of MMP-9 mRNA expression are shown in Figure 4.12. When mice were treated with BSA, MMP-9 mRNA levels were significantly induced. In contrast, when mice treated with BSA and BB-94, the mRNA expression of MMP-9 was significantly reduced compared with the BSA treated mice. The mRNA expression was increased more than 10-fold in POP mice compared to the saline-treated control group. BB-94 treatment resulted in an apparent 8-fold reduction in MMP-9 mRNA expression compared to the BSA treated mice. These results indicate that BB-94 can be used as a regulator of MMP-9 gene expression.

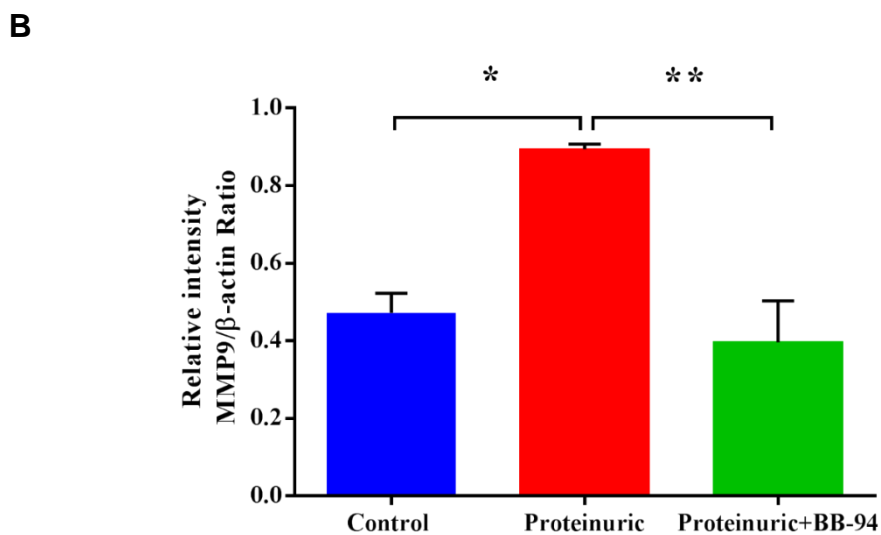
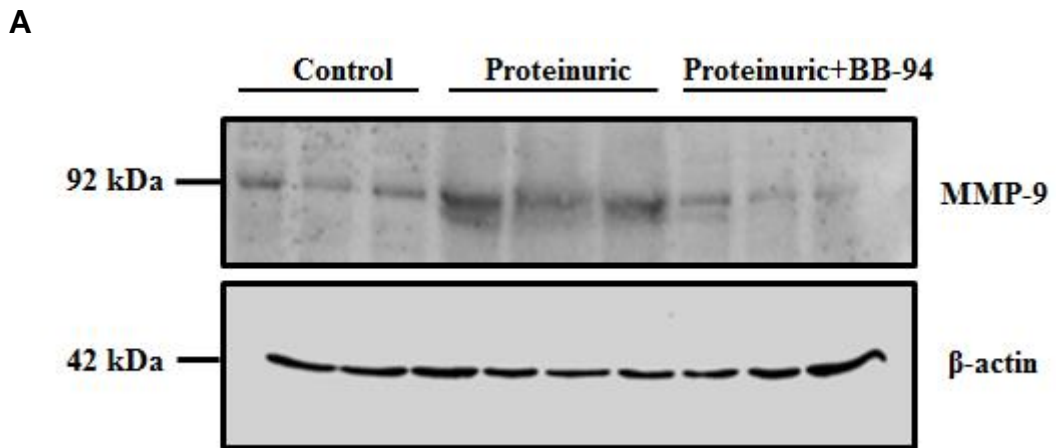


Figure 4.9: BB-94 treatment reduced MMP-9 expression in POP mice. A) Representative western blot for MMP-9 and β -actin of lysates from saline-injected control, POP and POP+BB-94 groups. B) Densitometry analysis of MMP-9 expression in the three groups. Results are expressed as mean \pm SEM of 3 mice per group. * $P < 0.05$ compared with the saline-treated control group (ANOVA), ** $P < 0.05$ compared with POP+BB-94 group (ANOVA).

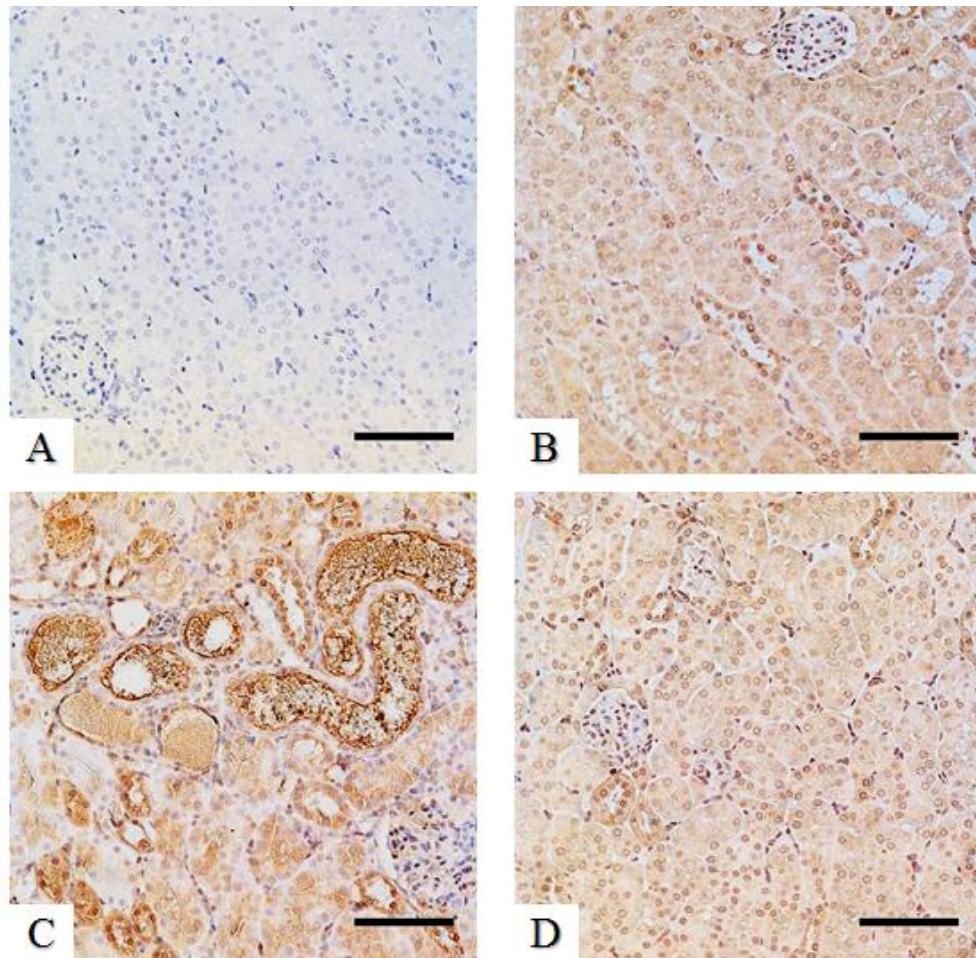


Figure 4.10: Expression of MMP-9 in the cortex of kidneys from saline-treated control, POP and POP+BB-94 groups. Representative photomicrographs showing immunohistochemical staining of MMP-9 in the kidney of saline-injected control (B), POP (C) and POP+BB-94 (D) groups. (A) Negative control (without primary antibody). Scale bar: 100 μ m.

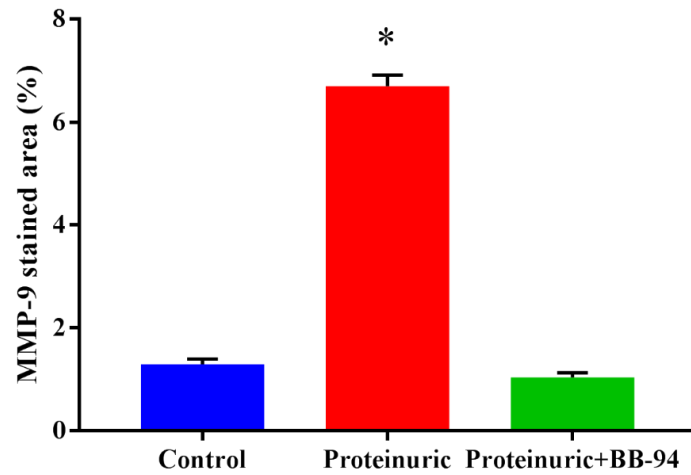


Figure 4.11: Quantification of renal MMP-9 staining in saline-treated control, POP and POP+BB-94 groups. MMP-9 staining was performed after BSA or BSA+BB-94 administration for 14 days. Results are expressed as mean \pm SEM of 4 mice per group. * $P < 0.05$ compared with saline-treated control and POP+BB-94 groups (ANOVA).

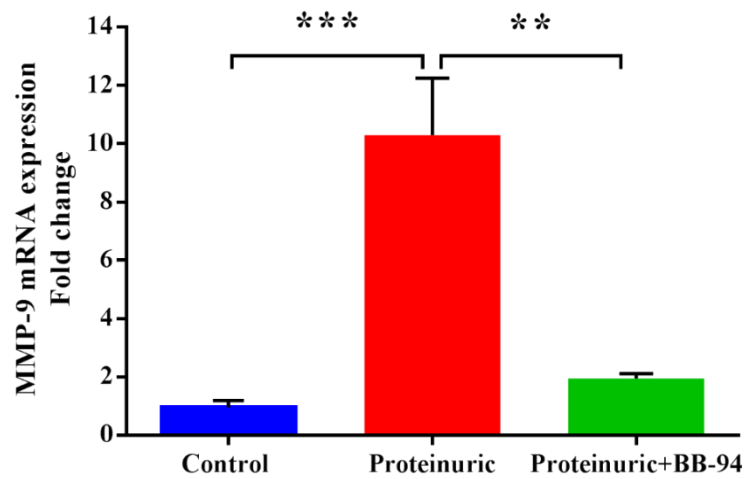


Figure 4.12: Effect of BB-94 treatment on MMP-9 mRNA expression in POP mice. The levels of MMP-9 mRNA were determined in saline-treated control, POP and POP+BB-94 groups. Results are expressed as mean \pm SEM of 4 mice per group. *** $P < 0.05$ compared with saline-injected control group (ANOVA), ** $P < 0.05$ compared with the POP+BB-94 group (ANOVA).

4.2.9 BB-94 preserves the expression of megalin in proximal tubules in mice with POP

In our previous studies it was demonstrated that proteinuria is associated with reduced megalin expression at PT cell surface. This downregulation was hypothesised to be related to the RIP of megalin as significant amounts of megalin were detected in the urine of proteinuric animals. It is well-known that RIP is dependent on activation of MMPs. Therefore, in order to determine whether MMPs activity inhibition could prevent the reduction of megalin in kidney in proteinuria, three groups of four animals were treated with saline, BSA or BSA+BB-94 for 14 days.

WB results confirmed that proximal tubular expression of megalin was markedly reduced in POP mice compared to saline-treated controls. In contrast, BSA+BB-94 treated mice showed a similar expression pattern of megalin in the kidney as saline-injected control animals, indicating that an important aspect in the basal reduction of megalin in kidney is mediated by MMP activity.

As shown in Figure 4.13A, rabbit polyclonal antibody to megalin recognised a protein at approximately 600 kDa in kidney homogenates. The amount of megalin present in the kidney homogenates from POP mice was low, whereas more intense bands in saline-injected control and POP+BB-94 mice indicate preserved megalin expression in these animals.

As shown in Figure 4.13B, when quantified, a significant reduction (0.29 ± 0.02 relative intensity) in megalin expression was found in POP mice compared to saline-treated controls (1.92 ± 0.11 relative intensity). Conversely, megalin expression was not significantly different (1.32 ± 0.27 relative intensity) to saline-injected controls (1.92 ± 0.11 relative intensity) after treatment of POP mice with BB-94. There was a statistical difference between POP (0.29 ± 0.01 relative intensity) and POP+BB-94 groups (1.32 ± 0.27 relative intensity).

By IHC, in POP sections, megalin expression was absent in many PTs and very weakly seen in the others (Figure 4.14 C). Saline-treated control sections showed clear megalin staining in almost all PTs especially those around glomeruli (Figure 4.14 B). Similar to saline-injected controls, megalin staining

seemed prominent in POP+BB-94 treated kidney sections (Figure 4.14 D). When quantified, the intensity of megalin staining was significantly decreased (8.99 ± 0.43 % stained area) in POP animals compared to saline-treated controls (21.27 ± 0.85 % stained area). BB-94 treatment of POP mice significantly protected megalin expression (19.73 ± 0.89). No significant difference was found in megalin expression between saline-injected controls and POP+BB-94 treated animals (Figure 4.15).

4.2.10 The effect of BB-94 treatment on megalin mRNA expression in POP mice

The effect of BB-94 on megalin gene expression was also studied. Megalin mRNA expression was significantly increased in POP animals compared to saline-injected controls as previously observed. In contrast, the mRNA levels of megalin was not significantly different in POP mice treated with BB-94 compared to saline-treated control animals. There was, on the other hand, a significant decrease in megalin mRNA expression in POP+BB-94 treated mice compared to POP mice, indicating that BB-94 treatment can effectively normalise megalin gene expression (Figure 4.16).

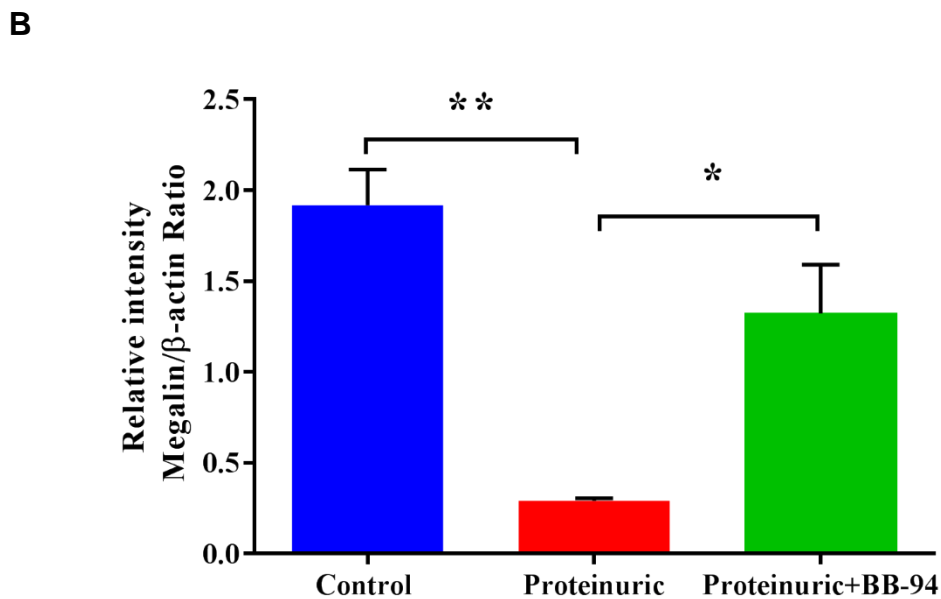
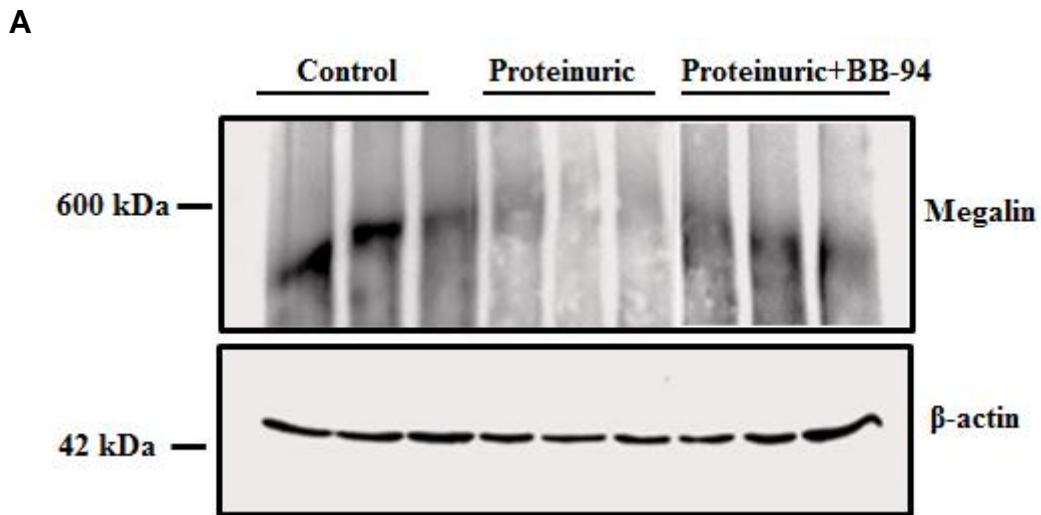


Figure 4.13: Downregulation of megalin in POP mice is prevented with BB-94 treatment. A) Representative Immunoblot for megalin and β -actin of kidney lysates from saline-treated control, POP and POP+BB-94 treated mice. B) Densitometry analysis of megalin expression in the three groups. Results are expressed as mean \pm SEM of 3 mice per group. ** $P < 0.05$ compared with saline-injected control group (ANOVA), * $P < 0.05$ compared with POP+BB-94 group (ANOVA).

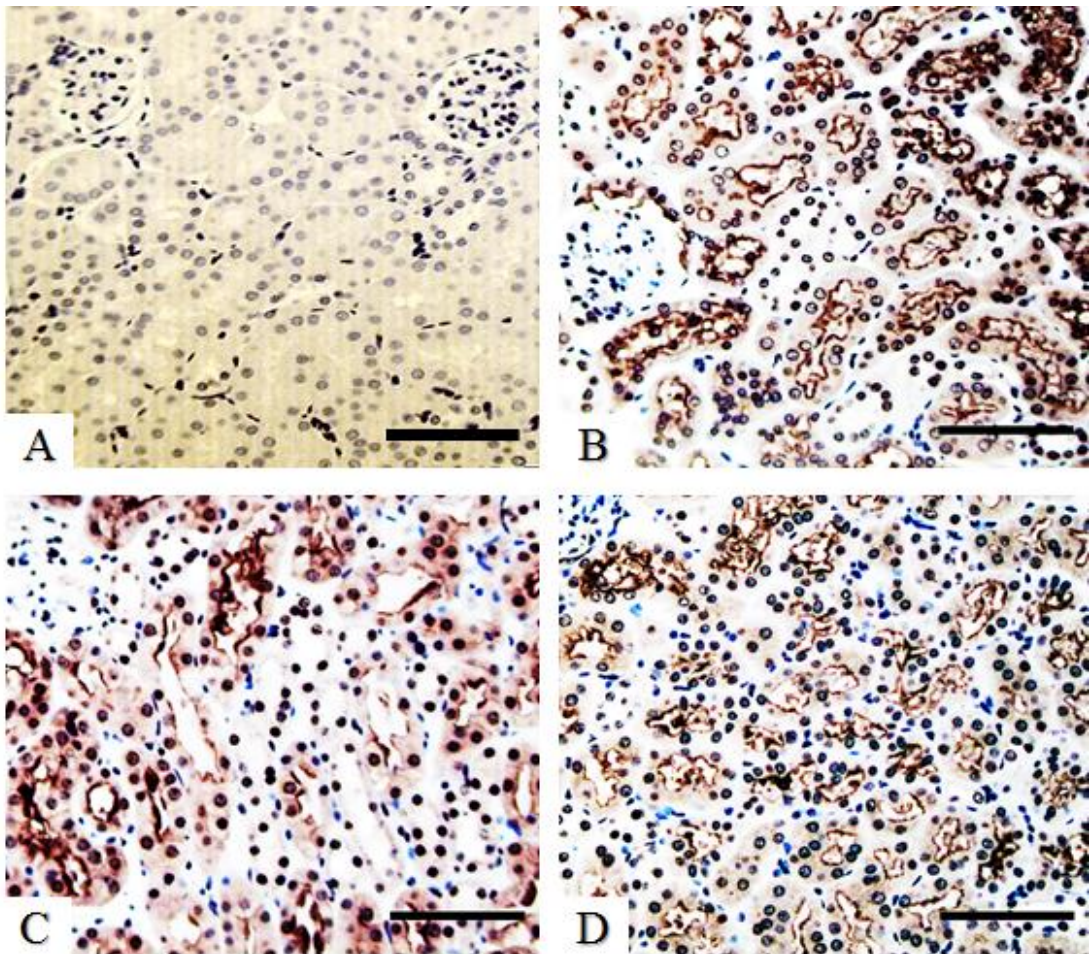


Figure 4.14: Expression of megalin in the cortex of kidneys from saline-treated control, POP and POP+BB-94 mice. Representative photomicrographs depicting megalin expression in the kidney of saline-treated control (B), POP (C) and POP+BB-94 (D) groups. (A) Negative control (without primary antibody). Scale bar: 100 μ m.

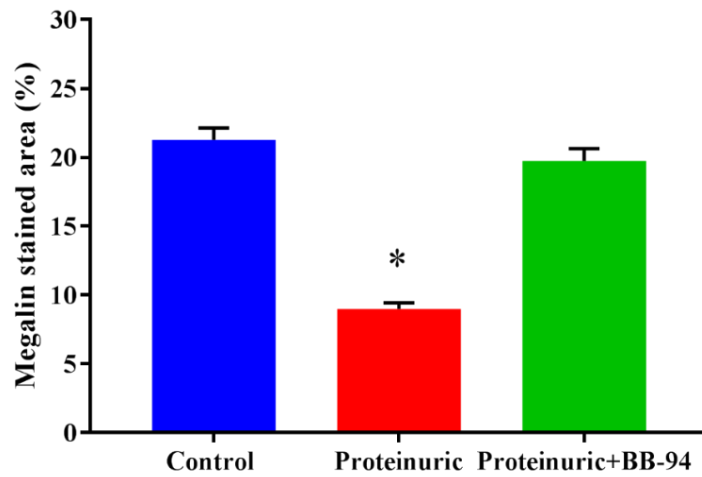


Figure 4.15: Quantification of renal megalin staining in saline-treated control, POP and POP+BB-94 groups. Megalin staining was performed 14 days after BSA or BSA plus BB-94 administration. Results are expressed as mean \pm SEM of 4 mice per group. * $P < 0.05$ compared with saline-injected control and POP+BB-94 groups (ANOVA).

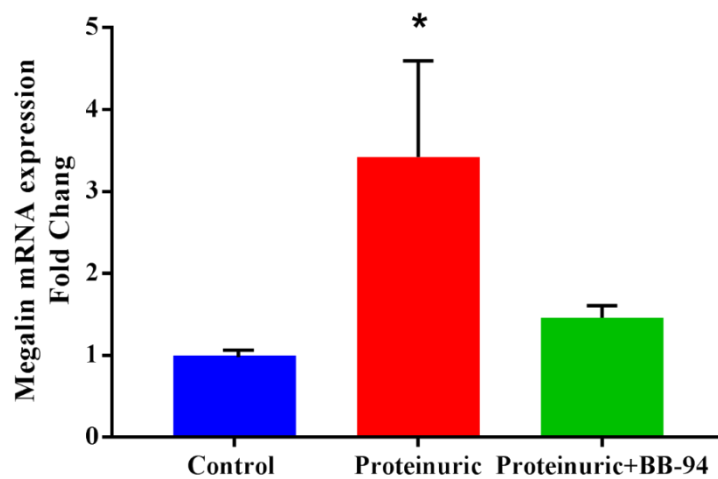


Figure 4.16: Effect of BB-94 treatment on renal megalin mRNA levels in POP group. The levels of megalin mRNA were determined in saline-treated control mice or POP mice with or without the BB-94. Results are expressed as mean \pm SEM of 4 mice per group. * $P < 0.05$ compared with saline-treated control and POP+BB-94 groups (ANOVA).

4.2.11 Assessment of FcRn protein expression after BB-94 treatment in POP mice

The expression of FcRn was assessed by WB analysis and IHC. WB of mouse kidney lysates at approximately 42 kDa showed a well-defined band immunoreacting with rabbit polyclonal FcRn antibody. Figure 4.17A shows the bands of FcRn in saline-treated controls, POP and POP+BB-94 treated mice. Reduced FcRn protein expression was evident in the cortical homogenates from POP mice, but FcRn expression was preserved in kidneys from POP animals treated with BB-94. Saline-injected control homogenates showed clear expression of FcRn. Results were quantified by densitometry and are shown in Figure 4.17B. A significant decrease (0.65 ± 0.08 relative intensity) in FcRn expression was found in POP animals compared to saline-treated controls (1.41 ± 0.12 relative intensity), but in contrast, when POP mice treated with BB-94, the expression of FcRn was maintained (1.15 ± 0.12 relative intensity) compared with POP animals (0.65 ± 0.08 relative intensity).

Results of IHC are shown in Figure 4.18. Cortical sections from all mice were immunostained with anti-FcRn antibody. The intensity of IHC staining for FcRn was variable in the sections. In POP sections, very weak immunoreactivity of FcRn was detected in most of the PTs compared to a very strong immunoreactive signals observed in saline-treated control sections (Figure 4.18C vs 4.18B). A strong immunoreactive signal was observed in number of the majority of PTs in the kidney sections from POP+BB-94 treated animals (Figure 4.18D). To quantify the intensity of immunostaining, ImageJ was performed. As shown in Figure 4.19, the expression of FcRn was significantly reduced (8.07 ± 0.31 % stained area) in POP animals compared to saline-treated controls (15.82 ± 0.65 % stained area). BB-94 treatment of POP animals seemed to attenuate FcRn expression significantly (14.71 ± 0.69 % stained area) compared to POP animals (8.07 ± 0.31 % stained area). Proximal tubular expression of FcRn showed no significant difference between saline-treated control and POP+BB-94 treated mice (15.82 ± 0.65 % vs 14.71 ± 0.69 % stained area).

4.2.12 mRNA expression of FcRn receptor in proteinuric mice after BB-94 treatment

qPCR was used to determine whether mRNA of the FcRn receptor is changed in the PTEC of POP mouse kidneys and treated with or without BB-94. Figure 4.20 shows qPCR results expressed as fold change and normalised to GAPDH. As shown, a significant increase in mRNA level of FcRn were observed in kidney cortex of POP mice compared with saline-treated control mice. When POP mice treated with BB-94, the mRNA level of FcRn was not significantly decreased compared to POP animals. There was also a significant difference in FcRn mRNA expression between POP+BB-94 treated animals and saline-treated control animals.

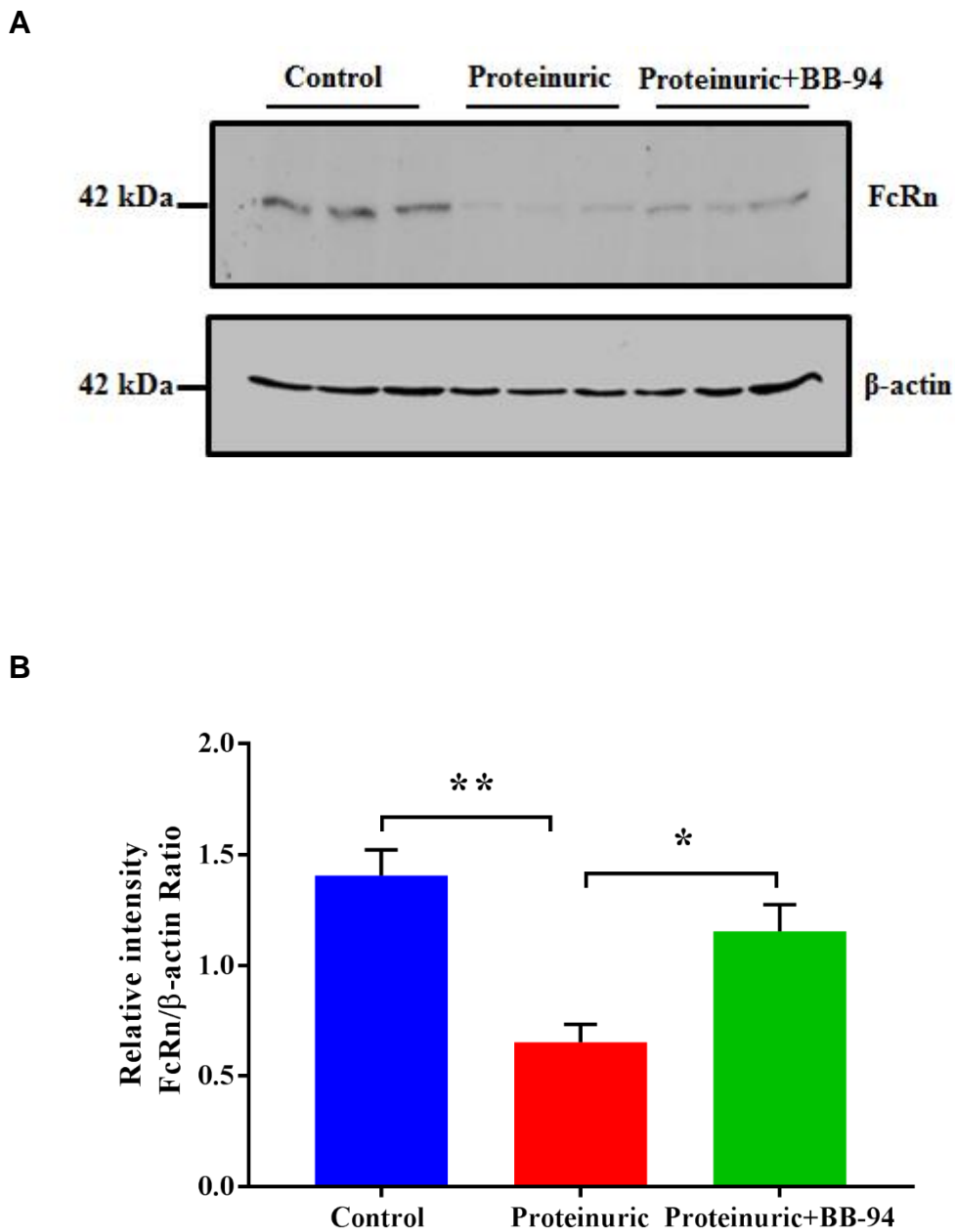


Figure 4.17: Downregulation of FcRn in POP mice is prevented with BB-94 treatment. A) Representative Immunoblot for FcRn and β -actin of kidney lysates from saline-treated control, POP and POP+BB-94 treated mice. B) Densitometry analysis of FcRn expression in the three groups. Results are expressed as mean \pm SEM of 3 mice per group. ** $P < 0.05$ (ANOVA) compared with saline-treated control group, * $P < 0.05$ compared with POP+BB-94 treated group (ANOVA).

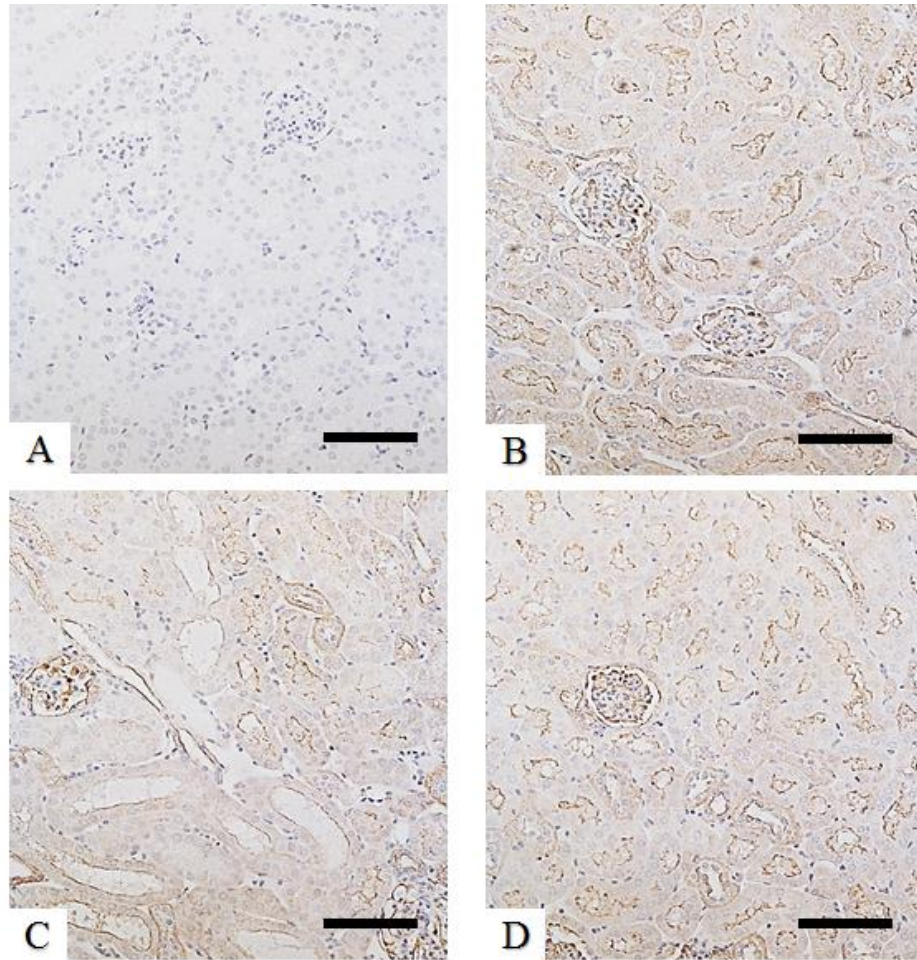


Figure 4.18: Expression of FcRn in the cortex of kidneys from saline-treated control, POP and POP+BB-94 groups. Representative photomicrographs depicting FcRn expression in the kidney of saline-injected control (B), POP (C) and POP+BB-94 (D) groups. (A) Negative control (without primary antibody). Scale bar: 100 μ m.

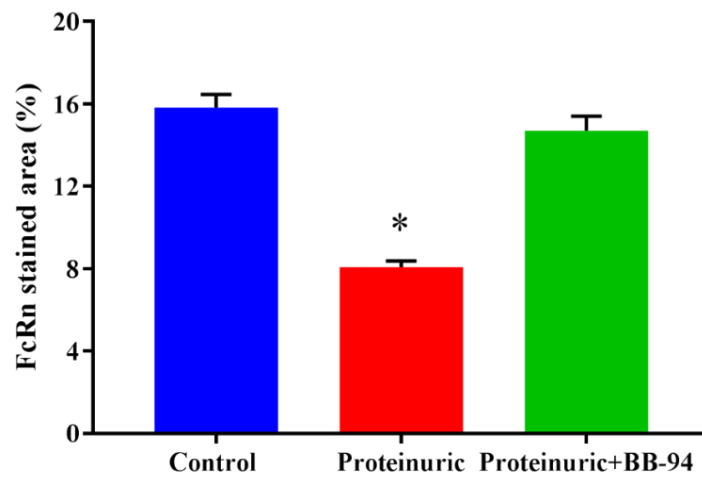


Figure 4.19: Quantification of renal FcRn staining in saline-treated control, POP and POP+BB-94 groups. FcRn staining was performed after 14 days of BSA or BSA+BB-94 treatment. Results are expressed as mean \pm SEM of 4 mice per group. * $P < 0.05$ compared with saline-treated control and POP+BB-94 treated groups (ANOVA).

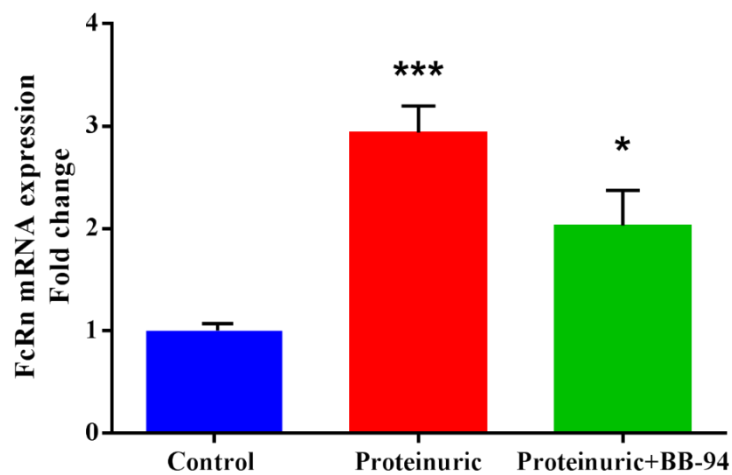


Figure 4.20: Effect of BB-94 treatment on renal FcRn mRNA levels in POP mice. The levels of FcRn mRNA were determined in saline-treated control mice or POP mice with or without the BB-94. Results are expressed as mean \pm SEM of 4 mice per group. *** $P < 0.05$ compared with saline-treated control group (ANOVA), * $P < 0.05$ compared with saline-injected control group (ANOVA).

4.2.13 BB-94 treatment leads to reduced urinary excretion of megalin in POP mice

In the previous studies POP in mice was associated with increased urinary excretion of megalin. To investigate whether BB-94 treatment can reduce the amount of megalin shedding into the urine of POP mice, urine samples from animals treated with saline, BSA or BSA+BB-94 were analysed for the detection of megalin by ELISA (Figure 4.21). In accordance with previous results, POP led to a significant increase (305.5 ± 35.77 ng/ml) in megalin excretion in the urine compared to saline-treated controls (24.32 ± 14.02 ng/ml). Administration of BB-94 to POP mice significantly decreased urinary excretion of megalin (15.95 ± 6.03 ng/ml), indicating the potential importance of BB-94 in reducing MMP-mediated megalin cleavage and resulting shedding into urine. There was no statistically significant difference in *P* between POP+BB-94 treated animals and saline-injected control animals in urinary megalin excretion.

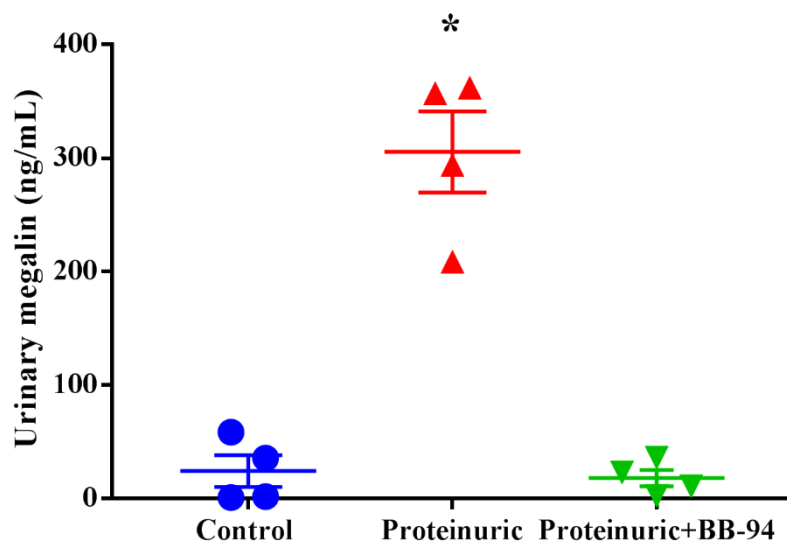


Figure 4.21: Increased urinary excretion of megalin in POP mice is reduced by BB-94 treatment. Urinary megalin excretion was measured in saline-treated control mice or POP mice with or without the BB-94. Results are expressed as mean \pm SEM of 4 mice per group. * $P < 0.05$ compared with saline-treated control and POP+BB-94 treated groups (ANOVA).

4.2.14 BB-94 treatment leads to reduced urinary excretion of FcRn in POP mice

In our previous studies it was shown that POP led to increased urinary excretion of FcRn in POP mice. To determine whether BB-94 treatment can reduce increased urinary excretion of FcRn, three groups of four animals received saline, BSA or BSA+BB-94. The levels of FcRn were evaluated in the urine of all animals by ELISA. Figure 4.22 shows concentrations of FcRn present in the urine of all treated mice. Consistent with the first study, POP mice showed a significant increase (484 ± 104.1 pg/ml) in urinary FcRn excretion compared to saline-treated controls (25.03 ± 13 pg/ml). The urinary excretion of FcRn was significantly decreased (90.28 ± 30.95 pg/ml) in POP+BB-94 treated animals compared to POP animals (484 ± 104.1 pg/ml). There was no significant difference in urinary FcRn excretion between POP+BB-94 treated animals and saline-treated control mice. These data indicate that BB-94 treatment reduces FcRn from shedding and excretion.

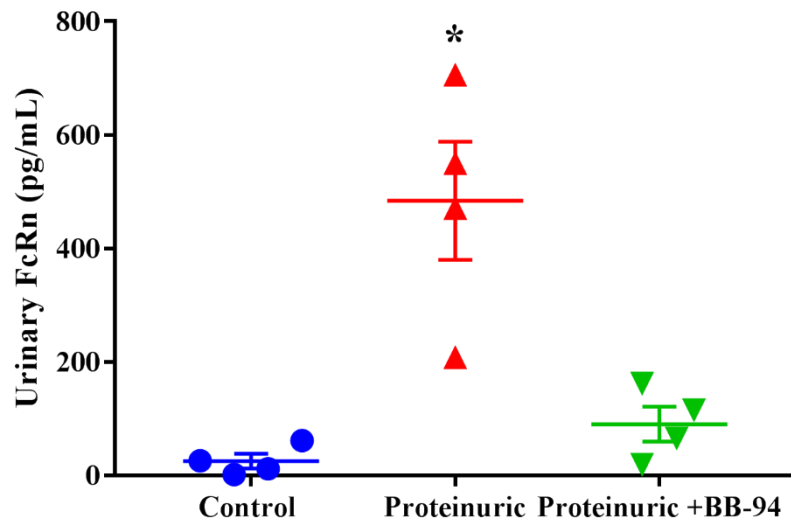


Figure 4.22: Increased urinary excretion of FcRn in POP mice is reduced by BB-94 treatment. FcRn was measured in the urine of saline-treated control mice or POP mice with or without the BB-94. Results are expressed as mean \pm SEM of 4 mice per group. * $P < 0.05$ compared with saline-treated control and POP+BB-94 treated groups (ANOVA).

4.3 Discussion

The findings of these experiments clearly show that inhibition of MMPs reduces proteinuria and preserves the cell surface expression of megalin and FcRn by PTEC. It is very well-known that MMPs also mediate the cleavage of the extracellular domain of megalin under certain conditions (Biemesderfer, 2006, Li et al., 2008, Zou et al., 2004). This megalin domain is responsible for the reabsorption of a wide range of glomerular ultrafiltered proteins, including albumin (Caruso-Neves et al., 2006, Christensen et al., 2009, Chang et al., 2011).

In the absence of the extracellular domain due to shedding, cell surface availability of these receptors is likely to be reduced thus potentially contributing to the loss of filtered proteins in the urine. The cleavage of intracellular domain of megalin, which is processed by gamma secretase, is also believed to be dependent on the ectodomain shedding of these receptors (Biemesderfer, 2006). This domain of megalin is thought to be highly involved in the regulation of megalin gene expression. A recent study has demonstrated that increased megalin mRNA expression is closely associated with the amount of intracellular domain of megalin (Li et al., 2008). All the above events could be inhibited by blocking the activity of MMPs.

Some megalin ligands such as albumin have been shown to effectively increase the expression and enhance the activity of MMPs. Fang et al. (2009) found that BSA at different doses can increase both the expression and activity of MMP-2 and MMP-9 in mouse podocytes. Similarly, in vitro albumin overload led to overexpression and activation of MMP-9 in the glomerular parietal epithelial cells and this was via the activation of P44/42 MAPK pathway (Zhang et al., 2015). In a mouse model similar to the present study, protein overload increased modestly, but non-significantly, the activity of MMP-9 compared to control mice (Eddy et al., 2000). These observations are consistent with the results of the current work that show significant increase in MMP-9 activity in proteinuric animals. This activation of MMP in the kidney of proteinuric mice may then contribute to the proximal tubular shedding of endocytic receptors. In addition to MMP-9, the current work showed a modest increase in MMP-3 and

MMP-7 protein and mRNA expression in proteinuric animals but not in the same content as MMP-9 (data not shown).

The present results also demonstrate that the activity of γ -secretase is increased in the PT of the proteinuric mice. Thus, enhanced γ -secretase activity may be related to both downstream effect of megalin ectodomain shedding and protein overload in this model. Immunohistochemical studies showed that PS-1, the active component of the γ -secretase enzymatic complex (Ramdya et al., 2003), is localised to the renal brush border where megalin is expressed. This finding is in line with the previous studies showing that high levels of PS-1 protein are enriched in renal brush border membrane vesicles (Zou et al., 2004).

It was previously demonstrated that the intracellular domain of megalin is cleaved by γ -secretase in vitro (Zou et al., 2004, Li et al., 2008). Although the current work was not able to study the cleavage of megalin intracellular domain, increased PS-1 expression may indicate that the process could be occurred in vivo. It is believed that the intracellular domain of megalin is involved in the regulation of megalin gene expression in the PTEC (Biemesderfer, 2006). However, recent study showed that, despite its synthesis in large quantities in the PTEC, the soluble intracellular domain of megalin does not have correlation to any of the regulatory processes, including megalin expression, endocytic retrieval of proteins, or gene expression in the kidney (Christ et al., 2010).

The current results demonstrate that BB-94 reduced both the activity and expression of MMPs in proteinuric mice. BB-94 is a broad-spectrum MMP inhibitor that mediates its action by binding to active zinc site on the MMPs (Beckett et al., 1996, Wojtowicz-Praga et al., 1997). The way by which the majority of MMP inhibitors exert their inhibitory effects is similar. BB-94 contains hydroxamate (-CONHOH) group that binds to the active site and inhibits the activity of metalloproteinases (Denis and Verweij, 1997). Previously, studies have shown that BB-94 reduced and inhibited the activity of MMPs in various tissues, including lungs and muscle. For example, BB-94 in a dose of 30mg/kg/day reduced the increased activity of MMP-2 and MMP-9 in bronchoalveolar lavage of mouse in a murine model of pulmonary fibrosis

induced by bleomycin (Corbel et al., 2001). Similarly, Kumar et al. (2010) found that the enzymatic activity of MMPs was significantly decreased in skeletal muscle of *mdx* mice treated with BB-94. In addition, in vitro BB-94 has shown to inhibit the activity of gelatinases, gelatinase A and B at the concentrations greater than 5 μ M (Low et al., 1996). Consistent with these studies, the results of the current work show that BB-94 significantly reduced the increased MMP activity in proteinuric animals.

Although BB-94 is designed to inhibit the activity of MMPs, mechanisms leading to decrease the expression of MMPs by this synthetic inhibitor has not been described yet. Hanemaaijer et al. (2001) suggested that both MMP activation and synthesis are sensitive to tetracycline, a synthetic inhibitor of MMPs. In addition, several studies have demonstrated the reduced expression of MMPs in animals treated with MMP inhibitor or in patients received doxycycline, a synthetic MMP inhibitor. In rats treated with doxycycline, the increased expression and production of MMP-9 was reduced after both 7 and 14 days of doxycycline treatment (Petrinec et al., 1996). Similarly, Curci et al. (2000) have shown that both increased protein and mRNA expressions of MMP-9 are significantly reduced in the aneurysm tissues of patients treated with doxycycline, indicating the effect of this exogenous inhibitor on the production of MMPs in the aneurysm. According to Liu et al. (2003), the expression of both MMP-2 and MMP-9 are reduced in cultured human aortic smooth muscle cells and abdominal aortic aneurysm tissue explants treated with doxycycline at therapeutic serum concentrations, and in case of MMP-2 reduced protein expression was associated with the reduced MMP-2 mRNA stability.

In the present study, BB-94 reduced the increased expression of both protein and mRNA of MMP-9 in proteinuric mice. In addition, BB-94 treatment reduced the expression of other MMPs such as MMP-3 and MMP-7 in POP mice but not in the same pattern as MMP-9 (data not shown). The reduced expression of MMP-9 by BB-94 might be related to the effect of this broad spectrum inhibitor on the production and synthesis of this proteinase in the kidney. Consistent with these results, Urso et al. (2012) demonstrated that administration of BB-94 significantly reduced the increased mRNA expressions of MMP-3 (7.2-fold decrease) and MMP-9 (9.7-fold decrease) in mice subjected to skeletal muscle

trauma. It appears that BB-94 is also effective in reducing the expression of MMPs, but the mechanisms of this downregulation still need to be elucidated.

Previous studies have shown that BB-94 is effective in reducing the risk of developing various kidney diseases such as prevention of cyst formation and reduction of kidney weight in a rat model of polycystic kidney disease (Obermüller et al., 2001), reducing proteinuria in transplanted animals (Ermolli et al., 2003) and in the lung reduced pulmonary fibrosis induced by bleomycin in mice (Corbel et al., 2001). In the present study, BB-94 reduced proteinuria and improved renal function in proteinuric animals suggesting that MMP activity may be contributing to altered proximal tubular endocytic receptor expression or glomerular permselectivity in proteinuria. A recent study supports the antiproteinuric effect of BB-94 by demonstrating that proteinuria are markedly reduced in hypertensive Dah1 salt-sensitive rats and type 2 DN rats treated with the two newly available MMP inhibitors, XL081 and XL784 (Williams et al., 2011). Williams et al. (2011) also demonstrated that these proteinase inhibitors also reduced glomerulosclerosis and renal injury in these animals, indicating that XL081 and XL784 might reduce proteinuria through reducing glomerular and renal injury. Conversely Obermüller et al. (2011) found that the urinary protein excretion was significantly higher in BB-94 treated rats than non-treated wild type controls. Another study revealed that early inhibition of MMPs is important to reduce 24h protein in chronic allograft nephropathy (Lutz et al., 2005).

Inhibiting MMPs with other synthetic inhibitors such as GM6001, improves renal function in cisplatin-induced injury and salt-sensitive hypertension in experimental animals (Ramesh and Reeves, 2002, Pushpakumar et al., 2013). In the first study, reduced blood urea nitrogen due to the effect of MMP inhibitor GM6001 was associated with the improvement of tubular injury induced by cisplatin in mice (Ramesh and Reeves, 2002). Moreover, Kunugi et al. (2011) showed that minocycline and synthetic peptide MMP inhibitor reduced acute tubular injury and improved renal function by lowering serum creatinine after 24h in mice with ischemic AKI. Consistent with these studies, inhibition of MMPs using BB-94 reduced serum creatinine in proteinuric animals indicating

better renal function. Finally, BB-94 treated animals did not show any signs of major toxicity and all were healthy (Wojtowicz-Praga et al., 1997).

Another important point is that BB-94 reduced the urinary excretion of megalin in proteinuric mice. In addition, the whole megalin can also be excreted into the urine under certain conditions. It appears that the majority of megalin found in the urine of proteinuric mice are the extracellular domain because antibodies used in determining megalin in the urine are specific to the extracellular domain of this receptor. Furthermore, inhibition of MMP activity with BB-94 greatly reduced the amount of megalin in the urine indicating that megalin may be vulnerable to cleavage and loss from cell membrane under proteinuric conditions. At least one study has demonstrated the importance of MMPs inhibition in protecting the cleavage of megalin in vitro. Zou et al. (2004) found that constitutive ectodomain shedding of megalin can be prevented by several broad spectrum inhibitors (MMP inhibitor III and tumour necrosis factor- α protease inhibitor-1 and -2) of MMPs activity.

The results demonstrate that BB-94 preserved megalin cell surface expression in proteinuric mice. Our previous study and this by Cabezas and his colleagues showed that protein overload caused a significant decrease in megalin protein expression in the PTs of proteinuric mice (Cabezas et al., 2011). Different mechanisms can regulate the expression of megalin in the PTs exposed to BSA overload. For example, Cabezas et al. (2011) showed that megalin protein expression can be regulated by PPARs and using agonists of PPARs, the expression of megalin is largely ameliorated. In the present study, megalin expression might be regulated in the PTEC by MMPs. Both the results of urinary megalin excretion and protein expression showed that inhibition of MMPs are essential in preserving megalin at cell surface. Furthermore, urinary excretion of megalin ligands such as albumin appeared to be reduced in BB-94 treated animals, indicating the better megalin expression in the PTEC. These observations support that maintenance of megalin expression is important in reducing proteinuria, and the subsequent renal injury, including inflammations and fibrosis.

FcRn like megalin has an extracellular domain that might be susceptible to cleavage by MMPs and then excreted into the urine, however no evidence

exists suggesting that FcRn undergoes such cleavage. Therefore, although the results of the present study demonstrate that inhibition of MMP activity significantly reduced the urinary excretion of FcRn, the mechanism of this effect is unclear.

Although mechanisms underlying FcRn downregulation in the PTEC are not described yet, MMPs activity may be involved in the regulation of FcRn protein expression in the PTEC of proteinuric mice. MMPs, in addition to their role in degradation of ECM, act on membrane proteins and release them (Van Lint and Libert, 2017). However, the role of MMPs in the cleavage of FcRn is not identified. The present study showed that inhibition of MMPs using synthetic inhibitor BB-94, the expression of FcRn was maintained suggesting that MMPs may be contributing to the cleavage and regulation of this receptor in the PTEC.

Most interesting is that BB-94 treatment down regulated the mRNA expression of megalin while it did not affect the mRNA expression of FcRn in proteinuric mice. In case of megalin, the mechanism of this regulation could be related to the intracellular domain of this receptor. Previous studies have reported different roles for intracellular domain in the regulation of megalin mRNA in the PTs. According to Christ et al. (2010), the soluble intracellular domain does not have any effect on global gene transcription of megalin using genetically modified mice. While, Li et al. (2008) found that inhibition of gamma secretase activity, which is responsible for the intracellular cleavage of megalin, in transfected megalin intracellular domain cells resulted in an 8- to 10-fold increase in megalin mRNA expression.

The above evidence suggests that MMPI reduced the activity of MMP in the PTs rather than kidney glomeruli because this synthetic inhibitor as shown reduced the PT shedding and preserved the expression of endocytic receptors. Therefore, the reduced urinary excretion of plasma proteins is likely due to the effect of MMPI (BB-94) on the availability of megalin and FcRn in the PT.

4.4 Conclusions

- MMPs are major mediators of ectodomain shedding, and their activity is increased in the kidneys of proteinuric animals.
- The increased expression of PS-1 did not have any effect on the mRNA expression of megalin and FcRn.
- BB-94 treatment improved renal function in proteinuric animals as the serum creatinine and proteinuria are both reduced to normal range.
- BB-94 treatment reduced the increased MMP activity and expression in proteinuric mice.
- Reduced MMP activity decreased urinary excretion of megalin in proteinuric animals which in turn increased cell surface expression of the receptor.
- BB-94 treatment reduced FcRn urinary excretion by unknown mechanism and preserved cell surface expression of FcRn in proteinuric animals.
- BB-94 treatment reduced megalin mRNA expression by unknown mechanism but did not change the level of FcRn mRNA significantly.

5 Matrix Metalloproteinase Inhibitor (BB-94) Reduces Renal Tubulointerstitial Fibrosis in Proteinuric Mice

5.1 Introduction

The morphological hallmark of progressive chronic renal disease (CKD) is tubulointerstitial fibrosis and inflammation, which is mainly characterised by interstitial infiltrate of mononuclear cells and macrophages as well as excessive accumulation and deposition of ECM proteins in the interstitial space (Genovese et al., 2014). In all the progressive renal diseases, impaired kidney function is strongly associated with the severity of tubulointerstitial damage (Tramonti et al., 2009).

Protein overload is very well known to induce tubulointerstitial damage dose-dependently in experimental animals. Histologically, the kidneys of these animals show interstitial macrophage infiltration, tubular atrophy and excessive ECM deposition in the interstitium (Eddy, 1989, Eddy et al., 1995, Eddy et al., 2000, Landgraf et al., 2014). Other markers of renal fibrosis such as TGF- β and TNF- α also increase in response to BSA overload (Eddy et al., 1995, Okamura et al., 2013, Wu et al., 2014). In addition, as discussed earlier in this thesis, an increase in MMP expression and activity was detected in cortical kidney tissues. However, the role of MMPs in the development of renal fibrosis and inflammation is not yet clear. The aim of the present study was therefore to investigate the effect of BB-94 on the development of fibrotic lesions and interstitial inflammation in a mouse model of POP to induce tubulointerstitial fibrosis and inflammation.

5.2 Results

5.2.1 Effects of BB-94 treatment on morphological changes in the kidney of POP mice

H&E staining was performed to assess tubular injury in mice treated with BSA, as well as the effects of BB-94 on tissue damage (Figure 5.1). The kidney structure showed no obvious histological changes in saline-treated control mice sections. By contrast, sections from BSA treated mice exhibited marked histological changes. The changes observed included, tubular cell brush border loss, tubular dilation, intratubular blood cast, interstitial inflammation, acute tubular necrosis, and fibrosis. Interestingly, BB-94 treatment effectively reduced tubular lesions in BSA treated mice. Sections were scored according to the severity of tubulointerstitial scarring after two weeks of BSA and BSA plus BB-94 injections. There was a significant increase (2.76 ± 0.14) in tubulointerstitial scarring score in BSA treated mice compared to saline-treated control animals, whereas tubulointerstitial injury score was significantly attenuated in POP+BB-94 treated mice (0.64 ± 0.098) (Figure 5.2).

Semiquantitative analysis used herein and described in the materials and methods is widely used to investigate structural changes in various kidney conditions. This scoring system allows to measure different parameters at histological levels, including tubular brush border loss, tubular dilation, and necrosis. One of the disadvantage of this method is that the scores are measured in numbers i.e. 1, 2, 3 and 4 and does not count 0.5 etc.

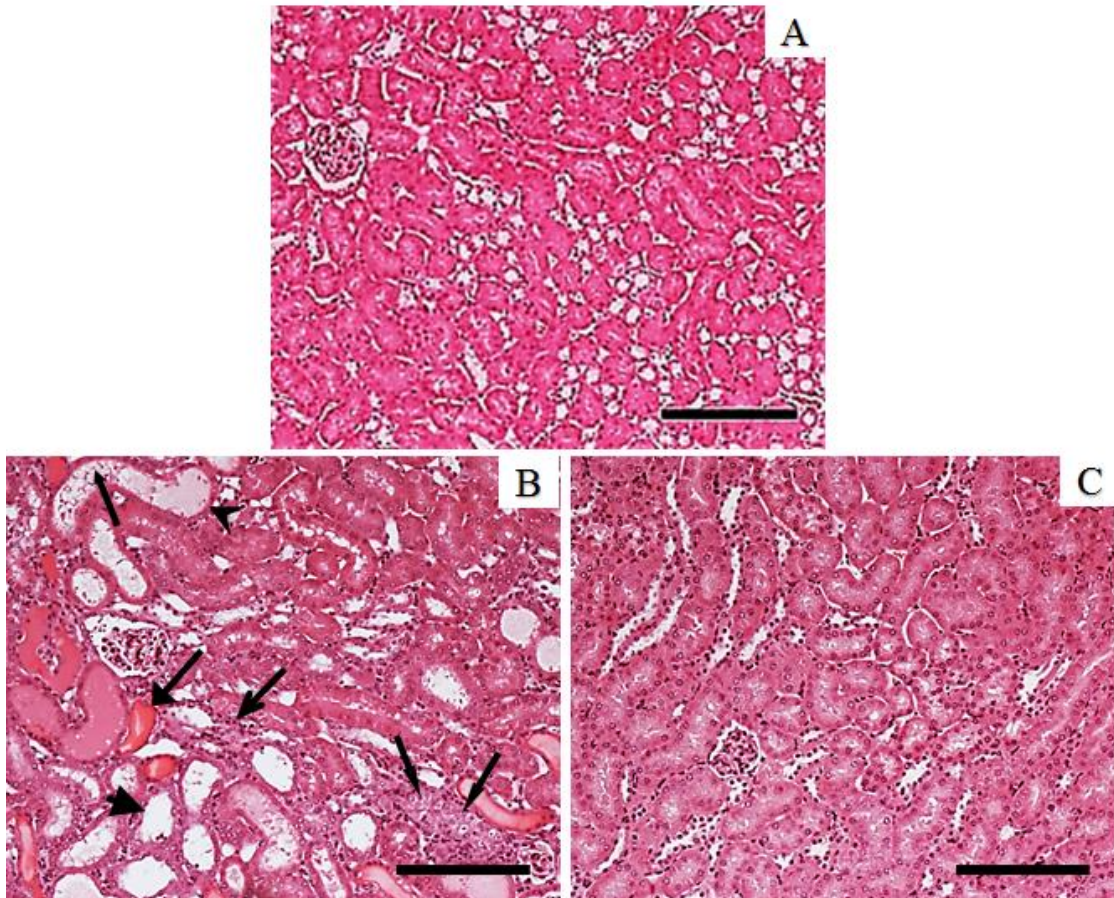


Figure 5.1: Representative photomicrographs of H&E staining of the kidney of saline-treated control (A), POP (B) and POP+BB-94 groups. Histological changes: Tubular brush border loss (→), tubular dilation (➤), intratubular blood cast (→), interstitial inflammation (➤) acute tubular necrosis (➔) and fibrosis (➔). Scale bar: 100 μ m.

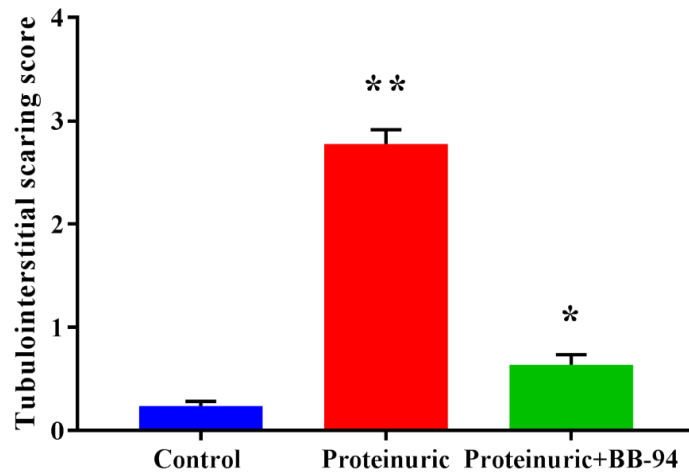


Figure 5.2: BB-94 treatment attenuated renal tubular injury scores in POP mice. Nephrectomised mice were treated with saline, BSA or BSA+BB-94 for two weeks. Results are presented as mean \pm SEM of 4 mice per group. ** $P < 0.05$ compared with saline-treated control and POP+BB-94 groups (ANOVA), * $P < 0.05$ compared with saline-injected control group (ANOVA).

5.2.2 BB-94 treatment reduced collagen deposition in POP mice

Sirius red staining was performed to assess collagen deposition in the kidney of animals. Collagen deposition was barely detected in renal tissues from saline-treated control mice (Figure 5.3A). POP mice exhibited an increase in collagen deposition in the renal cortex (Figure 5.3B), whereas BB-94 treatment was markedly reduced collagen deposition in the kidney of POP mice (Figure 5.3C).

To quantify renal interstitial fibrosis, the area of collagen staining was measured using ImageJ. Figure 5.4 shows that renal interstitial fibrosis was significantly higher (10.15 ± 0.68 % stained area) in POP mice compared to saline-treated control mice (3.66 ± 0.19 % stained area). Conversely, BB-94 treatment significantly reduced (5.15 ± 0.14 % stained area) renal interstitial fibrosis in POP mice. This data indicate that the development of renal fibrosis can be effectively suppressed by BB-94 treatment.

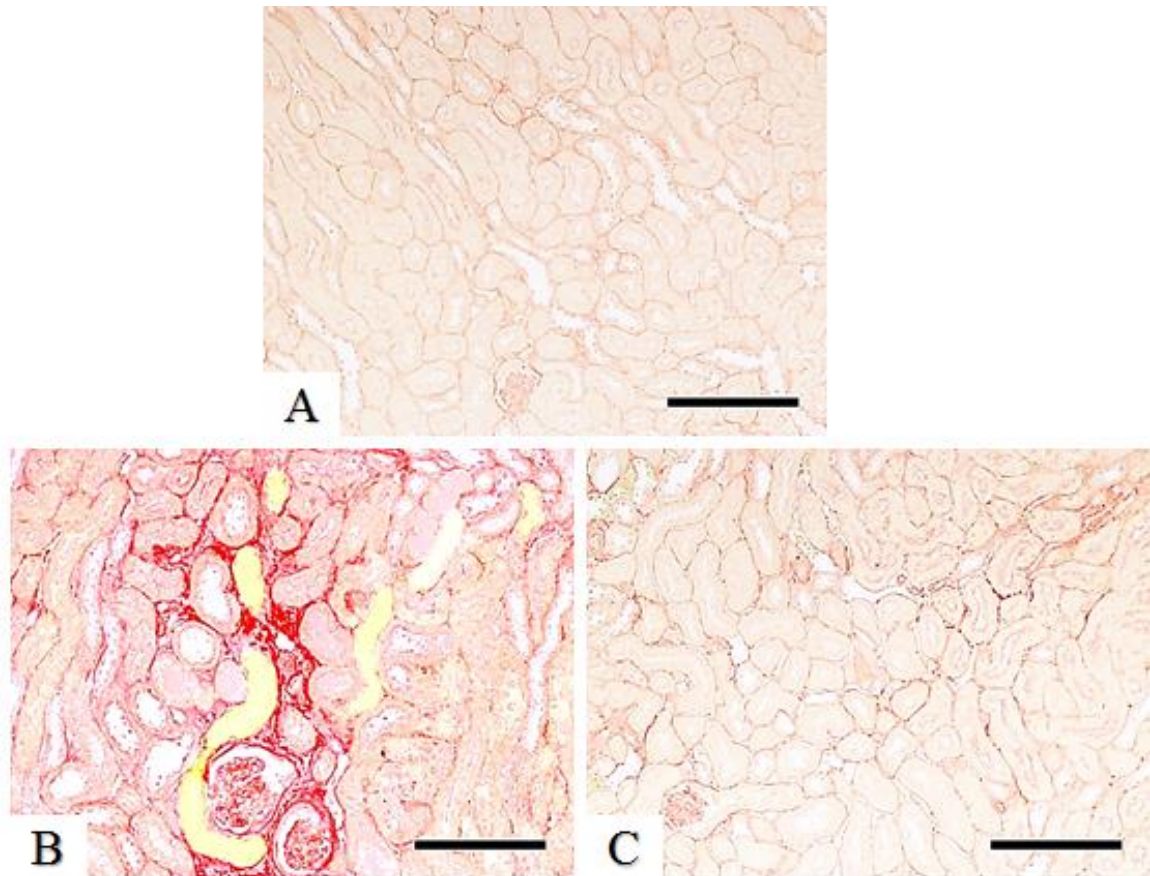


Figure 5.3: Representative photomicrographs of sirius red staining showing collagen deposition in the kidney of saline-treated control (A), POP (B) and POP+BB-94 (C) groups. Scale bar: 100 μ m.

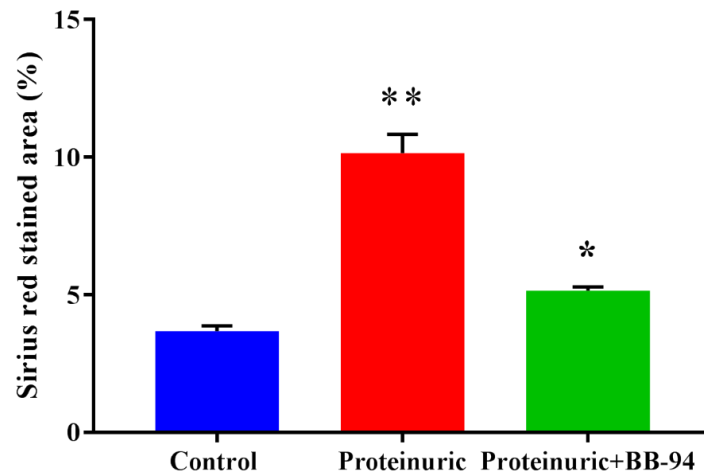


Figure 5.4: BB-94 treatment reduced collagen deposition in the kidney of POP mice. Sirius red staining was performed 14 days after BSA or BSA+BB-94 treatment. Results are expressed as mean \pm SEM of 4 mice per group. ** $P < 0.05$ compared with saline-injected control and POP+BB-94 groups (ANOVA), * $P < 0.05$ compared with saline-treated control group (ANOVA).

5.2.3 Effect of BB-94 treatment on the interstitial accumulation of inflammatory cells in mice with POP

WB analysis revealed that POP caused an increase in macrophage infiltration into the kidney interstitium. While treatment with BB-94 resulted in a markedly reduced infiltration of macrophage into the kidney interstitium of POP mice. Figure 5.5A shows a single protein bands at 102 kDa immunoreacting with rabbit polyclonal F4/80 antibody. The intensity of WB bands was measured using ImageJ software and normalised to the intensity of β -actin bands (Figure 5.5B). The expression of F4/80 was significantly increased (1.26 ± 0.36 relative intensity) in POP, whereas BB-94 treatment was significantly reduced (0.21 ± 0.09 relative intensity) macrophage infiltration in POP mice.

WB results were confirmed by IHC. Mouse kidney sections were immunostained for macrophage aggregation using rabbit polyclonal anti-mouse F4/80 antibody. F4/80 staining was very faint and barely detected in kidney sections from saline-treated control group (Figure 5.6B). By contrast, strong F4/80 staining was observed in kidney sections from POP mice (Figure 5.6C). This strong F4/80 staining was not found in kidney sections from POP+BB-94 group (Figure 5.6D). To measure the intensity of interstitial F4/80 staining, ImageJ software was used (Figure 5.7). There was a significant increase in macrophage infiltration in POP (10.06 ± 0.27 % stained area) compared to saline-treated controls (0.6 ± 0.02 % stained area). Treatment with BB-94 significantly reduced macrophage aggregation in the kidney interstitium (3.31 ± 0.11 % stained area). Together with WB results, IHC results revealed that kidney inflammation can be reduced by BB-94 treatment.

5.2.4 BB-94 treatment reduced mRNA expression of F4/80 in the kidney of POP mice

To determine whether the enhanced mRNA expression of F4/80 can be down regulated in POP, uni-nephrectomised mice were treated with BB-94. The mRNA levels of F4/80 in the kidney tissues were determined using qPCR analysis. The obtained Ct values of F4/80 were normalised to a reference gene, GAPDH. Figure 5.8 shows fold change in F4/80 mRNA expression in the kidney cortex of POP and POP+BB-94 groups. As shown, the mRNA expression of F4/80 was significantly increased (about 8.93-fold) in POP mice. Whereas, treatment of POP mice with BB-94 significantly reduced F4/80 expression (about 7.46-fold) in the proximal tubule cells. These data indicate that BB-94 can be used to regulate the mRNA expression of F4/80 in the kidney of POP mice.

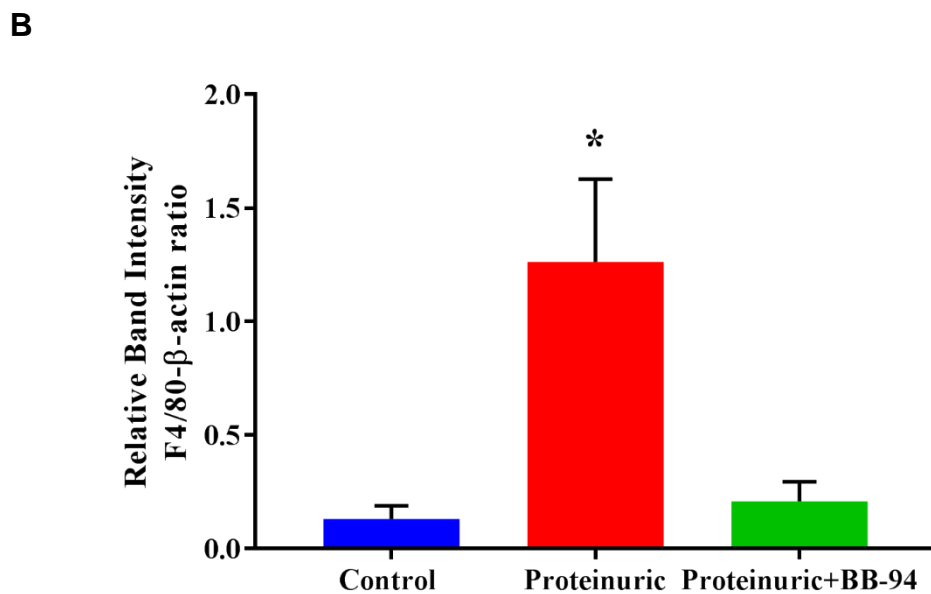
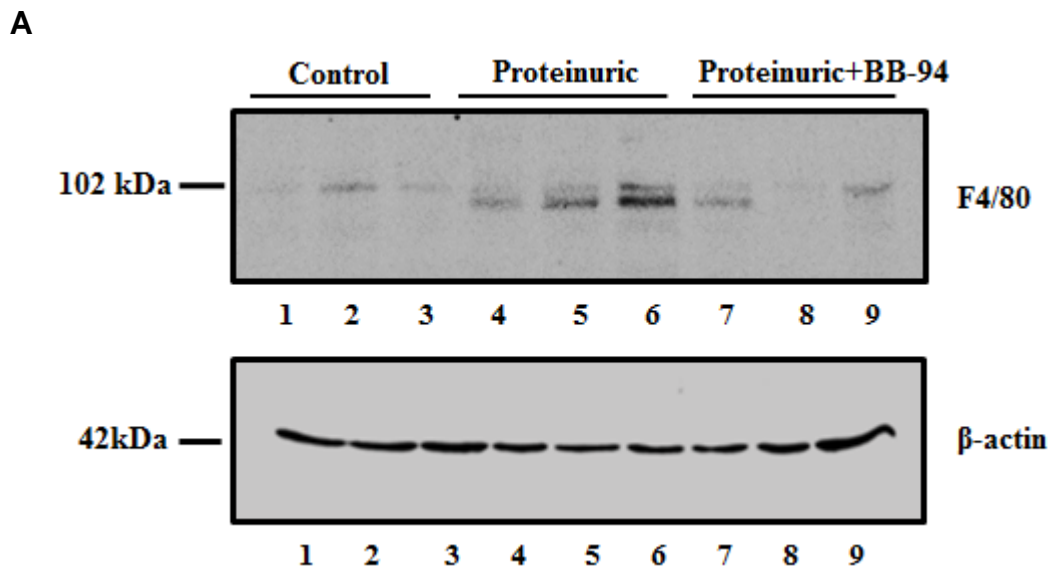


Figure 5.5: BB-94 treatment reduced macrophage infiltration into the kidney of POP mice. A) Representative WB of F4/80 and β -actin. B) Densitometric analysis of F4/80 expression. Results are expressed as mean \pm SEM of 3 mice per group. * $P < 0.05$ compared with saline-treated control and POP+BB-94 groups (ANOVA).

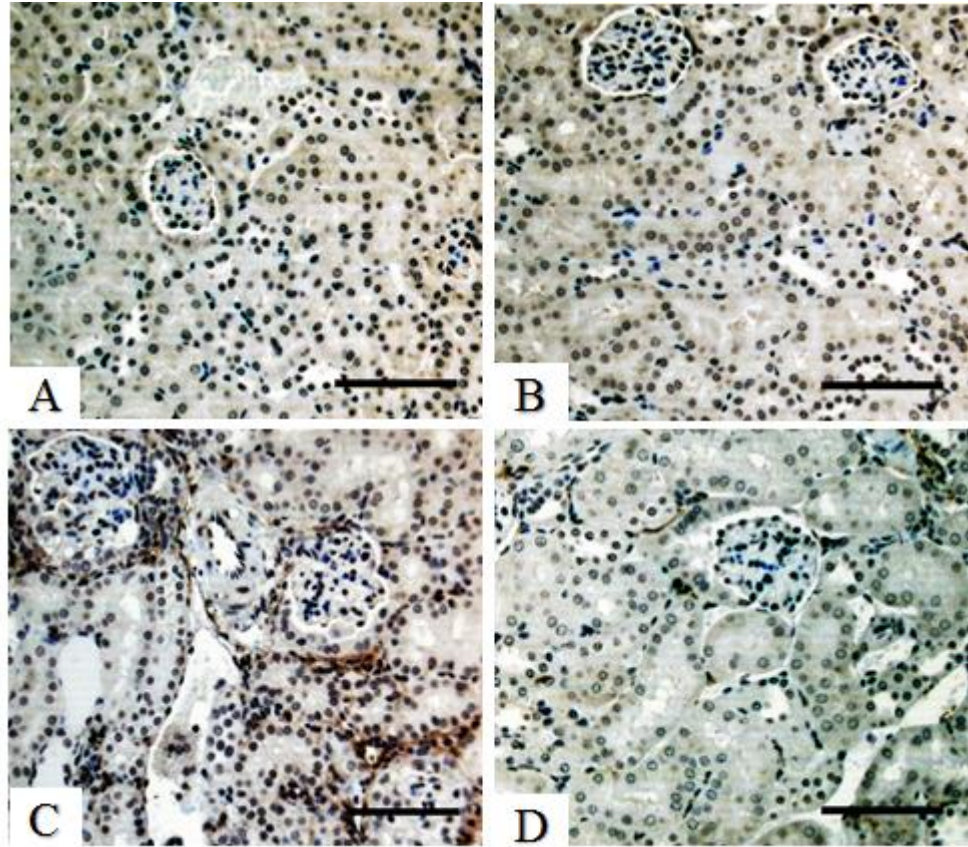


Figure 5.6: Representative photomicrographs showing macrophage infiltration into renal interstitium assessed by immunohistochemistry of F4/80 in the saline-treated control (B), POP (C), and POP+BB-94 (D) groups at day 14. (A) Negative control (without primary antibody). Scale bar: 100 μ m.

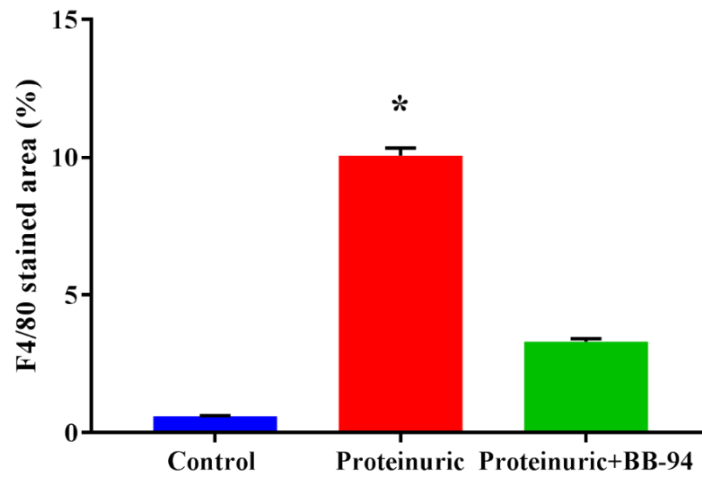


Figure 5.7: Quantification of macrophage infiltration in the kidney of saline-treated control, POP and POP+BB-94 groups. Staining for F4/80 was performed 14 days after BSA or BSA+BB-94 administration. Results are expressed as mean \pm SEM of 4 mice per group. * $P < 0.05$ compared with saline-injected control and POP+BB-94 groups (ANOVA).

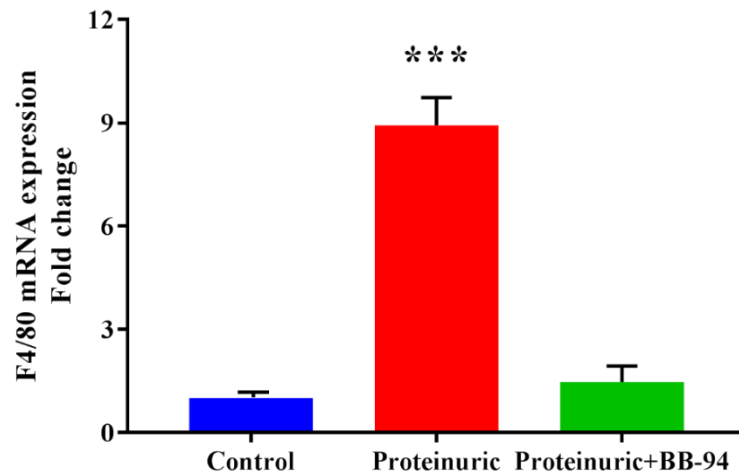


Figure 5.8: BB-94 treatment reduced mRNA expression of F4/80 in POP mice. The mRNA levels of F4/80 were determined in saline-treated control mice or POP mice with or without the BB-94. Results are expressed as mean \pm SEM of 4 mice per group. *** $P < 0.05$ compared with saline-treated control and POP+BB-94 treated groups (ANOVA).

5.2.5 Effect of BB-94 treatment on transforming growth factor-beta (TGF- β) expression in the kidney of POP mice

To determine whether BB-94 treatment could reduce the increased protein expression of TGF- β in POP, uni-nephrectomised mice were treated with BB-94 up to two weeks, beginning on day 1 of BSA injection. The expression of TGF- β was assessed in renal cortical tissues using WB analysis, IHC and ELISA. WB of mouse kidney cortical tissues showed a protein band at approximately 44 kDa immunoreacting with rabbit polyclonal mouse anti-TGF- β antibody. Figure 5.9A shows TGF- β bands in saline-injected controls, POP and POP+BB-94 treated kidney lysates. Increased expression of TGF- β was evident in kidney homogenates of POP mice, whereas very low levels of TGF- β was observed in POP+BB-94 treated and saline-treated control mice. By ImageJ analysis (Figure 5.9B), the expression of TGF- β was significantly increased in the kidney of POP mice (1.45 ± 0.12 relative intensity) compared to saline-treated control mice (0.09 ± 0.01 relative intensity). On the other hand, POP+BB-94 group showed a significant decrease (0.11 ± 0.07 relative intensity) in TGF- β expression compared to POP mice.

To confirm WB results, IHC was performed to evaluate the kidney expression of TGF- β in POP and POP+BB-94 groups. Strong tubular staining for TGF- β was observed in POP group (Figure 5.10C), whereas staining was much less intense in saline-treated control and POP+BB-94 groups (Figure 5.10B&D). Semiquantitative scoring revealed a significant increase in TGF- β expression in mice that were challenged with BSA (2.85 ± 0.1). Whereas, the expression of TGF- β was significantly decreased in POP+BB-94 mice (0.85 ± 0.13) (Figure 5.11).

ELISA was also used to measure the concentration of TGF- β in mouse kidney tissues. The concentration of TGF- β in all three groups is shown in Figure 5.12. BSA administration caused a significant increase in TGF- β protein levels (184.6 ± 22.97 pg/100 μ g protein) compared to saline-treated group (57.86 ± 10.99 pg/100 μ g protein). Whereas, BB-94 treatment was significantly reduced the protein levels of TGF- β (107.9 ± 13.19 pg/100 μ g protein).

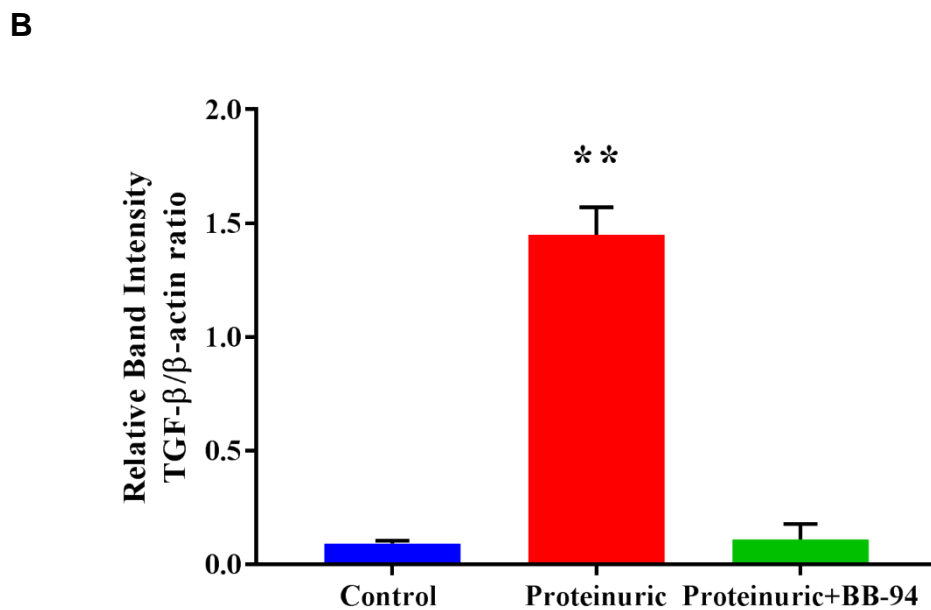
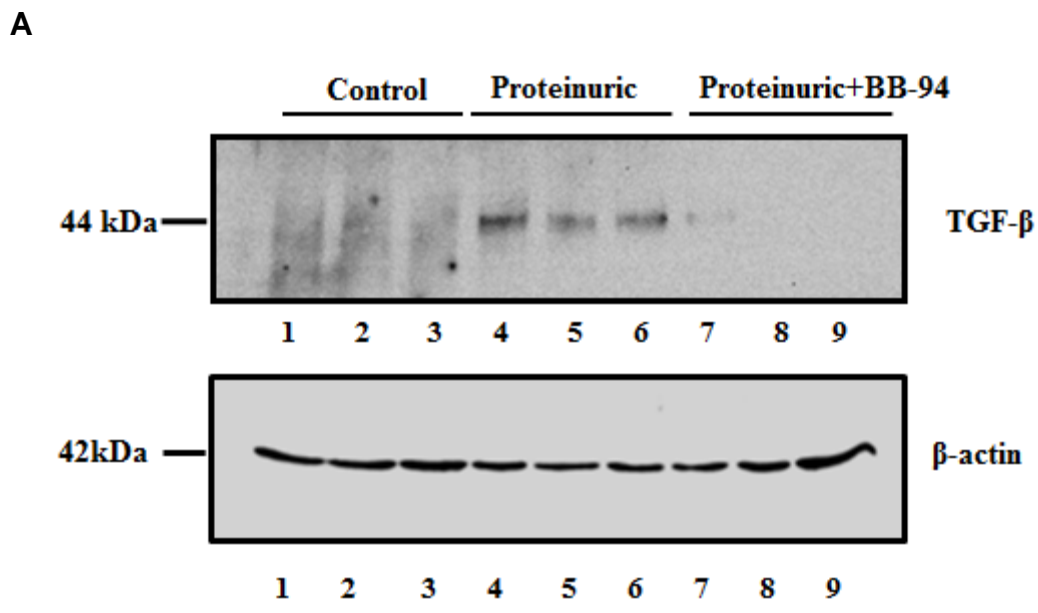


Figure 5.9: Effects of BB-94 treatment on renal TGF-β expression in POP mice. A) Expression of TGF-β in kidney tissues from mice treated with saline, BSA or BSA+BB-94 was evaluated by WB analysis. B) Densitometric analysis of TGF-β expression. Results are expressed as mean ± SEM of 3 mice per group. ** $P < 0.05$ compared with saline-treated control and POP+BB-94 groups (ANOVA).

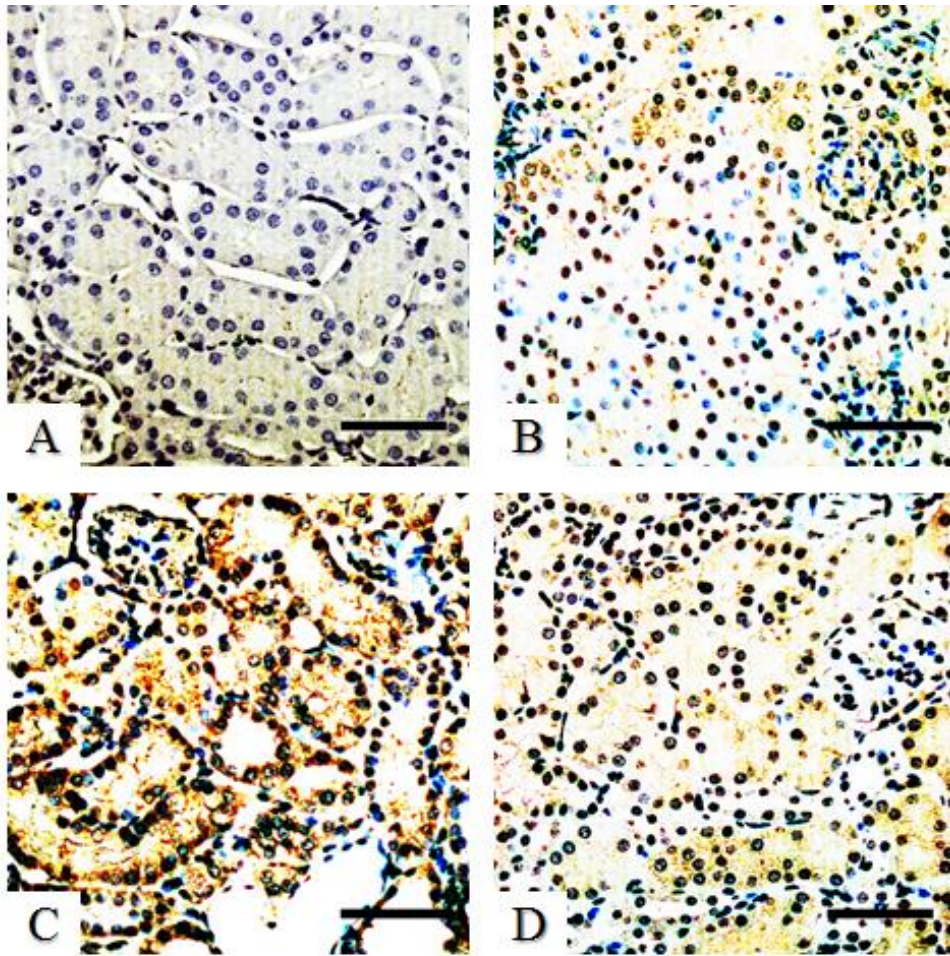


Figure 5.10: Expression of TGF- β in the cortex of kidneys from saline-treated control, POP and POP+BB-94 groups. Representative photomicrographs showing TGF- β expression assessed by IHC in the kidneys of saline-treated control (B), POP (C) and POP+BB-94 (D) groups. (A) Negative control (without primary antibody). Scale bar: 100 μ m.

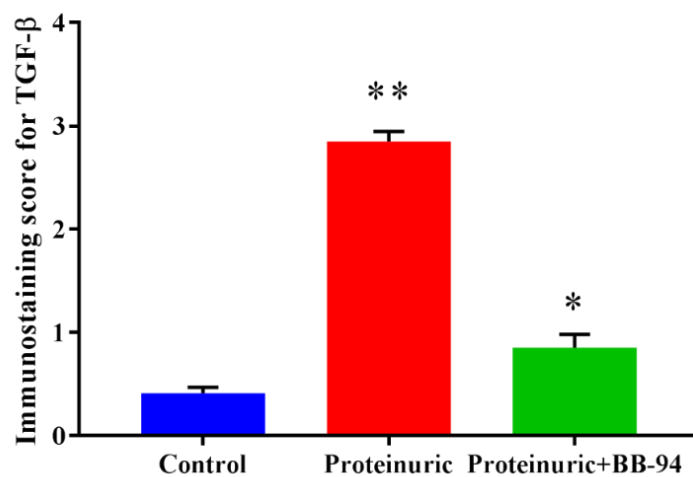


Figure 5.11: Immunostaining score for TGF- β staining in the kidney of saline-treated control, POP and POP+BB-94 groups. TGF- β staining was performed 14 days after BSA or BSA+BB-94 treatment. Results are expressed as mean \pm SEM of 4 mice per group. ** $P < 0.05$ compared with saline-treated control and POP+BB-94 groups (ANOVA), * $P < 0.05$ compared with saline-treated control group (ANOVA).

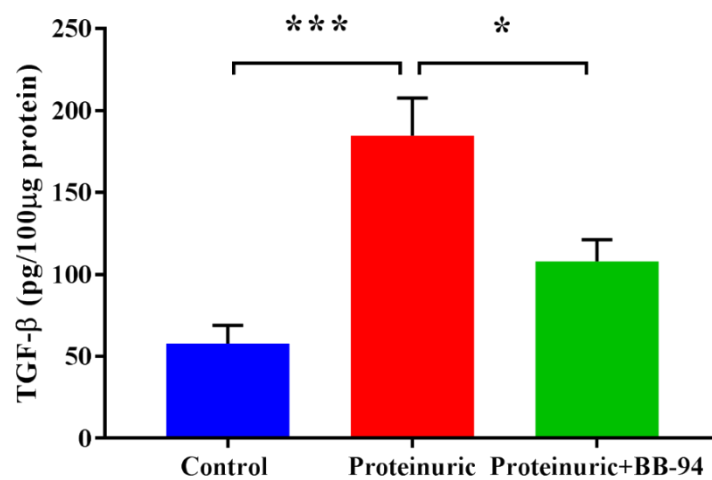


Figure 5.12: Effects of BB-94 treatment on renal TGF- β levels in POP mice. TGF- β levels were measured in the kidney of saline-treated control mice or POP mice with or without the BB-94 by ELISA. Results are expressed as means \pm SEM of 4 mice per group. *** $P < 0.05$ compared with saline-treated control group (ANOVA), * $P < 0.05$ compared with POP+BB-94 treated group (ANOVA).

5.2.6 Effect of BB-94 treatment on tumour necrosis factor-alpha (TNF- α) expression in POP mice

Since the expression and release of TNF- α are increased in response to albumin exposure in podocytes (Okamura et al., 2013) and PTEC (Wu et al., 2014) and is an indicator of renal inflammation (Vielhauer and Mayadas 2007), we therefore investigated the effect of BB-94 on TNF- α expression and production in POP mice. The expression of TNF- α in renal cortical tissues was analysed by WB analysis, IHC and ELISA. A representative WB is shown in Figure 5.13A. Rabbit polyclonal anti-mouse TNF- α recognised a major protein band with an estimated molecular mass of 25 kDa in kidney lysates from saline-treated control, POP and POP+BB-94 mice. Strong immunoreactivity was detected in POP group, whereas very faint or undetectable bands in both saline-treated control and POP+BB-94 treated groups indicated a very weak immunoreaction. To quantify the protein levels of TNF- α in kidney lysates, the intensity of protein bands was measured and normalised to the intensity of β -actin bands using ImageJ software (Figure 5.13B). TNF- α protein levels were significantly higher in POP group than in saline-treated control group (1.27 ± 0.15 vs 0.1 ± 0.03 relative intensity). The BB-94 treatment of POP mice was significantly lowered the protein levels of TNF- α (0.22 ± 0.07 relative intensity).

The WB results were confirmed by IHC (Figure 5.14). Renal cortical sections were immunostained with an antibody specific to mouse TNF- α . Strong immunolabeling for TNF- α was found in kidney tubules of POP mice (Figure 5.14C), whereas saline-treated control and POP+BB-94 treated mice showed very weak immunoreactive signals for TNF- α in kidney tubules (Figure 5.14B&D). The intensity of TNF- α staining was measured with a use of ImageJ software. As shown in Figure 5.15, the expression of TNF- α was significantly increased in BSA treated mice (7.91 ± 0.62 % stained area), whereas BB-94 treatment was significantly reduced the expression of TNF- α (4.15 ± 0.14 % stained area).

ELISA was also performed to measure protein levels of TNF- α in the kidney cortex of saline-treated control, POP and POP+BB-94 treated mice. TNF- α concentrations in all three groups is shown in Figure 5.16. As demonstrated, BSA administration caused a significant increase in protein levels of TNF- α (408.7 ± 46.5 pg/100 μ g protein) compared with saline-injected control group (163.6 ± 9.707 pg/100 μ g protein). Whereas, BB-94 treatment was significantly decreased the protein levels of TNF- α (266 ± 32.83 pg/ μ g protein) compared to BSA-challenged mice. Altogether, these results indicate that BB-94 treatment might be useful in reducing renal inflammation *via* decreasing TNF- α production in proteinuric conditions.

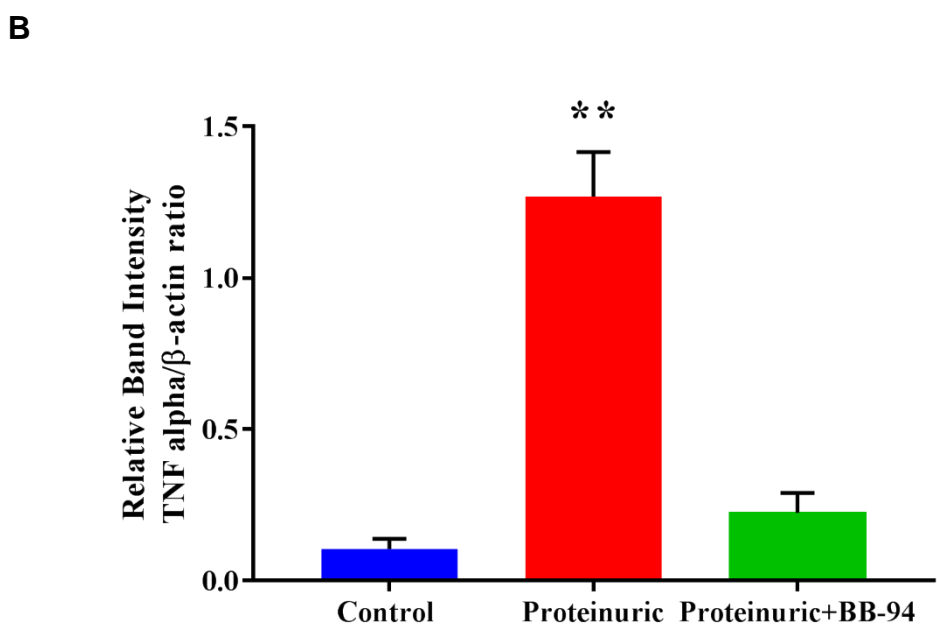
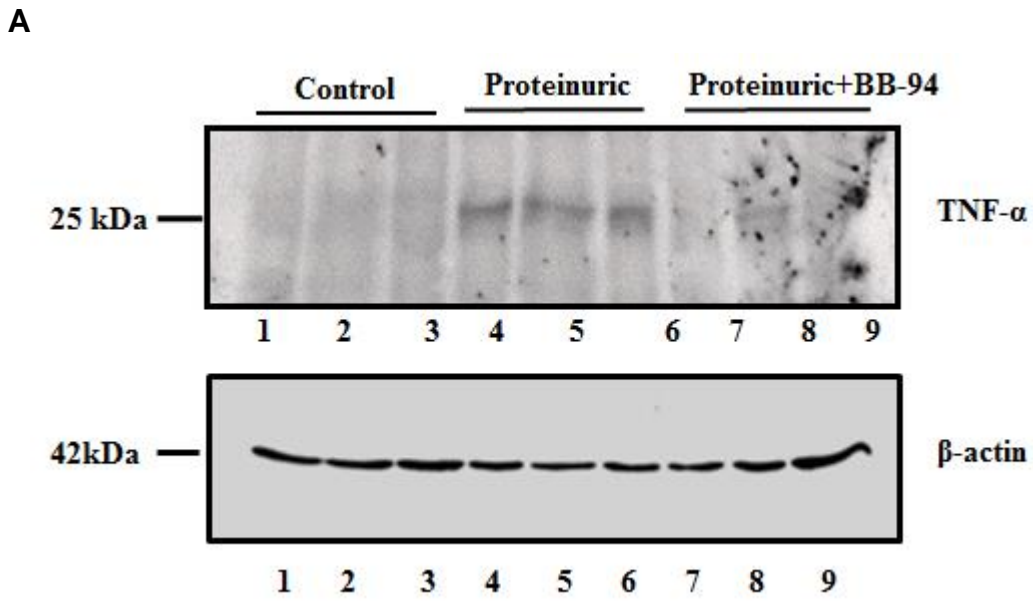


Figure 5.13: BB-94 treatment reduced TNF- α expression in the kidney of POP mice. A) Expression of TNF- α in kidney tissues from mice treated with saline, BSA or BSA+BB-94 was evaluated by WB analysis. B) Densitometric analysis of TNF- α expression is presented as the relative ratio to β -actin. Results are expressed as mean \pm SEM of 3 mice per group. ** $P < 0.05$ compared with saline-treated control and POP+BB-94 groups (ANOVA).

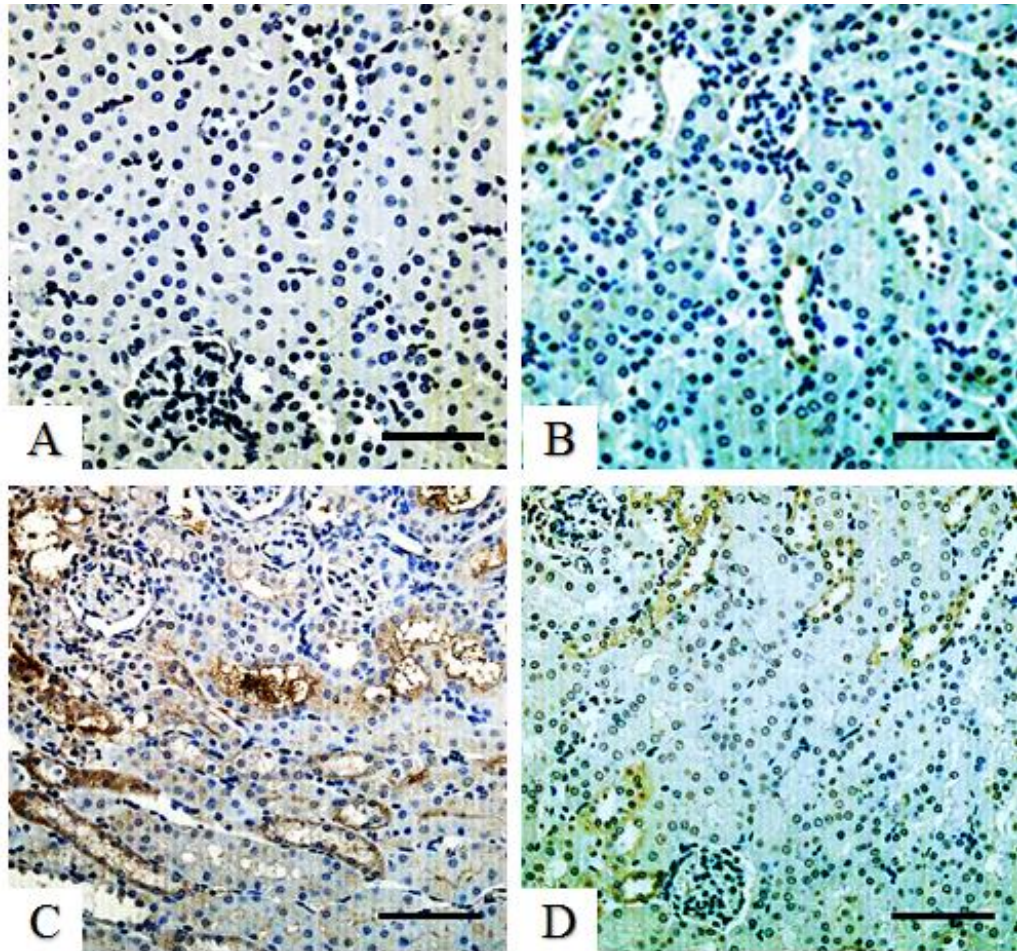


Figure 5.14: Expression of TNF- α in the cortex of kidneys from saline-treated control, POP and POP+BB-94 groups. Representative photomicrographs showing TNF- α expression assessed by IHC in the kidneys of saline-treated control (B), POP (C) and POP+BB-94 (D) groups. (A) Negative control (without primary antibody). Scale bar: 100 μ m.

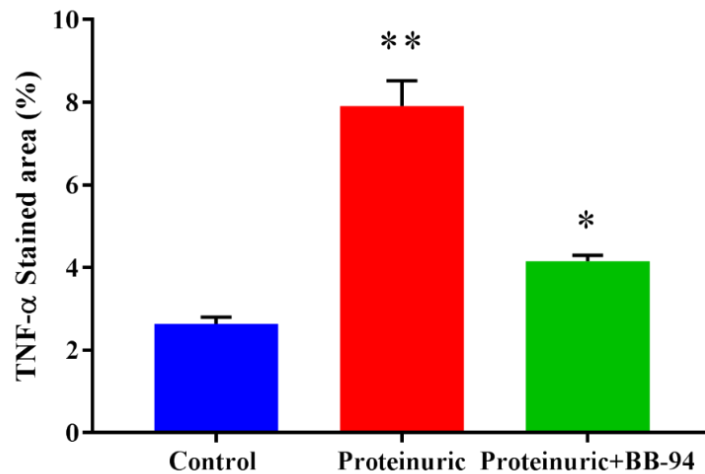


Figure 5.15: Quantification of TNF- α staining in the kidneys of saline-treated control, POP and POP+BB-94 groups. TNF- α staining was performed 14 days after BSA or BSA+BB-94 treatment. Results are expressed as mean \pm SEM of 4 mice per group. ** $P < 0.05$ compared with saline-treated control and POP+BB-94 groups (ANOVA), * $P < 0.05$ compared with saline-injected control group (ANOVA).

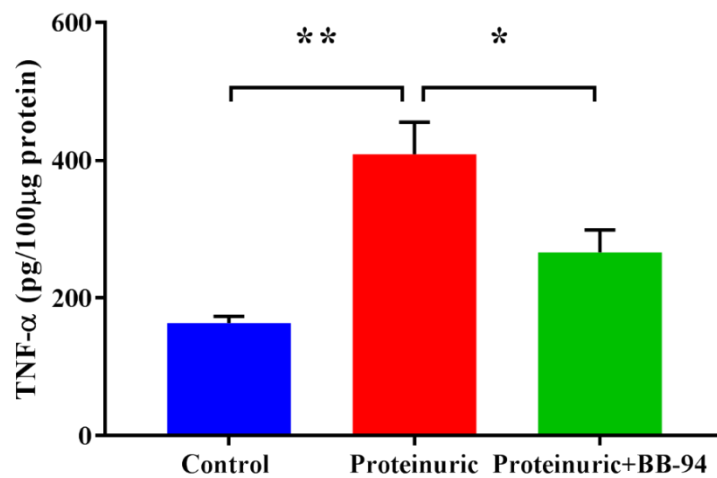


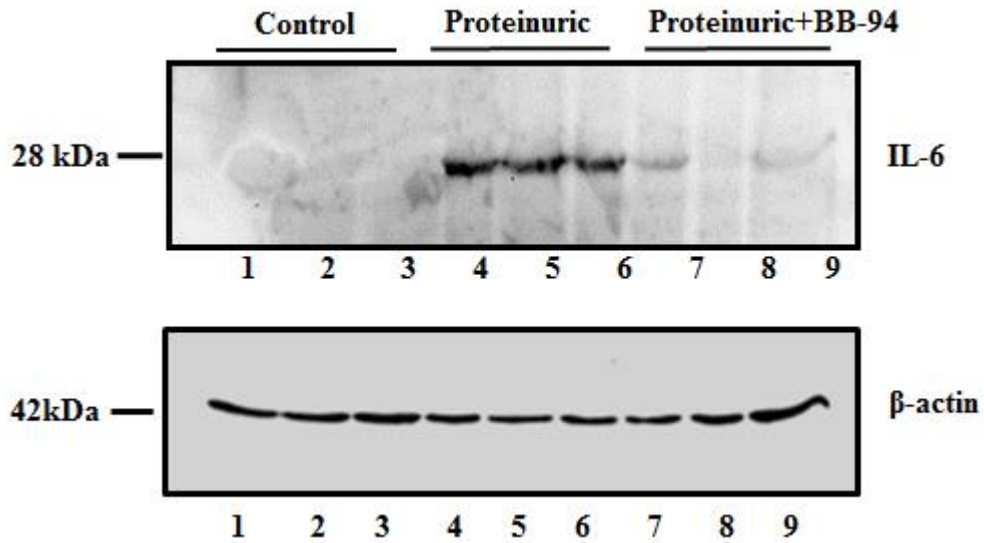
Figure 5.16: Effects of BB-94 treatment on renal TNF- α levels in POP mice. TNF- α levels were measured in the kidneys of saline-treated control mice or POP mice with or without the BB-94 by ELISA. Results are expressed as means \pm SEM of 4 mice per group. ** $P < 0.05$ compared with saline-treated control group (ANOVA), * $P < 0.05$ compared with POP+BB-94 treated group (ANOVA).

5.2.7 Effects of BB-94 treatment on interleukin-6 (IL-6) expression in POP mice

Elevated protein levels of IL-6 may promote the progression of CKD (Kayama et al., 1997). We therefore assessed protein IL-6 levels by WB analysis and IHC. WB results revealed that the protein levels of IL-6 were significantly increased in POP group (1.73 ± 0.1 % relative intensity) compared with saline-treated control group (0.07 ± 0.02 relative intensity). The administration of BB-94 ameliorated the BSA-induced increase in protein levels of IL-6 (0.26 ± 0.13 relative intensity) (Figure 5.17A&B).

WB results were confirmed by IHC. Mouse kidney sections were immunostained with rabbit polyclonal anti-mouse IL-6 antibody. Strong IL-6 immunostaining was observed in POP group (Figure 5.18C). While weak-to-moderate IL-6 immunostaining was seen in POP+BB-94 treated group (Figure 5.18D). The intensity of IL-6 immunostaining was very weak in saline-treated control group (Figure 5.18B). To quantify the protein levels of IL-6 in kidney sections, the intensity of brown staining was measured using ImageJ software. As demonstrated in Figure 5.19, the protein levels of IL-6 was significantly increased in POP mice (6.71 ± 0.52 % stained area), whereas BB-94 administration was significantly reduced the protein levels of IL-6 (2.72 ± 0.15 % stained area).

A



B

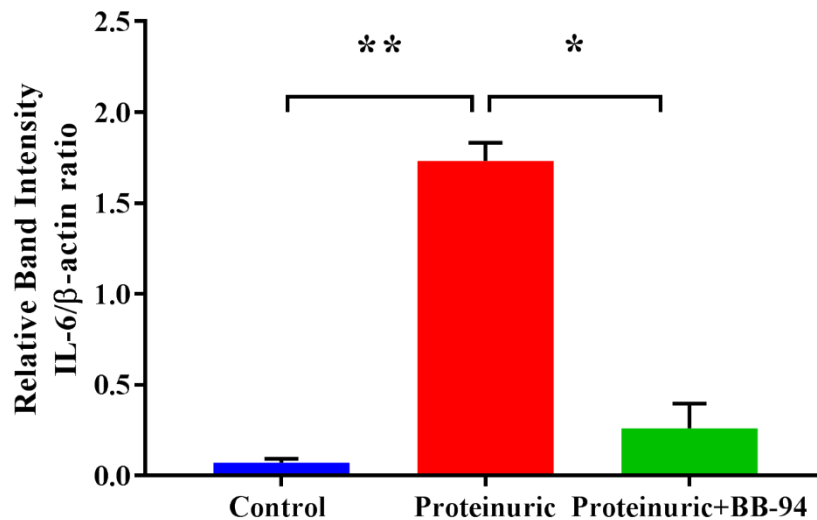


Figure 5.17: Effects of BB-94 treatment on renal IL-6 expression in POP mice. A) Expression of IL-6 in kidney tissues from saline, BSA or BSA+BB-94 treated mice was evaluated by WB analysis. B) Densitometric analysis of IL-6 expression is presented as the relative ratio to β -actin. Results are expressed as mean \pm SEM of 3 mice per group. ** $P < 0.05$ compared with saline-treated control group (ANOVA), * $P < 0.05$ compared with POP+BB-94 treated group (ANOVA).

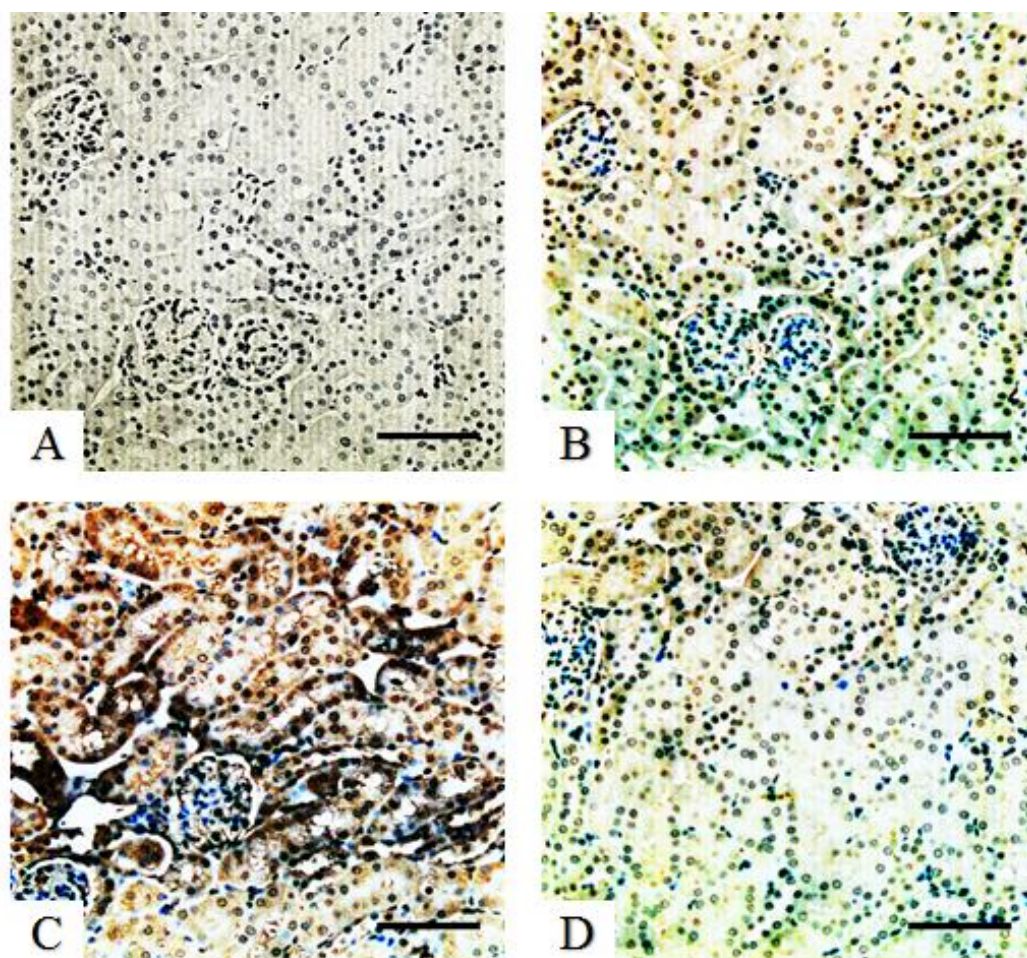


Figure 5.18: Expression of IL-6 in the cortex of kidneys from saline-treated control, POP and POP+BB-94 groups. Representative microphotographs showing IL-6 expression assessed by IHC in the kidneys of saline-injected control (B), POP (C), and POP+BB-94 (D) groups. (A) Negative control (without primary antibody). Scale bar: 100 μ m.

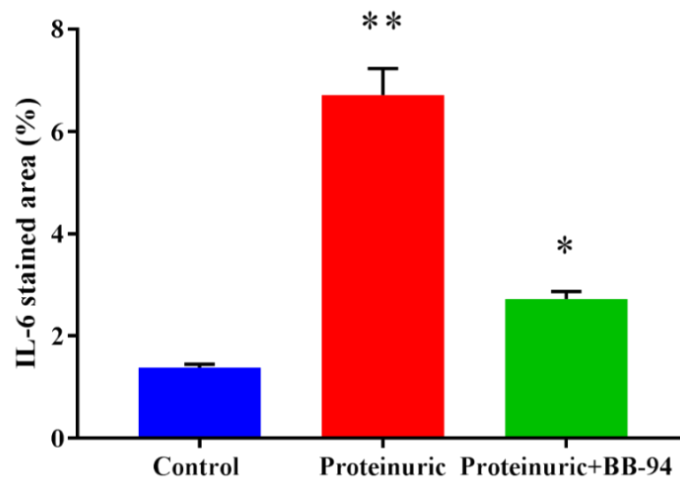


Figure 5.19: Quantification of IL-6 staining in the kidneys of saline-treated control, POP and POP+BB-94 groups. IL-6 staining was performed 14 days after BSA or BSA+BB-94 treatment. Results are expressed as mean \pm SEM of 4 mice per group. ** $P < 0.05$ compared with saline-treated control and POP+BB-94 groups (ANOVA), * $P < 0.05$ compared with saline-injected control group (ANOVA).

5.3 Discussion

The current studies demonstrate that MMPs play an important role in the development of renal interstitial inflammation and fibrosis in proteinuria. In addition, blockade of MMP greatly abrogates the progression of kidney disease in POP and improves renal function. The results demonstrate that BB-94 significantly reduced interstitial inflammation and fibrosis by decreasing the expression of proinflammatory cytokines and interstitial infiltration of macrophages.

MMPs control the structural alterations in collagen and laminin during renal fibrosis (Zhao et al., 2013). MMPs such as MMP-2, MMP-7 and MMP-9 are the main proteinases found in the kidney which are responsible for cleavage of collagen type IV and laminin (Lenz et al., 2000, Sbardella et al., 2012). Collagen type IV and laminin are the basic components of the tubular basement membrane (TBM) (Tan and Liu, 2012, Zhao et al., 2013).

Consistent with the current results, Landgraf et al. (2014) showed that collagen deposition is increased in the kidney interstitium of BSA treated mice after 7 days of administration. In support of the view that activation of MMPs is the main cause of accumulated collagen in the interstitial space of protein overload animals detected herein, Du et al. (2012) reported that collagen deposition, which was prominent in the kidney of mice after unilateral ureteral obstruction (UUO) is associated with increased MMP-2 and MMP-9 activity in MMP-2^{+/+} mice.

Most importantly, increased collagen deposition and other markers of interstitial fibrosis were not observed in MMP-2^{-/-} mice and minocycline-treated MMP-2^{+/+} mice, minocycline is an inhibitor of MMP, suggesting that MMPs play an important role in both renal fibrosis and collagen deposition (Du et al., 2012). Ślusarz et al. (2013) reported that the two collagen genes, Col1a2 and Col3a1 are elevated in MMP-7 overexpressed NRK-52E cells and in aged rat kidneys which showed increased MMP-7 expression as well, indicating the role of MMP-7 in regulating collagen production in the kidney. In agreement with these studies, blockade of MMP activity in proteinuric animals significantly reduced collagen deposition and interstitial fibrosis.

It is widely accepted that collagens, such as type I and III are the main constituents of different fibrotic lesions and excessive accumulation of these fibres may lead to alterations in tissue structure and function (Giannandrea and Parks, 2014). It has been demonstrated that degradation of collagen type IV and laminin by MMPs contributes to the tubular cell epithelial mesenchymal transition (EMT) via disruption of TBM integrity and this process has shown to be involved in the development of renal fibrosis through ECM deposition (Liu et al., 2006, Zhao et al., 2013). In vitro and in vivo studies have shown that the EMT is associated with the increased expression of MMP-2 and MMP-9 (Strutz et al., 2002, Yang et al., 2002). Similarly, renal fibrosis appears to be related with the MMP-7 induced EMT (Tan and Liu, 2012).

Several investigators have highlighted the important role for MMPs in causing EMT and renal fibrosis. Du et al. (2012) reported that MMP-2 deficient mice and minocycline-treated mice exhibit less renal interstitial fibrosis and the EMT induced molecules are also inhibited in these animals. In obstructive nephropathy, inactivation of MMP-9 using tissue-type plasminogen activator (t-PA) deficient mice preserved tubular basement membrane integrity with reduced tubular cell EMT and renal fibrosis (Yang et al., 2002). The results of above study are consistent with recent study conducted in MMP-9 KO mice with obstructive nephropathy (Wang et al., 2010). Therefore, inhibition of MMP activity in the present study might have similar effects on the EMT and renal fibrosis.

The results of the present study showed that macrophage infiltration, assessed by F4/80 immunostaining and WB, significantly increased in the kidney of POP mice. F4/80 is a specific antigen marker found on the surface of macrophages (Nishimura et al. 1998) and it is widely used by the previous investigators to estimate the degree of renal inflammation in POP studies (Abbate et al., 2008, Donadelli et al., 2003). Previously, protein overload has been shown to increase macrophage infiltration into the interstitium of proteinuric mice (Eddy et al., 2000, Landgraf et al., 2014). In the present study, increased macrophage was shown to be associated with increased MMP activity in proteinuric animals. This data is consistent with a previous study showing that MMP-2 increases macrophage infiltration into the kidney of UUO mice and this is possibly due to

the increased degradation of ECM (Nishida et al., 2007). With inhibition of MMPs activity the recruitment of macrophages into the kidney was reduced. Consistent with the current work, Nishida et al. (2007) found that inhibition of MMP-2 significantly reduced macrophage infiltration and kidney fibrosis in UUO mice.

The mechanisms by which BB-94 treatment reduces macrophage infiltration might be similar to those found by others. BB-94 reduces the activity of MMPs and in turn macrophage infiltration into the kidney interstitium in proteinuric mice. This might be due to the reduced components of ECM or other molecules which are chemotactic and play a major role in the attracting of inflammatory cells such as macrophages into the site of inflammation. For example, MMPs can increase the number of macrophages through the cleavage of OPN and the MMP-cleaved OPN has well been defined as a macrophage chemoattractant molecule (Agnihotri et al., 2001, Takafuji et al., 2007). In obstructed mice, inhibition of MMPs such as MMP-2 and MMP-9 significantly reduced MMP-cleaved OPN and macrophage infiltration (Tan et al., 2013), indicating the involvement of MMP-2 and MMP-9 both in OPN cleavage and the recruitment of macrophages to the interstitial space. Another study reported that inhibition of MMPs with minocycline is effective in reducing macrophage infiltration (Du et al., 2012). In the present work, BB-94 reduced macrophage infiltration in proteinuric animals and this might be related to the reduced production of chemotactic molecules such as MMP-cleaved OPN by MMPs. It has also been demonstrated that BB-94 reduces macrophage infiltration in mice treated with bleomycin to induce pulmonary fibrosis in mice (Corbel et al., 2001).

Macrophages has long been recognised to play an important role in the development of renal injury and fibrosis. For example, Henderson et al. (2008) found that specific reduction of macrophages using CD11b-DTR mice is associated with the reduced severity of renal fibrosis after UUO in these mice. Another study demonstrated that depletion of macrophages is linked to the reduced myofibroblasts and renal fibrosis in UUO mice (Duffield et al., 2005). Consistent with these observations, the current study showed that reduction in macrophage infiltration using BB-94 reduced renal fibrosis in proteinuric mice.

The current study showed that BB-94 markedly reduced TGF- β expression in proteinuric mice. It is well known that TGF- β is a fibrogenic cytokine and plays an important role in the kidney fibrosis (Zhao et al., 2013, Rodrigues-Díez et al., 2015). Numerous studies have reported that in the kidney increased TGF- β expression is associated with interstitial fibrosis (Tamaki et al., 1994, Eddy et al., 1995). In agreement with the present study, at least two studies have demonstrated that TGF- β expression is increased in BSA overload mice and was associated with interstitial fibrosis as collagen deposition was increasingly detected (Eddy et al., 2000, Landgraf et al., 2014). While TGF- β is a key modulator of interstitial fibrosis in these studies, its inhibition might be beneficial in reducing the development of renal fibrosis. Previously, TGF- β has shown to induce kidney fibrosis through the induction of tubular cell EMT (Lan, 2003). Recent study showed that inhibition of MMP-9 reduces TGF- β induced tubular cell EMT (Tan et al., 2010), indicating that MMPs might be involved in the regulation of TGF- β in the interstitium or the EMT itself. It has been demonstrated that MMPs can modulate growth factors and their receptors (TGF- β , FGF-R1), adhesion molecules, cytokines and chemokines (Catania et al., 2007, Genovese et al., 2014). Thus, the reduced TGF- β expression in the current work might be related to the inhibition of MMPs by BB-94. However, in a murine model of pulmonary fibrosis BB-94 is failed to reduce TGF- β in the bronchoalveolar lavage (Corbel et al., 2001).

In addition, macrophages are known to produce and release TGF- β in various tissues (Nacu et al., 2008, Zhao et al., 2013). Diamond et al. (1994) showed that the mRNA levels of TGF- β 1 is significantly increased in the renal cortex of UUO mice and was associated with the increased macrophage infiltration to the interstitium. In the present study, the same correlation was detected between macrophage infiltration and TGF- β expression in proteinuric animals. Therefore, reduced TGF- β in BB-94 treated animals might be related to the reduced macrophage numbers as discussed earlier.

The results demonstrate that BB-94 dramatically reduced the expression of TNF- α in proteinuric mice. MMPs have been shown to induce the release of TNF- α from macrophages and cells, which in turn increases the tissue level of TNF- α . Haro et al. (2000) demonstrated that MMP-7 expression is essential for

the release of cytokine TNF- α from peritoneal macrophages. Another study showed that the release of TNF- α from cells can be inhibited by hydroxamic acid-based inhibitors (MMP inhibitor), indicating the involvement of MMPs in increasing the level of this cytokine in the tissue (Black et al., 1997). Consistent with the present study using inhibitors of TNF- α production such as GM6001 (MMP inhibitor), the serum and kidney protein levels of TNF- α was reduced in cisplatin induced nephrotoxicity model (Ramesh and Reeves, 2002).

Lee et al. (2009) believes that secreted MMP-9 from macrophages are involved in tissue destruction and inflammation through proteolytic activation of cytokines/chemokines and degradation of matrix proteins. In vivo inhibition of MMPs markedly reduced the increased numbers of inflammatory cells and the increased mRNA and protein expression of proinflammatory cytokines such as IL-1 and TNF- α in both lung tissues and bronchoalveolar lavage fluids in a murine model of toluene diisocyanate (TDI)-induced asthma (Lee et al., 2003).

The role of TNF- α in kidney inflammation and injury has been well documented. It has been shown that, both genetic TNF- α deficiency and pharmacological inhibition of this cytokine attenuate the progression of renal disease by reducing inflammation and crescent formation in an experimental model of crescentic glomerulopathy (Karkar et al., 2001). Furthermore, in cisplatin-induced nephrotoxicity, inhibition of TNF- α release appears to be protective against inflammation and the development of kidney injury (Ramesh and Reeves, 2002, Ramesh and Reeves, 2003). Similarly, Knotek et al. (2001) found that mice treated with TNFRp55, which binds to TNF- α and neutralises it, exhibited better renal function indicating less inflammation and tissue injury. Consistent with the above studies, reduced TNF- α expression using MMP inhibitor (BB-94) attenuates BSA-induced tubular damage in POP model.

Another proinflammatory marker reduced by BB-94 treatment in proteinuric mice is IL-6. Within the kidney, a significant correlation has been detected between increased IL-6 expression and kidney injury (Grigoryev et al., 2008). At least one study showed that IL-6 deficiency protects the kidney from further injury. In this study, reduced AKI was shown to be associated with reduced neutrophil accumulation suggesting the role of IL-6 in the recruitment of

inflammatory cells during inflammation (Nechemia-Arbely et al., 2008). In the current study, together with the other inflammatory markers, reduction in IL-6 expression appeared more effective in reducing kidney inflammation.

Although no previous works have shown the mechanisms of the effect of BB-94 or other MMP inhibitors on the kidney expression of IL-6, the reduced IL-6 expression in the present work is more likely to be related with the reduced MMP activity and migration of inflammatory cells and proinflammatory cytokines

Reduced inflammation and fibrosis in MMPI treated mice as evidenced above could greatly be linked to the reduced proteinuria mentioned in the previous chapter. A bulk of evidence reveals that proteinuria is the major risk for CKD which is characterised by the presence of kidney inflammation and fibrosis as shown here in proteinuric mice.

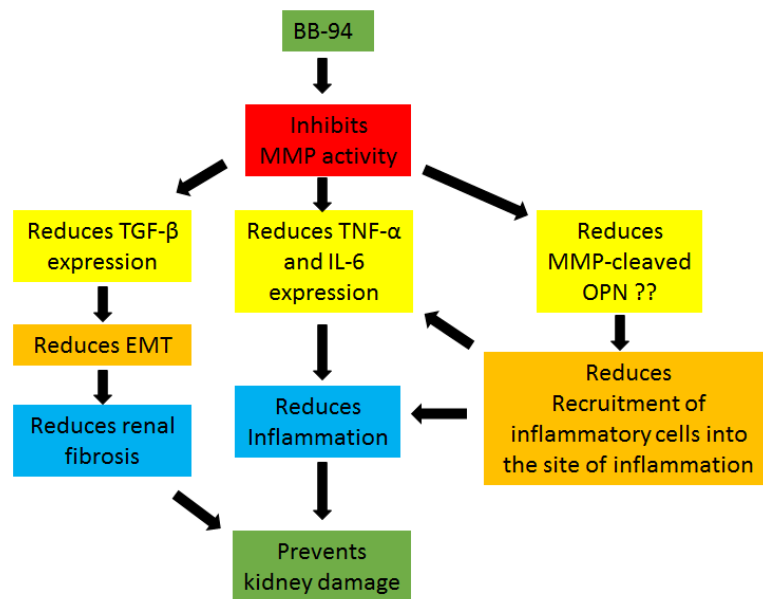


Figure 5.20: Mechanisms of MMP inhibition preventing renal tubulointerstitial inflammation and fibrosis. MMP inhibition abrogates the formation of MMP-cleaved OPN, a chemotactic molecule having role in the recruitment of inflammatory cells into the site of inflammation and leading to tubulointerstitial inflammation. MMP blockade reduces the expression of proinflammatory cytokines TNF- α and IL-6 and growth factor TGF- β which subsequently reduces inflammation and fibrosis. BB-94 = Broad spectrum MMP inhibitor, OPN = Osteopontin, EMT = Epithelial Mesenchymal Transformation.

5.4 Conclusions

- Overall BB-94 treatment ameliorated renal interstitial inflammation and fibrosis, and prevented the kidney from further damage in proteinuric animals.
- BB-94 treatment reduced macrophage infiltration into the interstitium of proteinuric mice.
- BB-94 treatment reduced proinflammatory markers such as TNF- α and IL-6 in the kidney of proteinuric mice.
- BB-94 treatment reduced collagen deposition and TGF- β expression in the kidney of proteinuric mice.

6 Thesis discussion

6.1 Thesis Summary

This thesis has demonstrated that megalin and FcRn protein are down-regulated in the PTEC of proteinuric kidney compared with non-proteinuric proximal epithelial cells, and this protein down-regulation was largely due to receptor shedding into the urine while the gene expression of these receptors was inversely increased in the PTEC exposed to BSA overload. Notably, the decreased expression of these receptors was associated with the increased urinary excretion of megalin and FcRn ligands such as albumin; increased enzymatic activity of metalloproteinases and increased megalin and FcRn excretion into the urine of proteinuric animals.

By investigating the mechanism of megalin and FcRn protein down-regulation in proteinuric animals, I have provided an insight into how the cell surface expression of megalin and FcRn are maintained in the PTEC. I have demonstrated that increased megalin and FcRn protein expression are important as in proteinuric animals when the expression and function of these endocytic receptors are downregulated, the urinary excretion of plasma proteins are increased. Activation of megalin and FcRn reduced urinary excretion of plasma proteins indicating the fundamental role of these receptors in normal reabsorption of glomerular filtered proteins in the kidney. Megalin and FcRn cell surface maintenance was largely due to the reduced activity of MMP that was inhibited by a broad spectrum MMP inhibitor (BB-94). Blockade of MMPs activity reduced megalin and FcRn shedding into the urine of proteinuric mice, which in turn increased the protein expression of these receptors in the PTEC.

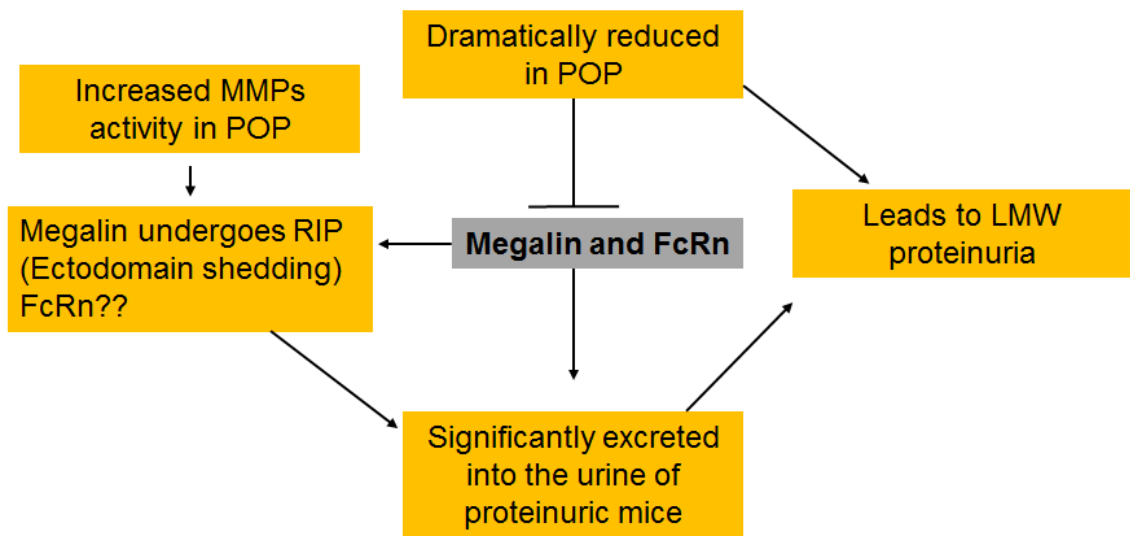


Figure 6.1: Schematic view of endocytic receptor down-regulation in proteinuria

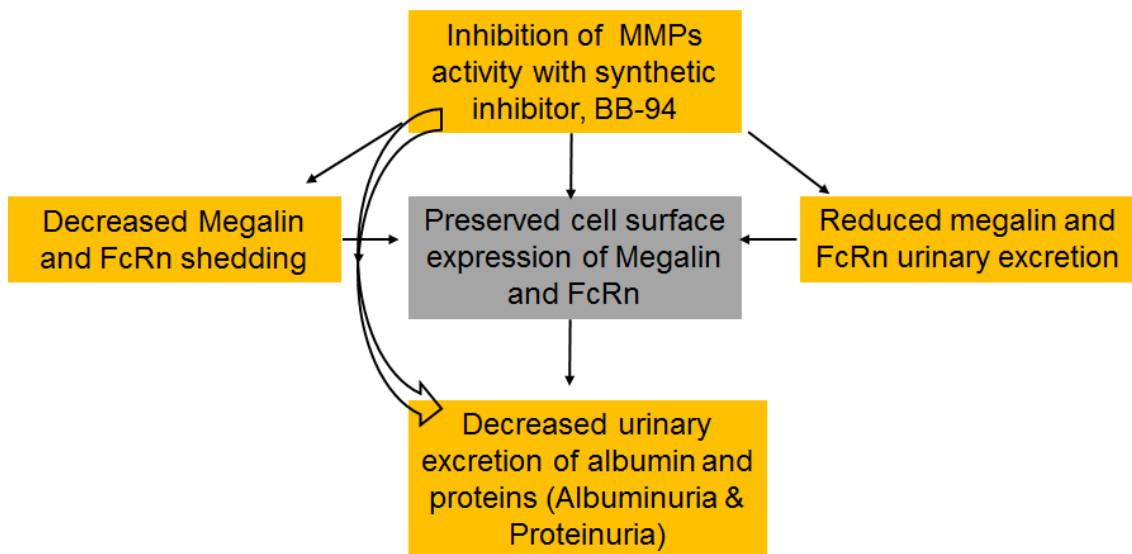


Figure 6.2: Schematic view showing how MMPs inhibition preserves cell surface expression of endocytic receptors in the proximal tubule cells in the kidney.

In Chapter 5, it is demonstrated that protein overload led to renal tubulointerstitial fibrosis and inflammation in experimental animals. Increased filtered proteins in the tubular lumen, in addition to the negative effects on proximal tubular expression of endocytic receptors, resulted in a marked increase in proinflammatory cytokines and chemokines (TNF- α , IL-6 and TGF- β). It also increased the recruitment of inflammatory cells such as macrophage into the kidney of proteinuric mice. Further, protein overload caused aberrant collagen deposition in the tubulointerstitial space of proteinuric mice. Finally, inhibition of MMPs activity in the kidney of proteinuric animals with BB-94 significantly ameliorated renal tubulointerstitial fibrosis and inflammation as the expression of TNF- α , IL-6 and TGF- β are all decreased; reduced macrophage infiltration into the interstitial space and decreased collagen deposition.

It is proposed that MMPs contribute to renal fibrosis through the induction of tubular EMT. In vitro and in vivo studies have demonstrated that MMP-2 and MMP-9 can cleave the basic components of the tubular basement membrane, type IV collagen and laminin, and subsequently may lead to tubular EMT and kidney fibrosis (Cheng and Lovet 2003, Strutz et al., 2002, Yang et al., 2002). In addition, MMPs play a major role in mediating the TGF- β induced EMT (Zhao et al., 2013). This may have a direct effect on the enhancement of TGF- β expression in the kidney, and the increase in kidney fibrosis.

It is of great importance to keep the intracellular activity of MMPs and increased MMPs activity may lead to collagen deposition in the kidney interstitium. This is largely because the deteriorated balance between ECM degradation and synthesis.

MMPs are involved in interstitial inflammation through the production of chemotactic molecules and degradation of ECM proteins. OPN is one of the proteins that cleaves by MMPs and produces MMP-cleaved OPN. This by-product of MMP has long been recognised to increase the number of macrophages in the kidney interstitium (Tan et al., 2013).

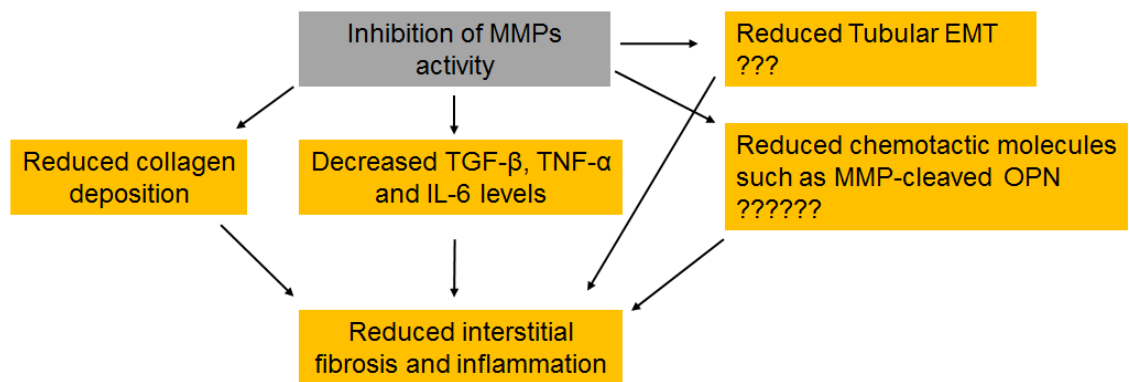


Figure 6.3: Schematic diagram showing how inhibition of MMPs activity reduces interstitial fibrosis and inflammation.

6.2 Conclusions

In conclusion, this thesis has demonstrated that the expression of endocytic receptors megalin and FcRn is greatly altered in the PTEC of proteinuric mice. The present study has also provided evidence showing that preserving megalin and FcRn cell surface expression may be of significant clinical importance, as treatment with MMP inhibitor was able to reduce proteinuria in proteinuric mice. Subsequent reduction in progressive tubulointerstitial fibrosis and inflammation has also reported in proteinuric animals and that was probably due to the reduced proteinuria. Although the expression and function of renal proximal endocytic receptors is an area of research which is at its inception, it is clear that megalin and FcRn could be physiological targets for the treatment of proteinuria and kidney diseases.

6.3 Future Work

- From the data obtained in this thesis, treatment with BB-94 was effective against proteinuria and reduced tubular injury in only two weeks duration of disease. Future studies will examine the efficacy of this MMP inhibitor in the treatment of proteinuria and tubulointerstitial fibrosis and inflammation in the later disease or long-term condition.
- Future studies examining gene expression of megalin and FcRn in the kidney tissues exposed to protein overload for longer duration will be critical to confirm the results of the present study.
- Identification of megalin and FcRn forms in the urine of proteinuric animals will provide more evidence for the mechanism of receptor shedding into the urine.

- Further investigation into the mechanisms of how the broad spectrum MMPI (BB-94) reduced kidney fibrosis and inflammation.
- The results presented suggest that inhibition of MMPs activity could be a therapeutic target for the treatment of proteinuria and kidney diseases.
- These studies found that MMP-9 is the most candidate responsible for the tubular events, therefore it is of great importance to use a specific inhibitor against MMP-9 activity rather than the broad spectrum MMP inhibitor.
- A mouse model of conditional MMP-9 knockout could be useful to study the effect of this endopeptidase on megalin and FcRn shedding.
- MMPI is never successful in treating cancer and tumour due to non-selectivity, therefore using MMP-9 inhibitor could have better effect on reducing proteinuria and kidney inflammation and fibrosis.

7 Appendices

7.1 Appendix A - Buffers and solutions used in this study

PBS:

137 mM NaCl
2.7 mM KCl
10 mM Na₂HPO₄
2 mM KH₂PO₄

TBS buffer:

20 mM Tris-base
100 mM NaCl

TBST buffer:

20 mM Tris-base
100 mM NaCl
0.05% Tween 20

SDS-running buffer:

25 mM Tris-base
192 mM Glycine
0.1% Sodium-dodecyl-sulphate (SDS) (w/v)

2X SDS Gel loading buffer:

100 mM Tris (pH 6.8)
20% Glycerol
4% SDS
0.2% Bromophenol blue
200 mM Dithiothreitol (DTT)

Transfer buffer:

39 mM glycine
48 mM Tris base
0.375 % SDS (w/v)
20% methanol (v/v)

4% SDS-PAGE gel (10 ml):

5.85 ml H₂O
1.34 ml 30% Acrylamide
2.6 ml Tris-base (pH 8.8)
0.1 ml 20% SDS
0.1 ml 10% ammonium persulfate (APS)
0.01 ml TEMED

10% SDS-PAGE gel (10 ml):

4.0 ml H₂O
3.3 ml 30% Acrylamide
2.5 ml 1.5 M Tris-base (pH 8.8)
0.1 ml 20% SDS
0.1 ml 10% APS
0.004 ml TEMED

Coomassie destaining solution:

90% Methanol: Distilled water 1:1
10% Glacial acetic acid

Lysis buffer 2 ml:

1.946 ml PBS
20 µl Triton x-100
20 µl Phenylmethanesulfonyl fluoride (PMSF)
2 µl Pepstatin
2 µl Aprotinin
20 µl Roche Factor

Citrate Buffer (pH 6.0):

10 mM Tri-sodium citrate (dehydrate)

5% blocking solution:

1 g milk powder

20 ml TBS

Blocking serum:

0.5% BSA

3% Milk powder

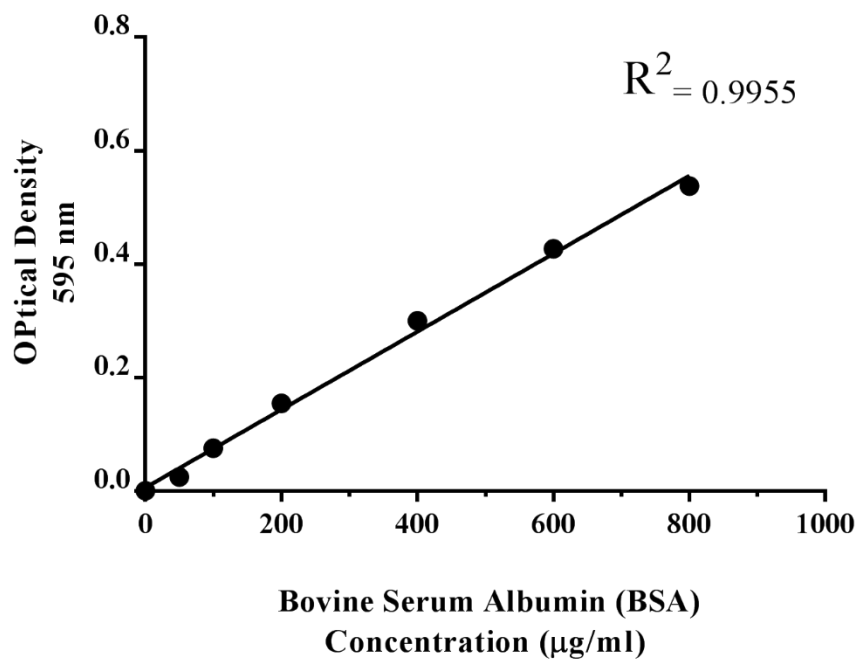
10% Goat serum

10% Goat serum:

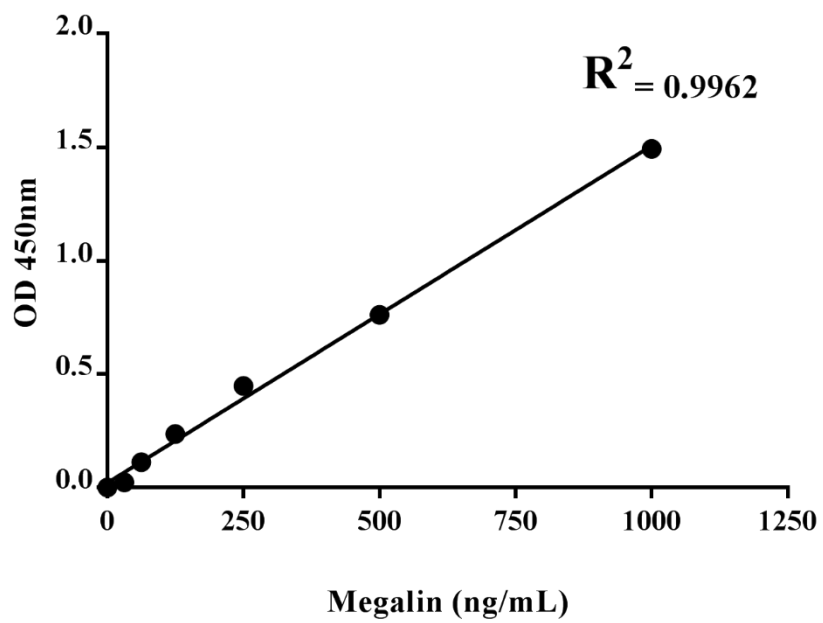
10 μ l Normal goat serum

90 μ l PBS

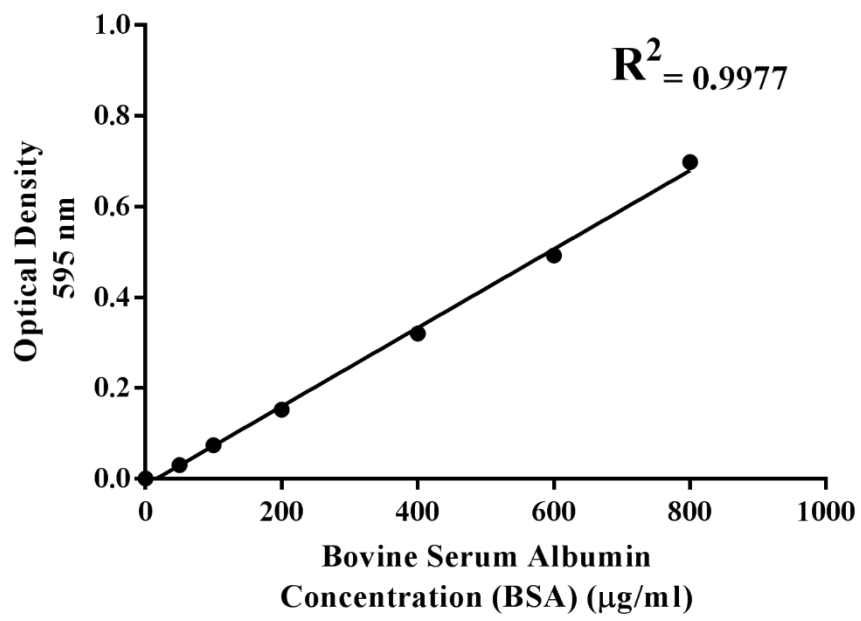
7.2 Appendix B - Standard curves



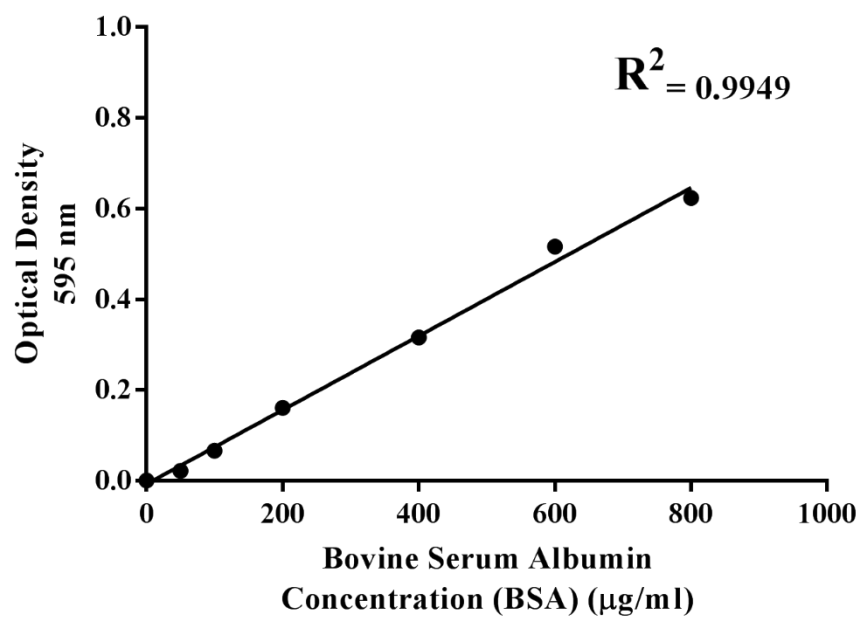
Standard curve for determining protein concentration in mouse urine. The relative optical density of BSA standards at 595 nm increases with the increase of BSA concentration. The linear regression was used to calculate the protein concentration of urine samples.



Standard curve for determining megalin concentration in mouse urine.



Standard curve for determining total serum protein concentration in mice.



An example of standard curve for determining protein concentration in mouse kidney homogenates.

7.3 Appendix C - Automated image analysis macro code

Below code for analysing IHC staining was kindly provided by Sami Alghadban, former PhD student in Lab 228.

//The code starts:

```
dir1 = getDirectory("Choose source directory");
list = getFileList(dir1);
dir2 = getDirectory("Choose destination directory");
setBatchMode(true);
for (i=0; i<list.length; i++) {
    path = dir1+list[i];
    open(path);
    title1= getTitle;
    title2 = File.nameWithoutExtension;
    run("Subtract Background...", "rolling=50 light");
    run("8-bit");
    setThreshold(0, 180);
    run("Convert to Mask");
    run("Set Measurements...", "area min max mean area fraction
redirect=None decimal=2");
    run("Measure");
    saveAs("tiff", dir2+"Threshold of "+title2+".tiff");
}
selectWindow("Results");
run("Summarize");
saveAs("txt", dir2+title2+".xls");
run("Close")
run("Close All");
```

//End of the code.

8 References

- Abbate, M., Zoja, C., Corna, D., Capitanio, M., Bertani, T. and Remuzzi, G., 1998. In progressive nephropathies, overload of tubular cells with filtered proteins translates glomerular permeability dysfunction into cellular signals of interstitial inflammation. *Journal of the American Society of Nephrology*, 9(7), pp.1213-1224.
- Abbate, M., Zoja, C., Rottoli, D., Corna, D., Perico, N., Bertani, T. and Remuzzi, G., 1999. Antiproteinuric therapy while preventing the abnormal protein traffic in proximal tubule abrogates protein- and complement-dependent interstitial inflammation in experimental renal disease. *Journal of the American Society of Nephrology*, 10(4), pp.804-813.
- Adler, S., 1992. Characterization of glomerular epithelial cell matrix receptors. *The American journal of pathology*, 141(3), p.571.
- Adler, S., 2004. Diabetic nephropathy: Linking histology, cell biology, and genetics. *Kidney International*, 66(5), pp.2095-2106.
- Agnihotri, R., Crawford, H.C., Haro, H., Matrisian, L.M., Havrda, M.C. and Liaw, L., 2001. Osteopontin, a novel substrate for matrix metalloproteinase-3 (stromelysin-1) and matrix metalloproteinase-7 (matrilysin). *Journal of Biological Chemistry*, 276(30), pp.28261-28267.
- Ahmed, A.K.H., 2009. Matrix metalloproteinases and their inhibitors in kidney scarring: culprits or innocents. *Journal of Health Science*, 55(4), pp.473-483.
- Akihiro, T.O.J.O., ONOZATO, M.L., Kurihara, H., Sakai, T. and FUJITA, T., 2003. Angiotensin II blockade restores albumin reabsorption in the proximal tubules of diabetic rats. *Hypertension Research*, 26(5), pp.413-419.
- Akilesh, S., Huber, T.B., Wu, H., Wang, G., Hartleben, B., Kopp, J.B., Miner, J.H., Roopenian, D.C., Unanue, E.R. and Shaw, A.S., 2008. Podocytes use FcRn to clear IgG from the glomerular basement membrane. *Proceedings of the National Academy of Sciences*, 105(3), pp.967-972.
- Amann, K., Koch, A., Hofstetter, J., Gross, M.L., Haas, C., Orth, S.R., Ehmke, H., Rump, L.C. and Ritz, E., 2001. Glomerulosclerosis and progression: Effect of subantihypertensive doses of α and β blockers. *Kidney International*, 60(4), pp.1309-1323.
- Amann, K., Rump, L.C., Simonaviciene, A., Oberhauser, V., Wessels, S., Orth, S.R., Gross, M.L., Koch, A., Bielenberg, G.W., Van Kats, J.P. and Ehmke, H., 2000. Effects of low dose sympathetic inhibition on glomerulosclerosis and albuminuria in subtotaly nephrectomized rats. *Journal of the American Society of Nephrology*, 11(8), pp.1469-1478.
- Aminoff, M., Carter, J.E., Chadwick, R.B., Johnson, C., Gräsbeck, R., Abdelaal, M.A., Broch, H., Jenner, L.B., Verroust, P.J., Moestrup, S.K. and Chapelle, A.D.L., 1999. Mutations in CUBN, encoding the intrinsic factor-vitamin B 12

receptor, cubilin, cause hereditary megaloblastic anaemia 1. *Nature Genetics*, 21(3).

Amsellem, S., Gburek, J., Hamard, G., Nielsen, R., Willnow, T.E., Devuyst, O., Nexo, E., Verroust, P.J., Christensen, E.I. and Kozyraki, R., 2010. Cubilin is essential for albumin reabsorption in the renal proximal tubule. *Journal of the American Society of Nephrology*, 21(11), pp.1859-1867.

Andersen, J.T., Dalhus, B., Cameron, J., Daba, M.B., Plumridge, A., Evans, L., Brennan, S.O., Gunnarsen, K.S., Bjørås, M., Sleep, D. and Sandlie, I., 2012. Structure-based mutagenesis reveals the albumin-binding site of the neonatal Fc receptor. *Nature Communications*, 3, p.610.

Andersen, J.T., Dee Qian, J. and Sandlie, I., 2006. The conserved histidine 166 residue of the human neonatal Fc receptor heavy chain is critical for the pH-dependent binding to albumin. *European Journal of Immunology*, 36(11), pp.3044-3051.

Anderson, S., Meyer, T.W., Rennke, H.G. and Brenner, B.M., 1985. Control of glomerular hypertension limits glomerular injury in rats with reduced renal mass. *Journal of Clinical Investigation*, 76(2), p.612.

Anderson, S., Rennke, H.G. and Brenner, B.M., 1986. Therapeutic advantage of converting enzyme inhibitors in arresting progressive renal disease associated with systemic hypertension in the rat. *Journal of Clinical Investigation*, 77(6), p.1993.

Andersson, E.R., Sandberg, R. and Lendahl, U., 2011. Notch signaling: simplicity in design, versatility in function. *Development*, 138(17), pp.3593-3612.

Arici, M., Chana, R., Lewington, A., Brown, J. and Brunskill, N.J., 2003. Stimulation of proximal tubular cell apoptosis by albumin-bound fatty acids mediated by peroxisome proliferator activated receptor- γ . *Journal of the American Society of Nephrology*, 14(1), pp.17-27.

Baines, R. J., 2010. *Megalin Cytoplasmic Tail Phosphorylation and Function in Kidney Proximal Tubular Cells*.

Baines, R.J. and Brunskill, N.J., 2008. The molecular interactions between filtered proteins and proximal tubular cells in proteinuria. *Nephron Experimental Nephrology*, 110(2), pp.e67-e71.

Baines, R.J. and Brunskill, N.J., 2011. Tubular toxicity of proteinuria. *Nature Reviews Nephrology*, 7(3), pp.177-180.

Bakoush, O., Grubb, A., Rippe, B. and Tencer, J., 2001. Urine excretion of protein HC in proteinuric glomerular diseases correlates to urine IgG but not to albuminuria. *Kidney International*, 60(5), pp.1904-1909.

Barth, J.L. and Argraves, W.S., 2001. Cubilin and megalin: partners in lipoprotein and vitamin metabolism. *Trends in Cardiovascular Medicine*, 11(1), pp.26-31.

- Beckett, R.P., Davidson, A.H., Drummond, A.H., Huxley, P. and Whittaker, M., 1996. Recent advances in matrix metalloproteinase inhibitor research. *Drug Discovery Today*, 1(1), pp.16-26.
- Benezra, M., Vlodavsky, I., Ishai-Michaeli, R., Neufeld, G. and Bar-Shavit, R., 1993. Thrombin-induced release of active basic fibroblast growth factor-heparan sulfate complexes from subendothelial extracellular matrix. *Blood*, 81(12), pp.3324-3331.
- Bern, M., Sand, K.M.K., Nilsen, J., Sandlie, I. and Andersen, J.T., 2015. The role of albumin receptors in regulation of albumin homeostasis: Implications for drug delivery. *Journal of Controlled Release*, 211, pp.144-162.
- Bernstein, L.S., Grillo, A.A., Loranger, S.S. and Linder, M.E., 2000. RGS4 binds to membranes through an amphipathic α -helix. *Journal of Biological Chemistry*, 275(24), pp.18520-18526.
- Bidani, A.K., Mitchell, K.D., Schwartz, M.M., Navar, L.G. and Lewis, E.J., 1990. Absence of glomerular injury or nephron loss in a normotensive rat remnant kidney model. *Kidney International*, 38(1), pp.28-38.
- Biemesderfer, D., 2006. Regulated intramembrane proteolysis of megalin: linking urinary protein and gene regulation in proximal tubule?. *Kidney International*, 69(10), pp.1717-1721.
- Birn, H. and Christensen, E.I., 2006. Renal albumin absorption in physiology and pathology. *Kidney International*, 69(3), pp.440-449.
- Birn, H., 2006. The kidney in vitamin B 12 and folate homeostasis: characterization of receptors for tubular uptake of vitamins and carrier proteins. *American Journal of Physiology-Renal Physiology*, 291(1), pp.F22-F36.
- Birn, H., Fyfe, J.C., Jacobsen, C., Mounier, F., Verroust, P.J., Ørskov, H., Willnow, T.E., Moestrup, S.K. and Christensen, E.I., 2000. Cubilin is an albumin binding protein important for renal tubular albumin reabsorption. *Journal of Clinical Investigation*, 105(10), p.1353.
- Black, R.A., Rauch, C.T., Kozlosky, C.J., Peschon, J.J., Slack, J.L., Wolfson, M.F., Castner, B.J., Stocking, K.L., Reddy, P., Srinivasan, S. and Nelson, N., 1997. A metalloproteinase disintegrin that releases tumour-necrosis factor- α from cells. *Nature*, 385(6618), p.729.
- Bode, W., Gomis-Rüth, F.X. and Stöckler, W., 1993. Astacins, serralytins, snake venom and matrix metalloproteinases exhibit identical zinc-binding environments (HEXXHXXGXXH and Met-turn) and topologies and should be grouped into a common family, the 'metzincins'. *FEBS Letters*, 331(1-2), pp.134-140.
- Broch, H., Imerslund, O., Monn, E., Hovig, T. and Seip, M., 1984. Imerslund Gräsbeck Anemia. *Acta Paediatrica*, 73(2), pp.248-253.

- Brown, P.D., 1995. Matrix metalloproteinase inhibitors: a novel class of anticancer agents. *Advances in Enzyme Regulation*, 35, pp.293-301.
- Brown, M.S. and Goldstein, J.L., 1997. The SREBP pathway: regulation of cholesterol metabolism by proteolysis of a membrane-bound transcription factor. *Cell*, 89(3), pp.331-340.
- Brunskill, N.J., Nahorski, S., Walls, J. and Brunskill, N., 1997. Characteristics of albumin binding to opossum kidney cells and identification of potential receptors. *Pflügers Archiv-European Journal of Physiology*, 433(4), pp.497-504.
- Brunskill, N.J., Cockcroft, N.E.I.L., Nahorski, S.T.E.F.A.N. and Walls, J.O.H.N., 1996. Albumin endocytosis is regulated by heterotrimeric GTP-binding protein G alpha i-3 in opossum kidney cells. *American Journal of Physiology-Renal Physiology*, 271(2), pp.F356-F364.
- Brunskill, N.J., Nahorski, S., Walls, J. and Brunskill, N., 1997. Characteristics of albumin binding to opossum kidney cells and identification of potential receptors. *Pflügers Archiv European Journal of Physiology*, 433(4), pp.497-504.
- Bu, G. and Marzolo, M.P., 2000. Role of rap in the biogenesis of lipoprotein receptors. *Trends in Cardiovascular Medicine*, 10(4), pp.148-155.
- Bulger, R.E., Eknayan, G.A.R.A.B.E.D., Purcell 2nd, D.J. and Dobyan, D.C., 1983. Endothelial characteristics of glomerular capillaries in normal, mercuric chloride-induced, and gentamicin-induced acute renal failure in the rat. *Journal of Clinical Investigation*, 72(1), p.128.
- Burton, C. and Harris, K.P.G., 1996. The role of proteinuria in the progression of chronic renal failure. *American Journal of Kidney Diseases*, 27(6), pp.765-775.
- Cabezas, F., Lagos, J., Céspedes, C., Vio, C.P., Bronfman, M. and Marzolo, M.P., 2011. Megalin/LRP2 expression is induced by peroxisome proliferator-activated receptor-alpha and-gamma: implications for PPARs' roles in renal function. *PLOS One*, 6(2), p.e16794.
- Caruso-Neves, C., Pinheiro, A.A.S., Cai, H., Souza-Menezes, J. and Guggino, W.B., 2006. PKB and megalin determine the survival or death of renal proximal tubule cells. *Proceedings of the National Academy of Sciences*, 103(49), pp.18810-18815.
- Catania, J.M., Chen, G. and Parrish, A.R., 2007. Role of matrix metalloproteinases in renal pathophysiology. *American Journal of Physiology-Renal Physiology*, 292(3), pp.F905-F911.
- Caulfield, J.P. and Farquhar, M.G., 1975. The permeability of glomerular capillaries of aminonucleoside nephrotic rats to graded dextrans. *Journal of Experimental Medicine*, 142(1), pp.61-83.
- Chadzinska, M., Baginski, P., Kolaczowska, E., Savelkoul, H.F. and Lidy Verburg-van Kemenade, B.M., 2008. Expression profiles of matrix metalloproteinase 9 in teleost fish provide evidence for its active role in initiation and resolution of inflammation. *Immunology*, 125(4), pp.601-610.

- Chang, A.M., Ohse, T., Krofft, R.D., Wu, J.S., Eddy, A.A., Pippin, J.W. and Shankland, S.J., 2011. Albumin-induced apoptosis of glomerular parietal epithelial cells is modulated by extracellular signal-regulated kinase 1/2. *Nephrology Dialysis Transplantation*, 27(4), pp.1330-1343.
- Chang, R.L., Ueki, I.F., Troy, J.L., Deen, W.M., Robertson, C.R. and Brenner, B.M., 1975. Permselectivity of the glomerular capillary wall to macromolecules. II. Experimental studies in rats using neutral dextran. *Biophysical Journal*, 15(9), pp.887-906.
- Chaudhury, C., Brooks, C.L., Carter, D.C., Robinson, J.M. and Anderson, C.L., 2006. Albumin binding to FcRn: Distinct from the FcRn- IgG interaction. *Biochemistry*, 45(15), pp.4983-4990.
- Chaudhury, C., Mehnaz, S., Robinson, J.M., Hayton, W.L., Pearl, D.K., Roopenian, D.C. and Anderson, C.L., 2003. The major histocompatibility complex-related Fc receptor for IgG (FcRn) binds albumin and prolongs its lifespan. *Journal of Experimental Medicine*, 197(3), pp.315-322.
- Chen, P., Li, C., Lang, S., Zhu, G., Rehemian, A., Spring, C.M., Freedman, J. and Ni, H., 2010. Animal model of fetal and neonatal immune thrombocytopenia: role of neonatal Fc receptor in the pathogenesis and therapy. *Blood*, 116(18), pp.3660-3668.
- Cheng, S. and Lovett, D.H., 2003. Gelatinase A (MMP-2) is necessary and sufficient for renal tubular cell epithelial-mesenchymal transformation. *The American Journal of Pathology*, 162(6), pp.1937-1949.
- Christ, A., Terryn, S., Schmidt, V., Christensen, E.I., Huska, M.R., Andrade-Navarro, M.A., Hübner, N., Devuyst, O., Hammes, A. and Willnow, T.E., 2010. The soluble intracellular domain of megalin does not affect renal proximal tubular function in vivo. *Kidney International*, 78(5), pp.473-477.
- Christensen, E., Birn, H., Verroust, P. and Moestrup, S.K., 1998. Membrane receptors for endocytosis in the renal proximal tubule. *International Review of Cytology*, 180, pp.237-284.
- Christensen, E.I. and Birn, H., 2001. Megalin and cubilin: synergistic endocytic receptors in renal proximal tubule. *American Journal of Physiology-Renal Physiology*, 280(4), pp.F562-F573.
- Christensen, E.I. and Birn, H., 2002. Megalin and cubilin: multifunctional endocytic receptors. *Nature Reviews. Molecular Cell Biology*, 3(4), p.256.
- Christensen, E.I. and Birn, H., 2013. Proteinuria: tubular handling of albumin—degradation or salvation?. *Nature Reviews Nephrology*, 9(12), pp.700-702.
- Christensen, E.I., Birn, H., Storm, T., Weyer, K. and Nielsen, R., 2012. Endocytic receptors in the renal proximal tubule. *Physiology*, 27(4), pp.223-236.
- Christensen, E.I., Verroust, P.J. and Nielsen, R., 2009. Receptor-mediated endocytosis in renal proximal tubule. *Pflügers Archiv-European Journal of Physiology*, 458(6), pp.1039-1048.

- Coffey, S., Costacou, T., Orchard, T. and Erkan, E., 2015. Akt links insulin signaling to albumin endocytosis in proximal tubule epithelial cells. *PLOS One*, 10(10), p.e0140417.
- Comper, W.D., Lee, A.S., Tay, M. and Adal, Y., 1993. Anionic charge concentration of rat kidney glomeruli and glomerular basement membrane. *Biochemical Journal*, 289(3), pp.647-652.
- Comper, W.D., Osicka, T.M., Clark, M., MacIsaac, R.J. and Jerums, G., 2004. Earlier detection of microalbuminuria in diabetic patients using a new urinary albumin assay. *Kidney International*, 65(5), pp.1850-1855.
- Comper, W.D., Hilliard, L.M., Nikolic-Paterson, D.J. and Russo, L.M., 2008. Disease-dependent mechanisms of albuminuria. *American Journal of Physiology-Renal Physiology*, 295(6), pp.F1589-F1600.
- Comper, W.D., 2008. Resolved: normal glomeruli filter nephrotic levels of albumin. *Journal of the American Society of Nephrology*, 19(3), pp.427-432.
- Connelly, J.C., Skidgel, R.A., Schulz, W.W., Johnson, A.R. and Erdös, E.G., 1985. Neutral endopeptidase 24.11 in human neutrophils: cleavage of chemotactic peptide. *Proceedings of the National Academy of Sciences*, 82(24), pp.8737-8741.
- Conner, S.D. and Schmid, S.L., 2003. Regulated portals of entry into the cell. *Nature*, 422(6927), p.37.
- Coppola, D., Lu, L., Fruehauf, J.P., Kyshtoobayeva, A., Karl, R.C., Nicosia, S.V. and Yeatman, T.J., 1998. Analysis of p53, p21WAF1, and TGF- β 1 in human ductal adenocarcinoma of the pancreas: TGF- β 1 protein expression predicts longer survival. *American Journal of Clinical Pathology*, 110(1), pp.16-23.
- Corbel, M., Caulet-Maugendre, S., Germain, N., Molet, S., Lagente, V. and Boichot, E., 2001. Inhibition of bleomycin-induced pulmonary fibrosis in mice by the matrix metalloproteinase inhibitor batimastat. *The Journal of Pathology*, 193(4), pp.538-545.
- Coudroy, G., Gburek, J., Kozyraki, R., Madsen, M., Trugnan, G., Moestrup, S.K., Verroust, P.J. and Maurice, M., 2005. Contribution of cubilin and amnionless to processing and membrane targeting of cubilin–amnionless complex. *Journal of the American Society of Nephrology*, 16(8), pp.2330-2337.
- Cui, S., Verroust, P.J., Moestrup, S.K. and Christensen, E.I., 1996. Megalin/gp330 mediates uptake of albumin in renal proximal tubule. *American Journal of Physiology-Renal Physiology*, 271(4), pp.F900-F907.
- Culhaci, N., Sagol, O., Karademir, S., Astarcioglu, H., Astarcioglu, I., Soy Turk, M., Oztop, I. and Obuz, F., 2005. Expression of transforming growth factor-beta-1 and p27 Kip1 in pancreatic adenocarcinomas: relation with cell-cycle-associated proteins and clinicopathologic characteristics. *BMC Cancer*, 5(1), p.98.

Curci, J.A., Mao, D., Bohner, D.G., Allen, B.T., Rubin, B.G., Reilly, J.M., Sicard, G.A. and Thompson, R.W., 2000. Preoperative treatment with doxycycline reduces aortic wall expression and activation of matrix metalloproteinases in patients with abdominal aortic aneurysms. *Journal of Vascular Surgery*, 31(2), pp.325-342.

D'Amico, G. and Bazzi, C., 2003. Pathophysiology of proteinuria. *Kidney International*, 63(3), pp.809-825.

De Zeeuw, D., Remuzzi, G., Parving, H.H., Keane, W.F., Zhang, Z., Shahinfar, S., Snapinn, S., Cooper, M.E., Mitch, W.E. and Brenner, B.M., 2004. Proteinuria, a target for renoprotection in patients with type 2 diabetic nephropathy: lessons from RENAAL. *Kidney International*, 65(6), pp.2309-2320.

Denis, L.J. and Verweij, J., 1997. Matrix metalloproteinase inhibitors: present achievements and future prospects. *Investigational New Drugs*, 15(3), pp.175-185.

Diamond, J.R., Kees-Folts, D., Ding, G., Frye, J.E. and Restrepo, N.C., 1994. Macrophages, monocyte chemoattractant peptide-1, and TGF-beta 1 in experimental hydronephrosis. *American Journal of Physiology-Renal Physiology*, 266(6), pp.F926-F933.

Dickson, L.E., Wagner, M.C., Sandoval, R.M. and Molitoris, B.A., 2014. The proximal tubule and albuminuria: really!. *Journal of the American Society of Nephrology*, 25(3), pp.443-453.

Diwakar, R., Pearson, A.L., Colville-Nash, P., Brunskill, N.J. and Dockrell, M.E., 2007. The role played by endocytosis in albumin-induced secretion of TGF- β 1 by proximal tubular epithelial cells. *American Journal of Physiology-Renal Physiology*, 292(5), pp.F1464-F1470.

Dixon, R. and BRUNSKILL, N.J., 2000. Albumin stimulates p44/p42 extracellular-signal-regulated mitogen-activated protein kinase in opossum kidney proximal tubular cells. *Clinical Science*, 98(3), pp.295-301.

Donadelli, R., Abbate, M., Zanchi, C., Corna, D., Tomasoni, S., Benigni, A., Remuzzi, G. and Zoja, C., 2000. Protein traffic activates NF- κ B gene signaling and promotes MCP-1-dependent interstitial inflammation. *American Journal of Kidney Diseases*, 36(6), pp.1226-1241.

Donadelli, R., Zanchi, C., Morigi, M., Buelli, S., Batani, C., Tomasoni, S., Corna, D., Rottoli, D., Benigni, A., Abbate, M. and Remuzzi, G., 2003. Protein Overload Induces Fractalkine Upregulation in Proximal Tubular Cells through Nuclear Factor κ B-and p38 Mitogen-Activated Protein Kinase-Dependent Pathways. *Journal of the American Society of Nephrology*, 14(10), pp.2436-2446.

Drake, C.J., Fleming, P.A., Larue, A.C., Barth, J.L., Chintalapudi, M.R. and Argaves, W.S., 2004. Differential distribution of cubilin and megalin expression in the mouse embryo. *The Anatomical Record Part A: Discoveries in Molecular, Cellular, and Evolutionary Biology*, 277(1), pp.163-170.

Du, X., Shimizu, A., Masuda, Y., Kuwahara, N., Arai, T., Kataoka, M., Uchiyama, M., Kaneko, T., Akimoto, T., Iino, Y. and Fukuda, Y., 2012. Involvement of matrix metalloproteinase-2 in the development of renal interstitial fibrosis in mouse obstructive nephropathy. *Laboratory Investigation*, 92(8), pp.1149-1160.

Dudek, R.W., 2006. *High-yield kidney*. Lippincott Williams & Wilkins. Page 53.

Duffield, J.S., Tipping, P.G., Kipari, T., Cailhier, J.F., Clay, S., Lang, R., Bonventre, J.V. and Hughes, J., 2005. Conditional ablation of macrophages halts progression of crescentic glomerulonephritis. *The American Journal of Pathology*, 167(5), pp.1207-1219.

Eddy, A.A. and Michael, A.F., 1988. Acute tubulointerstitial nephritis associated with aminonucleoside nephrosis. *Kidney International*, 33(1), pp.14-23.

Eddy, A.A., 1989. Interstitial nephritis induced by protein-overload proteinuria. *The American Journal of Pathology*, 135(4), p.719.

Eddy, A.A., 2001. Role of cellular infiltrates in response to proteinuria. *American Journal of Kidney Diseases*, 37(1), pp.S25-S29.

Eddy, A.A., 2004. Proteinuria and interstitial injury. *Nephrology Dialysis Transplantation*, 19(2), pp.277-281.

Eddy, A.A., Giachelli, C.M. and Liu, E., 1995. Renal expression of genes that promote interstitial inflammation and fibrosis in rats with protein-overload proteinuria. *Kidney International*, 47(6), pp.1546-1557.

Eddy, A.A., Kim, H., López-Guisa, J., Oda, T., Soloway, P.D., McCulloch, L., Liu, E. and Wing, D., 2000. Interstitial fibrosis in mice with overload proteinuria: deficiency of TIMP-1 is not protective. *Kidney International*, 58(2), pp.618-628.

Eddy, A.A., McCulloch, L., Liu, E. and Adams, J., 1991. A relationship between proteinuria and acute tubulointerstitial disease in rats with experimental nephrotic syndrome. *The American Journal of Pathology*, 138(5), p.1111.

El-Aouni, C., Herbach, N., Blattner, S.M., Henger, A., Rastaldi, M.P., Jarad, G., Miner, J.H., Moeller, M.J., St-Arnaud, R., Dedhar, S. and Holzman, L.B., 2006. Podocyte-specific deletion of integrin-linked kinase results in severe glomerular basement membrane alterations and progressive glomerulosclerosis. *Journal of the American Society of Nephrology*, 17(5), pp.1334-1344.

El-Nahas, A.M., Paraskevakou, H., Zoob, S., Rees, A.J. and Evans, D.J., 1983. Effect of dietary protein restriction on the development of renal failure after subtotal nephrectomy in rats. *Clinical Science*, 65(4), pp.399-406.

El Nahas, A.M., 1989. Glomerulosclerosis: insights into pathogenesis and treatment. *Nephrology, Dialysis, Transplantation*, 4(10), pp.843-853.

Ermolli, M., Schumacher, M., Lods, N., Hammoud, M. and Marti, H.P., 2003. Differential expression of MMP-2/MMP-9 and potential benefit of an MMP

inhibitor in experimental acute kidney allograft rejection. *Transplant Immunology*, 11(2), pp.137-145.

Falcone, D.J., McCaffrey, T.A., Haimovitz-Friedman, A., Vergilio, J.A. and Nicholson, A.C., 1993. Macrophage and foam cell release of matrix-bound growth factors. Role of plasminogen activation. *Journal of Biological Chemistry*, 268(16), pp.11951-11958.

Fang, Z., He, F., Chen, S., Sun, X., Zhu, Z. and Zhang, C., 2009. Albumin modulates the production of matrix metalloproteinases-2 and-9 in podocytes. *Journal of Huazhong University of Science and Technology--Medical Sciences--*, 29(6), pp.710-714.

Farquhar, M.G. and Palade, G.E., 1960. Segregation of ferritin in glomerular protein absorption droplets. *The Journal of Cell Biology*, 7(2), pp.297-304.

Fanjul-Fernández, M., Folgueras, A.R., Cabrera, S. and López-Otín, C., 2010. Matrix metalloproteinases: evolution, gene regulation and functional analysis in mouse models. *Biochimica et Biophysica Acta (BBA)-Molecular Cell Research*, 1803(1), pp.3-19.

Fingleton, B., 2007. Matrix metalloproteinases as valid clinical target. *Current Pharmaceutical Design*, 13(3), pp.333-346.

Fingleton, B., 2008, February. MMPs as therapeutic targets—still a viable option?. In *Seminars in Cell & Developmental Biology* (Vol. 19, No. 1, pp. 61-68). Academic Press.

Fyfe, J.C., Giger, U.R.S., Hall, C.A., Jezyk, P.F., Klumpp, S.A., Levine, J.S. and Patterson, D.F., 1991a. Inherited selective intestinal cobalamin malabsorption and cobalamin deficiency in dogs. *Pediatric Research*, 29(1), pp.24-31.

Fyfe, J.C., Madsen, M., Højrup, P., Christensen, E.I., Tanner, S.M., de la Chapelle, A., He, Q. and Moestrup, S.K., 2004. The functional cobalamin (vitamin B 12)–intrinsic factor receptor is a novel complex of cubilin and amnionless. *Blood*, 103(5), pp.1573-1579.

Fyfe, J.C., Ramanujam, K.S., Ramaswamy, K., Patterson, D.F. and Seetharam, B., 1991b. Defective brush-border expression of intrinsic factor-cobalamin receptor in canine inherited intestinal cobalamin malabsorption. *Journal of Biological Chemistry*, 266(7), pp.4489-4494.

Gekle, M., 2005. Renal tubule albumin transport. *Annual Review Physiology*, 67, pp.573-594.

Genovese, F., Manresa, A.A., Leeming, D.J., Karsdal, M.A. and Boor, P., 2014. The extracellular matrix in the kidney: a source of novel non-invasive biomarkers of kidney fibrosis?. *Fibrogenesis & Tissue Repair*, 7(1), p.4.

Gharagozlian, S., Svennevig, K., Bangstad, H.J., Winberg, J.O. and Kolset, S.O., 2009. Matrix metalloproteinases in subjects with type 1 diabetes. *BMC Clinical Pathology*, 9(7), pp.1628-1635.

- Gialeli, C., Theocharis, A.D. and Karamanos, N.K., 2011. Roles of matrix metalloproteinases in cancer progression and their pharmacological targeting. *The FEBS Journal*, 278(1), pp.16-27.
- Giannandrea, M. and Parks, W.C., 2014. Diverse functions of matrix metalloproteinases during fibrosis. *Disease Models & Mechanisms*, 7(2), pp.193-203.
- Gibb, D.M., Tomlinson, P.A., Dalton, N.R., Turner, C., Shah, V. and Barratt, T.M., 1989. Renal tubular proteinuria and microalbuminuria in diabetic patients. *Archives of Disease in Childhood*, 64(1), pp.129-134.
- Gibbons, G.H., Pratt, R. and Dzau, V.J., 1992. Vascular smooth muscle cell hypertrophy vs. hyperplasia. Autocrine transforming growth factor-beta 1 expression determines growth response to angiotensin II. *Journal of Clinical Investigation*, 90(2), p.456.
- Gorriz, J.L. and Martinez-Castelao, A., 2012. Proteinuria: detection and role in native renal disease progression. *Transplantation Reviews*, 26(1), pp.3-13.
- Grande, M.T., Pérez-Barriocanal, F. and López-Novoa, J.M., 2010. Role of inflammation in tubulo-interstitial damage associated to obstructive nephropathy. *Journal of Inflammation*, 7(1), p.19.
- Greka, A. and Mundel, P., 2012. Cell biology and pathology of podocytes. *Annual Review of Physiology*, 74, pp.299-323.
- Grigoryev, D.N., Liu, M., Hassoun, H.T., Cheadle, C., Barnes, K.C. and Rabb, H., 2008. The local and systemic inflammatory transcriptome after acute kidney injury. *Journal of the American Society of Nephrology*, 19(3), pp.547-558.
- Gross, J. and Lapiere, C.M., 1962. Collagenolytic activity in amphibian tissues: a tissue culture assay. *Proceedings of the National Academy of Sciences*, 48(6), pp.1014-1022.
- Guan, S., Ma, J., Zhang, Y., Gao, Y., Zhang, Y., Zhang, X., Wang, N., Xie, Y., Wang, J., Zhang, J. and Chu, L., 2013. Danshen (*Salvia miltiorrhiza*) injection suppresses kidney injury induced by iron overload in mice. *PLOS One*, 8(9), p.e74318.
- Guasch, A. and Myers, B.D., 1994. Determinants of glomerular hypofiltration in nephrotic patients with minimal change nephropathy. *Journal of the American Society of Nephrology*, 4(8), pp.1571-1581.
- Gudehithlu, K.P., Pegoraro, A.A., Dunea, G., Arruda, J.A. and Singh, A.K., 2004. Degradation of albumin by the renal proximal tubule cells and the subsequent fate of its fragments. *Kidney International*, 65(6), pp.2113-2122.
- Gupta, S.P. ed., 2012. *Matrix metalloproteinase inhibitors: specificity of binding and structure-activity relationships* (Vol. 103). Springer Science & Business Media.

Guyton, A. C. and Hall, J. E., 2000. *Textbook of Medical Physiology*. Philadelphia: WB Saunders Company.

Hanemaaijer, R., van Lent, N., Sorsa, T., Salo, T., Konttinen, T. and Lindeman, J., 2001. Inhibition of matrix metalloproteinases (MMPs) by tetracyclines. In *Tetracyclines in Biology, Chemistry and Medicine* (pp. 267-281). Birkhäuser Basel.

Haraldsson, B., Nyström, J. and Deen, W.M., 2008. Properties of the glomerular barrier and mechanisms of proteinuria. *Physiological Reviews*, 88(2), pp.451-487.

Haro, H., Crawford, H.C., Fingleton, B., Shinomiya, K., Spengler, D.M. and Matrisian, L.M., 2000. Matrix metalloproteinase-7–dependent release of tumor necrosis factor- α in a model of herniated disc resorption. *The Journal of Clinical Investigation*, 105(2), pp.143-150.

Hathaway, C.K., Gasim, A.M., Grant, R., Chang, A.S., Kim, H.S., Madden, V.J., Bagnell, C.R., Jennette, J.C., Smithies, O. and Kakoki, M., 2015. Low TGF β 1 expression prevents and high expression exacerbates diabetic nephropathy in mice. *Proceedings of the National Academy of Sciences*, 112(18), pp.5815-5820.

Haymann, J.P., Levrard, J.P., Bouet, S., Kappes, V., Hagege, J., Nguyen, G., Xu, Y., Rondeau, E. and Sraer, J.D., 2000. Characterization and localization of the neonatal Fc receptor in adult human kidney. *Journal of the American Society of Nephrology*, 11(4), pp.632-639.

Hebert, L.A., Bain, R.P., Verme, D., Cattran, D., Whittier, F.C., Tolchin, N., Rohde, R.D., Lewis, E.J., Lewis, E.J., Rohde, R. and Nemcek, M., 1994. Remission of nephrotic range proteinuria in type I diabetes. *Kidney International*, 46(6), pp.1688-1693.

Henderson, N.C., Mackinnon, A.C., Farnworth, S.L., Kipari, T., Haslett, C., Iredale, J.P., Liu, F.T., Hughes, J. and Sethi, T., 2008. Galectin-3 expression and secretion links macrophages to the promotion of renal fibrosis. *The American Journal of Pathology*, 172(2), pp.288-298.

Hjalmarsson, C., Johansson, B.R. and Haraldsson, B., 2004. Electron microscopic evaluation of the endothelial surface layer of glomerular capillaries. *Microvascular Research*, 67(1), pp.9-17.

Hostetter, T.H., Olson, J.L., Rennke, H.G., Venkatachalam, M.A. and Brenner, B.M., 1981. Hyperfiltration in remnant nephrons: a potentially adverse response to renal ablation. *American Journal of Physiology-Renal Physiology*, 241(1), pp.F85-F93.

Hou, F.F., Xie, D., Zhang, X., Chen, P.Y., Zhang, W.R., Liang, M., Guo, Z.J. and Jiang, J.P., 2007. Renoprotection of Optimal Antiproteinuric Doses (ROAD) Study: a randomized controlled study of benazepril and losartan in chronic renal insufficiency. *Journal of the American Society of Nephrology*, 18(6), pp.1889-1898.

- Huang, T.W. and Langlois, J.C., 1985. Podoendin. A new cell surface protein of the podocyte and endothelium. *Journal of Experimental Medicine*, 162(1), pp.245-267.
- Huby, A.C., Rastaldi, M.P., Caron, K., Smithies, O., Dussaule, J.C. and Chatziantoniou, C., 2009. Restoration of podocyte structure and improvement of chronic renal disease in transgenic mice overexpressing renin. *PLOS One*, 4(8), p.e6721.
- Hudson, B.G., Tryggvason, K., Sundaramoorthy, M. and Neilson, E.G., 2003. Alport's syndrome, Goodpasture's syndrome, and type IV collagen. *New England Journal of Medicine*, 348(25), pp.2543-2556.
- Inoue, C.N., Sunagawa, N., Morimoto, T., Ohnuma, S., Katsushima, F., Nishio, T., Kondo, Y. and Inuma, K., 2003. Reconstruction of tubular structures in three-dimensional collagen gel culture using proximal tubular epithelial cells voided in human urine. *In Vitro Cellular & Developmental Biology-Animal*, 39(8), pp.364-367.
- Ishola Jr, D.A., van der Giezen, D.M., Hahnel, B., Goldschmeding, R., Kriz, W., Koomans, H.A. and Joles, J.A., 2005. In mice, proteinuria and renal inflammatory responses to albumin overload are strain-dependent. *Nephrology Dialysis Transplantation*, 21(3), pp.591-597.
- Jakoi, E.R., Cambier, J. and Saslow, S., 1985. Transepithelial transport of maternal antibody: purification of IgG receptor from newborn rat intestine. *The Journal of Immunology*, 135(5), pp.3360-3364.
- Jarad, G. and Miner, J.H., 2009. Update on the glomerular filtration barrier. *Current Opinion in Nephrology and Hypertension*, 18(3), p.226.
- Jarad, G., Cunningham, J., Shaw, A.S. and Miner, J.H., 2006. Proteinuria precedes podocyte abnormalities in *Lamb2*^{-/-} mice, implicating the glomerular basement membrane as an albumin barrier. *The Journal of Clinical Investigation*, 116(8), p.2272.
- Jeansson, M. and Haraldsson, B., 2003. Glomerular size and charge selectivity in the mouse after exposure to glucosaminoglycan-degrading enzymes. *Journal of the American Society of Nephrology*, 14(7), pp.1756-1765.
- Jeansson, M. and Haraldsson, B., 2006. Morphological and functional evidence for an important role of the endothelial cell glycocalyx in the glomerular barrier. *American Journal of Physiology-Renal Physiology*, 290(1), pp.F111-F116.
- Jeansson, M., Björck, K., Tenstad, O. and Haraldsson, B., 2009. Adriamycin alters glomerular endothelium to induce proteinuria. *Journal of the American Society of Nephrology*, 20(1), pp.114-122.
- Johnson, R.J., Alpers, C.E., Yoshimura, A., Lombardi, D., Pritzl, P., Floege, J. and Schwartz, S.M., 1992. Renal injury from angiotensin II-mediated hypertension. *Hypertension*, 19(5), pp.464-474.

Jones, C.L., Buch, S., Post, M., McCulloch, L., Liu, E. and Eddy, A.A., 1992. Renal extracellular matrix accumulation in acute puromycin aminonucleoside nephrosis in rats. *The American Journal of Pathology*, 141(6), p.1381.

Jones, E.A., 1972. Immunoglobulins and the gut. *Gut*, 13(10), p.825.

Jones, C.B., Sane, D.C. and Herrington, D.M., 2003. Matrix metalloproteinases: a review of their structure and role in acute coronary syndrome. *Cardiovascular Research*, 59(4), pp.812-823.

Jørgensen, F., 1966. *The ultrastructure of the normal human glomerulus*. Copenhagen: Ejnar Munksgaard.

Kalluri, R. and Cosgrove, D., 2000. Assembly of Type IV Collagen INSIGHTS FROM $\alpha 3$ (IV) COLLAGEN-DEFICIENT MICE. *Journal of Biological Chemistry*, 275(17), pp.12719-12724.

Kalluri, R., 2006. Proteinuria with and without renal glomerular podocyte effacement. *Journal of the American Society of Nephrology*, 17(9), pp.2383-2389.

Kamijo, A., Kimura, K., Sugaya, T., Yamanouchi, M., Hase, H., Kaneko, T., Hirata, Y., Goto, A., Fujita, T. and Omata, M., 2002. Urinary free fatty acids bound to albumin aggravate tubulointerstitial damage. *Kidney International*, 62(5), pp.1628-1637.

Kanwar, Y.S., Linker, A. and Farquhar, M.G., 1980. Increased permeability of the glomerular basement membrane to ferritin after removal of glycosaminoglycans (heparan sulfate) by enzyme digestion. *The Journal of Cell Biology*, 86(2), pp.688-693.

Karkar, A.M., Smith, J. and Pusey, C.D., 2001. Prevention and treatment of experimental crescentic glomerulonephritis by blocking tumour necrosis factor- α . *Nephrology Dialysis Transplantation*, 16(3), pp.518-524.

Kaseda, R., Hosojima, M., Sato, H. and Saito, A., 2011. Role of megalin and cubilin in the metabolism of vitamin D3. *Therapeutic Apheresis and Dialysis*, 15(s1), pp.14-17.

Kayama, F., Yoshida, T., Kodama, Y., Matsui, T., Matheson, J.M. and Luster, M.I., 1997. Pro-inflammatory cytokines and interleukin 6 in the renal response to bacterial endotoxin. *Cytokine*, 9(9), pp.688-695.

Ke, J.T., Li, M., Xu, S.Q., Zhang, W.J., Jiang, Y.W., Cheng, L.Y., Chen, L., Lou, J.N. and Wu, W., 2014. Gliquidone decreases urinary protein by promoting tubular reabsorption in diabetic Goto-Kakizaki rats. *Journal of Endocrinology*, 220(2), pp.129-141.

Kerjaschki, D. and Farquhar, M.G., 1982. The pathogenic antigen of Heymann nephritis is a membrane glycoprotein of the renal proximal tubule brush border. *Proceedings of the National Academy of Sciences*, 79(18), pp.5557-5561.

- Kerjaschki, D., 2001. Caught flat-footed: podocyte damage and the molecular bases of focal glomerulosclerosis. *Journal of Clinical Investigation*, 108(11), p.1583.
- Kestilä, M., Lenkkeri, U., Männikkö, M., Lamerdin, J., McCready, P., Putaala, H., Ruotsalainen, V., Morita, T., Nissinen, M., Herva, R. and Kashtan, C.E., 1998. Positionally cloned gene for a novel glomerular protein—nephrin—is mutated in congenital nephrotic syndrome. *Molecular Cell*, 1(4), pp.575-582.
- Kim, J., Bronson, C.L., Hayton, W.L., Radmacher, M.D., Roopenian, D.C., Robinson, J.M. and Anderson, C.L., 2006. Albumin turnover: FcRn-mediated recycling saves as much albumin from degradation as the liver produces. *American Journal of Physiology-Gastrointestinal and Liver Physiology*, 290(2), pp.G352-G360.
- Kim, J.K., Firan, M., Radu, C.G., Kim, C.H., Ghetie, V. and Ward, E.S., 1999. Mapping the site on human IgG for binding of the MHC class I-related receptor, FcRn. *European Journal of Immunology*, 29(9), pp.2819-2825.
- Knotek, M., Rogachev, B., Wang, W., Ecdler, T., Melnikov, V., Gengaro, P.E., Esson, M., Edelstein, C.L., Dinarello, C.A. and Schrier, R.W., 2001. Endotoxemic renal failure in mice: role of tumor necrosis factor independent of inducible nitric oxide synthase. *Kidney International*, 59(6), pp.2243-2249.
- Kobayashi, N., Suzuki, Y., Tsuge, T., Okumura, K., Ra, C. and Tomino, Y., 2002. FcRn-mediated transcytosis of immunoglobulin G in human renal proximal tubular epithelial cells. *American Journal of Physiology-Renal Physiology*, 282(2), pp.F358-F365.
- Koeppen, B.M. and Stanton, B.A., 2012. Renal Physiology E-Book: Mosby Physiology Monograph Series. Elsevier Health Sciences. Page 583.
- Kristiansen, M., Kozyraki, R., Jacobsen, C., Nexø, E., Verroust, P.J. and Moestrup, S.K., 1999. Molecular dissection of the intrinsic factor-vitamin B12 receptor, cubilin, discloses regions important for membrane association and ligand binding. *Journal of Biological Chemistry*, 274(29), pp.20540-20544.
- Kumar, A., Bhatnagar, S. and Kumar, A., 2010. Matrix metalloproteinase inhibitor batimastat alleviates pathology and improves skeletal muscle function in dystrophin-deficient mdx mice. *The American Journal of Pathology*, 177(1), pp.248-260.
- Kunugi, S., Shimizu, A., Kuwahara, N., Du, X., Takahashi, M., Terasaki, Y., Fujita, E., Mii, A., Nagasaka, S., Akimoto, T. and Masuda, Y., 2011. Inhibition of matrix metalloproteinases reduces ischemia-reperfusion acute kidney injury. *Laboratory Investigation*, 91(2), p.170.
- Kuo, T.T., Baker, K., Yoshida, M., Qiao, S.W., Aveson, V.G., Lencer, W.I. and Blumberg, R.S., 2010. Neonatal Fc receptor: from immunity to therapeutics. *Journal of Clinical Immunology*, 30(6), pp.777-789.

- Lafayette, R.A., Druzin, M., Sibley, R., Derby, G., Malik, T., Huie, P., Polhemus, C., Deen, W.M. and Myers, B.D., 1998. Nature of glomerular dysfunction in pre-eclampsia. *Kidney International*, 54(4), pp.1240-1249.
- Lal, M. and Caplan, M., 2011. Regulated intramembrane proteolysis: signaling pathways and biological functions. *Physiology*, 26(1), pp.34-44.
- Lan, H.Y., 2003. Tubular epithelial-myofibroblast transdifferentiation mechanisms in proximal tubule cells. *Current Opinion in Nephrology and Hypertension*, 12(1), pp.25-29.
- Lan, H.Y., 2011. Diverse roles of TGF- β /Smads in renal fibrosis and inflammation. *International Journal of Biological Sciences*, 7(7), p.1056.
- Landgraf, S.S., Silva, L.S., Peruchetti, D.B., Sirtoli, G.M., Moraes-Santos, F., Portella, V.G., Silva-Filho, J.L., Pinheiro, C.S., Abreu, T.P., Takiya, C.M. and Benjamin, C.F., 2014. 5-Lipoxygenase products are involved in renal tubulointerstitial injury induced by albumin overload in proximal tubules in mice. *PLOS One*, 9(10), p.e107549.
- Lang, F. ed., 2009. *Encyclopedia of molecular mechanisms of disease*. Springer Science & Business Media.
- Lauhio, A., Sorsa, T., Srinivas, R., Stenman, M., Tervahartiala, T., Stenman, U.H., Grönhagen-Riska, C. and Honkanen, E., 2008. Urinary matrix metalloproteinase-8,-9,-14 and their regulators (TRY-1, TRY-2, TATI) in patients with diabetic nephropathy. *Annals of Medicine*, 40(4), pp.312-320.
- Lee, K.S., Jin, S.M., Kim, H.J. and Lee, Y.C., 2003. Matrix metalloproteinase inhibitor regulates inflammatory cell migration by reducing ICAM-1 and VCAM-1 expression in a murine model of toluene diisocyanate-induced asthma. *Journal of Allergy and Clinical Immunology*, 111(6), pp.1278-1284.
- Lee, Y.K., Kwon, T., Kim, D.J., Huh, W., Kim, Y.G., Oh, H.Y. and Kawachi, H., 2004. Ultrastructural study on nephrin expression in experimental puromycin aminonucleoside nephrosis. *Nephrology Dialysis Transplantation*, 19(12), pp.2981-2986.
- Lee, Y.S., Tran, H.T.L. and Van Ta, Q., 2009. Regulation of expression of matrix metalloproteinase-9 by JNK in Raw 264.7 cells: presence of inhibitory factor (s) suppressing MMP-9 induction in serum and conditioned media. *Experimental & Molecular Medicine*, 41(4), pp.259-268.
- Lehste, J.R., Rolinski, B., Vorum, H., Hilpert, J., Nykjaer, A., Jacobsen, C., Aucouturier, P., Moskaug, J.Ø., Otto, A., Christensen, E.I. and Willnow, T.E., 1999. Megalin knockout mice as an animal model of low molecular weight proteinuria. *The American Journal of Pathology*, 155(4), pp.1361-1370.
- Lenz, O., Elliot, S.J. and Stetler-Stevenson, W.G., 2000. Matrix metalloproteinases in renal development and disease. *Journal of the American Society of Nephrology*, 11(3), pp.574-581.

- Leonard, M., Ryan, M.P., Watson, A.J., Schramek, H. and Healy, E., 1999. Role of MAP kinase pathways in mediating IL-6 production in human primary mesangial and proximal tubular cells. *Kidney International*, 56(4), pp.1366-1377.
- Leontovich, A.A., Zhang, J., Shimokawa, K.I., Nagase, H. and Sarras, M.P., 2000. A novel hydra matrix metalloproteinase (HMMP) functions in extracellular matrix degradation, morphogenesis and the maintenance of differentiated cells in the foot process. *Development*, 127(4), pp.907-920.
- Lewis, J.B., Berl, T., Bain, R.P., Rohde, R.D., Lewis, E.J. and Collaborative Study Group, 1999. Effect of intensive blood pressure control on the course of type 1 diabetic nephropathy. *American journal of kidney diseases*, 34(5), pp.809-817.
- Lewy, J.E. and Pesce, A., 1973. Micropuncture study of albumin transfer in aminonucleoside nephrosis in the rat. *Pediatric Research*, 7(6), pp.553-559.
- Li, Y., Cong, R. and Biemesderfer, D., 2008. The COOH terminus of megalin regulates gene expression in opossum kidney proximal tubule cells. *American Journal of Physiology-Cell Physiology*, 295(2), pp.C529-C537.
- Lichtenthaler, S.F., Haass, C. and Steiner, H., 2011. Regulated intramembrane proteolysis—lessons from amyloid precursor protein processing. *Journal of Neurochemistry*, 117(5), pp.779-796.
- Liu, G., Thomas, L., Warren, R.A., Enns, C.A., Cunningham, C.C., Hartwig, J.H. and Thomas, G., 1997. Cytoskeletal protein ABP-280 directs the intracellular trafficking of furin and modulates proprotein processing in the endocytic pathway. *The Journal of Cell Biology*, 139(7), pp.1719-1733.
- Liu, J., Xiong, W., Baca-Regen, L., Nagase, H. and Baxter, B.T., 2003. Mechanism of inhibition of matrix metalloproteinase-2 expression by doxycycline in human aortic smooth muscle cells. *Journal of Vascular Surgery*, 38(6), pp.1376-1383.
- Liu, S., Li, Y., Zhao, H., Chen, D., Huang, Q., Wang, S., Zou, W., Zhang, Y., Li, X. and Huang, H., 2006. Increase in extracellular cross-linking by tissue transglutaminase and reduction in expression of MMP-9 contribute differentially to focal segmental glomerulosclerosis in rats. *Molecular and Cellular Biochemistry*, 284(1), pp.9-17.
- Liu, W., Yu, W.R., Carling, T., Juhlin, C., Rastad, J., Ridefelt, P., Akerstrom, G. and Hellman, P., 1998. Regulation of gp330/megalyn expression by vitamins A and D. *European Journal of Clinical Investigation*, 28(2), pp.100-107.
- Llano, E., Pendás, A.M., Aza-Blanc, P., Kornberg, T.B. and López-Otín, C., 2000. Dm1-MMP, a Matrix Metalloproteinase from *Drosophila* with a Potential Role in Extracellular Matrix Remodeling during Neural Development. *Journal of Biological Chemistry*, 275(46), pp.35978-35985.
- Löffek, S., Schilling, O. and Franzke, C.W., 2011. Biological role of matrix metalloproteinases: a critical balance.

- Lovejoy, B., Cleasby, A., Hassell, A.M., Longley, K., Luther, M.A., Weigl, D., McGeehan, G., McElroy, A.B., Drewry, D., Lambert, M.H. and Jordan, S.R., 1994. Structure of the catalytic domain of fibroblast collagenase complexed with an inhibitor. *Science-AAAS-Weekly Paper Edition-including Guide to Scientific Information*, 263(5145), pp.375-377.
- Low, J.A., Johnson, M.D., Bone, E.A. and Dickson, R.B., 1996. The matrix metalloproteinase inhibitor batimastat (BB-94) retards human breast cancer solid tumor growth but not ascites formation in nude mice. *Clinical Cancer Research*, 2(7), pp.1207-1214.
- Lund, U., Rippe, A., Venturoli, D., Tenstad, O., Grubb, A. and Rippe, B., 2003. Glomerular filtration rate dependence of sieving of albumin and some neutral proteins in rat kidneys. *American Journal of Physiology-Renal Physiology*, 284(6), pp.F1226-F1234.
- Lutz, J., Yao, Y., Song, E., Antus, B., Hamar, P., Liu, S. and Heemann, U., 2005. Inhibition of matrix metalloproteinases during chronic allograft nephropathy in rats. *Transplantation*, 79(6), pp.655-661.
- Maack, T.H.O.M.A.S. and Sigulem, D.A.N.I.E.L., 1974. Renal handling of lysozyme. *Lysozyme*, 100, p.101.
- Maack, T., 1975. Renal handling of low molecular weight proteins. *The American Journal of Medicine*, 58(1), pp.57-64.
- Maack, T., Johnson, V., Kau, S.T., Figueiredo, J. and Sigulem, D., 1979. Renal filtration, transport, and metabolism of low-molecular-weight proteins: a review. *Kidney International*, 16(3), pp.251-270.
- Machuca, E., Hummel, A., Nevo, F., Dantal, J., Martinez, F., Al-Sabban, E., Baudouin, V., Abel, L., Grünfeld, J.P. and Antignac, C., 2009. Clinical and epidemiological assessment of steroid-resistant nephrotic syndrome associated with the NPHS2 R229Q variant. *Kidney International*, 75(7), pp.727-735.
- Marzolo, M.P. and Farfán, P., 2011. New insights into the roles of megalin/LRP2 and the regulation of its functional expression. *Biological Research*, 44(1), pp.89-105.
- Marshansky, V., Bourgoin, S., Londoño, I., Bendayan, M., Maranda, B. and Vinay, P., 1997. Receptor-mediated endocytosis in kidney proximal tubules: Recent advances and hypothesis. *Electrophoresis*, 18(14), pp.2661-2676.
- Maunsbach, A.B., 1966. Observations on the segmentation of the proximal tubule in the rat kidney: Comparison of results from phase contrast, fluorescence and electron microscopy. *Journal of Ultrastructure Research*, 16(3-4), pp.239-258.
- Maynard, S.E., Min, J.Y., Merchan, J., Lim, K.H., Li, J., Mondal, S., Libermann, T.A., Morgan, J.P., Sellke, F.W., Stillman, I.E. and Epstein, F.H., 2003. Excess placental soluble fms-like tyrosine kinase 1 (sFlt1) may contribute to endothelial dysfunction, hypertension, and proteinuria in preeclampsia. *Journal of Clinical Investigation*, 111(5), p.649.

- McKenzie, L.M., Hendrickson, S.L., Briggs, W.A., Dart, R.A., Korbet, S.M., Mokrzycki, M.H., Kimmel, P.L., Ahuja, T.S., Berns, J.S., Simon, E.E. and Smith, M.C., 2007. NPHS2 variation in sporadic focal segmental glomerulosclerosis. *Journal of the American Society of Nephrology*, 18(11), pp.2987-2995.
- Medesan, C., Matesoi, D., Radu, C., Ghetie, V. and Ward, E.S., 1997. Delineation of the amino acid residues involved in transcytosis and catabolism of mouse IgG1. *The Journal of Immunology*, 158(5), pp.2211-2217.
- Medina, M. and Dotti, C.G., 2003. RIPped out by presenilin-dependent γ -secretase. *Cellular Signalling*, 15(9), pp.829-841.
- Menon, M.C., Chuang, P.Y. and He, C.J., 2012. The glomerular filtration barrier: components and crosstalk. *International Journal of Nephrology*, 2012.
- Messina, A., Davies, D. J., Dillane, P. C. and Ryan, G. B., 1987. 'Glomerular epithelial abnormalities associated with the onset of proteinuria in aminonucleoside nephrosis', *The American Journal of Pathology*, (126), 220-229.
- Mills, S.E., 2007. *Histology for pathologists*. Philadelphia.
- Miner, J.H. and Sanes, J.R., 1996. Molecular and functional defects in kidneys of mice lacking collagen alpha 3 (IV): implications for Alport syndrome. *The Journal of Cell Biology*, 135(5), pp.1403-1413.
- Miner, J.H., 2012. The glomerular basement membrane. *Experimental Cell Research*, 318(9), pp.973-978.
- Miner, J.H., Go, G., Cunningham, J., Patton, B.L. and Jarad, G., 2006. Transgenic isolation of skeletal muscle and kidney defects in laminin β 2 mutant mice: implications for Pierson syndrome. *Development*, 133(5), pp.967-975.
- Mirpuri, N. and Patel, P., 2000. Development, Structure and function of the kidney. In: L. Crowe editor. *Renal and urinary system*. London: Mosby, 3-80.
- Mishra, V.K. and Palgunachari, M.N., 1996. Interaction of model class A1, class A2, and class Y amphipathic helical peptides with membranes. *Biochemistry*, 35(34), pp.11210-11220.
- Mitani, O., Katoh, M. and Shigematsu, H., 2004. Participation of the matrix metalloproteinase inhibitor in Thy-1 nephritis. *Pathology International*, 54(4), pp.241-250.
- Moestrup, S.K. and Verroust, P.J., 2001. Megalin-and cubilin-mediated endocytosis of protein-bound vitamins, lipids, and hormones in polarized epithelia. *Annual Review of Nutrition*, 21(1), pp.407-428.
- Moestrup, S.K., Kozyraki, R., Kristiansen, M., Kaysen, J.H., Rasmussen, H.H., Brault, D., Pontillon, F., Goda, F.O., Christensen, E.I., Hammond, T.G. and Verroust, P.J., 1998. The intrinsic factor-vitamin B12 receptor and target of teratogenic antibodies is a megalin-binding peripheral membrane protein with

homology to developmental proteins. *Journal of Biological Chemistry*, 273(9), pp.5235-5242.

Mollet, G., Ratelade, J., Boyer, O., Muda, A.O., Morisset, L., Lavin, T.A., Kitzis, D., Dallman, M.J., Bugeon, L., Hubner, N. and Gubler, M.C., 2009. Podocin inactivation in mature kidneys causes focal segmental glomerulosclerosis and nephrotic syndrome. *Journal of the American Society of Nephrology*, 20(10), pp.2181-2189.

Molloy, S.S., Bresnahan, P.A., Leppla, S.H., Klimpel, K.R. and Thomas, G., 1992. Human furin is a calcium-dependent serine endoprotease that recognizes the sequence Arg-XX-Arg and efficiently cleaves anthrax toxin protective antigen. *Journal of Biological Chemistry*, 267(23), pp.16396-16402.

Mogensen, C.E. and Sølling, K., 1977. Studies on renal tubular protein reabsorption: partial and near complete inhibition by certain amino acids. *Scandinavian Journal of Clinical and Laboratory Investigation*, 37(6), pp.477-486.

Morello, R., Zhou, G., Dreyer, S.D., Harvey, S.J., Ninomiya, Y., Thorner, P.S., Miner, J.H., Cole, W., Winterpacht, A., Zabel, B. and Oberg, K.C., 2001. Regulation of glomerular basement membrane collagen expression by LMX1B contributes to renal disease in nail patella syndrome. *Nature Genetics*, 27(2), p.205.

Morelli, E., Loon, N., Meyer, T., Peters, W. and Myers, B.D., 1990. Effects of converting-enzyme inhibition on barrier function in diabetic glomerulopathy. *Diabetes*, 39(1), pp.76-82.

Morita, H., Yoshimura, A., Inui, K., Ideura, T., Watanabe, H., Wang, L., Soininen, R. and Tryggvason, K., 2005. Heparan sulfate of perlecan is involved in glomerular filtration. *Journal of the American Society of Nephrology*, 16(6), pp.1703-1710.

Morrison, C.J., Butler, G.S., Rodríguez, D. and Overall, C.M., 2009. Matrix metalloproteinase proteomics: substrates, targets, and therapy. *Current Opinion in Cell Biology*, 21(5), pp.645-653.

Motoyoshi, Y., Matsusaka, T., Saito, A., Pastan, I., Willnow, T.E., Mizutani, S. and Ichikawa, I., 2008. Megalin contributes to the early injury of proximal tubule cells during nonselective proteinuria. *Kidney International*, 74(10), pp.1262-1269.

Mukherjee, S., Ghosh, R.N. and Maxfield, F.R., 1997. Endocytosis. *Physiological Reviews*, 77(3), pp.759-803.

Mundel, P. and Kriz, W., 1995. Structure and function of podocytes: an update. *Anatomy and Embryology*, 192(5), pp.385-397.

Murphy, G., Stanton, H., Cowell, S., Butler, G., Knäuper, V., Atkinson, S. and Gavrilovic, J., 1999. Mechanisms for pro matrix metalloproteinase activation. *APMIS*, 107(1-6), pp.38-44.

- Murphy, M. P. and LeVine III, H., 2010. Alzheimer's disease and the β -Amyloid Peptide. *Journal Alzheimers Disease*, 19(1): 311.
- Nacu, N., Luzina, I.G., Highsmith, K., Lockett, V., Pochetuh, K., Cooper, Z.A., Gillmeister, M.P., Todd, N.W. and Atamas, S.P., 2008. Macrophages produce TGF- β -induced (β -ig-h3) following ingestion of apoptotic cells and regulate MMP14 levels and collagen turnover in fibroblasts. *The Journal of Immunology*, 180(7), pp.5036-5044.
- Nagase, H., 1997. Activation mechanisms of matrix metalloproteinases. *Biological Chemistry*, 378(3-4), pp.151-160.
- Nagase, H. and Woessner, J.F., 1999. Matrix metalloproteinases. *Journal of Biological Chemistry*, 274(31), pp.21491-21494.
- Nakajima, H., Takenaka, M., Kaimori, J.Y., Hamano, T., Iwatani, H., Sugaya, T., Ito, T., Hori, M. and Imai, E., 2004. Activation of the signal transducer and activator of transcription signaling pathway in renal proximal tubular cells by albumin. *Journal of the American Society of Nephrology*, 15(2), pp.276-285.
- Navarro-González, J.F. and Mora-Fernández, C., 2008. The role of inflammatory cytokines in diabetic nephropathy. *Journal of the American Society of Nephrology*, 19(3), pp.433-442.
- Nechemia-Arbely, Y., Barkan, D., Pizov, G., Shriki, A., Rose-John, S., Galun, E. and Axelrod, J.H., 2008. IL-6/IL-6R axis plays a critical role in acute kidney injury. *Journal of the American Society of Nephrology*, 19(6), pp.1106-1115.
- Nielsen, R., Christensen, E.I. and Birn, H., 2016. Megalin and cubilin in proximal tubule protein reabsorption: from experimental models to human disease. *Kidney International*, 89(1), pp.58-67.
- Nishida, M., Okumura, Y., Ozawa, S.I., Shiraishi, I., Itoi, T. and Hamaoka, K., 2007. MMP-2 inhibition reduces renal macrophage infiltration with increased fibrosis in UO. *Biochemical and Biophysical Research Communications*, 354(1), pp.133-139.
- Norden, A.G., Lapsley, M., Lee, P.J., Pusey, C.D., Scheinman, S.J., Tam, F.W., Thakker, R.V., Unwin, R.J. and Wrong, O., 2001. Glomerular protein sieving and implications for renal failure in Fanconi syndrome. *Kidney International*, 60(5), pp.1885-1892.
- Norden, A.G., Lapsley, M., Igarashi, T., Kelleher, C.L., Lee, P.J., Matsuyama, T., Scheinman, S.J., Shiraga, H., Sundin, D.P., Thakker, R.V. and Unwin, R.J., 2002. Urinary megalin deficiency implicates abnormal tubular endocytic function in Fanconi syndrome. *Journal of the American Society of Nephrology*, 13(1), pp.125-133.
- Norden, A.G., Scheinman, S.J., Deschodt-Lanckman, M.M., Lapsley, M., Nortier, J.L., Thakker, R.V., Unwin, R.J. and Wrong, O., 2000. Tubular proteinuria defined by a study of Dent's (CLCN5 mutation) and other tubular diseases. *Kidney International*, 57(1), pp.240-249.

- Novak, K.B., Le, H.D., Christison-Lagay, E.R., Nose, V., Doiron, R.J., Moses, M.A. and Puder, M., 2010. Effects of metalloproteinase inhibition in a murine model of renal ischemia-reperfusion injury. *Pediatric Research*, 67(3), pp.257-262.
- Novick, A.C., Gephardt, G., Guz, B., Steinmuller, D. and Tubbs, R.R., 1991. Long-term follow-up after partial removal of a solitary kidney. *New England Journal of Medicine*, 325(15), pp.1058-1062.
- Nykjaer, A., Fyfe, J.C., Kozyraki, R., Leheste, J.R., Jacobsen, C., Nielsen, M.S., Verroust, P.J., Aminoff, M., de la Chapelle, A., Moestrup, S.K. and Ray, R., 2001. Cubilin dysfunction causes abnormal metabolism of the steroid hormone 25 (OH) vitamin D3. *Proceedings of the National Academy of Sciences*, 98(24), pp.13895-13900.
- Obermüller, N., Morente, N., Kränzlin, B., Gretz, N. and Witzgall, R., 2001. A possible role for metalloproteinases in renal cyst development. *American Journal of Physiology-Renal Physiology*, 280(3), pp.F540-F550.
- Odera, K., Goto, S. and Takahashi, R., 2007. Age-related change of endocytic receptors megalin and cubilin in the kidney in rats. *Biogerontology*, 8(5), pp.505-515.
- Ogasawara, S., Hosojima, M., Kaseda, R., Kabasawa, H., Yamamoto-Kabasawa, K., Kurosawa, H., Sato, H., Iino, N., Takeda, T., Suzuki, Y. and Narita, I., 2012. Significance of urinary full-length and ectodomain forms of megalin in patients with type 2 diabetes. *Diabetes Care*, 35(5), pp.1112-1118.
- Ohlson, M., Sörensson, J., Lindström, K., Blom, A.M., Fries, E. and Haraldsson, B., 2001. Effects of filtration rate on the glomerular barrier and clearance of four differently shaped molecules. *American Journal of Physiology-Renal Physiology*, 281(1), pp.F103-F113.
- Okamura, K., Dummer, P., Kopp, J., Qiu, L., Levi, M., Faubel, S. and Blaine, J., 2013. Endocytosis of albumin by podocytes elicits an inflammatory response and induces apoptotic cell death. *PLOS One*, 8(1), p.e54817.
- Oken, D.E. and Flamenbaum, W., 1971. Micropuncture studies of proximal tubule albumin concentrations in normal and nephrotic rats. *Journal of Clinical Investigation*, 50(7), p.1498.
- Oleinikov, A.V., Jun, Z.H.A.O. and Makker, S.P., 2000. Cytosolic adaptor protein Dab2 is an intracellular ligand of endocytic receptor gp600/megalyn. *Biochemical Journal*, 347(3), pp.613-621.
- Osicka, T.M., Panagiotopoulos, S., Jerums, G. and Comper, W.D., 1997. Fractional clearance of albumin is influenced by its degradation during renal passage. *Clinical Science*, 93(6), pp.557-564.
- Otaki, Y., Miyauchi, N., Higa, M., Takada, A., Kuroda, T., Gejyo, F., Shimizu, F. and Kawachi, H., 2008. Dissociation of NEPH1 from nephrin is involved in development of a rat model of focal segmental glomerulosclerosis. *American Journal of Physiology-Renal Physiology*, 295(5), pp.F1376-F1387.

- Overall, C.M. and López-Otín, C., 2002. Strategies for MMP inhibition in cancer: innovations for the post-trial era. *Nature Reviews. Cancer*, 2(9), p.657.
- Park, C.H. and Maack, T., 1984. Albumin absorption and catabolism by isolated perfused proximal convoluted tubules of the rabbit. *Journal of Clinical Investigation*, 73(3), p.767.
- Pavenstädt, H., Kriz, W. and Kretzler, M., 2003. Cell biology of the glomerular podocyte. *Physiological Reviews*, 83(1), pp.253-307.
- Pearson, A. L., Colville-Nash, P., Kwan, J. T. and Dockrell M. E., 2008. Albumin induces interleukin-6 release from primary human proximal tubule epithelial cells. *Journal of Nephrology*, 21(6), pp.887-893.
- Peng, W.J., Yan, J.W., Wan, Y.N., Wang, B.X., Tao, J.H., Yang, G.J., Pan, H.F. and Wang, J., 2012. Matrix metalloproteinases: a review of their structure and role in systemic sclerosis. *Journal of Clinical Immunology*, 32(6), pp.1409-1414.
- Peterson, J.C., Adler, S., Burkart, J.M., Greene, T., Hebert, L.A., Hunsicker, L.G., King, A.J., Klahr, S., Massry, S.G. and Seifter, J.L., 1995. Blood Pressure Control, Proteinuria, and the Progression of Renal DiseaseThe Modification of Diet in Renal Disease Study. *Annals of Internal Medicine*, 123(10), pp.754-762.
- Peti-Peterdi, J., 2009. Independent two-photon measurements of albumin GSC give low values. *American Journal of Physiology-Renal Physiology*, 296(6), pp.F1255-F1257.
- Petrinec, D., Liao, S., Holmes, D.R., Reilly, J.M., Parks, W.C. and Thompson, R.W., 1996. Doxycycline inhibition of aneurysmal degeneration in an elastase-induced rat model of abdominal aortic aneurysm: preservation of aortic elastin associated with suppressed production of 92 kD gelatinase. *Journal of Vascular Surgery*, 23(2), pp.336-346.
- Pisitkun, T., Shen, R.F. and Knepper, M.A., 2004. Identification and proteomic profiling of exosomes in human urine. *Proceedings of the national academy of sciences of the United States of America*, 101(36), pp.13368-13373.
- Pollak, M.R., Quaggin, S.E., Hoenig, M.P. and Dworkin, L.D., 2014. The glomerulus: the sphere of influence. *Clinical Journal of the American Society of Nephrology*, pp.CJN-09400913.
- Prontera, C., Mariani, B., Rossi, C., Poggi, A. and Rotilio, D., 1999. Inhibition of gelatinase A (MMP-2) by batimastat and captopril reduces tumor growth and lung metastases in mice bearing Lewis lung carcinoma. *International Journal of Cancer*, 81(5), pp.761-766.
- Pushpakumar, S.B., Kundu, S., Metreveli, N., Tyagi, S.C. and Sen, U., 2013. Matrix metalloproteinase inhibition mitigates renovascular remodeling in salt-sensitive hypertension. *Physiological Reports*, 1(3).
- Putala, H., Soininen, R., Kilpeläinen, P., Wartiovaara, J. and Tryggvason, K., 2001. The murine nephrin gene is specifically expressed in kidney, brain and

pancreas: inactivation of the gene leads to massive proteinuria and neonatal death. *Human Molecular Genetics*, 10(1), pp.1-8.

Raghavan, M., Bonagura, V.R., Morrison, S.L. and Bjorkman, P.J., 1995. Analysis of the pH dependence of the neonatal Fc receptor/immunoglobulin G interaction using antibody and receptor variants. *Biochemistry*, 34(45), pp.14649-14657.

Raghavan, M., Chen, M.Y., Gastinel, L.N. and Bjorkman, P.J., 1994. Investigation of the interaction between the class I MHC-related Fc receptor and its immunoglobulin G ligand. *Immunity*, 1(4), pp.303-315.

Ramdyia, P., Skoch, J., Bacskai, B.J., Hyman, B.T. and Berezovska, O., 2003. Activated Notch1 associates with a presenilin-1/ γ -secretase docking site. *Journal of Neurochemistry*, 87(4), pp.843-850.

Ramesh, G. and Reeves, W.B., 2002. TNF- α mediates chemokine and cytokine expression and renal injury in cisplatin nephrotoxicity. *The Journal of Clinical Investigation*, 110(6), pp.835-842.

Ramesh, G. and Reeves, W.B., 2003. TNFR2-mediated apoptosis and necrosis in cisplatin-induced acute renal failure. *American Journal of Physiology-Renal Physiology*, 285(4), pp.F610-F618.

Ramesh, G. and Reeves, W.B., 2004. Inflammatory cytokines in acute renal failure. *Kidney International*, 66, pp.S56-S61.

Rasmussen, H.S. and McCann, P.P., 1997. Matrix metalloproteinase inhibition as a novel anticancer strategy: a review with special focus on batimastat and marimastat. *Pharmacology & Therapeutics*, 75(1), pp.69-75.

Reich, H., Tritchler, D., Herzenberg, A.M., Kassiri, Z., Zhou, X., Gao, W. and Scholey, J.W., 2005. Albumin activates ERK via EGF receptor in human renal epithelial cells. *Journal of the American Society of Nephrology*, 16(5), pp.1266-1278.

Remuzzi, G., 1999. Nephropathic nature of proteinuria. *Current Opinion in Nephrology and Hypertension*, 8(6), pp.655-663.

Remuzzi, A., Puntorieri, S., Battaglia, C., Bertani, T. and Remuzzi, G., 1990. Angiotensin converting enzyme inhibition ameliorates glomerular filtration of macromolecules and water and lessens glomerular injury in the rat. *Journal of Clinical Investigation*, 85(2), p.541.

Rodriguez-Díez, R., Rayego-Mateos, S., Orejudo, M., Aroeira, L.S., Selgas, R., Ortiz, A., Egido, J. and Ruiz-Ortega, M., 2015. TGF-beta blockade increases renal inflammation caused by the C-terminal module of the CCN2. *Mediators of Inflammation*, 2015.

Rodríguez-Iturbe, B. and García, G.G., 2010. The role of tubulointerstitial inflammation in the progression of chronic renal failure. *Nephron Clinical Practice*, 116(2), pp.c81-c88.

Romanic, A.M., Burns-Kurtis, C.L., Ao, Z., Arleth, A.J. and Ohlstein, E.H., 2001. Upregulated expression of human membrane type-5 matrix metalloproteinase in kidneys from diabetic patients. *American Journal of Physiology-Renal Physiology*, 281(2), pp.F309-F317.

Roopenian, D.C. and Akilesh, S., 2007. FcRn: the neonatal Fc receptor comes of age. *Nature Reviews. Immunology*, 7(9), p.715.

Roopenian, D.C., Christianson, G.J., Sproule, T.J., Brown, A.C., Akilesh, S., Jung, N., Petkova, S., Avanesian, L., Choi, E.Y., Shaffer, D.J. and Eden, P.A., 2003. The MHC class I-like IgG receptor controls perinatal IgG transport, IgG homeostasis, and fate of IgG-Fc-coupled drugs. *The Journal of Immunology*, 170(7), pp.3528-3533.

Rosenzweig, L.J. and Kanwar Y. S. 1982. Removal of sulfated (heparan sulfate) or nonsulfated (hyaluronic acid) glycosaminoglycans results in increased permeability of the glomerular basement membrane to 125I-bovine serum albumin. *Laboratory Investigation*, 47, pp.177-184.

Ross, M. H., Romrell, L. J. and Kaye, G. I. 1995. Urinary system. In: P. A. Coryell, editor. *Histology A Text and Atlas*. 3rd ed. ed. Baltimore, USA: Williams & Wilkins, 558-595.

Ruggenti, P., Perna, A., Gherardi, G., Gaspari, F., Benini, R., Remuzzi, G. and Gruppo Italiano di Studi Epidemiologici in Nefrologia, 1998. Renal function and requirement for dialysis in chronic nephropathy patients on long-term ramipril: REIN follow-up trial. *The Lancet*, 352(9136), pp.1252-1256.

Ruotsalainen, V., Ljungberg, P., Wartiovaara, J., Lenkkeri, U., Kestilä, M., Jalanko, H., Holmberg, C. and Tryggvason, K., 1999. Nephritin is specifically located at the slit diaphragm of glomerular podocytes. *Proceedings of the National Academy of Sciences*, 96(14), pp.7962-7967.

Russo, L.M., Sandoval, R.M., McKee, M., Osicka, T.M., Collins, A.B., Brown, D., Molitoris, B.A. and Comper, W.D., 2007. The normal kidney filters nephrotic levels of albumin retrieved by proximal tubule cells: retrieval is disrupted in nephrotic states. *Kidney International*, 71(6), pp.504-513.

Sahali, D., Mulliez, N., Chatelet, F., Laurent-Winter, C., Citadelle, D., Roux, C., Ronco, P. and Verroust, P., 1992. Coexpression in humans by kidney and fetal envelopes of a 280 kDa-coated pit-restricted protein. Similarity with the murine target of teratogenic antibodies. *The American Journal of Pathology*, 140(1), p.33.

Sahali, D.J.I.L.L.A.L.I., Mulliez, N., Chatelet, F., Laurent-Winter, C., Citadelle, D., Sabourin, J.C., Roux, C., Ronco, P. and Verroust, P., 1993. Comparative immunochemistry and ontogeny of two closely related coated pit proteins. The 280-kd target of teratogenic antibodies and the 330-kd target of nephritogenic antibodies. *The American Journal of Pathology*, 142(5), p.1654.

Sand, K.M.K., Bern, M., Nilsen, J., Noordzij, H.T., Sandlie, I. and Andersen, J.T., 2015. Unraveling the interaction between FcRn and albumin: opportunities for design of albumin-based therapeutics. *Frontiers in Immunology*, 5, p.682.

Sankari, S.L., Krupaa, R.J., Kumar, G.K. and Balachander, N., 2016. MMP-Matrix Metalloproteinase. *Biomedical and Pharmacology Journal*, 9(2), pp.885-888.

Sarav, M., Wang, Y., Hack, B.K., Chang, A., Jensen, M., Bao, L. and Quigg, R.J., 2009. Renal FcRn reclaims albumin but facilitates elimination of IgG. *Journal of the American Society of Nephrology*, 20(9), pp.1941-1952.

Sawada, H., Stukenbrok, H., Kerjaschki, D. and Farquhar, M.G., 1986. Epithelial polyanion (podocalyxin) is found on the sides but not the soles of the foot processes of the glomerular epithelium. *The American Journal of Pathology*, 125(2), p.309.

Sbardella, D., Fasciglione, G.F., Gioia, M., Ciaccio, C., Tundo, G.R., Marini, S. and Coletta, M., 2012. Human matrix metalloproteinases: an ubiquitous class of enzymes involved in several pathological processes. *Molecular Aspects of Medicine*, 33(2), pp.119-208.

Schmid, S.L., 1997. Clathrin-coated vesicle formation and protein sorting: an integrated process. *Annual Review of Biochemistry*, 66(1), pp.511-548.

Scott, R.P., Hawley, S.P., Ruston, J., Du, J., Brakebusch, C., Jones, N. and Pawson, T., 2012. Podocyte-specific loss of Cdc42 leads to congenital nephropathy. *Journal of the American Society of Nephrology*, pp.ASN-2011121206.

Seetharam, B., Alpers, D.H. and Allen, R.H., 1981. Isolation and characterization of the ileal receptor for intrinsic factor-cobalamin. *Journal of Biological Chemistry*, 256(8), pp.3785-3790.

Seki, T., Asanuma, K., Asao, R., Nonaka, K., Sasaki, Y., Trejo, J.A.O., Kurosawa, H., Hirayama, Y., Horikoshi, S., Tomino, Y. and Saito, A., 2014. Significance of urinary full-length megalin in patients with IgA nephropathy. *PLOS One*, 9(12), p.e114400.

Shah, M., Baterina, O.Y., Taupin, V. and Farquhar, M.G., 2013. ARH directs megalin to the endocytic recycling compartment to regulate its proteolysis and gene expression. *The Journal of Cell Biology*, 202(1), pp.113-127.

Shea, S.M. and Morrison, A.B., 1975. A stereological study of the glomerular filter in the rat. Morphometry of the slit diaphragm and basement membrane. *The Journal of Cell Biology*, 67(2), pp.436-443.

Shimamura, T. and Morrison, A.B., 1975. A progressive glomerulosclerosis occurring in partial five-sixths nephrectomized rats. *The American Journal of Pathology*, 79(1), p.95.

Simister, N.E. and Mostov, K.E., 1989. An Fc receptor structurally related to MHC class I antigens. *Nature*, 337(6203), pp.184-187.

- Simister, N.E. and Rees, A.R., 1985. Isolation and characterization of an Fc receptor from neonatal rat small intestine. *European Journal of Immunology*, 15(7), pp.733-738.
- Simister, N.E., Story, C.M., Chen, H.L. and Hunt, J.S., 1996. An IgG-transporting Fc receptor expressed in the syncytiotrophoblast of human placenta. *European Journal of Immunology*, 26(7), pp.1527-1531.
- Simpson, R.J., Jensen, S.S. and Lim, J.W., 2008. Proteomic profiling of exosomes: current perspectives. *Proteomics*, 8(19), pp.4083-4099.
- Ślusarz, A., Nichols, L.A., Grunz-Borgmann, E.A., Chen, G., Akintola, A.D., Catania, J.M., Burghardt, R.C., Trzeciakowski, J.P. and Parrish, A.R., 2013. Overexpression of MMP-7 increases collagen 1A2 in the aging kidney. *Physiological Reports*, 1(5), p.e00090.
- Sorbi, D., Fadly, M., Hicks, R., Alexander, S. and Arbeit, L., 1993. Captopril inhibits the 72 kDa and 92 kDa matrix metalloproteinases. *Kidney International*, 44(6), pp.1266-1272.
- Sörensson, J., Björnson, A., Ohlson, M., Ballermann, B.J. and Haraldsson, B., 2003. Synthesis of sulfated proteoglycans by bovine glomerular endothelial cells in culture. *American Journal of Physiology-Renal Physiology*, 284(2), pp.F373-F380.
- Stillman, I.E. and Karumanchi, S.A., 2007. The glomerular injury of preeclampsia. *Journal of the American Society of Nephrology*, 18(8), pp.2281-2284.
- Story, C.M., Mikulska, J.E. and Simister, N.E., 1994. A major histocompatibility complex class I-like Fc receptor cloned from human placenta: possible role in transfer of immunoglobulin G from mother to fetus. *Journal of Experimental Medicine*, 180(6), pp.2377-2381.
- Strutz, F., Zeisberg, M., Ziyadeh, F.N., Yang, C.Q., Kalluri, R., Müller, G.A., Neilson, E.G., Renziehausen, A. and Sisic, Z., 2002. Role of basic fibroblast growth factor-2 in epithelial-mesenchymal transformation. *Kidney International*, 61(5), pp.1714-1728.
- Sugimoto, H., Mundel, T.M., Sund, M., Xie, L., Cosgrove, D. and Kalluri, R., 2006. Bone-marrow-derived stem cells repair basement membrane collagen defects and reverse genetic kidney disease. *Proceedings of the National Academy of Sciences*, 103(19), pp.7321-7326.
- Sumpio, B.E. and Maack, T., 1982. Kinetics, competition, and selectivity of tubular absorption of proteins. *American Journal of Physiology-Renal Physiology*, 243(4), pp.F379-F392.
- Supuran, C. T. and Scozzafaca, A., 2002. Matrix Metalloproteinases, In Proteinase and Peptidase Inhibition; Recent Potential Targets for Drug Development. Smith, H.J. and C. Simons (Eds.), Taylor and Francis: London and New York, pp: 35-61.

- Taal, M.W., Chertow, G.M., Marsden, P.A., Skorecki, K., Alan, S.L. and Brenner, B.M., 2011. Brenner and Rector's The Kidney E-Book. Elsevier Health Sciences. Taipale, J., Koli, K. and Keski-Oja, J., 1992. Release of transforming growth factor-beta 1 from the pericellular matrix of cultured fibroblasts and fibrosarcoma cells by plasmin and thrombin. *Journal of Biological Chemistry*, 267(35), pp.25378-25384.
- Takafuji, V., Forgues, M., Unsworth, E., Goldsmith, P. and Wang, X.W., 2007. An osteopontin fragment is essential for tumor cell invasion in hepatocellular carcinoma. *Oncogene*, 26(44), pp.6361-6371.
- Takase, O., Hirahashi, J., Takayanagi, A., Chikaraishi, A., Marumo, T., Ozawa, Y., Hayashi, M., Shimizu, N. and Saruta, T., 2003. Gene transfer of truncated $\text{I}\kappa\text{B}\alpha$ prevents tubulointerstitial injury. *Kidney International*, 63(2), pp.501-513.
- Takaya, K., Koya, D., Isono, M., Sugimoto, T., Sugaya, T., Kashiwagi, A. and Haneda, M., 2003. Involvement of ERK pathway in albumin-induced MCP-1 expression in mouse proximal tubular cells. *American Journal of Physiology-Renal Physiology*, 284(5), pp.F1037-F1045.
- Takeda, T., Yamazaki, H. and Farquhar, M.G., 2003. Identification of an apical sorting determinant in the cytoplasmic tail of megalin. *American Journal of Physiology-Cell Physiology*, 284(5), pp.C1105-C1113.
- Tamaki, K., Okuda, S., Ando, T., Iwamoto, T., Nakayama, M. and Fujishima, M., 1994. TGF- β 1 in glomerulosclerosis and interstitial fibrosis of adriamycin nephropathy. *Kidney International*, 45(2), pp.525-536.
- Tan, R.J. and Liu, Y., 2012. Matrix metalloproteinases in kidney homeostasis and diseases. *American Journal of Physiology-Renal Physiology*, 302(11), pp.F1351-F1361.
- Tan, T.K., Zheng, G., Hsu, T.T., Lee, S.R., Zhang, J., Zhao, Y., Tian, X., Wang, Y., Wang, Y.M., Cao, Q. and Wang, Y., 2013. Matrix metalloproteinase-9 of tubular and macrophage origin contributes to the pathogenesis of renal fibrosis via macrophage recruitment through osteopontin cleavage. *Laboratory Investigation*, 93(4), pp.434-449.
- Tan, T.K., Zheng, G., Hsu, T.T., Wang, Y., Lee, V.W., Tian, X., Wang, Y., Cao, Q., Wang, Y. and Harris, D.C., 2010. Macrophage matrix metalloproteinase-9 mediates epithelial-mesenchymal transition in vitro in murine renal tubular cells. *The American Journal of Pathology*, 176(3), pp.1256-1270.
- Tang, S., Lai, K.N., Chan, T.M., Lan, H.Y., Ho, S.K. and Sacks, S.H., 2001. Transferrin but not albumin mediates stimulation of complement C3 biosynthesis in human proximal tubular epithelial cells. *American Journal of Kidney Diseases*, 37(1), pp.94-103.
- Tang, W.W., Qi, M., Warren, J.S. and Van, G.Y., 1997. Chemokine expression in experimental tubulointerstitial nephritis. *The Journal of Immunology*, 159(2), pp.870-876.

- Tashiro, K., Koyanagi, I., Ohara, I., Ito, T., Saitoh, A., Horikoshi, S. and Tomino, Y., 2004. Levels of urinary matrix metalloproteinase-9 (MMP-9) and renal injuries in patients with type 2 diabetic nephropathy. *Journal of Clinical Laboratory Analysis*, 18(3), pp.206-210.
- Tencer, J., Frick, I.M., Öquist, B.W., Alm, P. and Rippe, B., 1998. Size-selectivity of the glomerular barrier to high molecular weight proteins: upper size limitations of shunt pathways. *Kidney International*, 53(3), pp.709-715.
- Tenten, V., Menzel, S., Kunter, U., Sicking, E.M., van Roeyen, C.R., Sanden, S.K., Kaldenbach, M., Boor, P., Fuss, A., Uhlig, S. and Lanzmich, R., 2013. Albumin is recycled from the primary urine by tubular transcytosis. *Journal of the American Society of Nephrology*, 24(12), pp.1966-1980.
- Tewari, R., Nada, R., Rayat, C.S., Boruah, D., Dudeja, P., Joshi, K. and Sakhuja, V., 2015. Correlation of proteinuria with podocyte foot process effacement in IgA nephropathy: an ultrastructural study. *Ultrastructural Pathology*, 39(2), pp.147-151.
- Thelle, K., Christensen, E.I., Vorum, H. and Birn, H., 2006. Characterization of proteinuria and tubular protein uptake in a new model of oral L-lysine administration in rats. *Kidney International*, 69(8), pp.1333-1340.
- Thomas, M.E., Brunskill, N.J., Harris, K.P., Bailey, E., Pringle, J.H., Furness, P.N. and Walls, J., 1999. Proteinuria induces tubular cell turnover: A potential mechanism for tubular atrophy. *Kidney International*, 55(3), pp.890-898.
- Thomas, M.E., Harris, K.P., Walls, J., Furness, P.N. and Brunskill, N.J., 2002. Fatty acids exacerbate tubulointerstitial injury in protein-overload proteinuria. *American Journal of Physiology-Renal Physiology*, 283(4), pp.F640-F647.
- Thraillkill, K.M., Bunn, R.C. and Fowlkes, J.L., 2009a. Matrix metalloproteinases: their potential role in the pathogenesis of diabetic nephropathy. *Endocrine*, 35(1), pp.1-10.
- Thraillkill, K.M., Nimmo, T., Bunn, R.C., Cockrell, G.E., Moreau, C.S., Mackintosh, S., Edmondson, R.D. and Fowlkes, J.L., 2009b. Microalbuminuria in type 1 diabetes is associated with enhanced excretion of the endocytic multiligand receptors megalin and cubilin. *Diabetes Care*, 32(7), pp.1266-1268.
- Toblli, J.E., Bevione, P., Di Gennaro, F., Madalena, L., Cao, G. and Angerosa, M., 2012. Understanding the mechanisms of proteinuria: therapeutic implications. *International Journal of Nephrology*, 2012.
- Tojo, A. and Endou, H., 1992. Intrarenal handling of proteins in rats using fractional micropuncture technique. *American Journal of Physiology-Renal Physiology*, 263(4), pp.F601-F606.
- Tojo, A. and Kinugasa, S., 2012. Mechanisms of glomerular albumin filtration and tubular reabsorption. *International Journal of Nephrology*, 2012.

- Tojo, A., Onozato, M., Ha, H., Kurihara, H., Sakai, T., Goto, A., Fujita, T. and Endou, H., 2001. Reduced albumin reabsorption in the proximal tubule of early-stage diabetic rats. *Histochemistry and Cell Biology*, 116(3), pp.269-276.
- Tokito, A. and Jougasaki, M., 2016. Matrix metalloproteinases in non-neoplastic disorders. *International Journal of Molecular Sciences*, 17(7), p.1178.
- Tramonti, G., Romiti, N. and Chieli, E., 2009. Albumin influences expression and function of the membrane transporter P-glycoprotein in HK-2 human proximal tubular cells. *Journal of Nephrology*, 22(2), pp.263-272.
- Tryggvason, K., 1999. Unraveling the Mechanisms of Glomerular Ultrafiltration Nephron, a Key Component of the Slit Diaphragm. *Journal of the American Society of Nephrology*, 10(11), pp.2440-2445.
- Tveita, A., Rekvig, O.P. and Zykova, S.N., 2008. Glomerular matrix metalloproteinases and their regulators in the pathogenesis of lupus nephritis. *Arthritis Research & Therapy*, 10(6), p.229.
- Urso, M.L., Strohbach, C.A., Eustis, H.L. and Warren, G.L., 2012. Matrix metalloprotease inhibitor Batimastat does not improve skeletal muscle function post-traumatic injury. *The FASEB Journal*, 26(1 Supplement), pp.1086-2.
- Van den Bergh Weerman, M.A., Assmann, K.J., Weening, J.J. and Florquin, S., 2004. Podocyte foot process effacement is not correlated with the level of proteinuria in human glomerulopathies. *Kidney International*, 66(5), pp.1901-1906.
- Van der Zijl, N.J., Hanemaaijer, R., Tushuizen, M.E., Schindhelm, R.K., Boerop, J., Rustemeijer, C., Bilo, H.J., Verheijen, J.H. and Diamant, M., 2010. Urinary matrix metalloproteinase-8 and-9 activities in type 2 diabetic subjects: A marker of incipient diabetic nephropathy?. *Clinical Biochemistry*, 43(7), pp.635-639.
- Van Leeuwen, A.M. and Bladh, M.L., 2016. Textbook of Laboratory and Diagnostic Testing: Practical Application of Nursing Process at the Bedside. FA Davis. Page 532.
- Van Lint, P. and Libert, C., 2007. Chemokine and cytokine processing by matrix metalloproteinases and its effect on leukocyte migration and inflammation. *Journal of Leukocyte Biology*, 82(6), pp.1375-1381.
- Van Praet, O., Argraves, W.S. and Morales, C.R., 2003. Co-expression and interaction of cubilin and megalin in the adult male rat reproductive system. *Molecular Reproduction and Development*, 64(2), pp.129-135.
- Van Wart, H.E. and Birkedal-Hansen, H., 1990. The cysteine switch: a principle of regulation of metalloproteinase activity with potential applicability to the entire matrix metalloproteinase gene family. *Proceedings of the National Academy of Sciences*, 87(14), pp.5578-5582.
- Vaughn, D.E., Milburn, C.M., Penny, D.M., Martin, W.L., Johnson, J.L. and Bjorkman, P.J., 1997. Identification of critical IgG binding epitopes on the neonatal Fc receptor. *Journal of Molecular Biology*, 274(4), pp.597-607.

- Verlander, J.W., 1998. Normal ultrastructure of the kidney and lower urinary tract. *Toxicologic Pathology*, 26(1), pp.1-17.
- Verma, R.P. and Hansch, C., 2007. Matrix metalloproteinases (MMPs): chemical–biological functions and (Q) SARs. *Bioorganic & Medicinal Chemistry*, 15(6), pp.2223-2268.
- Vielhauer, V. and Mayadas, T.N., 2007, May. Functions of TNF and its receptors in renal disease: distinct roles in inflammatory tissue injury and immune regulation. In *Seminars in Nephrology* (Vol. 27, No. 3, pp. 286-308). WB Saunders.
- Vinge, L., Lees, G.E., Nielsen, R., Kashtan, C.E., Bahr, A. and Christensen, E.I., 2010. The effect of progressive glomerular disease on megalin-mediated endocytosis in the kidney. *Nephrology Dialysis Transplantation*, 25(8), pp.2458-2467.
- Viswanathan, V. and Rani, A. A., 2016. Proteinuria in nondiabetic patients: Clinical significance. *Hypertension Journal*, 2(3), pp.118-123.
- Visse, R. and Nagase, H., 2003. Matrix metalloproteinases and tissue inhibitors of metalloproteinases. *Circulation Research*, 92(8), pp.827-839.
- Wang, X., Fu, X., Brown, P.D., Crimmin, M.J. and Hoffman, R.M., 1994. Matrix metalloproteinase inhibitor BB-94 (batimastat) inhibits human colon tumor growth and spread in a patient-like orthotopic model in nude mice. *Cancer Research*, 54(17), pp.4726-4728.
- Wang, X., Zhou, Y., Tan, R., Xiong, M., He, W., Fang, L., Wen, P., Jiang, L. and Yang, J., 2010. Mice lacking the matrix metalloproteinase-9 gene reduce renal interstitial fibrosis in obstructive nephropathy. *American Journal of Physiology-Renal Physiology*, 299(5), pp.F973-F982.
- Wasserstein, A.G., 1997. Membranous glomerulonephritis. *Journal of the American Society of Nephrology*, 8(4), pp.664-674.
- Watson, S.A., Morris, T.M., Parsons, S.L., Steele, R.J. and Brown, P.D., 1996. Therapeutic effect of the matrix metalloproteinase inhibitor, batimastat, in a human colorectal cancer ascites model. *British Journal of Cancer*, 74(9), p.1354.
- Welling, L.W. and Welling, D.J., 1975. Surface areas of brush border and lateral cell walls in the rabbit proximal nephron. *Kidney International*, 8(6), pp.343-348.
- West, B.L., Picken, M.M. and Leehey, D.J., 2006. Albuminuria in acute tubular necrosis. *Nephrology Dialysis Transplantation*, 21(10), pp.2953-2956.
- Whaley-Connell, A.T., Morris, E.M., Rehmer, N., Yaghoubian, J.C., Wei, Y., Hayden, M.R., Habibi, J., Stump, C.S. and Sowers, J.R., 2007. Albumin activation of NAD (P) H oxidase activity is mediated via Rac1 in proximal tubule cells. *American Journal of Nephrology*, 27(1), pp.15-23.

- Wheeler, D.S., Giuliano, J.S., Lahni, P.M., Denenberg, A., Wong, H.R. and Zingarelli, B., 2011. The immunomodulatory effects of albumin in vitro and in vivo. *Advances in Pharmacological Sciences*, 2011.
- Whiteside, C.I., Cameron, R., Munk, S. and Levy, J., 1993. Podocytic cytoskeletal disaggregation and basement-membrane detachment in puromycin aminonucleoside nephrosis. *The American Journal of Pathology*, 142(5), p.1641.
- Whittaker, M., Floyd, C.D., Brown, P. and Gearing, A.J., 1999. Design and therapeutic application of matrix metalloproteinase inhibitors. *Chemical Reviews*, 99(9), pp.2735-2776.
- Wicher, G., Larsson, M., Rask, L. and Aldskogius, H., 2005. Low-density lipoprotein receptor-related protein (LRP) -2/megalin is transiently expressed in a subpopulation of neural progenitors in the embryonic mouse spinal cord. *Journal of Comparative Neurology*, 492(2), pp.123-131.
- Wilmer, M.J., Christensen, E.I., van den Heuvel, L.P., Monnens, L.A. and Levtchenko, E.N., 2008. Urinary protein excretion pattern and renal expression of megalin and cubilin in nephropathic cystinosis. *American Journal of Kidney Diseases*, 51(6), pp.893-903.
- Williams, A.J., Baker, F. and Walls, J., 1987. Effect of varying quantity and quality of dietary protein intake in experimental renal disease in rats. *Nephron*, 46(1), pp.83-90.
- Williams, J.D. and Coles, G.A., 1994. Proteinuria—A direct cause of renal morbidity?. *Kidney International*, 45(2), pp.443-450.
- Williams, J.M., Zhang, J., North, P., Lacy, S., Yakes, M., Dahly-Vernon, A. and Roman, R.J., 2011. Evaluation of metalloprotease inhibitors on hypertension and diabetic nephropathy. *American Journal of Physiology-Renal Physiology*, 300(4), pp.F983-F998.
- Williams, M.E., 2005. Diabetic nephropathy: the proteinuria hypothesis. *American Journal of Nephrology*, 25(2), pp.77-94.
- Willnow, T.E., Hilpert, J., Armstrong, S.A., Rohlmann, A., Hammer, R.E., Burns, D.K. and Herz, J., 1996. Defective forebrain development in mice lacking gp330/megalin. *Proceedings of the National Academy of Sciences*, 93(16), pp.8460-8464.
- Wojtowicz-Praga, S.M., Dickson, R.B. and Hawkins, M.J., 1997. Matrix metalloproteinase inhibitors. *Investigational New Drugs*, 15(1), pp.61-75.
- Wu, H.J., Yiu, W.H., Li, R.X., Wong, D.W., Leung, J.C., Chan, L.Y., Zhang, Y., Lian, Q., Lin, M., Tse, H.F. and Lai, K.N., 2014. Mesenchymal stem cells modulate albumin-induced renal tubular inflammation and fibrosis. *PLOS One*, 9(3), p.e90883.

- Xu, D., Kozyraki, R., Newman, T.C. and Fyfe, J.C., 1999. Genetic evidence of an accessory activity required specifically for cubilin brush-border expression and intrinsic factor-cobalamin absorption. *Blood*, 94(10), pp.3604-3606.
- Xu, X., Jackson, P.L., Tanner, S., Hardison, M.T., Roda, M.A., Blalock, J.E. and Gaggar, A., 2011. A self-propagating matrix metalloprotease-9 (MMP-9) dependent cycle of chronic neutrophilic inflammation. *PLOS One*, 6(1), p.e15781.
- Xu, T.H., Yan, Y., Kang, Y., Jiang, Y., Melcher, K. and Xu, H.E., 2016. Alzheimer's disease-associated mutations increase amyloid precursor protein resistance to γ -secretase cleavage and the A β 42/A β 40 ratio. *Cell Discovery*, 2.
- Yammani, R.R., Seetharam, S. and Seetharam, B., 2001. Cubilin and megalin expression and their interaction in the rat intestine: effect of thyroidectomy. *American Journal of Physiology-Endocrinology and Metabolism*, 281(5), pp.E900-E907.
- Yang, J., Shultz, R.W., Mars, W.M., Wegner, R.E., Li, Y., Dai, C., Nejak, K. and Liu, Y., 2002. Disruption of tissue-type plasminogen activator gene in mice reduces renal interstitial fibrosis in obstructive nephropathy. *The Journal of Clinical Investigation*, 110(10), pp.1525-1538.
- Yang, X., Kume, S., Tanaka, Y., Isshiki, K., Araki, S.I., Chin-Kanasaki, M., Sugimoto, T., Koya, D., Haneda, M., Sugaya, T. and Li, D., 2011. GW501516, a PPAR δ agonist, ameliorates tubulointerstitial inflammation in proteinuric kidney disease via inhibition of TAK1-NF κ B pathway in mice. *PLOS One*, 6(9), p.e25271.
- Yuseff, M.I., Farfan, P., Bu, G. and Marzolo, M.P., 2007. A cytoplasmic PPPSP motif determines megalin's phosphorylation and regulates receptor's recycling and surface expression. *Traffic*, 8(9), pp.1215-1230.
- Zatz, R., Dunn, B.R., Meyer, T.W., Anderson, S., Rennke, H.G. and Brenner, B.M., 1986. Prevention of diabetic glomerulopathy by pharmacological amelioration of glomerular capillary hypertension. *Journal of Clinical Investigation*, 77(6), p.1925.
- Zhang, Y.N., Dean, W.L. and Gray, R.D., 1997. Cooperative binding of Ca²⁺ to human interstitial collagenase assessed by circular dichroism, fluorescence, and catalytic activity. *Journal of Biological Chemistry*, 272(3), pp.1444-1447.
- Zhang, Y., George, J., Li, Y., Olufade, R. and Zhao, X., 2015. Matrix Metalloproteinase-9 Expression Is Enhanced in Renal Parietal Epithelial Cells of Zucker Diabetic Fatty Rats and Is Induced by Albumin in In Vitro Primary Parietal Cell Culture. *PLOS One*, 10(4), p.e0123276.
- Zhao, H., Dong, Y., Tian, X., Tan, T.K., Liu, Z., Zhao, Y., Zhang, Y., Harris, D.C. and Zheng, G., 2013. Matrix metalloproteinases contribute to kidney fibrosis in chronic kidney diseases. *World Journal of Nephrology*, 2(3), p.84.
- Zheng, G., Lyons, J.G., Tan, T.K., Wang, Y., Hsu, T.T., Min, D., Succar, L., Rangan, G.K., Hu, M., Henderson, B.R. and Alexander, S.I., 2009. Disruption of

E-cadherin by matrix metalloproteinase directly mediates epithelial-mesenchymal transition downstream of transforming growth factor- β 1 in renal tubular epithelial cells. *The American Journal of Pathology*, 175(2), pp.580-591.

Zhuo, J.L. and Li, X.C., 2013. Proximal nephron. *Comprehensive Physiology*.

Zoja, C., Benigni, A. and Remuzzi, G., 1999. Protein overload activates proximal tubular cells to release vasoactive and inflammatory mediators. *Nephron Experimental Nephrology*, 7(5-6), pp.420-428.

Zoja, C., Donadelli, R., Colleoni, S., Figliuzzi, M., Bonazzola, S., Morigi, M. and Remuzzi, G., 1998. Protein overload stimulates RANTES production by proximal tubular cells depending on NF- κ B activation. *Kidney International*, 53(6), pp.1608-1615.

Zoja, C., Benigni, A. and Remuzzi, G., 1999. Protein overload activates proximal tubular cells to release vasoactive and inflammatory mediators. *Nephron Experimental Nephrology*, 7(5-6), pp.420-428.

Zou, Z., Chung, B., Nguyen, T., Mentone, S., Thomson, B. and Biemesderfer, D., 2004. Linking receptor-mediated endocytosis and cell signaling evidence for regulated intramembrane proteolysis of megalin in proximal tubule. *Journal of Biological Chemistry*, 279(33), pp.34302-34310.